

Circular floor system for residential buildings

Development of a post-tensioned and modular floor system applicable as a storey floor in ground-based housing units and apartment buildings

L.S. Schuyffel (4248295)
CIE5060-09 MSc Thesis
Thesis report

June 2, 2022



Circular floor system for residential buildings

Development of a post-tensioned and modular floor system applicable as a storey floor in ground-based housing units and apartment buildings

by

L.S. (Luke) Schuyffel

in partial fulfilment of the requirements for the degree of

Master of Science
in Civil Engineering
Structural Engineering - Concrete Structures

at the Delft University of Technology,
to be defended publicly on Thursday June 9, 2022 at 13:00.

In collaboration with:



ONDERDEEL VAN IV-BOUW

Student number:	4248295	
Project duration:	September 1, 2021 – June 9, 2022	
Thesis committee:	Prof. dr. ir. M.A.N. (Max) Hendriks	TU Delft, chair
	Dr. ir. Y. (Yuguang) Yang	TU Delft, supervisor
	Ir. A.C.B. (Marco) Schuurman	TU Delft, supervisor
	Ir. R.J. (Rinske) Daniëls-de Waard	CAE, supervisor

An electronic version of this thesis is available at <http://repository.tudelft.nl/>.

Cover image retrieved from <https://www.bamb2020.eu/>

Preface

This thesis marks the final achievement in order to obtain the degree of Master of Science in Structural Engineering, with the specialisation Concrete Structures, at the faculty of Civil Engineering and Geosciences at Delft University of Technology. The research has been performed in collaboration with C.A.E. B.V. in Delft, and took place during the period from September 2021 until June 2022. In this report, the findings of my research into the topic of circular design in residential and utility buildings, specifically focused on the development of a post-tensioned and modular load bearing floor system, are presented. The driving forces behind this research are related to the imminent introduction of the circular economy and the capriciousness of the Dutch housing market at the present day.

First of all, I would like to take the opportunity to express my gratitude to the members of my graduation committee for their contributions, insights and support throughout the thesis project. I would like to thank dr. ir. Yuguang Yang for his expertise and help regarding all structural parameters included in the highly iterative design process and accompanying analyses that have been performed. Besides, I would like to thank ir. Marco Schuurman for his realistic and practical views and, moreover, for his ideas on my research to enlarge my knowledge on the project. Furthermore, I would like to thank prof. dr. ir. Max Hendriks, as the chair of the committee, for guarding my progress and constantly pointing out to zoom out and keep an eye on the bigger picture, which was very challenging sometimes, but resulted in a lesson for life. Moreover, I would like to thank C.A.E. B.V. and all colleagues for providing me the opportunity and freedom for my research project and for a supportive working environment. In particular, my thanks go to ir. Rinske Daniëls-de Waard as my daily supervisor at C.A.E. B.V. for all her guidance, support, ideas, expertise and constructive feedback throughout the entire project.

Finally, I would like to express my gratitude to my family and friends who supported me during the writing of my thesis. My friends for providing me with moments of distraction, support and advice which helped me to reload my batteries and to continue my work with enthusiasm. Secondly, my parents for their unconditional support in every thinkable way and providing me the opportunity to become the third generation of 'ingenieur' of the family. Last but not least, I would like to express my gratitude to my girlfriend for her persistent support through better and worse moments and to remove all obstacles out of my way, so I could fully focus on writing my final thesis.

I wish you most pleasant reading!

*L.S. (Luke) Schuyffel
Voorburg, June 2022*

Abstract

Sustained economic growth based on a linear production model is not feasible on a planet with finite resources and a limited capacity to absorb wastes. By 2050, the world's population has grown exponentially to 9.7 billion and a tripling of the global use of materials can be realistically expected. Therefore, the transition towards a circular economy has become one of the top priorities of the European Union and its national governments. The Dutch government has stated the ambition to achieve a fully circular economy by 2050 at the latest.

Worldwide, the construction sector contributes to approximately 13% of the global economy and employment of over 110 million workers. However, the construction sector is also responsible for 50% of the total raw material consumption, 40% of the energy usage and for 39% of all carbon dioxide emissions. The construction sector therefore shows excellent potential for the transition to a more circular production model. One of the initiatives in the Netherlands to accelerate this transition is called 'het betonakkoord'. This initiative aims to make the concrete supply chain more sustainable by focusing on high quality application of recycled or reused building materials and on circular design.

Another interesting development is ongoing in the Netherlands. Since 2019, the housing shortage is 300.000 units and is continuously increasing to approximately 400.000 units by 2025. Combined with the economic growth of the past decade has resulted in skyrocketing house prices. One of the most effective solutions to overcome this problem is to simply built new houses. However, taken into consideration the transition towards a circular economy, raises a fundamental question of how to design sustainable residential buildings with regard to circular principles. This question is quite extensive and consists of a variety of both structural and non-structural aspects. This thesis project focuses on the circular design of a load-bearing floor system for utilisation as a storey floor.

First, extensive literature review is performed in order to identify circular principles and strategies in the design phase of buildings. This thesis project adopted the framework of Cheshire. The framework consist of six nested circles which represent the hierarchy of the framework. Within the framework, Cheshire proposes five design principles in his book: building in layers, designing-out waste, design for adaptability, design for disassembly and material selection. This thesis project expanded the design principles of Cheshire, by defining and providing hands-on strategies or criteria for each design principle. In total, 42 criteria are proposed for transposition into a comprehensive framework for application in practice.

Next, several recent residential and utility building projects are reviewed to determine the state-of-the-art regarding the implementation of circular design principles in practice. The general tendency is that these projects take the deconstructability and, to a limited extent, the selection of materials of the buildings into account. The common denominator in all recent projects, and especially for residential buildings, is the reduction of environmental impact through the realisation of net zero energy buildings.

Concrete floor systems are still widely used in newly built residential and utility buildings, due to their favourable characteristics. Therefore, the four most commonly used concrete floor systems are reviewed and discussed, These four floor systems are primarily designed in accordance with the demands of users and contractors. As a result of this thesis project, a newly designed floor system is proposed which is fundamentally based on the theoretical design framework developed in this report. Implementation of all five design principles was not considered feasible given the current state-of-the-art and regulatory barriers. Therefore, the newly proposed floor system is based on strategies and criteria related to the design principles of adaptability and disassembly. These design principles form the starting point of the multi-criteria analysis conducted in this report. The multi-criteria analysis is conducted in the first place to evaluate the performances of the four most commonly used concrete floor systems in the context of the considered circular design principles and secondly to compare the newly proposed floor system with the four most commonly used concrete floor systems. Based on

the weighted rating scale, a maximum score of one hundred can be obtained. Results from the multi-criteria analysis reveal that three out of four commonly used concrete floor systems score well (scoring between 60 and 80) regarding the circular design principles. The newly proposed floor system scores excellent (scoring between 80 and 100).

The structural resistance of the newly proposed floor system is verified in accordance with codes of practice and state-of-the-art research under normal loading conditions. Horizontal wind loading is taken into consideration as well with respect to the stability of floor systems. Moreover, several stakeholder prerequisites are included in the design. Possibilities for recesses, staircases or vertical shafts for example, and building services are provided and suggested. Buildability aspects, such as the fabrication and assembly process are discussed in the report as well.

This thesis project is conducted from an academic perspective with limited scope in order to fit within a predetermined time frame. Several aspects require further research to determine the successful application of the system in practice. Broad financial aspects, such as costs and new business models are not included in this research. Cross-sectional optimisation and more comprehensive inclusion of buildability aspects and stakeholder requirements are recommended for future research. However, the developed circular design framework of this thesis project, based on the design principles of Cheshire, reveals additional valuable dimensions in the design of concrete floor systems and buildings in general. As the multi-criteria analysis has shown, the newly proposed floor system translates these valuable dimensions and design criteria into the design to a higher extent compared to the commonly used concrete floor systems. Nevertheless, the proposed floor system provides sufficient room for improvements in future research. However, in conclusion, the newly proposed floor system, but especially its analogy, provide additional valuable dimensions into the design of concrete floor systems and is therefore a more comprehensive, yet practical alternative for application in residential buildings.

Table of Contents

Preface	i
Abstract	iii
Table of Contents	vi
List of Figures	viii
List of Tables	ix
I Research Framework	1
1 Introduction	2
1.1 Background and Motivation	2
1.1.1 Circular Economy Concept	2
1.1.2 Transition Towards a Circular Economy	4
1.1.3 The Construction Industry	5
1.2 Problem Statement	6
1.3 Problem Definition	7
2 Research plan	9
2.1 Research Scope	9
2.2 Research Aim and Objectives	9
2.3 Research Questions	10
II Theoretical Framework	11
3 Design for a Circular Economy	12
3.1 General CE Framework	12
3.2 CE Framework for the Built Environment	13
3.2.1 Theory of Layers	15
3.2.2 Designing out Waste	16
3.2.3 Design for Adaptability	18
3.2.4 Design for Disassembly	19
3.2.5 Selecting Materials	21
3.3 Conclusions	26
4 Recent Projects	27
4.1 Utility Building Projects	27
4.1.1 Park 20 20	27
4.1.2 Temporary Courthouse Amsterdam	27
4.1.3 Pavilion Circl	28
4.1.4 People's Pavilion	29
4.2 Residential Building Project	30
4.2.1 Superlocal	30
4.3 Conclusions	30
5 Floor Systems	31
5.1 Hollow Core Slab	31
5.2 Service-integrated floor	32
5.3 Reinforced Plank Floor	32
5.4 Bestcon floor systems	34

III	Design	35
6	Design and Validation	36
6.1	Evaluation common floor systems	36
6.2	Design Starting Points	37
6.3	Newly Proposed System	39
6.4	Validation floor systems	40
7	Design Verification	44
7.1	Calculation procedure	44
7.2	Classification and imposed loading	44
7.2.1	Classification	44
7.2.2	Imposed vertical loading	45
7.2.3	Load combinations	45
7.2.4	Cross-sectional and material properties	47
7.3	Required amount of prestressing	47
7.4	Prestressing losses.	49
7.4.1	Immediate prestressing losses.	49
7.4.2	Time dependent prestressing losses	51
7.5	Cross-sectional checks in SLS.	54
7.5.1	Cross-sectional stresses	54
7.5.2	Deformations	55
7.5.3	Vibrations	58
7.6	Bending moment resistance in ULS	58
7.6.1	Previously conducted research	59
7.6.2	Codes of practice	63
7.6.3	Results	65
7.7	Shear resistance in ULS	68
7.7.1	Shear resistance cross-section	68
7.7.2	Shear resistance interfaces	69
8	Buildability Aspects	73
8.1	Fabrication and Assembly Procedure	73
8.2	Building Services	74
8.2.1	Raised floor systems	76
8.2.2	Suspended ceilings.	76
8.3	Recesses	78
8.4	Stability	81
IV	Conclusion	88
9	Discussion	89
10	Conclusions	91
10.1	Sub-questions	91
10.2	Central research question	93
11	Recommendations	94
11.1	Expansion of the analogy or analysis of the system	94
11.2	Developments of the proposed design	94
	Bibliography	102
	Appendices	102
A	Calculation results for Group I	103
B	Calculation results for Group II	111
C	Calculation results for Group III	123
D	European Technical Assessment Post Tensioning system	139

E	Calculation sheet	180
F	Case study Project	214

List of Figures

1.1	Three economical models: Linear Economy, Recycling Economy, Circular Economy . . .	3
1.2	Additions to the housing stock through transformation in 2019	6
1.3	Experimental test set-up of Ortlepp et al.	8
1.4	Shape, sizes and geometry of the concrete blocks and slab	8
3.1	The 9R Framework of Potting et al.	13
3.2	Applying circular economy principles to building design	14
3.3	Interaction between building layers	16
3.4	Circular design framework with hands-on criteria or strategies	25
4.1	Overview of Park 20 20 in Hoofddorp	28
4.2	The Temporary Courthouse building in Amsterdam and demountable beam-slab connection	28
4.3	Overview of Pavilion Circl in Amsterdam	29
4.4	People's Pavilion building in Eindhoven	29
4.5	Overview of the Superlocal project in Kerkrade	30
5.1	Hollow core slabs	32
5.2	Service-integrated floor systems	33
5.3	Examples of a reinforced plank floor and cast-in building services	34
5.4	Bestcon floor slabs	34
6.1	Schematic side view of the system with an element size of: 1200x1200 millimeters	38
6.2	Schematic cross-sectional view of the system with an element size of 1200x1200 millimeters	39
6.3	Dimensions group I: width = 0.6 meters	41
6.4	Dimensions group II: width = 1.2 meters	41
6.5	Dimensions group III: width = 1.8 meters	42
6.6	Cross-sectional views of the exact dimensions for an element width of 1200 millimeters	42
7.1	Loading scheme system	46
7.2	Calculation values for loads	46
7.3	Example of the kern area of a T-shaped beam	55
7.4	Stresses in the cross-section for a span length of 5.4 m	56
7.5	Stresses in the cross-section for a span length of 7.8 m	56
7.6	Vertical components of the deflections defined by	56
7.7	Deflection lines according to the frequent load combination	57
7.8	Values of parameters under typical load situations and tendon profiles	62
7.9	Δf_{ps} prediction versus experimental results by Naaman and Alkhairi	63
7.10	Δf_{ps} prediction versus experimental results by He and Liu	63
7.11	Δf_{ps} prediction versus experimental results by Alqam et al.	64
7.12	Adopted kinematic failure model due to the imposed loading	66
7.13	Bending moment diagrams due to the imposed loading	66
7.14	Cross-sectional equilibrium at ultimate limit state	66
7.15	Shear force diagrams due to the imposed loading	70
8.1	Assembly procedure for the proposed floor system in top view	75
8.2	Hydraulic jack from Dywidag for post tensioning tendons	76
8.3	Assembly procedure for the proposed floor system in side view	76
8.4	Examples of raised floor systems	77

8.5	Examples of suspended ceilings	77
8.6	Location of recesses for a span length of $l = 7.8m$ in illustrative cross-sectional view	78
8.7	Location of recesses for a span length of $l = 7.8m$ in illustrative top view	78
8.8	Loading scheme with an additional trimmer beam	79
8.9	System and local slab overviews with the application of a trimmer beam	80
8.10	Representation of the interaction between shear and torsion	80
8.11	Stability walls of the case study building and various wind directions	83
8.12	Wind loading on the considered floor system	84
8.13	Composite action for beams: (a) no composite action; (b) full composite action	85
8.14	Two mechanisms for determination of tendon forces under wind loading	86
8.15	Dry connections with a bolt anchor embedded in the concrete (left) and bolts penetrating through the concrete	87

List of Tables

1.1	Explicit definitions of Circular Economy	3
1.2	Structural parameters of Ortlepp et al.	7
3.1	Layers of Duffy and Henney	15
3.2	Layers of Brand	15
3.3	Strategies of DfD and their relevance to the hierarchic levels of recycling	22
3.4	Groups and corresponding factors for DfD and corresponding weights	23
5.1	General characteristics of hollow core slabs	32
5.2	General characteristics of service-integrated floors	33
5.3	General characteristics of reinforced plank floors	33
5.4	General characteristics of the Bestcon floor systems	34
6.1	Multi-criteria analysis of the four commonly used and newly proposed floor system	43
7.1	Classification of residential buildings of the case study	45
7.2	Vertical loading on the residential units	45
7.3	Combination factors ψ	46
7.4	Required amount of prestressing steel for all span lengths	49
7.5	Immediate prestressing losses due to friction, wedge set and elastic deformation	50
7.6	Total prestressing losses due to immediate and time-dependent effects	54
7.7	Vertical deformation limits for buildings	57
7.8	Results regarding deflections for all span lengths	57
7.9	Unity checks regarding the bending moment capacity for all span lengths	68
7.10	Unity checks regarding the shear force capacity for all span lengths	69
7.11	Interface roughness factors	71
7.12	Unity checks regarding the shear stress at the interfaces for all span lengths	72
8.1	Required amount of prestressing steel for all span lengths with a trimmer beam	79
8.2	Results regarding deflections for all span lengths with a trimmer beam	80
8.3	Unity checks regarding the bending moment capacity for all span lengths with a trimmer beam	81
8.4	Unity checks regarding the shear force capacity for all span lengths with a trimmer beam	82
8.5	Unity checks regarding the shear stress at the interfaces for all span lengths with a trimmer beam	82



Research Framework

Introduction

In this first chapter, a general description of the problem is introduced. The background and motivation for the topic are explained in section 1.1. The problem statement is presented in section 1.2 and this chapter is finalized by stating the problem definition in section 1.3.

1.1. Background and Motivation

All research projects aim to expand knowledge about societal questions and to develop ever better solutions. The overarching objective of this thesis project is to explore an issue currently present in society. In the first paragraph, the concept of the circular economy is defined. The second paragraph highlights the initiatives towards a circular economy on European and national level. The last paragraph zooms in on the central sector in this thesis; the building industry.

1.1.1. Circular Economy Concept

Sustained economic growth based on a linear production model is not feasible in a planet with finite resources and a limited capacity to absorb wastes [1]. Despite numerous attempts to address the ecological issues, the pressures on the global environment have been constantly growing. In this context, Circular Economy (CE) is regarded as an alternative which may give rise to economic and ecological benefits [2].

The term circular economy has both a linguistic and a descriptive meaning. Linguistically it is an antonym of a linear economy. A linear economy is characterised by a 'take-make-consume and dispose' pattern [3]. The production of waste leads to the deterioration of the environment in two ways: **(i)**: by the removal of natural capital from the environment, through mining or unsustainable harvesting **(ii)**: by the reduction of the value of natural capital caused by pollution from waste. Pollution can also occur at the resource acquisition stage [4].

This is a one-way system and an economy based on such a system has been referred to as a cowboy economy. A cowboy economy is an economy that behaves as if natural resources are infinite and all wastes can be absorbed by nature [5].

A circular economy is envisaged as having no net effect on the environment. The word circular has a second, descriptive meaning, which relates to the concept of a cycle [4]. The linear, recycling and circular economical models are depicted in figure 1.1. However, in scientific literature, many descriptions of the circular economy concept can be found. Examples of description of the circular economy concept are presented in table 1.1. It can be concluded that the circular economy concept has not reached a mainstream yet [6].

According to Suárez-Eiroa et al. [2], three common theoretical strategies are found under the circular economy paradigm: **i)**: minimizing inputs of raw materials and outputs of waste **ii)**: keeping resource value as long as possible within the system and **iii)**: reintegrating products into the system when they reach the end-of-life. The circular economy concept should be implemented on three levels: micro,

meso and macro. The micro level refers to the implementation in, for example, a company. The meso level refers to the interaction within the inter-firm network, or the so-called eco-industrial parks [7]. The macro level refers to the implementation in cities, regions, nations or society as a whole.

Definition	Reference
Circular Economy systems keep the added value in products for as long as possible and eliminates waste. They keep resources within the economy when a product has reached the end of its life, so that they can be productively used again and again and hence create further value	European Commission [3]
The Circular Economy is one that is restorative and regenerative by design and aims to keep products, components, and materials at their highest utility and value at all times, distinguishing between technical and biological cycles. This new economic model seeks to ultimately decouple global economic development from finite resource consumption. It enables key policy objectives such as generating economic growth, creating jobs, and reducing environmental impacts, including carbon emissions	Ellen MacArthur Foundation [8]
Model of production and consumption of goods through closed loop material flows that internalize environmental externalities linked to virgin resource extraction and the generation of waste (including pollution)	Sauvé et al. [9]
We define the Circular Economy as a regenerative system in which resource input and waste, emission, and energy leakage are minimised by slowing, closing, and narrowing material and energy loops. This can be achieved through long-lasting design, maintenance, repair, reuse, re manufacturing, refurbishing, and recycling	Geissdoerfer et al. [10]
The Circular Economy is an economic model wherein planning, resourcing, procurement, production and reprocessing are designed and managed, as both process and output, to maximize ecosystem functioning and human well-being	Murray et al. [4]
Circular Economy is a sustainable development initiative with the objective of reducing the societal production-consumption systems' linear material and energy throughput flows by applying materials cycles, renewable and cascade-type energy flows to the linear system. Circular Economy promotes high value material cycles alongside more traditional recycling and develops systems approaches to the cooperation of producers, consumers and other societal actors in sustainable development work	Korhonen et al. [11]
A circular economy is a regenerative production-consumption system that aims to maintain extraction rates of resources and generation rates of wastes and emissions under suitable values for planetary boundaries, through closing the system, reducing its size and maintaining the resource's value as long as possible within the system, mainly leaning on design and education, and with capacity to be implemented at any scale	Suárez-Eiroa et al. [2]

Table 1.1: Explicit definitions of Circular Economy

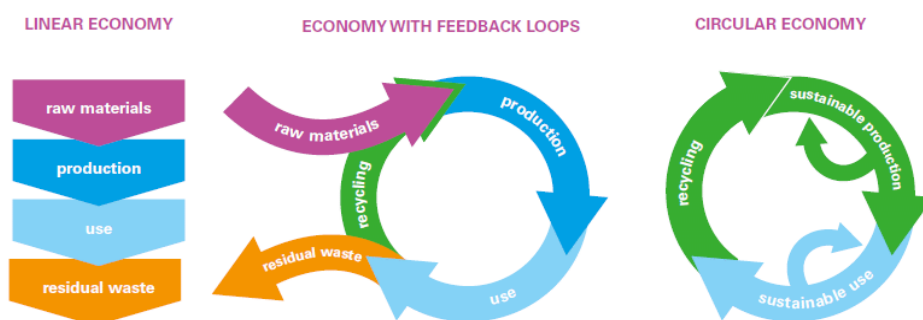


Figure 1.1: Three economical models: Linear Economy (left), Recycling Economy (middle), Circular Economy (right) [12]

In conclusion to this paragraph, this thesis adopts the definition of circular economy proposed by Kirchherr et al. [7] :

Circular Economy: "A circular economy describes an economic system that is based on business models which replace the 'end-of-life' concept with reducing, alternatively reusing, recycling and recovering materials in production/distribution and consumption processes, thus operational at the micro level (products, companies, consumers), meso level (eco-industrial parks) and macro level (city, region, nation and beyond), with the aim to accomplish sustainable development, which implies creating environmental quality, economic prosperity and social equity, to the benefit of current and future generations."

1.1.2. Transition Towards a Circular Economy

The circular economy concept is not new. In Germany, in the early 1990's, the circular economy concept was introduced into environmental policy with the intent to address issues associated with raw material and natural resource use for sustained economic growth [13]. Nowadays, circular economy is becoming increasingly commonplace. One of the most important driving forces behind this is the high environmental impact, caused by the explosive demand for natural resources. In the course of the 20th century, the world's population has started to consume 34 times more materials, 27 times more minerals and 12 times more fossil fuels, compared to the 19th century [14]. Since the global population continues to grow to around 9.7 billion in 2050 [15], a tripling of the global use of materials in 2050 can realistically be expected, in relation to the base year 2000 [12].

Policy on European level

The transition from a linear towards a circular economy is one of the European Union's priorities, accelerating from the past decade. The European Commission expressed the transition in numerous programs and intermediate guidelines. A concise timeline, with the most important initiatives, is presented underneath.

2010: In the aftermath of the economic and financial crisis, the European Commission presents the: *Europe 2020: A strategy for smart, sustainable and inclusive growth*. This strategy aims to achieve: (i) smart growth: developing an economy based on knowledge and innovation (ii) sustainable growth: promoting a more resource efficient, greener and more competitive economy (iii) inclusive growth: fostering a high-employment economy delivering social and territorial cohesion [16].

2014: The European Commission presents the proposal: *Towards a circular economy: A zero waste programme for Europe* [3]. This proposal emphasizes on (i) defining waste targets for a move to a recycling society (ii) delivering simplification and better implementation of waste legislation (iii) tackling specific waste challenges.

2015: The first circular economy action plan is adopted by the European Commission: *Closing the loop: An EU action plan for the circular economy*. The action plan establishes concrete and ambitious actions, with measures covering the whole life cycle from production and consumption to waste management and the market for secondary raw materials and a revised legislative proposal on waste [17].

2018: Monitoring trends and patterns is key to understand how the various elements of the circular economy are developing over time, to help identify success factors in Member States and to assess whether sufficient action has been taken. For this reason, the European Commission presents the: *Monitoring framework for the circular economy* [18]. This monitoring framework captures, in a concise set of indicators, the main elements of the circular economy, including the life-cycle of products and materials, the priority areas and sectors, and the impacts on competitiveness, innovation and jobs.

2019: The European Commission presents in December the assumptions of the new growth strategy: *The European Green Deal*. The main objective of the European Green Deal is to transform the European Union into a fair and prosperous society, with a modern, resource-efficient and competitive economy where there are no net emissions of greenhouse gases in 2050 and where economic growth is decoupled from resource use. The Green Deal

also aims to protect, conserve and enhance the European Union's natural capital, and protect the health and well-being of citizens from environment-related risks and impacts [19].

2020: An updated version of the first circular economy action plan [17] is presented by the European Commission: *A new Circular Economy Action Plan: For a cleaner and more competitive Europe*. This new circular economy action plan provides a future-oriented agenda for achieving a cleaner and more competitive Europe in co-creation with economic actors, consumers, citizens and civil society organisations. It introduces legislative and non-legislative measures targeting areas where action, at the European Union level, brings real added value [20]. Moreover, it is one of the main building blocks of the European Green Deal [19].

Policy on national level

Following the ambitions of the European Union, the Dutch government has set out three goals aimed at making the Dutch economy circular as quickly as possible: **(i)** ensure efficient raw material use **(ii)** emphasize on using sustainably produced, renewable, raw materials instead of non-renewable raw materials **(iii)** develop new production methods and design products to be circular [21].

The Dutch government has set itself the goal to become a fully circular economy in 2050. A concise timeline, with the most important initiatives, is presented underneath.

2016: The Dutch government publishes the report: *A circular economy in the Netherlands by 2050* [22]. This report is a government-wide program that outlines how the Dutch economy can be transformed into a sustainable, fully circular economy. It adopts the advisory reports of (i) the Social and Economic Council of the Netherlands (in Dutch: 'Sociaal Economische Raad') [14] and (ii) the Council for the Environment and Infrastructure (in Dutch: 'Raad voor de leefomgeving en infrastructuur') [12].

2017: Stakeholders, both from the government and industry, sign the Raw Material Agreement (in Dutch: 'Grondstoffenakkoord'), which sets out what should be done to ensure that the Dutch economy can run on renewable resources [23]. Within this agreement, the signatories actively cooperate to draw up the transition agendas.

2018: The government and the signatories of the Raw Material Agreement finalize the transition agendas, focusing on five sectors and value chains that are important to the economy, but also have a high environmental burden. The agendas set out how each sector can become circular and what actions need to be taken. The five sectors and supply chains are: **(i)** biomass and food **(ii)** plastics **(iii)** manufacturing industry **(iv)** consumer goods **(v)** construction [24].

2019: The Circular Economy Implementation Program is presented by the government. This program translates the transition agendas into concrete actions and projects between 2019 and 2023. The Implementation Program will be updated every five years by the government. The Environmental Assessment Agency (in Dutch: 'Planbureau voor de Leefomgeving') will publish a progress report every two years [25].

1.1.3. The Construction Industry

Worldwide, the construction industry contributes to approximately 13% of the global economy and employment of over 110 million workers [26]. Despite its significance to the global economy, the environmental impact of the industry is raising concerns, especially under the currently prevailing linear production model. The industry accounts for 50% of the total raw material extractions, 40% of the energy consumption and is responsible for 39% of the total carbon dioxide (CO₂)-emissions [20, 27]. The numbers in the Netherlands are in line with the global statistics; the industry is responsible for 50% of the raw material consumption, 40% of the energy consumption and for approximately 35% of the CO₂-emissions [22].

In total, in European and sector-wide context, thirty-five official reports are published to accelerate the transition towards a circular economy [28]. The emphasis for the construction industry is on more efficient use of (raw) materials, both at the beginning and at the end of the life cycle, in order to contribute to reducing the environmental impact and resource depletion [29].

Apart from, but analogously to, the transition agenda for the construction industry [30], several private and public parties in the Netherlands have signed an agreement in July 2018 to make the concrete supply chain more sustainable. This agreement is called (in Dutch) 'Het Betonakkoord' [31]. 'Het Betonakkoord' aims to achieve: (i) CO₂-emission reduction: a reduction of 30-49 percent by the end of this decade, compared to 1990 (ii) circularity: focus on circular design and high-quality application of recycled- or reused building materials or components; 100 percent of the concrete waste residue should be recycled in such a way that it is suitable for new concrete from 2030 onwards (iii) natural capital: the concrete supply chain aims to have a net positive value of natural capital, across the entire chain, by 2030 (iv) innovation, knowledge and education: stimulate innovation and participate in knowledge development and dissemination throughout the sector and seek connection with educational institutes.

The scope of 'het Betonakkoord' concerns all concrete applications, both structural and non-structural, and within the construction of buildings and civil engineering works (in Dutch: 'Burgerlijke en Utiliteitsbouw alsmede de Grond-, Weg- en Waterbouw').

1.2. Problem Statement

In the Netherlands there is a continuously increasing housing shortage. In 2019, the registered housing shortage is 300.000 units. The prognosis is that by the year of 2025, the housing shortage is increased to approximately 400.000 units [32]. Due to this increasing shortage, combined with the economic growth of the past few years, the house prices have skyrocketed. The price index of existing houses has increased with 83.9%, compared to 2015 [33]. The increasing prices and scarcity make it more difficult to buy a house, especially for starters.

Another upcoming development is the transformation from existing buildings into housing. In 2019, approximately 12.500 housing units have been created in this way. Almost half originate from vacant office buildings [34]. Figure 1.2a presents the newly created houses, through transformation, as a percentage of the total additions to the housing stock of all municipalities in the Netherlands. The absolute numbers of the top ten municipalities are presented in Figure 1.2b.

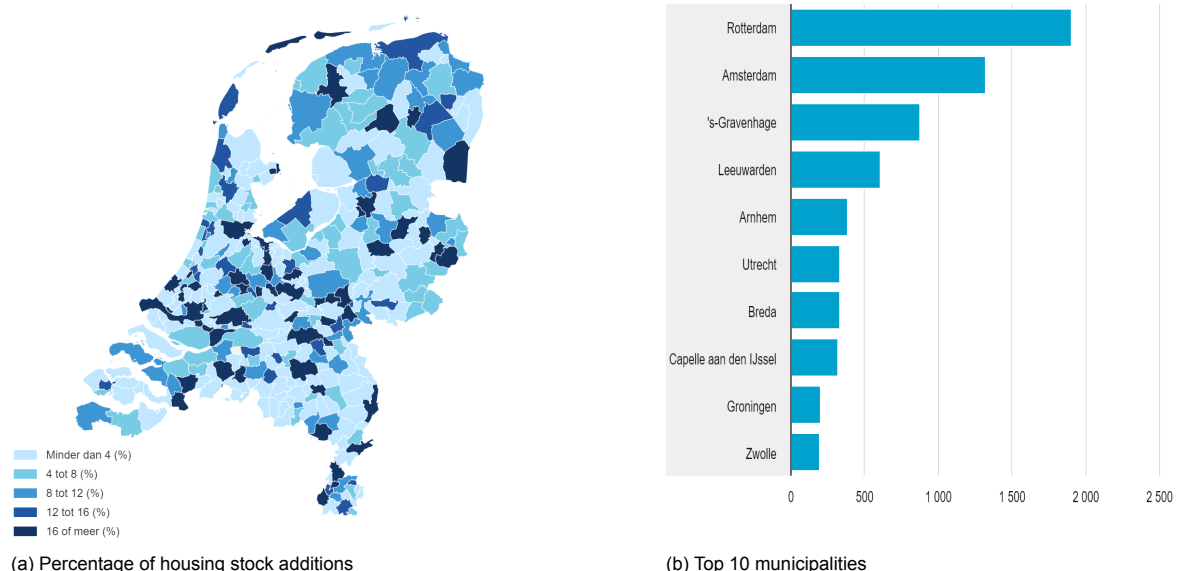


Figure 1.2: Additions to the housing stock through transformation in 2019 [34]

Due to the COVID-19 pandemic, working from home has become the new standard for most nonessential jobs in 2020 and 2021. Although the opinions are divided regarding working from home, it is likely that a hybrid form of remote work will stay. Due to this hybrid form of remote work, companies expect to require less office space [35, 36]. This will eventually lead to more vacancy in commercial real estate.

The transformation from existing buildings to houses can be a valuable part of the solution for the continuously increasing housing shortage. However, due to the very high demand the coming years, it cannot solve the problem on its own. Perhaps the most effective solution would simply be to build new houses. However, one should note that this is easier said than done. Many parties, public and private, are involved in approving and developing new construction projects. These projects usually take eight to ten years from head to tail. Meanwhile, many people need a house right now. Peter Boelhouwer, professor Housing Systems at the Delft University of Technology, states that it will not be enough to keep up with the demand, without a temporary and flexible layer around the existing housing system [37]. Therefore, a solution can be found in constructing temporary houses. Houses that can be: **(i)** built rapidly using prefabricated elements **(ii)** have a service life of a few years **(iii)** can be deconstructed afterwards and **(iv)** rebuilt at a different location.

Whether the previously mentioned points **(ii)** and **(iv)** are applied the coming years is subject of debate between the public and private parties and is, therefore, out of scope for this research. As stated in 'Het Betonakkoord' [31], one of the main pillars is to focus on circular design from 2030 onwards. Points **(i)** and **(iii)** comply with this focus. Therefore, the question arises: *How can sustainable buildings be designed, taken into account circularity and demountability?* This question is quite comprehensive. In chapter 2 the research scope, research aim and objectives and the research questions are explained.

1.3. Problem Definition

Literature review shows a wide interest of implementing circular principles in the economy. Specifically for the building industry, Durmisevic [38] argues that the aim of sustainable buildings should be on designing transformable buildings, made of components, assembled in a systematic order, so that it becomes suitable for maintenance and replacement of individual parts. The purpose of this section is to introduce one specific topic in line with this field of research.

In 2015, a conference paper [39] was published that examined the applicability of prefabricated elements in a modular load-bearing floor slab. The purpose of the conference paper was exclusively to present the potential technical solution and discuss its feasibility. The adopted design consists of calcium silicate blocks, assembled bondless with unbonded post-tensioning tendons. A simple numerical model has been used to gain information about the practicability, size and span of the slab. Next, the slab was subjected to a bending test. The aim of the bending test is to determine the deformation behaviour under loading. The slab was subjected to a quasi-surface load, introduced via a whippetree system. The experimental test set-up is depicted in figure 1.3. The slab was equipped with inductive displacement transducers (IDT) to determine the deflection. Shape and sizes of the calcium silicate blocks and the geometry of the slab are presented in figure 1.4. The blocks are placed in half-shift arrangement. Rows one, three, five and seven include two complete blocks, where as rows two, four, six and eight consist of one complete and two half blocks. The structural parameters provided are provided in table 1.2

More detailed description of the analysis can be retrieved from the paper. Experimental results demonstrate an ultimate limit surface load of 25 kPa, which is equivalent to 25 kN/m², in addition to the self-weight. Hereby, Ortlepp et al. [39] conclude that the feasibility is demonstrated. However, the load bearing capacity is not sufficient yet to compete against commonly applied concrete slabs. For a substantial progress in that case, further developments into the block material are essential.

Parameters blocks		Parameters tendons	
Strength	26 MPa	Strength	950 MPa
Density	1800 kg/m ³	Diameter	26.5 mm
Size	0.5 x 0.5 x 0.24 m	Yield load	525 kN

Table 1.2: Structural parameters of Ortlepp et al. [39]

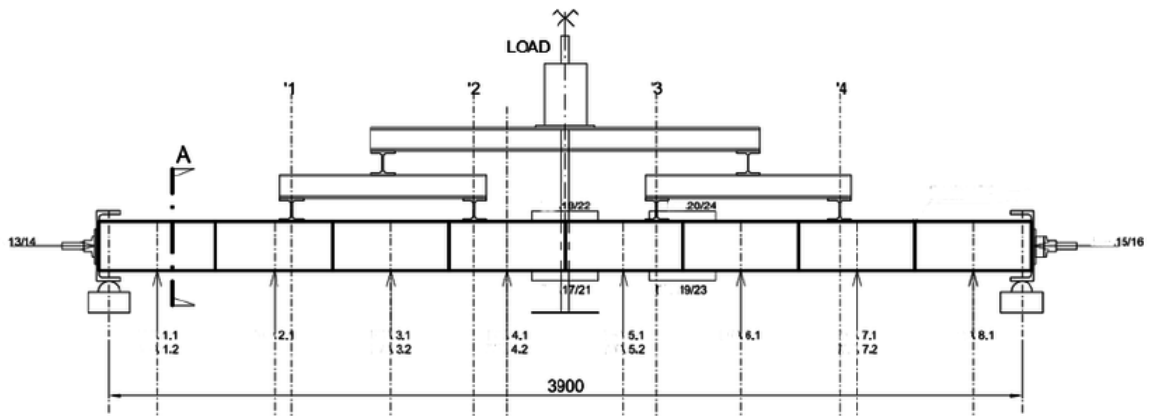


Figure 1.3: Experimental test set-up of Ortlepp et al. [39]

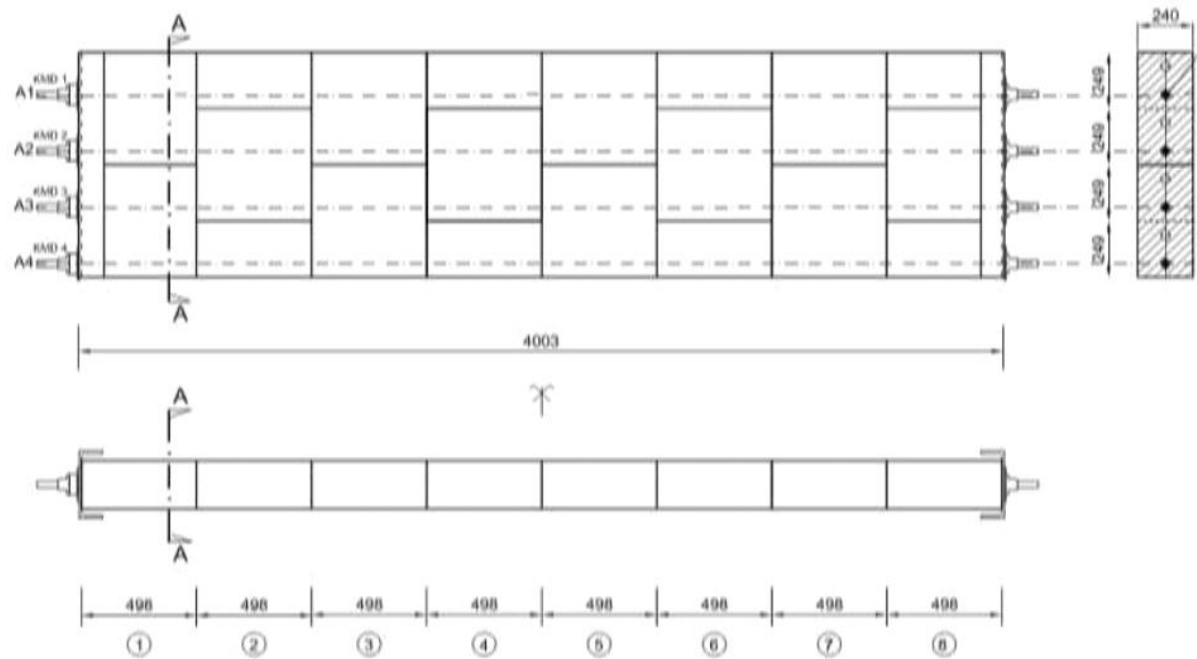


Figure 1.4: Shape, sizes and geometry of the concrete blocks and slab [39]

2

Research plan

In this second chapter the research plan is worked out in more detail. Following up from the problem statement and problem definition, the research scope is addressed in section 2.1. The research aim and objectives are presented in section 2.2 and this chapter is finalized with elaborating the research questions in section 2.3.

2.1. Research Scope

From the foregoing, it has become evident that the transition towards a circular economy is accelerating. Numerous programs, guidelines and legislation have been presented to streamline this transition. The construction industry has a significant environmental burden and is considered to have great potential for moving towards a circular economy.

Following up on the problem statement, the main sector of interest is the building industry. With respect to the increasing housing shortage in the Netherlands and implementation of the circular economy concept, the question arises: how can sustainable buildings be designed in the context of a circular economy? Not specifically designed for, but applicable in temporary houses. Both structural and non-structural aspects can be considered in order to formulate an answer to this question. In order to stay within a reasonable time schedule and taking into account the personal interest of the author of this thesis, it was chosen to mainly focus on structural aspects. To be more precise, inspired by Ortlepp et al. [39], this thesis zooms in on one structural component: a load bearing floor system.

2.2. Research Aim and Objectives

The aim of this research is to design and optimize prefabricated concrete modules, applicable in a modular floor system for the building industry. With an initial focus on ground-based housing units and low-rise apartment buildings.

The research objectives to achieve the research aim are:

- Identify the state-of-the-art frameworks and principles for a circular economy
- Investigate to what extent circular principles are already applied in buildings
- Investigate which floor systems are commonly used in practice
- Investigate and discuss the possibilities for integration of building services and other stakeholder prerequisites
- Determine structural parameters and calculation models for verification of modular floor systems

2.3. Research Questions

In order to achieve the research aim, a central research question, supported by several research sub-questions, have been formulated. The research sub-questions are in favor of answering the central research question. The research sub-questions are formulated in such a way that the answers comply with the objectives. The answer on the central research question presents an value judgement for the research aim.

Central research question

To what extent can a modular floor system, consisting of prefabricated concrete elements, be designed to meet the structural, circular and stakeholder requirements for application in residential buildings?

Research sub-question

- i What are the state-of-the-art frameworks and principles for a circular economy?
 - (a) How can circular principles be implemented in the design phase for the built environment?
 - (b) What criteria can be distinguished in order to evaluate the design?
 - (c) Are there any barriers or limitations to implementing circular design criteria?
- ii How and to what extent are circular principles recently applied in building projects?
- iii Which concrete floor systems are currently widely used in the built environment, both for residential and utility buildings and why?
- iv What are other requirements for a floor system, apart from circular principles?
 - (a) Which structural aspects are of importance and how can the load-bearing capacity be ensured?
 - (b) Does the Dutch Building Decree set certain requirements?
 - (c) What are stakeholder prerequisites for a floor system?
- v How does the newly proposed floor system compare to the current market offer?



Theoretical Framework

3

Design for a Circular Economy

This chapter contains a literature review on implementing design principles in the context of a circular economy. A brief introduction to general CE principles and frameworks, which are applicable throughout the economy, is presented in section 3.1. Specifically for the built environment, a CE framework is provided in section 3.2. The CE framework for the built environment consists of five main pillars or strategies in the design phase. These five strategies are elaborated in sections 3.2.1 to 3.2.5. To summarise the framework and underlying criteria for each design principle, an overview is visualised in figure 3.4. Conclusions on the developed design framework are presented in section 3.3.

3.1. General CE Framework

The relevance of the circular economy is, as mentioned earlier, gaining recognition among researchers and practitioners in industry, society and academia [40]. The circular economy concept on material conservation is already successfully applied to a number of products, from electronic goods to clothing, but to a lesser extent for buildings and building components [41].

One of the well-known frameworks towards circular design is the Cradle-to-Cradle (C2C) concept, developed by McDonough and Braungart [42]. The first focus of the C2C concept is that it considers all materials involved in industrial processes as nutrients for a process they called: technical metabolism. Similar as in nature, where waste does not exist and one organism's waste is food for another. The second focus of the C2C concept is the use of solar energy as a sustainable energy source. The third focus of the C2C concept is to celebrate diversity. One of the key principles of the circular economy is that most recycling is considered as a form of downcycling, since the material quality reduces over time. Therefore, it is suggested to fundamentally rethink production, distribution and consumption processes prior to pursuing recycling [7, 43].

The Chinese government, among the front-runners regarding implementation of the circular economy concept, started to show increasingly interest by adopting explicit policies in 2002 and 2009. Initially, the Chinese literature framed the concept around the three R principle: Reduce, Reuse and Recycle (3R). Wherein, reducing refers to the action of minimizing inputs and outputs such as raw materials and waste. Reusing is the operation of using a product again for the same purpose when it reaches its end-of-life. Recycling is the process of recovering waste to manufacture a new product [44].

In 1979, Lansink [45] developed a hierarchy for waste management. Nowadays, the 'ladder van Lansink' forms the basis of all developed R-strategies [46]. The core of the European Union Waste Framework [47] is based on an expansion of the 3R-framework by introducing a fourth R: Recover. Sihvonen and Ritola [48] expanded the 4R-framework into a 6R-framework and Potting et al. [46] proposed a 9R-framework. All R-strategies resemble each other and differ mainly in the number of circularity strategies they put forward [46]. Therefore, it can be concluded that the 9R-framework is the most nuanced one for the transition towards a circular economy. The 9R-framework is depicted in figure 3.1.

Figure 3.1 presents a range of strategies ordered from high circularity (low R number) to low circularity (high R number). Three overarching strategies within the framework can be observed: **(i)**: smarter product use and manufacture (R0-R2), **(ii)**: extension of the product lifespan (R3-R7) and **(iii)**: useful application of materials (R8-R9). These three overarching strategies are listed in order of priority. Thus, smarter product use and manufacture are preferred over the product lifespan extension strategies. Interesting to note that, contradictory to the C2C concept, material recycling and energy recovery have the lowest priority in this framework.

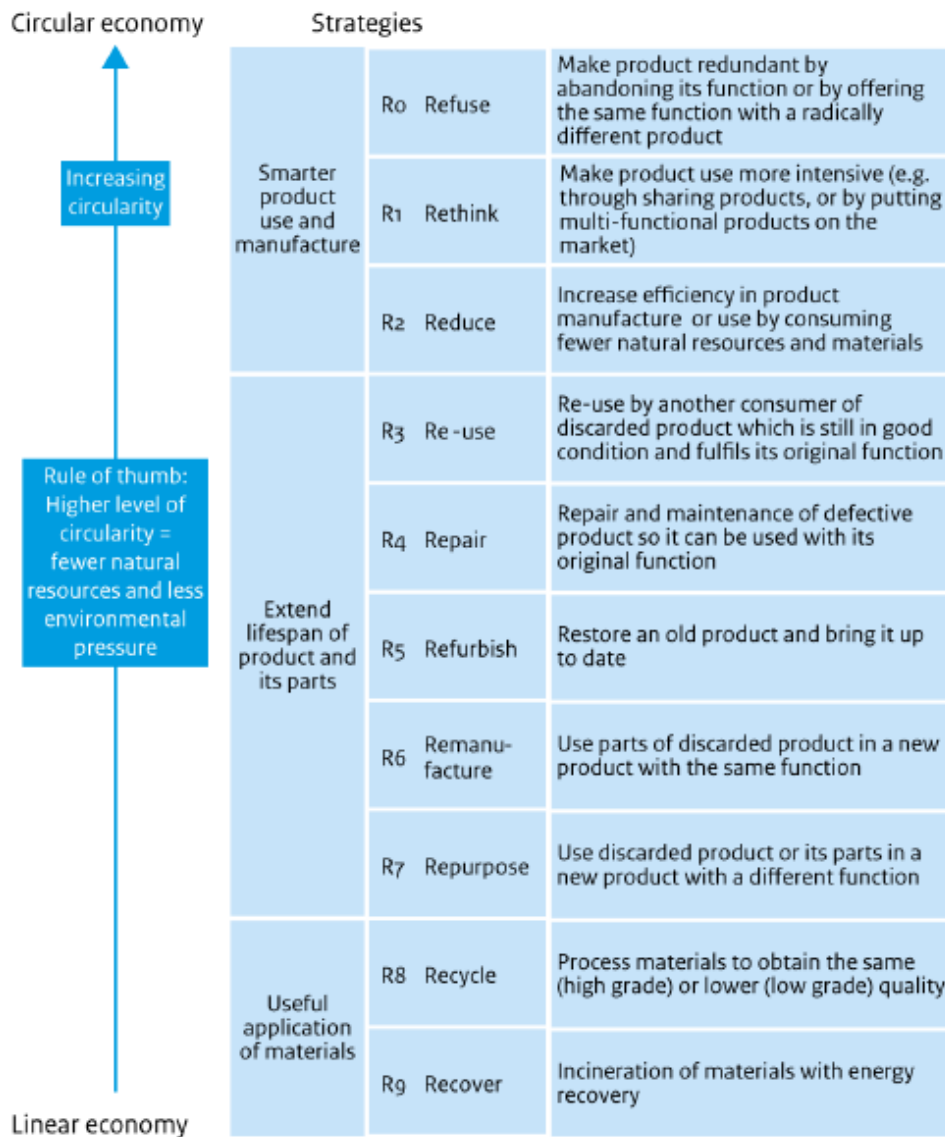


Figure 3.1: The 9R Framework of Potting et al. [46]

3.2. CE Framework for the Built Environment

Campbell [49] argues that, while there is significant information about how concepts are brought together within a circular economy overall, there is less information related to how this concept is fitted to the building industry. Two notable exceptions are the publications of Arup [50] and Cheshire [51].

The Ellen MacArthur Foundation [8] outlined three key principles on which the circular economy rests: **(i)**: Preserve and enhance natural capital by controlling finite stocks and balancing renewable resource flow, **(ii)**: optimize resource yields by sharing or looping products, components and materials in order to extend lifetimes and **(iii)**: foster system effectiveness by revealing and designing out negative external-

ities. Moreover, Ellen MacArthur Foundation [8] proposed the ReSOLVE framework for implementing circular principles into the economy. The ReSOLVE framework outlines six actions to guide the transition towards a circular economy: **(i): Regenerate (ii): Share (iii): Optimise (iv): Loop (v): Virtualise and (vi): Exchange**. Arup [50] adopted the ReSOLVE framework and intended to raise awareness of the circular approach and to identify the main challenges, enablers and opportunities in making a circular economy reality, specifically for the built environment. Through numerous examples mentioned in their report, the authors concluded that a collaborative, all-encompassing framework is still missing. The authors suggest that, in order to develop and benefit from the circular economy, the following steps should be taken:

- Analysis of new business models and services
- Consultation with clients to implement new business models
- Circular economy framework with respect to design principles
- Investigate the challenges of finance and contractual agreements

This thesis focuses mainly on the technical aspects of circular design. The investigation of business models and contractual agreements are just as important. However, in order to remain within the scope of this research, only the circular economy framework with respect to design principles will be further elaborated.

Applying the three key circular economy principles from the Ellen MacArthur Foundation [8], inspired Cheshire [51] to develop a framework for the built environment. In his book, Cheshire extensively focuses on design principles. The framework can be summarized in nested circles. The nested circles are presented in figure 3.2. The nested circles show the hierarchy of the framework, with the three inner circles as the most desirable ones. Retaining is the least invasive and, therefore, considered as the most resource-efficient. Next to retaining, refitting and refurbishment are considered as more demanding interventions. For the fourth and fifth circle, the priority is to reuse or re-manufacture. The sixth and last circle is to recycle components into materials that are applicable in new products. The outer ring in the diagram represents the underlying models that can be applied to enable a more circular economy across the buildings sector.

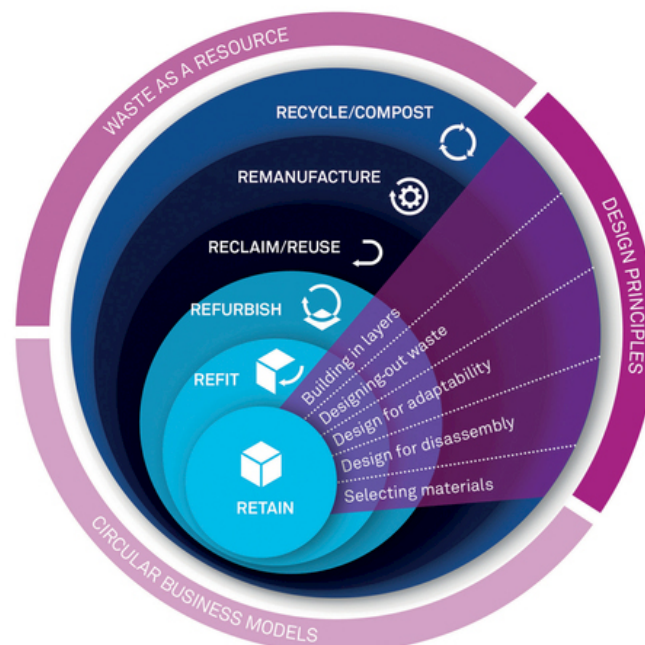


Figure 3.2: Applying circular economy principles to building design [51]

The five segments superimposed on the nested circles show the design principles that can be applied. Application of circular design principles is considered most important at the design stage of buildings,

due to the fact that at this stage, decisions on materials, connections and specifications of components are made [52]. These decisions can be used to ensure that waste and building components are managed properly. The five segments of figure 3.2 are: **(i)**: building in layers, **(ii)**: designing out waste, **(iii)**: design for adaptability, **(iv)**: design for disassembly and **(v)**: selecting appropriate materials. In the following sections, the five segments are further elaborated.

3.2.1. Theory of Layers

Considering buildings as one whole, singular object is still a common misconception in the construction industry. Buildings are no longer conceived, designed, constructed and used as complete entities. Only few buildings remain in their initial state for, at most, a couple of decades. Environmental conditions, technological advancement and changing user demands alter buildings over their lifespan, as illustrated in section 1.2. It can be argued that there is, in fact, not one singular building at all, but a series of different buildings over time [53].

The first writing about dissecting the buildings into layers originate from the Japanese Metabolism architects and John Habraken in the 1960's. In later writing, Habraken [54] discusses 'the traditions of two stage building' in which buildings are constructed first as a primary structural frame which typically supports the roof, then a secondary system of construction which defines the internal spaces [53]. Following up on Habraken, Duffy and Henney [55] expand the two layer theory into four layers. Moreover, Duffy and Henny assign a service life to each of the layers. The expected service life is based on experience of: **(i)**: changing user demands and **(ii)**: the necessity to upgrade or expand the plant and equipment [53]. The four layers and their service life are presented in table 3.1

Layer	Description	Service Life
Shell	Foundation and load-bearing elements	50 years
Services	Technical installations like: heating, ventilation and data	10-15 years
Scenery	Internal partitioning system, finishes and furniture	5-7 years
Sets	Movable items of users	Days or weeks

Table 3.1: Layers of Duffy and Henny [55]

The concept of dissecting buildings into layers is key to expose that some parts in buildings, with a shorter lifespan, can be separated from other parts of the building with a longer lifespan. Duffy and Henney limited their model to the internal parts and the shell of buildings, or the so-called 'hard' layers. Brand [56] expanded this model by: **(i)**: splitting up the shell layer into structure and skin, **(ii)**: adding a sixth dimensional layer (site) and **(iii)**: extending the service lives. The six layers of Brand are presented in table 3.2.

Layer	Description	Service Life
Site	Geographical setting on which the building stands	Eternal
Skin	Cladding and roofing systems that exclude the natural elements from the interior	20 years
Structure	Foundation and load-bearing elements	30-300 years
Services	Technical installations like: heating, ventilation and data	7-15 years
Space plan	Internal partitioning system, finishes and furniture	3-30 years
Stuff	Movable items of users and furniture	Days or weeks

Table 3.2: Layers of Brand [56]

Recently conducted research by Schmidt III and Austin [57] extended Brand's model, by including three 'soft' layers: social, space and surroundings. Moreover, they indicated the interaction between different layers. These interactions or interdependencies are important to assess further adaptations in buildings. Figure 3.3 shows the interactions between the different layers. The severity of the interaction between

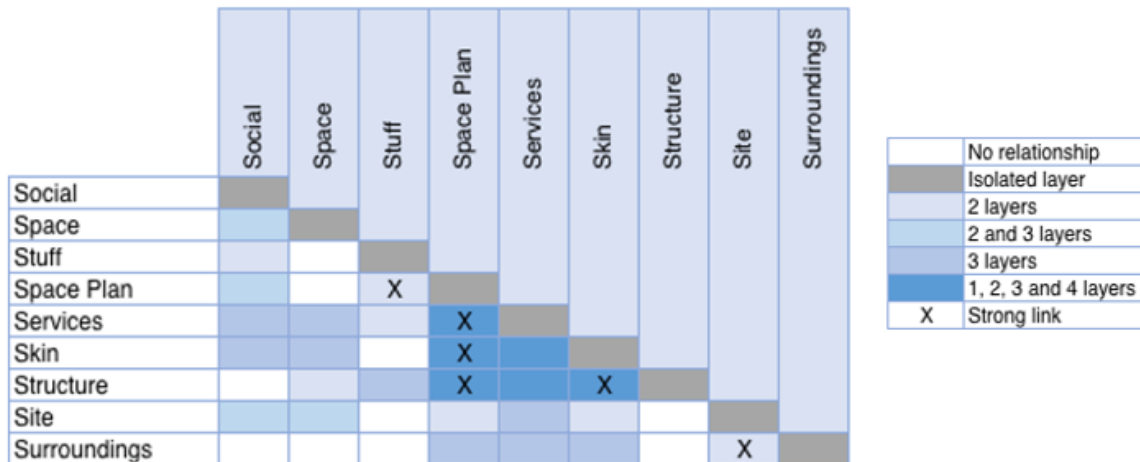


Figure 3.3: Interaction between building layers [57]

different layers is illustrated with colours. So-called 'strong links' are emphasized as well. From figure 3.3 can be concluded that the structure has significant influence on the space plan and the skin of a building. This is quite straightforward, since the foundation and load bearing elements form the backbone of a building and, therefore, changing the structural system severely impacts the space plan and skin of a building. For this reason it is feasible to design for a longer lifespan of the structural system than for a space plan or skin, just from an economic perspective.

In the context of this thesis, it is of interest to consider the interaction of the structural system and services as well. As can be seen in figure 3.3, the structural system has a considerable influence on the services of a building. Modern load bearing floor systems provide integration possibilities of building services within the structural system. One brief example is concrete core activation of reinforced plank floors (in Dutch: 'breedplaatvloeren'). Some floor systems, such as a Slimline floor, are designed for integrating building services. This section does not further elaborate the different floor systems. For now, it is evident that the structural system and services have considerable interaction.

The building layers and the components that make up each layer, can be seen as a hierarchy of materials, which represents the way in which materials and components are arranged in buildings. Durmisevic [38] argues that dissectable structures should be seen as a hierarchy of sub-assemblies. The sub-assemblies exist at different levels of technical composition of a building. Such specification of buildings is based on a top-down approach. A system at one level is a component (or sub-system) at another level. Defining buildings in such a way, hierarchical levels of building composition or decomposition can be defined. The highest level in this hierarchy is the building level, which represents the arrangement of systems, which are carriers of main building functions (load bearing construction, enclosure, partitioning and servicing). The second level is the system level and represents the arrangement of components, which are carriers of the system functions (bearing, finishing, insulation, reflection etc) - the sub-functions of the building. The third level is the component level and represents the arrangement of elements and materials, which are carriers of component functions, being sub-functions of the system.

3.2.2. Designing out Waste

The construction sector is responsible for a large part of the raw material consumption, as mentioned in section 1.1.3. Together with the increasing global population, the consumption needs will increase over the coming decades. In 2012, the construction industry produced more than three times the amount of waste than all households combined in the Netherlands [58]. Although many of the construction and demolition waste is recycled, often as road base material or landfill, recycling should not be the favorable option for high quality building materials.

By changing the way that buildings are designed, the amount of waste generated on construction sites

can be reduced considerably. The design decisions made at the start of a project will have a profound influence on the amount of waste generated [51, 52]. Most of the waste management studies in the construction sector focus on the actual construction stage itself. This mainly results into guidelines for achieving one of the R-strategies. By implementing waste management efforts in the design phase and in the whole design process, up to a third of construction waste can be prevented [59].

Ajayi and Oyedele [59] applied structural equation modeling, which is a multivariate statistical technique used for analyzing the relationship between variables, in order to identify factors that promote waste-efficient design. Out of the 39 identified measures, four key factors are distilled: **(i)**: standardisation and dimensional coordination, **(ii)**: collaborative design process, **(iii)**: design for modern methods of construction and **(iv)**: waste-efficient design documentation. These four factors mentioned are explained in more detail.

Standardisation and dimensional coordination is the first key factor. Standardizing and coordination of dimensions has several advantages. One of them is the improved buildability and constructability. A second advantage is the minimization of off-cuts, not only in structural elements, but also in individual elements, such as windows and door openings. However, these individual elements should be dimensioned according to available market sizes. Another benefit of standardisation and dimensional coordination is the possibility to reuse the elements or components after their allocated service life [59].

Collaborative design process is the second key factor. Improving the communication and early collaboration between architects, engineers and contractors could prevent waste generation [59, 60]. One important prerequisite is adequate information sharing between the stakeholders. One of the potential solutions is Building Information Modeling (BIM). In short, a BIM model is a digital representation of physical and functional characteristics of a construction project, which is commonly used in the architecture, engineering and construction industry. Since BIM models contain a wealth of information, for example: material resources and geometry, construction and demolition (C&D) waste, throughout the life cycle of buildings, can be reduced in two ways: **(i)**: issues due to design changes can be avoided by improved coordination among the project stakeholders and **(ii)**: Better construction planning and management can lead to avoidance of rework, unnecessary material handling and efficient usage of raw materials based on accurate measurement for material ordering, layout and cutting [60]. However, Rahla et al. [44] argue that the use of BIM for the management of the end-of-life of buildings is still in its early stage and requires more commitment from the construction industry.

Designing for modern methods of construction, the third mentioned key factor, refers to the situation in which various components of buildings are manufactured in a factory-controlled environment and transported to the building site, where the components can be assembled. The construction process is, in this way, primarily focused on the assembly of components rather than on traditional construction techniques, in order to effectively reduce the waste generated on site. It is highlighted that modular construction is an important driver for modern construction methods and thus for designing out waste [51, 59].

Completeness and the level of accuracy of design documents is important for reducing waste generated by construction activities. Ajayi and Oyedele [59] refer to this as waste-efficient design documentation and represents the fourth and final key factor. Proper documentation is characterised by: **(i)**: adequate detailing in order to minimize execution errors during construction **(ii)**: conventional language which is easily understood by all stakeholders involved and **(iii)**: incorporation of all features that are site specific [59]. However, proper design documentation should not be limited to the construction phase of buildings only. Numerous authors [51, 59, 61, 62] stress out the importance of a deconstruction plan for the end of the allocated service life of buildings. Especially considering that the majority of the demolition waste is processed as road base material or landfill, as mentioned earlier in this section. Design for deconstruction is considered as one of the five principles for applying the circular economy concept in building design [51]. This principle will be further elaborated in section 3.2.4. Regarding designing out waste, the availability of a deconstruction plan would open up the possibilities for recovering and/or reusing of building components and, thereby, reduce the waste generated by the industry. In other words, the waste efficiency is determined by the degree of implementation of a deconstruction plan in the design phase.

3.2.3. Design for Adaptability

Cheshire [51] and Crowther [53] argue that it is rare for buildings to remain in its original layout during its functional lifespan. Especially in the case of commercial real estate, such as office buildings, technological changes or different occupants bring new demands to the space and, therefore, require the building to adapt to the governing circumstances. If a building has insufficient adaptive capacity, obsolescence can occur, leading to unnecessary renovations or demolitions. In a broad sense, adaptability means the ability to be changed or modified to make suitable for a particular purpose [63]. Within literature, little agreement on the terminology of adaptability is present. The same situation occurs in the build environment [57]. The comprehensive study of Munaro et al. [64] outlines the different expressions related to the adaptability of buildings. The most common terms used in literature, with overlap to design for adaptability, are: adaptive reuse, deployable design, design for flexibility, design for durability and design for change. Munaro et al. [64] conclude that, while some authors use these terms as synonyms, other distinguish in conflicting ways, linking flexibility as a characteristic of adaptability and vice versa.

The intention of this section is not to elaborate on the different terminology, nor on the interchangeable use of terms. The point is to provide a simple and comprehensive definition of the principle - design for adaptability - and its main components or enablers. The definition of adaptability for buildings is retrieved from Ross et al. [65]: the ease in which buildings can be physically modified, deconstructed, refurbished, reconfigured, re-purposed and/or expanded. A similar definition is found from Schmidt III and Austin [57]. Taking adaptability into account in the design phase is referred to as design for adaptability. The goal of designing adaptable buildings is to minimise obsolescence in order to extend its functional lifespan. The separation of building layers and the consideration of interaction between building layers, as described in section 3.2.1, is an important instrument to extend the lifespan of buildings and, implicitly, determining its adaptability.

Rockow [66] recommends seven strategies to owners, architecture design firms and builders who wish to implement adaptability of buildings in the design phase. The seven strategies are: **(i)**: reserve capacity, **(ii)**: quality materials, **(iii)**: floor-plan openness, **(iv)**: floor-to-floor heights, **(v)**: simplicity in building design, **(vi)**: separated layers and **(vii)**: accurate plans. These seven strategies are briefly explained.

Functional changes of buildings result in changes of the required design loads. The Eurocode includes different categories with corresponding design loads for buildings. One common example is the transformation of office buildings into residential units. Structural components designed with reserve capacity often have a higher end-of-life salvage value. Integration of reserve capacity is most effective in building components with a low replacement frequency, such as structural components and foundations [65].

Material selection can influence the adaptability of buildings in several ways. Ross et al. [65] refers to this as selecting appropriate materials, while Rockow [66] speaks of quality materials. The commonality in the message is related to the durability of the material. Durability is considered crucial for components that are intended to last throughout their current functional life span and beyond.

Openness of the floor plan is the third strategy mentioned. Large open floor plans, without structural or mechanical obstructions, offers users the freedom to arrange the space to suit their needs. Ross et al. [65] argue that, by keeping large portions of the building free of components in the structural and service layers, components in the space plan layer can be more easily reconfigured to suit changing functional requirements.

Sufficient floor-to-floor heights in buildings provide flexibility regarding the installation of services. The height of spaces should be large enough to accommodate changing service requirements [51, 66]. Especially regarding heating, ventilation and air conditioning (HVAC) systems, where the changing requirements have been accelerated by introduction of nearly zero energy (NZE) buildings. However, from a financial point of view, it is desirable to keep the floor-to-floor height to a minimum, especially in multi-story buildings, because: **(i)**: facade elements are the most expensive component of a building and **(ii)**: it may be possible to realise extra stories and, therefore, increasing the usable floor space. The Dutch Building Decree [67] sets (minimum) requirements for floor-to-floor heights for buildings

with specific functions. This generates a field of tension between the two perspectives. In conclusion, designers should carefully consider both perspectives in the design phase.

Designing for simplicity in buildings, for example: repeating layouts and larger but fewer structural components, reduce the uncertainty for designers working on adaptation [68]. Ross et al. [65] argue that repeating layouts can result in more straightforward load paths, which can help future modification or replacement of components. Furthermore, larger components reduce the amount of connections and increase the likelihood of recovery. The strategy to design for simplicity in buildings is, therefore, not only related to the adaptability, but also to the deconstructability of buildings. As with many strategies proposed in literature, the overlap with other design principles is evident. Rockow [66] outlines that the simplicity of the building design is characterized by having repetitive and standardised components throughout the building, which can be considered as a strategy on its own [65, 69].

Layering of building components is the sixth strategy mentioned by Rockow [66], but is commonly reported in literature as a design-based enabler [65]. Dissecting a building into different layers has the advantage that each component or system of a building is separated and allows for maintenance or modification. Regarding the adaptability, the less the interaction between layers, the better the adaptability of each layer and thus the entire building. The dissection of layers does not only affect the adaptability of a building, it affects the deconstructability of buildings as well. Therefore, in line with Cheshire [51], it is reasoned that the layering of building components is more than just a strategy under adaptability and should be considered a design principle in itself.

Availability of accurate information about existing buildings, such as: as-built plans, models or maintenance documentation is the last strategy proposed by Rockow [66]. Appropriate documentation can assist designers in making decisions for adaptation and minimizes risk and uncertainty. One powerful tool for sharing and organizing information is BIM [65]. The availability of proper documentation can also help reduce waste generated throughout the entire life span of buildings, as described in section 3.2.2. As with many strategies, the overlap with various design principles is evident.

To conclude this section about strategies with respect to designing for adaptability, two last strategies are adopted from Iperen [70]. These two strategies encourage the reconfigurability and scalability of structural components. Reconfigurability relates to the possibility of building components to rearrange elements in relation to each other [70]. When structural components are designed with reconfigurability in mind, the components are more versatile and flexible in use, thus increasing the adaptability of structural components. Scalability relates to the capacity of building components to change in size or capacity [70]. Using structural elements in components that can be applied in a certain bandwidth, for example span lengths, generates freedom in design and therefore improves the adaptability of structural components.

3.2.4. Design for Disassembly

Design for disassembly, or design for deconstruction (DfD), is a term that is generally used to describe the strategy of designing products in such a way that components can be easily dismantled after their allocated lifespan. In relation to the building industry, this means that buildings should be designed so that its components can be easily dismantled after their (initial) life cycle. With respect to the definition of the circular economy [7] and the hierarchical levels of building composition of Durmisevic [38], entire buildings or (structural) components of buildings should either be completely reused or recycled, in which reuse is the most favorable option. Important to note is that the terms deconstruction and disassembly are often used interchangeably throughout literature. This thesis does not distinguish between both terms either.

There is a vast amount of research on designing buildings for deconstruction. Many researchers have set out guidelines to follow. One of the first and more elaborated models for DfD was developed by Crowther [71]. Review of architectural history (and related industries) resulted in two relevant types of knowledge with respect to designing for deconstruction. Firstly, there are broad themes that address the issues of why, what, where, and when to disassemble, and secondly there are specific design principles of how to design for disassembly. Three broad themes that significantly impact on the decision making process of designing a building for future disassembly are: **(i)**: a holistic model of environmentally sustainable construction, **(ii)**: awareness of building layers and corresponding service lives and **(iii)**:

a recycling hierarchy that recognises different benefits of different end-of-life scenarios [71]. The first and third point mentioned will be further explained in the following paragraphs. The second point has already been discussed in section 3.2.1.

Regarding the first point mentioned, a holistic model of environmentally sustainable construction, Crowther [71] argues that the consequences should be understood within a wider picture of the global environment. Designing for reuse has the obvious benefit of material conservation. However, potential environmental costs, such as greater initial energy consumption and possible use of (more) toxic materials to improve durability, could be present. Although it is reasonable to expect that these costs will have a smaller impact, they should be considered [71]. One commonly known concept is a life cycle assessment (LCA). LCA of a product identifies all inputs (materials or energy) and outputs (waste or polluting emissions) during the entire life cycle in order to quantify its environmental performance. Usually, LCA models plot the environmental impacts against the stages of life. However, this does not offer strategies for dealing with unwanted impacts, for example resource depletion. One solution to this issue has been proposed by Kibert [72]: the addition of a third axis of: 'principles for environmental responsibility' to the two-dimensions of LCA. The model proposed by Kibert [72] makes designers aware of possible conflicts that could occur between alternative principles of DfD. The main purpose of the model is to assist designers of why and when designing for deconstruction.

Hierarchies of recycling refer to different production models. The currently prevailing model in the construction industry is linear, characterized by the take-make-consume-dispose pattern. A more detailed discussion is provided in section 1.1. As has been stated repeatedly, a (more) cyclical or circular model makes recycling or reusing of components feasible. With designing for disassembly recycling or reusing can occur in different ways. Crowther [71] points out four possible end-of-life scenarios: **(i)**: relocation of entire buildings, **(ii)**: component reuse in a new building, **(iii)**: material reuse in the manufacture of new building components and **(iv)**: recycling materials (down-cycling) into new building materials. These four end-of-life scenarios are very similar to the R-strategies proposed by many authors in literature and within the context of Cheshire [51] as well. The main purpose of Crowther [71] with the understanding of a hierarchy of recycling is to offer guidance to designers about what to disassemble for any given end-of-life scenario. However, it should be noted that it might not always be preferable to design for deconstruction. For certain projects, other environmental aspects may outweigh the benefit of designing for deconstruction [71].

Although the three broad themes set valuable criteria to help designers with designing for deconstruction, the specific question of how to design for deconstruction, has not been answered yet. For that, a number of strategies are required. Crowther [71] formulates 27 design strategies for answering the how-question and rates each strategy against the four end-of-life scenarios with: 'highly relevant', 'relevant' or 'not normally relevant'. This list is presented in table 3.3.

Crowther [71] primarily addresses the technical aspects related to DfD. However, recent research by Akinade et al. [61] shows that non-technical aspects also play a key role in designing for deconstruction. Thorough literature review and conducting four focus group discussions, resulted in the identification of 43 DfD factors. After reliability analysis, the amount of factors was reduced to 38. The result of factor analysis revealed an underlying structure of five DfD groups: **(i)**: stringent legislation and policy, **(ii)**: deconstruction design process and competencies, **(iii)**: design for material recovery, **(iv)**: design for material reuse and **(v)**: design for building flexibility [61]. The 38 identified factors are assigned to these five groups. Each group has its normative weight in the overall analysis, indicating the relative importance of each group. Analogous to this, each factor has its weight within the group, indicating the relative importance within the group. The results are presented in table 3.4. The analysis shows that policy and legislation are the most significant success factors.

The findings of Akinade et al. [61] on the potential for policy and legislation were confirmed by previous research [50, 73]. Arup [50] argues that the built environment can benefit from improved policy and legislation by:

- Removing barriers by altering the definition of waste in order to facilitate reuse and minimise landfill, creating new markets for secondary materials and unlock new revenue streams
- Strengthening industry targets for waste and reuse, as well as incentives to promote extending

products lifespans and re-manufacturing

- Accelerating procurement that promotes a whole life-cycle approach
- Supporting organisations that seek to up-skill their workforce, innovation projects and incentives to create a more secure environment for investors

In line with these findings, Rios et al. [73] emphasize that a good partnership between public and private parties is crucial for the overall success of the implementation of DfD and thus of circular economy principles in general in the built environment. Arup [50] goes one step further by concluding that policy and legislation are a good driver to catalyse action, however, the development of a circular economy at scale should come from the industry itself.

3.2.5. Selecting Materials

Economic benefits of reuse are only realised when materials and components are recovered from the building. Buildings or components designed for a long functional lifespan, potentially decades, do not fit with the general interest of the industry in making (short-term) profits [74]. This indicates that successful implementation of CE in the construction industry should result from a balance of short-term profits and long-term sustainability objectives. The combination of these two interests could be a valuable solution. Eberhardt et al. [74] argue that reusing building components and modules may be more suitable for short- and medium-lived buildings, whereas social housing projects that have a frequent change in users over time, may be looking for other CE strategies, such as DfD, to facilitate easy adaptability and maintenance.

Buildings are complex products and, concluding from section 3.2.1, should not be considered as one singular entity. The shearing layers of Brand [56] illustrated the multitude of products with different functions, characteristics and varying rates of replacements, resulting in several possibilities for reuse and recycling over the lifespan of buildings. Eberhardt et al. [74] views buildings as a system of temporary storage and constant flow of resources that should be managed individually. This indicates that CE strategies should not limit the focus on entire buildings, but also on the differentiation between flow of material and component groups, in order to facilitate short-, medium- and long-term benefits throughout the lifespan of buildings [74].

Currently, less than 1% of the existing building stock is fully demountable and, although DfD is a promising tool for implementing CE in the built environment, it is not yet a mainstream concept [62]. As many previously built structures reach their end-of-life, they can become a valuable resource for new buildings. By following the hierarchy of the R-strategies, components that are not suitable for reuse or adaptation, should be designed with attention to their recyclability potential [41]. According to Cheshire [51], materials and component selection forms the bedrock of a circular economy. Therefore, materials should be selected based on: **(i)**: the lifespan of the considered element, **(ii)**: the distinction between technical or biological materials, **(iii)**: preservation of purity by avoiding mixing biological and technical substances and contamination by toxic substances, **(iv)**: application of reclaimed materials and **(v)**: disassembling of elements at the end-of-life with the ability to remanufacture or reclaim materials.

Minunno et al. [41] identified seven most common strategies from a review of literature on CE and how it is applied in practice. Three of these are relevant for the selection of materials, namely: **(i)**: integration of scrap, waste and by-products into new components, **(ii)**: design for recycling of construction materials and **(iii)**: systems to track materials and components within their supply chain. Regarding the integration of scrap, waste and by-products, the authors claim that many CE experts consider this as one of the leading strategies to close the waste-resource loop and, in most cases, to be more efficient than recycling [41]. One example is the search for a greener alternative to ordinary Portland cement (OPC). A recent development is the application of geopolymers binders in concrete. Geopolymer technology utilises many by-product materials, such as: fly-ash, granulated blast furnace slag or mining wastes. Geopolymer concrete (GPC) has shown the potential to be an appropriate alternative for conventional cement concrete [75]. One substantial benefit of GPC is that the production generates up to 90% less CO₂-emissions than conventional cement concrete [75]. However, due to differences in by-product quality, the same mixtures may have different mechanical and physical properties. Therefore, further research on underlying relationships between variables and a global acceptance of uniform

	Principle	Material recycling	Component remanufacture	Component reuse	Building relocation
1.	Use recycled and recyclable materials	●	●	•	•
2.	Minimize the number of different types of material	●	●	•	•
3.	Avoid toxic and hazardous materials	●	●	•	•
4.	Make inseparable sub-assemblies from the same material	●	●	•	•
5.	Avoid secondary finishes to materials	●	●	•	•
6.	Provide identification of material types	●	●	•	•
7.	Minimize the number of different types of components	●	●	•	•
8.	Use mechanical not chemical connections	•	•	●	●
9.	Use an open building system not a closed one	•	•	●	•
10.	Use modular design	•	•	●	•
11.	Design to use common tools and equipment, avoid specialist plant	•	•	●	●
12.	Separate the structure from the cladding for parallel disassembly	•	•	●	•
13.	Provide access to all parts and connection points	•	•	●	●
14.	Make components sized to suit the means of handling	•	•	●	●
15.	Provide a means of handling and locating	•	•	●	●
16.	Provide realistic tolerances for assembly and disassembly	•	•	●	●
17.	Use a minimum number of connectors	•	•	●	●
18.	Use a minimum number of different types of connectors	•	•	●	●
19.	Design joints and components to withstand repeated use	•	•	●	●
20.	Allow for parallel disassembly	●	●	●	•
21.	Provide identification of component type	●	●	●	•
22.	Use a standard structural grid for set outs	•	•	•	●
23.	Use prefabrication and mass production	•	•	●	●
24.	Use lightweight materials and components	●	●	●	●
25.	Identify points of disassembly	•	•	●	●
26.	Provide spare parts and on site storage for them and parts during disassembly	•	•	•	●
27.	Retain all information of the building components and materials	•	•	•	●

Legend of symbols: • Not normally relevant ● Relevant ● Highly relevant

Table 3.3: Strategies of DfD and their relevance to the hierarchic levels of recycling [71]

	Weight within group [%]	Norm. weight [%]
I. Stringent legislation and policy		39.15
1. Award of more points for building deconstructability in sustainable appraisal	26.86	
2. Government legislation to set target for material recovery and reuse	26.45	
3. Project contractual clauses that will favour building material recovery and reuse	22.31	
4. Legislation to make deconstruction plan compulsory at the planning permission stage	24.38	
II. Deconstruction design process and competencies		18.32
5. Improved education of professionals on design for building deconstruction	7.24	
6. Effective communication of disassembly needs to other project participants	8.01	
7. Effective pre-design disassembly review meetings	9.40	
8. Design conformance to codes and standards for deconstruction	10.02	
9. Early involvement of demolition and deconstruction professionals during design stage	9.09	
10. Production of a site waste management plan	12.79	
11. The use of BIM to estimate end-of-life property of materials	10.17	
12. Preparation of a deconstruction plan	12.17	
13. The use of BIM to simulate the process and sequence of building disassembly	14.48	
14. Production of COBie to retain information of the building components	6.63	
III. Design for material recovery		15.55
15. Use bolted joints instead of chemical joints such as gluing and nail joints	15.40	
16. Avoid composite materials during design specification	16.40	
17. Design foundations to be retractable from ground	14.00	
18. Specify building materials and components with long life span	13.40	
19. Specify lightweight materials and components	9.80	
20. Use joints and connectors that can withstand repeated use	9.40	
21. Minimise the number of components and connectors	8.60	
22. Minimise the types of components and connectors	13.00	
IV. Design for material reuse		14.01
23. Knowledge of end-of-life performances of building materials	32.62	
24. Avoid toxic and hazardous materials during design specification	13.19	
25. Making inseparable products from the same material	20.55	
26. Avoid specifying materials with secondary finishes	12.58	
27. Specify materials that can be reused or recycled	15.95	
28. Design for steel construction	14.11	
V. Design for building flexibility		12.97
29. Use open building system for flexible space management	12.44	
30. Using of interchangeable building components	12.28	
31. Design for modular construction	8.13	
32. Design for pre-assembled components	7.97	
33. Design for the repetition of similar building components	8.61	
34. Ensure dimensional coordination of building components	10.85	
35. Separate building structure from the cladding	11.48	
36. Standardising building form and layout	7.50	
37. Use standard structural grid	10.05	
38. Structure building components according to their lifespan	10.69	

Table 3.4: Groups and corresponding factors for DfD and corresponding weights [61]

guidelines for mixture designs for GPC is necessary [75, 76].

The second strategy is related to designing for recycling of construction materials. As stated before, most concrete waste is down-cycled as road base material, thereby reducing the quality of the second life product. However, for concrete mixtures, implementation of recycled content in the design of new elements is limited due to code prescriptions. A recent study, performed by Tošić et al. [77], suggested a revised upper limit for recycled aggregates (RA), which is 40% for reinforced concrete elements and 20% for prestressed concrete elements. Although, these limits are only valid for RA complying with classification type A. Despite current regulations on RA and the fact that both the transport and recycling process of concrete is carbon-intensive, further research into the recyclability of concrete is necessary in order to consider it as an option for the existing building stock [41].

Lastly, the strategy on systems for tracing materials and components is adopted. Radio-frequency identification (RFID) or standard barcodes allow companies to identify and track products as they move through the supply chain. In combination with BIM, valuable information becomes accessible about the mechanical characteristics, location, age and expected lifespan. Integrating RFID systems into prefabricated buildings optimizes the potential to create a closed-loop supply chain, due to the fact that prefabricated buildings are manufactured at a central location, allowing for inventory of materials and safe storage, whereas traditional construction techniques causes components to have a low degree of movability and deconstructability [41].

Implementing the strategies of Minunno et al. [41] and Cheshire [51] can turn buildings into material banks. By cataloguing the used materials and calculating the residual value of components, a new market for second-hand products can be established. This so-called catalogue is referred to as materials passport (MP). In short, a MP is a digital report containing circular economy relevant data that is entered into and then extracted from a centralised database in the form of reports customised to the needs of diverse users [78]. The scope of a MP is focused on different hierarchy levels. The hierarchy includes the levels of materials, components, products and systems that make up a building. Values for recovery of materials can be defined in a MP. For products and systems, general characteristics that make them valuable for recovery, such as: the design for disassembly or details of the application of an individual product or system. For example, the connection of a product to a building is essential to understand its value for recovery [79].

Through MP, the relevant parts can be assessed before the demolition of a building, because the relevant properties and history are documented. This allows time for planning a selected disassembly process and finding markets for recovered components at an early stage. Material passports can therefore reduce potential risks and barriers by providing the relevant information for actors in the value chain. As buildings and components have long lifetimes and can have multiple changes of ownership and responsibilities, the data should be kept up to date and passed on the relevant actors in a systematic way. Circular supply chains require incentives to endure the participation of all parties. The availability of material data is the core of a functioning circular economy and thus a prerequisite for the development towards a sustainable and more circular future [78].

A multitude of factors, barriers and opportunities related to MP are evaluated in the comprehensive study of Heinrich and Lang [78]. The study addresses the material data for a circular economy, life cycle management, assessment and certification, potentials of digitisation and information exchange among actors. It can be concluded from the study that material passports are strongly related to other design principles, such as: design for adaptability and design for deconstruction. Regarding the selection of materials, which are of particular interest in this section, Heinrich and Lang [78] propose ten criteria for imposing CE into the design phase, namely: **(i)**: use of renewable materials, **(ii)**: use of materials with recycled content, **(iii)**: use of regional products, **(iv)**: use of products that can be recycled or re-used, **(v)**: use of materials that can be produced with minimal effort, **(vi)**: use of materials with long residence times, **(vii)**: use of simple constructions with minimal material mixes, **(viii)**: avoiding products that release pollutants during installation and use, **(ix)**: avoiding products that negatively effect the environment and health and **(x)**: avoiding materials that need to be deposited as hazardous waste.

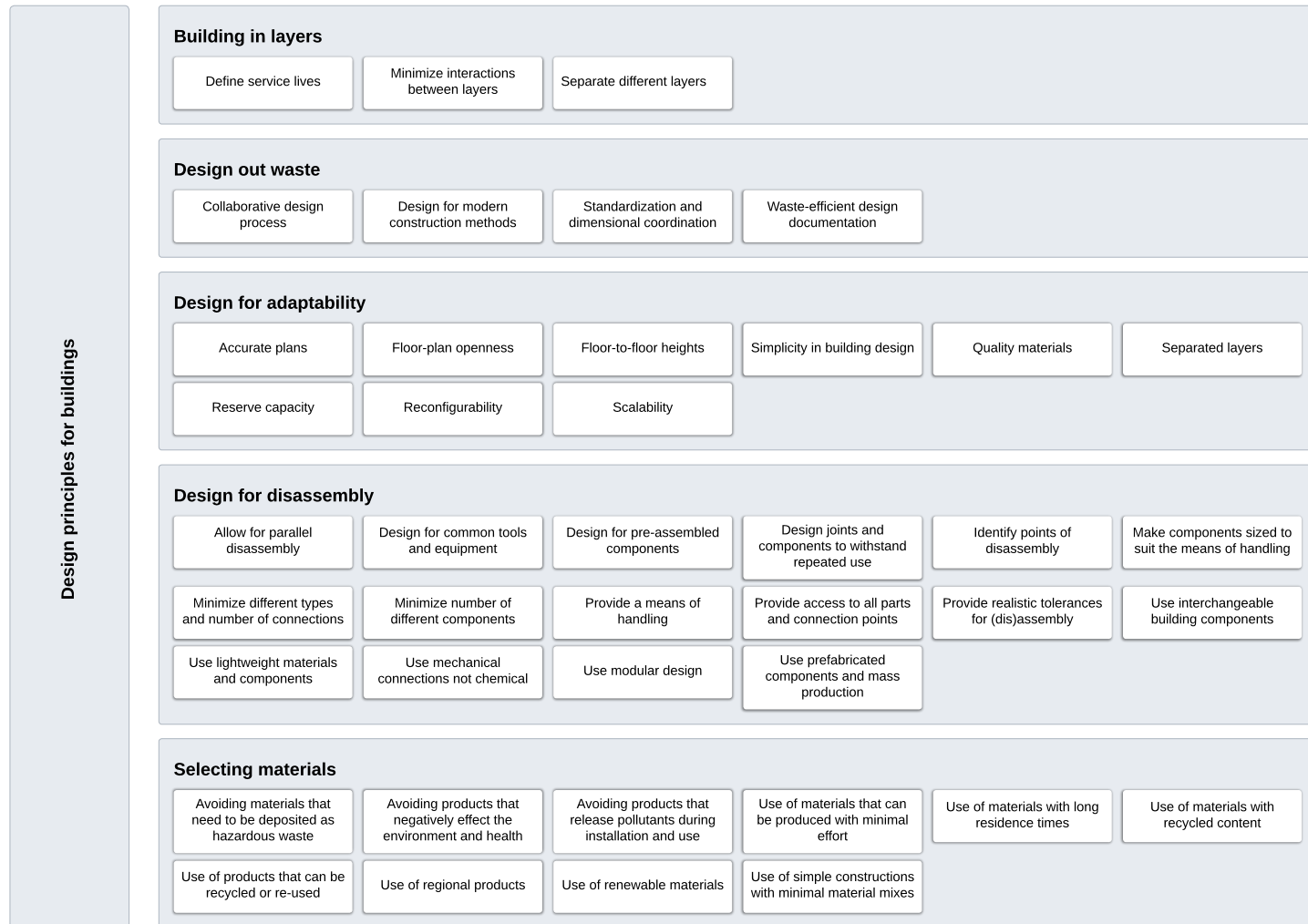


Figure 3.4: Circular design framework with hands-on criteria or strategies

3.3. Conclusions

From literature review, it can be concluded that substantial amounts of information on general circular economy concepts or principles are present. One example is the variety of nuances in the different R-strategies. The circular concept on material conservation has already been successfully integrated in several industries, but to a limited extent in the construction sector. Although awareness of circular concepts in the built environment is gaining momentum, resulting in many eco-design principles in literature, eighteen identified by Munaro et al. [64], only a handful of combined strategies in a comprehensive framework for buildings are proposed.

Between different design principles, a certain degree of overlap is present. Regarding the strategies for design for deconstruction proposed by Crowther [71], criteria 3. - avoidance of toxic and hazardous materials - fits well under the umbrella of selecting materials and criteria 9. - use an open building system - could be categorised as a strategy for design for adaptability. Moreover, some design principles are merged into a new concept, for example: design for adaptability and disassembly (DfAD).

Even though different principles or criteria sometimes overlap, conflicts can occur as well. For example, design for adaptability criteria 3. - floor-to-floor heights - proposed by Rockow [66], sufficient space for building services should be accommodated for. With respect to the replacement rates and changing requirements, as a result of the introduction of nearly zero energy buildings, the space necessary is likely to increase. This could interfere with minimum storey height set by the Dutch Building Decree and from financial perspectives, as highlighted in section 3.2.3.

The final conclusion on the theoretical framework concerns the selection of materials. Integration of by-products or designing for material recycling is still at an early stage due to insufficient scientific consensus and strict regulatory requirements. A similar situation occurs with the integration of BIM for the end-of-life management of buildings. More background information is given in sections 3.2.2 and 3.2.5.

4

Recent Projects

This section reviews several recent projects that specifically focus on circular design principles as proposed by Cheshire [51]. In section 4.1 examples of utility buildings are reviewed and discussed. Only one residential building project is reviewed and discussed in section 4.2. Implementation of circular design principles other than application of recycled construction materials is very rare in residential building projects. From state-of-the-art review, it became evident that the primary focus for residential buildings is on realising net zero energy buildings. This section is finalised with conclusions on the considered recent projects section 4.3.

4.1. Utility Building Projects

4.1.1. Park 20|20

The first utility building project considered is Park 20|20. Park 20|20 is a business park located in Hoofddorp, where several office buildings have been built and are still under development. In 1999, the consortium of Delta Development Group, VolkerWessels and Reggeborgh Groep purchased the Fokker production facility in the Schiphol area and redeveloped the plot into a mixed-use area [80]. Park 20|20 combines innovation and sustainability in its design. The circular core element in the design of the business park is the Cradle-to-Cradle concept. As discussed in section 3.1, the Cradle-to-Cradle philosophy is that waste equals food, for elements both in the biosphere and the technosphere.

All buildings in Park 20|20 are designed for disassembly. Structural components can be dismantled after the initial life cycle and reused in other buildings or at different locations. One example of a demountable structural component is the application of the Slimline floor system. The hollow space of the Slimline floor system enables installation of cables and building services that can be replaced or dismantled easily. Selection of materials is also considered in the project. Recycled building resources as well as biological materials are used to reduce carbon emissions. Another aspect that goes beyond the framework of Cheshire [51] is the energy generation and consumption of the business park. Solar panels are placed on top of buildings for supply of cleaner and renewable energy. Moreover, water stewardship is implemented as well, to keep water in a closed system, in order to minimise the amount of wastewater and sewage discharge from the site [81].

4.1.2. Temporary Courthouse Amsterdam

The Temporary Courthouse in Amsterdam has been designed to be a fully demountable and reusable building with an initial service life of five years. After its first life cycle, the building is dismantled and reconstructed 150 kilometers away in Enschede. The Temporary Courthouse was opened in November 2016 and the deconstruction process started in November 2021. The building will be taken back into service at the new location in early 2023.

Steel columns and beams function as the main support structure for the building. Bolted connections of the steel elements enable demountability and remountability. The columns are executed in hollow



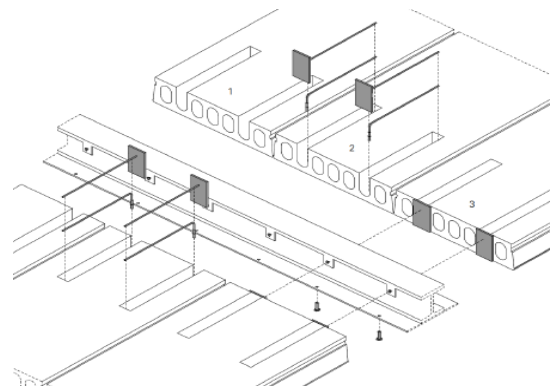
Figure 4.1: Overview of Park 20|20 in Hoofddorp [82]

box sections (in Dutch: 'kokerprofielen'). The beams are mainly executed in slim floor beams (SFB). Regarding the structural floor systems, several alternatives have been considered. Eventually, hollow core slabs are chosen [83].

For the stability of the building, various vertical braces are installed. In order to transfer the horizontal forces, such as wind loads, to the vertical braces, the hollow-core slabs are encased in a steel frame. Loose hollow core slabs are not able to transfer horizontal forces. Therefore a demountable moment-resisting connection was developed [83]. This demountable moment-resisting connection is depicted in figure ref. At the bottom, the hollow core slabs are connected to the flange of the steel beam, where tensile forces can be transmitted. At the top, compressive forces can be transferred by means of a threaded plate and bolts. In addition, the position of the hollow core slab can be adjusted [83]. The anchors were installed during construction on site and after installation concrete is poured into the slots (in Dutch: 'stekken'). A raised floor system is used to provide an even floor finishing.



(a) The Temporary Courthouse Building



(b) Schematic representation of the beam-slab connection

Figure 4.2: The Temporary Courthouse building in Amsterdam and demountable beam-slab connection [83]

4.1.3. Pavilion Circl

The Pavilion Circl is designed as a utility building of approximately 2000 square meters that facilitates flexible meeting and office spaces as well as restaurant facilities. Moreover, it provided a testing ground for the latest promising innovations, but have not proven their value in practise. This testing ground is called: 'living lab' and the Delft University of Technology was closely involved from the beginning. The pavilion is located in Amsterdam right besides the ABN Amro headquarters, which is also the client of the project. ABN Amro aims to develop circular business models and engage other organisations in expanding the circular economy [84].

From the engineering perspective, the main load bearing elements are constructed in timber. Only the basement is constructed in concrete. The expected service life of the timber supporting structure is thirty years. After the initial service life, the timber components are returned to the supplier for future

re-use. Therefore, the structural components should be designed for disassembly. The designers included the principles of designing out-waste and material selection of Cheshire [51] as well. All materials and components are captured in material passports and a BIM for the end-of-life management of the building. Regarding the selection of materials: the structural timber elements are made of locally harvested larch trees and the floor finishing consists of either refurbished timber window frames or pulverised recycled concrete [84].



Figure 4.3: Overview of Pavilion Circl in Amsterdam [84]

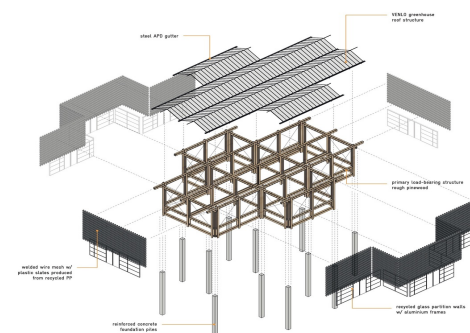
4.1.4. People's Pavilion

The People's Pavilion is a 250 square meter building constructed for the Dutch Design Week and the World Design Event, organised by the city of Eindhoven in 2017. The building has been used as a meeting place and hang-out for visitors and served as a venue for music and theater. In total, 600 people could be accommodated in the building. According to the architects, the pavilion is a design statement of the new circular economy [85]. Different from the previously mentioned projects, this building consists of 100% borrowed construction materials, which were returned to the owners and suppliers after decommissioning and deconstruction of the building. The designers realised a building without using screws, glue, drills or saws [85].

The main load bearing structure is made up of twelve reused reinforced concrete foundation piles and nineteen timber frames. The frames consists of unplanned timber beams with standard dimensions and are held together using steel straps. Concrete piles and frames are connected with 350 tensioning straps, resulting in a total building height of eight meters. The glass roof was adopted from a system that is often used in the greenhouse industry. The glass facade elements on the ground floor are leftovers from a refurbished office building. Most conspicuous is the facade of the building, which consists of recycled plastic tiles in a variety of colours. These tiles are made from plastic household waste materials, collected from the inhabitants of Eindhoven. All other interior elements, such as lighting, heating or furniture of the People's Pavilion were borrowed as well [85].



(a) Building overview



(b) Primary structural elements

Figure 4.4: People's Pavilion building in Eindhoven [85]

4.2. Residential Building Project

4.2.1. Superlocal

The Superlocal project is a renovation project in Kerkrade in which three of the four high-rise apartment buildings are transformed to approximately 125 new residential units. The apartment buildings originate from 1967 and no longer meet the requirements of the present day. The demolition and dismantling of the first apartment buildings was initiated in 2017. Several apartments from the tenth floor have been sawn out of the building for implementation in a newly constructed exhibition building to present the generic possibilities for circular reuse of building components. The exhibition building does not meet the regulations for residential units, but it is wind and watertight [86].

In the second phase of the transformation project, three circularly designed pilot (or test) houses consist of at least 90% of locally reclaimed materials. For these three houses, cast in-situ concrete with a high percentage of recycled granulate has been used. Other new materials are bio-based. In the third phase, fifteen energy-neutral ground based housing units are constructed. For the walls, 100 % of the gravel is replaced by recycled granulate. The floor systems consist of a lower percentage of granulate, due to imposed regulations of the Dutch Building Decree which resulted in a thicker floor slab. A thicker floor slab negates the benefits of the reduced CO₂-emissions. Moreover, all fifteen ground-based housing units are designed to be demountable after their service lives. For the last apartment building, half of concrete shell of the building is demolished and half is retained and renovated [86]. Figure 4.5 presents an overview of the finished project. In the bottom left of the figure, the three pilot houses can be seen. In the center to bottom right of the figure, the fifteen demountable and energy-neutral ground-based housing units can be seen. The renovated apartment building is visible at the top of the figure.



Figure 4.5: Overview of the Superlocal project in Kerkrade

4.3. Conclusions

Implementation of circular design principles is still sparsely applied. However, as discussed in the previous sections, some projects stand out for their active and innovative role in the transition to a more circular economy. Park 20|20 in Hoofddorp is one of the first large scale projects which actively implemented the principle of material selection in the design of buildings. The Temporary Courthouse in Amsterdam is characterised by the demountability of the structural system and of the other building components. Pavilion Circl in Amsterdam and the People's Pavilion in Eindhoven combined the demountability of the (structural) components and the material selection to a considerable extent.

For residential buildings, implementation of circular design principles, as described by the framework of Cheshire [51], is mainly limited to demountability of the components and application of recycled construction materials. However, as discussed in section 3.2.5 and as became evident in section 4.2.1, strict regulations are an impediment for the implementation of recycled materials. Moreover, the number of recent projects for residential buildings is even more scarce compared to utility buildings. Therefore, implementation of more (comprehensive) circular design principles in the design of residential buildings, combined with their current scarcity, offers excellent opportunities for further developments.

5

Floor Systems

This section reviews several concrete floor systems currently available on the market and commonly used in practice. Concrete floors have favorable characteristics in terms of: strength, rigidity, acoustic and thermal insulation, fire resistance and span lengths. Concrete floor systems are generally well available and offer a variety of suppliers. Due to the standardisation of the production process, the costs are relatively low. Timber and steel-concrete composite floor systems are not taken into consideration due to moderate availability, costs and additional measures to meet regulations imposed by the Dutch Building Decree (in Dutch: 'Bouwbesluit') on acoustic and thermal insulation for example. The four reviewed concrete floor systems in this section are: hollow core slabs, service-integrated floors, reinforced plank floors and the Bestcon floor systems.

5.1. Hollow Core Slab

Hollow core slabs are one of the commonly used load-bearing floor systems in the Netherlands. These are flat concrete slabs that have cavities in the longitudinal direction of the span to reduce self-weight of the system. Usually, hollow core slabs are provided with eccentric prestressing reinforcement only. The prestressing reinforcement is stressed at the ends of a long prestressing bed. After casting and hardening of the concrete, the elements are cut to length. Hollow core slabs are usually delivered in a standard width of 1200 millimeters, although smaller widths, to serve as fitting plates (in Dutch: 'pasplaten'), are available upon request [87]. The slabs are placed side by side and the longitudinal joint between the slabs is filled with mortar to form a shear joint. This shear joint transmits shear forces for horizontal stability. Therefore, hollow core slabs transfer loads along the length of the slab and can be classified as a one-way load bearing slab. In order to improve the horizontal stability or load distribution of localised vertical loads, hollow core slabs are usually provided with a (structural) concrete topping. Additionally, application of a concrete topping also has a beneficial effect on the sound and thermal insulation of entire floor system.

Regarding building services, small recesses of up to 25 millimeters can be drilled in the centre of a cavity [87]. Drilling holes in the webs is not recommended, due to the presence of longitudinal prestressing reinforcement. Larger recesses, for example for staircases, can be made using a trimmer beam (in Dutch: 'raveelijzer'). It is not possible to implement (larger) building services in a hollow core slab without application of a non-structural filling layer or additional measures such as a suspended ceiling or raised floor system. An example of a hollow core slab is presented in figure 5.1a. Illustrative use of a trimmer beam is depicted in figure 5.1b. The general characteristics of hollow core slabs are presented in table 5.1.

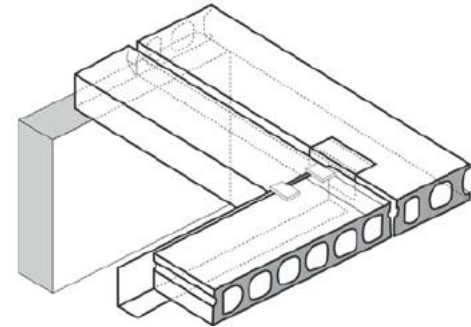
Hollow core slabs

Span lengths	5.0 – 16.0 meters	VBI [87]
Height	150 – 400 millimeters	VBI [87]
Self-weight	268 – 490 kg/m ² (including joint filling)	VBI [87]
Fire safety	60 – 120 minutes	VBI [87]

Table 5.1: General characteristics of hollow core slabs



(a) Geometrical layout [88]



(b) Utilisation of a trimmer beam [88]

Figure 5.1: Hollow core slabs

5.2. Service-integrated floor

The main disadvantage from hollow core slabs is the lack of integration of building services into the load-bearing structure, in order to reduce the total height of the floor system. This is usually a concern for application in apartment buildings. Therefore, a further development of a hollow core slab is a service-integrated floor system (in Dutch: 'leidingplaatvloer'). Service-integrated floor systems are optimised for the integration of building services within the load-bearing structure. The grooves (or trenches) for the building services can either be pre-determined or applied straight before the final construction phase (in Dutch: 'afbouw-fase'), depending on the supplier.

Betonson [89] developed the wing floor system. The system consists of a 1200 millimeter wide hollow core slab in the middle and 600 millimeter wide wing sections on either side. The floor system is shown in figure 5.2a. In the transverse direction, several channels are implemented for the passage of pipes for adjacent wing floors. When two wing floors are placed next to each other, a groove of 1200 millimeters is established in the direction of the span. Depending on the accessibility in the use phase, the grooves can be filled either with structural reinforced concrete or non-structural foam concrete [89]. VBI [87] developed a piping floor system (in Dutch: 'leidingplaatvloer') for integration of building services within the structural system. The piping floor systems consist of prefabricated and prestressed hollow core slabs. However, the main differences with ordinary hollow core slabs are: the thickness of the lower shell and the cavities. For a piping floor, the cavities are smaller and located in the top shell of the system. Hence, the thickness of the lower shell is larger. An example of a piping floor is shown in figure 5.2b. Grooves can be made shortly before the final construction phase. Ring grooves can be made around the entire floor field, providing maximum flexibility for future adjustments [87]. The grooves can be filled with a non-structural filling after installation of the building services. General characteristics of both service-integrated floor systems are presented in table 5.2.

5.3. Reinforced Plank Floor

Massive floor systems are still widely used in residential and utility buildings in the Netherlands, due to favorable acoustic and thermal insulation properties. One of the commonly used massive floor systems is a reinforced plank floor (in Dutch: 'breedplaatvloer'). Reinforced plank floors consists of a prefabricated concrete bottom shell and a cast in-situ concrete topping. The bottom shell contains

Service-integrated floor systems		
Span lengths	6.0 – 16.0 meters	Betonsol [89]
	≤ 7.6 or ≤ 9.0 meters	VBI [87]
Height	180 – 420 millimeters	Betonsol [89]
	200 or 260 millimeters	VBI [87]
Self-weight	225 – 427 kg/m ² (including joint filling)	Betonsol [89]
	386 or 511 kg/m ² (including joint filling)	VBI [87]
Fire safety	standard 60 minutes	Betonsol [89]
	90 or 120 minutes	VBI [87]

Table 5.2: General characteristics of service-integrated floors



(a) Wing floor system [89]



(b) Piping floor [90]

Figure 5.2: Service-integrated floor systems

conventional reinforcement and lattice girders. These lattice girders serve as supporting elements for the top reinforcement and ensure composite action of the lower shell and concrete topping and provide strength during transport, lifting and assembly [88]. The standard width of reinforced plank floors is 3000 millimeters. However, alternative widths are available upon request [91]. The thickness of the bottom shell varies from 50 to 100 millimeters [91]. Thin reinforced plank floors usually transfer the load along the length of the slab. However, for thicker reinforced plank floors, load transfer in the transverse direction is also possible, that is: a two-way load bearing slab. An example of a reinforced plank floor is presented in figure 5.3a.

Advantages of using reinforced plank floors are related to the cast in-situ nature of the floor slab. Building services can be installed freely in the floor field and therefore provide a lot of freedom upon installation. An example of integrated building services within a reinforced plank floor is presented in figure 5.3b. Additionally, during the design phase, recesses for piping or staircases can easily be implemented in the floor slab. Moreover, horizontal stability is optimal due to the monolithic character of reinforced plank floors. Self-weight and fire resistance of the system depends on the height of the concrete top layer, the latter is usually determined by the required cover of the reinforcement. General characteristics of reinforced plank floor systems are presented in table 5.3.

Reinforced plank floors		
Span lengths	0.8 – 10.0 meters	Dycore [91]
Height	50 – 100 millimeters (excluding concrete top layer)	Dycore [91]
Self-weight	125 – 250 kg/m ² (excluding concrete top layer)	Dycore [91]
Fire safety	≤ 120 minutes (depending on reinforcement cover)	Dycore [91]

Table 5.3: General characteristics of reinforced plank floors



(a) Reinforced plank floor without concrete topping [88]



(b) Cast-in building services in a reinforced plank floor [92]

Figure 5.3: Examples of a reinforced plank floor and cast-in building services

5.4. Bestcon floor systems

The last considered concrete floor system is developed by Bestcon [93]. The Bestcon floor system shows similarities with hollow core slabs and reinforced plank floors. The Bestcon MPV140 and MPV160 are designed for application for ground-based housing units, whereas the Bestcon-60 floor system is designed for application in apartment or utility buildings. Standard width of the first two floor systems is 3500 millimeters and 3600 millimeters for the third floor system, but fitting plates are available upon request [93]. All three floor systems consist of a prestressed massive concrete slab with a varying thickness. However, in case of smaller span lengths, the massive concrete slabs are traditionally reinforced only. Building services are separated from the load-bearing structure in a non-structural filling layer (in Dutch: 'vullaag') on top of the prestressed concrete slab and, therefore, offering a high degree of flexibility in the layout of building services. Considering the large width of each element, the required lifting operations is reduced and thus the speed of construction is increased, which is particularly beneficial for medium to high-rise buildings in densely urbanised areas. Large recesses for piping or staircases can be accounted for during the design phase. Moreover, diaphragm action of the Bestcon-60 floor system is ensured [93]. The general layout all three systems is presented in figure 5.4. General characteristics obtained from Bestcon [93] are presented in table 5.4.

Bestcon floor systems

Height	140 or 160 millimeters	MPV140-160 [93]
	200 millimeters	Bestcon-60 [93]
Fire safety	≤ 120 minutes	MPV140-160 [93]
	≤ 120 minutes	Bestcon-60 [93]

Table 5.4: General characteristics of the Bestcon floor systems

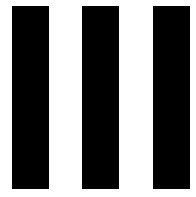


(a) Bestcon floor slab with integrated recess [93]



(b) Separation of building services in Bestcon floor systems [93]

Figure 5.4: Bestcon floor slabs



Design

6

Design and Validation

The purpose of this chapter is to further explain the design principles and geometric variables. Certain design decisions will also be discussed. In chapter 3, a large number of design principles and criteria are presented to achieve circular design. Chapter 4 presents a number of recent projects which, in varying degrees, are based on circular thinking. To finalise the theoretical framework, chapter 5, presents the (most) used concrete floor systems in the Dutch building industry. In section 6.1, these floor systems are briefly repeated with their key advantages. Section 6.2 focuses on the design starting points and discusses some design decisions. Section 6.3 presents the newly proposed floor system and dimensions. This chapter is finalised with a multi-criteria analysis of the four commonly used concrete floor system and the newly proposed floor system in section 6.4.

6.1. Evaluation common floor systems

As a brief summary of section 5, the general layout and advantages or favorable characteristics of the four most commonly used floor systems in Dutch residential and utility buildings are addressed in this section. The four considered floor systems are: **(i)**: hollow core slabs, **(ii)**: service-integrated floors, **(iv)**: reinforced plank floors and **(iii)**: Bestcon floor systems.

Hollow core slabs are flat concrete slabs with cavities in the longitudinal direction of the span to reduce the self-weight of the system. Usually, hollow core slabs are provided with bonded eccentric prestressing reinforcement only. Small recesses (≤ 25 millimeter) can be drilled in the centre of a cavity. Building services, however, cannot be integrated within the floor system and require additional measures, such as a suspended ceiling or raised floor system. Advantages of hollow core slabs are: **(i)**: realisation of long spans (up to 16 meters [87]), **(ii)**: high construction speed (propping is usually not required) and **(iii)**: good availability on the market due to multiple suppliers.

Service-integrated floors are a further development of hollow core slabs. These floor systems are designed to install building services in the structural system. Note that the building services are not embedded within the structural layer and are therefore relatively easily accessible. The location of the grooves for the building services can either be fixed in advance or provided at a later stage of construction, depending on the supplier. Key advantages of service-integrated floors are: **(i)**: large freedom in building service layout and **(ii)**: reduced height of the entire floor package.

Reinforced plank floors are massive systems, where a concrete top layer is poured onto a prefabricated concrete bottom shell with lattice girders. The monolithic character of reinforced plank floors provides favorable characteristics related to: **(i)**: acoustic and thermal insulation for ground-based housing units or apartment buildings, **(ii)**: large freedom in building service layout and recesses and **(iii)**: good diaphragm action for horizontal loads.

Lastly, the Bestcon floor systems are reviewed in section 5. Bestcon floor systems are an alternative for ordinary reinforced plank floors. The system consists of a massive prefabricated concrete layer, which is prestressed for normal to large span lengths in buildings. The main difference with reinforced

plank floors and service-integrated floors is that the top layer of the system is smooth and, therefore, free of grooves or lattice girders. Thus, building services can be installed freely in a non-structural filling layer. Similar to reinforced plank floors, large recesses for piping or staircases can be implemented in the design phase.

Each of the reviewed floor systems has their distinct advantages and disadvantages. Apart from all favorable characteristics mentioned, the selection of which specific floor system is chosen depends on several considerations, such as: structural limitations or execution aspects. Building in densely urbanised areas imposes different prerequisites compared to more rural areas. Moreover, experience of the contractor plays an important role as well. Furthermore, financial aspects should never be underestimated or neglected for the decision of a specific floor system. It is common knowledge that the construction industry is not known for its progressive nature. However, as mentioned previously throughout this thesis, circular thinking is gaining momentum in society and introduction of more stringent legislation is imminent. Therefore, initiatives such as 'Het Betonakkoord' are good incentives for innovation and implementation of circular principles. The second aspiration point of 'Het Betonakkoord' is on circular design and high-quality application of recycled- or reused building components. In line with this aspiration, the framework of chapter 3 has been developed to provide insight into design principles, together with hands-on criteria, in order to assess current and newly developed systems within the context of a circular economy.

6.2. Design Starting Points

From sections 1.1.3 and 6.1 it has become clear that implementation of circular thinking should be incorporated in the decision for specific building components. Moreover, for newly developed systems, legislation regarding the implementation of circular principles and criteria, such as those outlined in section 3, is coming at an increasing pace. Adopting circular thinking at this very moment adds an extra dimension which is generally not yet incorporated in current practices. Therefore, there is a great opportunity to design future floor systems that do comply with circular thinking.

With respect to the context of this thesis, the main challenge is to develop a new floor system that includes circular principles that cannot be found in the current market offer. Ideally, a new floor system should meet all circular principles and criteria, expressed in figure 3.4. However, concluding from section 3.3, the starting point for this thesis is related to the 25 criteria listed by the principles of adaptability and disassembly. The remainder of this section is to provide background information on the newly designed floor system and intermediate decisions that are made. The cornerstones of the new proposed floor system are: **(i)**: demountability, **(ii)**: reconfigurability, **(iii)**: scalability and **(iv)**: modularity.

The best way to describe this new system is to make the comparison with building with LEGO bricks. LEGO is a construction toy that consists of interlocking plastic bricks in different colours. These bricks can be connected in many ways to construct a variety of objects, such as buildings and vehicles. Anything that has been made can, in principle, be taken apart and the bricks or components can be reused to make new things again. The application of generic building blocks in larger components or systems, which can be deconstructed without intrusive modifications afterwards, in order to enable reuse of these building blocks or components, are very well in line with the circularity principles opposed before. Prefabricating these building blocks in a factory environment can guarantee certain quality aspects.

Starting from this perspective, the new floor system should be made from blocks or modules. The terms blocks and modules are commonly used throughout this thesis. No significant difference exists between both terms and they are therefore used interchangeably. A challenge to overcome is the connection between modules. The circular design framework prescribes the use of dry connections instead of chemical ones. Therefore, in concrete constructions, so-called wet joints should be avoided. Besides, wet joints require (more) intrusive modifications to separate the modules, which decreases the overall demountability and reusability of the system. One way of combining individual modules into a system is by applying a compressive force to the system at both ends. Usually, the compressive force to the system is provided by tensioning steel tendons. For concrete structures, this compressive force can be applied in two distinct ways:

- Pre-tensioning: by exerting a tension force to the tendons before pouring of the concrete. By definition this results in bonded tendons
- Post-tensioning: the tension force is exerted after the concrete has gained its minimum required strength. In this case, the tendons can either be bonded with the concrete by grouting or remain unbonded

An example of the utilisation of prestressed tendons in a floor system is the previously discussed hollow core slab. Hollow core slabs use bonded tendons as prestressing reinforcement. Research conducted by Glias [94] revealed that the reconfigurability of this floor system is very limited and reuse is only beneficial in the original dimensions. Therefore, bonded tendons in general should not be the favourable option. The best manner of realising a reconfigurable and demountable system is therefore the utilisation of unbonded post-tensioned tendons.

Regarding the modules, as a starting point, they are designed as solid square elements. The module widths are the same as those of hollow core slabs, namely 1200 millimeters and, since the elements are square, the depth of the modules is 1200 millimeters as well. The height of the elements follow later from the analysis. However, the disadvantage of solid slab elements is that the self-weight has significant impact on the load bearing capacity of the system. Again, analogous to hollow core slabs, weight-reducing voids can be implemented to reduce this effect. Since many parameters are yet unknown at this point, the shear force capacity can become an issue when choosing for weight-reducing voids. Particularly near the supports of the system. Moreover, the prestressing force is introduced at the ends of the system and should be transferred properly into the concrete in order to avoid local tensile splitting. Therefore, it is chosen to subdivide the building modules into two fundamental building blocks, as illustrated in figure 6.1, where:

1. Solid elements, located at both ends of the system where the prestressing tendons are anchored
2. Weight-reduced elements, located in between the end elements that can be adjusted for the required span length of the system

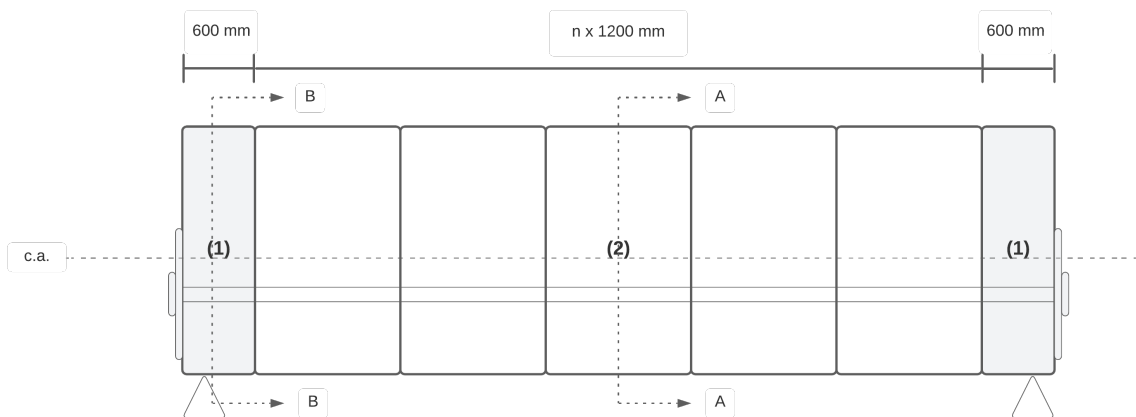


Figure 6.1: Schematic side view of the system with an element size of: 1200x1200 millimeters

Depicted in figure 6.1 are the different depths of the two fundamental elements. The solid end elements have fixed depth of 600 millimeters for all element sizes. Figure 6.2 presents a schematic cross-sectional view of the system. Cross-section A-A refers to the weight-reduced elements and cross-section B-B refers to the solid elements. For the sake of illustration, the unbonded tendons and anchorage are included in this figure.

Noticeable in figures 6.1 and 6.2 is the eccentric position of the unbonded tendons. This eccentricity is beneficial for the bending moment resistance of the system. Determining the eccentricity of the tendons is one of the major design challenges. The eccentricity is primarily dictated by:

- Allowable stresses in the cross-section. Since the system is post-tensioned and consists of a variety of elements, tensile stresses or opening of the interfaces (joints) between the elements

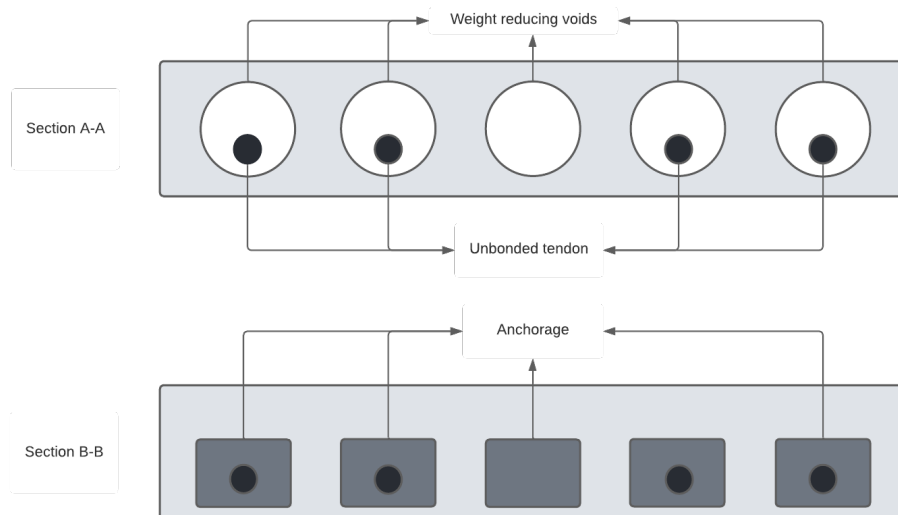


Figure 6.2: Schematic cross-sectional view of the system with an element size of 1200x1200 millimeters

should be avoided in serviceability limit state. This is referred to as a fully-prestressed situation. To meet this requirement, the axial compressive force should be applied within the kern area of the cross-section

- Different types of post-tensioning systems. The most commonly used post-tensioning systems are strands and bars. Both systems have their distinct advantages and disadvantages. Manufacturers of these systems can impose boundary conditions, such as: **(i)**: center-to-center or edge distances, **(ii)**: minimum concrete strength or **(iii)**: anchor plate dimensions. Moreover, additional splitting reinforcement could be required to distribute the prestressing forces into the concrete.

The last geometrical parameter is the height of the new system. The height is strongly affected by the desired market where the floor system should operate in. The initial purpose of this new system is to be used in residential buildings, specifically in ground-based houses (in Dutch: 'grondgebonden woningen') and apartment buildings to serve as a storey floor (in Dutch: 'verdiepingsvloer'). The most common span lengths for generic residential buildings is between 5.4 meters and 7.8 meters, with intermediate steps of 0.6 meters. The height of the new floor system should be in line with those currently offered in the market. Therefore, the height of the elements is initially set at 0.24 meters and later verified in section 7.

6.3. Newly Proposed System

In the foregoing section, the concept of newly proposed floor system is explained and illustrated. To meet the requirements regarding span lengths and common grid sizes, a variety of element sizes is offered to satisfy the market demands. Grid sizes for residential and utility buildings are usually in increments of 1.2 meters, whereas span lengths (in Dutch: 'beukmaten') are in increments of 0.6 meters. For low to medium-rise apartment buildings the construction speed can be increased by the applications of slabs wider than 1.2 meters, as is common for reinforced plank floors and the Bestcon floor system. Therefore, the proposed floor system consists of multiple elements that can be used interchangeably within their allocated group. In total, three different element widths are adopted. An overview of all dimensions is depicted in figures 6.3, 6.4 and 6.5.

Figure 6.6 presents a cross-sectional view of the newly proposed system, together with all relevant dimensions for a slab width of 1.2 meters. The geometrical properties comply with the requirements imposed by the manufacturer of the post-tensioning system. Other geometrical and material parameters are highlighted in section 7.2.4. The manufacturer of the monostrands is Dywidag [95]. Detailed information about the post tensioning system and anchorages is provided in Appendix E. The stressing

anchors used are of type SK6. Each monostrand consists of 7-wire strands, resulting in a nominal diameter of 15.7 millimeter. For each span length, a varying number of unbonded monostrands is required under the imposed loading. Corrosion protection is provided by PE-sheathing and a corrosion protection filling material [95]. Additional reinforcement is suggested by Dywidag [95] near the anchor plates of the system to properly transfer the prestressing forces into the concrete. Indicated in figure 6.6a the additional longitudinal reinforcement consists of 2 \varnothing 8 millimeter and the stirrups consist of \varnothing 8 millimeter. Figures 6.6 serve as an example for the required additional reinforcement for the elements of Group II. The same amount of additional reinforcement should be implemented in the design of elements of Groups I and III. Practical reinforcement to increase the robustness of the elements is not provided in the overview and is recommended to be implemented in (improved) designs in future research.

6.4. Validation floor systems

The newly proposed floor system and the four aforementioned floor systems should be reviewed in a quantitative manner in order to highlight the differences and potential improvements of each floor system. In order to make the analysis as objective as possible, a weighted scoring mechanism should be adopted. A widely used tool to make quantitative assessments is a multi-criteria analysis. Multi-criteria analysis is an evaluation method for making a rational choice between various alternatives on the basis of more than one distinguishing criterion. In general, a multi-criteria analysis consists of five intermediate steps:

1. Define the context
2. Identify the available options
3. Decide the objective and select the criteria or sub-criteria
4. Determine the relative importance of each criterion and impose a weighted rating scale
5. Calculate the results

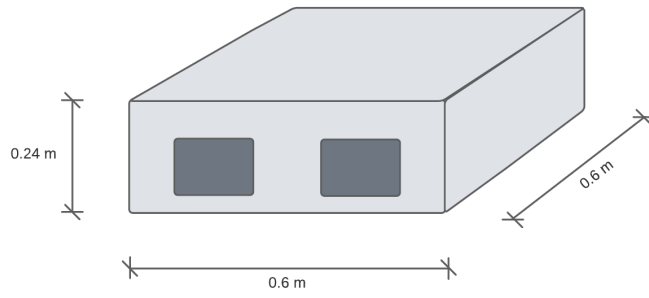
First, the context should be defined. The context of this thesis and, therefore, for this multi-criteria analysis as well, is the application of a concrete floor system in newly-built residential buildings to serve as a storey floor. The available options which are currently available on the market are reviewed in section 5. Section 6.3 proposes a new floor system, which should be included in the multi-criteria analysis. The objective of the multi-criteria analysis is to assess how the newly proposed floor system compares with the commonly used concrete floor systems in the context of a circular design. Considering the conclusions from section 3.3, the multi-criteria analysis is based upon the 25 strategies regarding design for adaptability and design for disassembly. Since each design strategy is considered of equal importance, the weight of each criterion is 1.0. A rating scale or score should be established in order to calculate the results, as is required for step five of the multi-criteria analysis. The score ranges from zero to four, where zero is the lowest and four is the highest attainable score. For all considered floor systems, the scores are added together, due to the weighing factor of 1.0. In this way, a theoretical maximum score of 100 can be achieved if all criteria are met.

Assumptions related to the installation of building services are made before step five of the multi-criteria analysis. These assumptions serve as a starting point, which are based on common practice for the various floor systems. The following assumptions have been adopted:

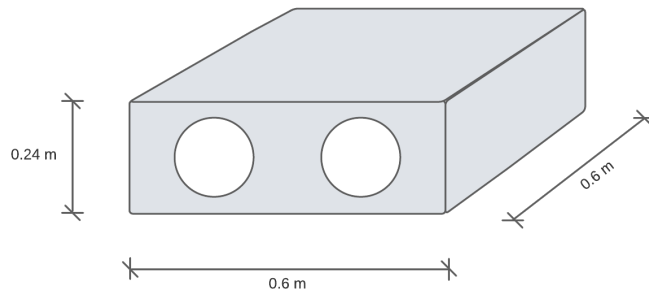
Building services

Hollow core slabs:	installed in the plenum of either a suspended ceiling or raised floor system
Service-integrated floor:	in the grooves of the structural system
Reinforced plank floor:	embedded within the cast in-situ concrete top layer
Beston:	installed in a non-structural filling layer
Newly proposed:	installed in the plenum of either a suspended ceiling or raised floor system

The results of the multi-criteria analysis are presented in table 6.1. Concluding from table 6.1: hollow core slabs score 67 out of 100, service-integrated floor systems score 67 out of 100, reinforced plank floors score 44 out of 100, Bestcon floor systems score 69 out of 100 and the newly proposed floor system scores 85 out of 100. Therefore, it can be concluded that the newly proposed floor system is the best option regarding implementation of circular design principles.

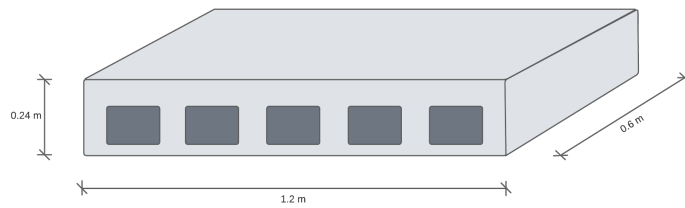


(a) Dimensions of anchorage element 0.6 x 0.6 meters

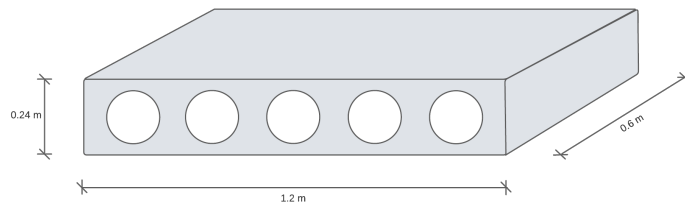


(b) Dimensions of weight-reduced element 0.6 x 0.6 meters

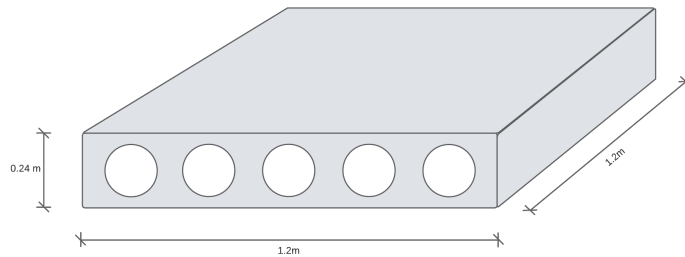
Figure 6.3: Dimensions group I: width = 0.6 meters



(a) Dimensions of anchorage element 1.2 x 0.6 meters

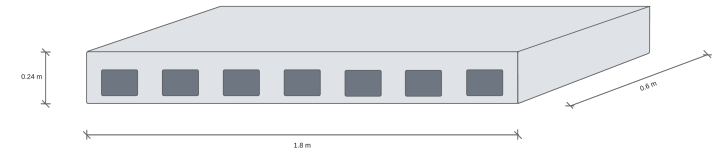


(b) Dimensions of weight-reduced element 1.2 x 0.6 meters

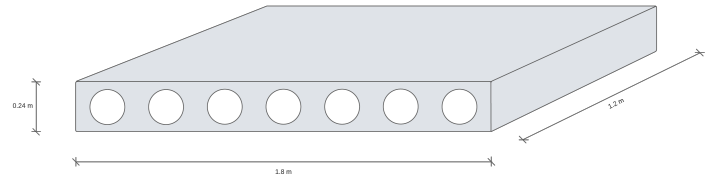


(c) Dimensions of weight-reduced element 1.2 x 1.2 meters

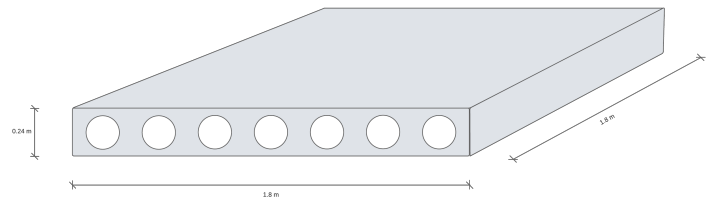
Figure 6.4: Dimensions group II: width = 1.2 meters



(a) Dimensions of anchorage element 1.8 x 0.6 meters

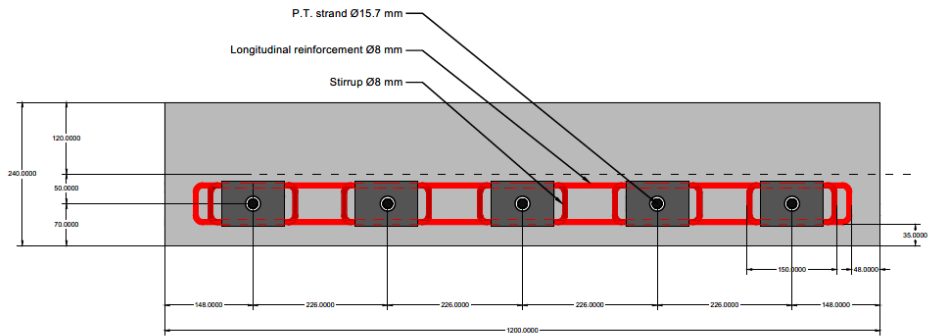


(b) Dimensions of weight-reduced element 1.8x1.2 meters

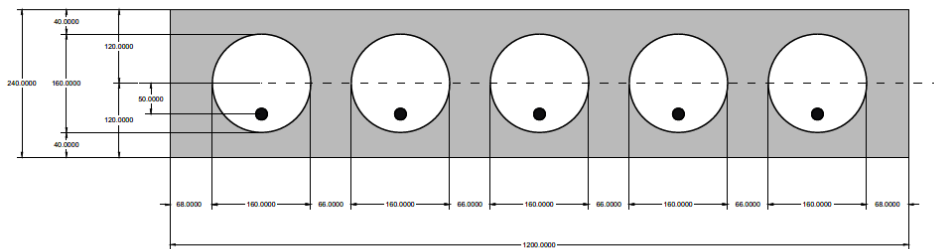


(c) Dimensions of weight-reduced element 1.8x1.8 meters

Figure 6.5: Dimensions group III: width = 1.8 meters



(a) Dimensions new floor system for the solid end elements in cross-sectional view



(b) Dimensions new floor system for the weight-reduces elements in cross-sectional view

Figure 6.6: Cross-sectional views of the exact dimensions for an element width of 1200 millimeters

Design criteria	Hollow core slab	Service-integrated floor	Reinforced plank floor	Bestcon	Newly proposed
1. Accurate plans	4	4	4	4	4
2. Floor-plan openness	3	3	4	4	3
3. Floor-to-floor heights	2	4	4	2	2
4. Simplicity in building design	4	4	4	4	4
5. Quality materials	4	4	2	4	4
6. Separated layers	3	1	0	2	4
7. Reserve capacity	3	3	4	4	3
8. Reconfigurability	1	1	0	1	4
9. Scalability	0	0	0	0	4
10. Allow for parallel disassembly	2	2	0	2	3
11. Design for common tools and equipment	4	4	4	4	4
12. Design for pre-assembled components	4	4	2	3	4
13. Design joints and components to withstand repeated use	2	2	0	2	3
14. Identify points of disassembly	2	2	0	2	3
15. Make components sized to suit handling	4	4	4	4	4
16. Minimize different types and number of connections	2	2	1	3	3
17. Minimize number of different components	3	3	2	3	3
18. Provide a means of handling	4	4	4	4	4
19. Provide access to all parts and connection points	2	2	0	2	3
20. Provide realistic tolerances for disassembly	3	3	0	3	3
21. Use interchangeable building components	3	3	2	3	4
22. Use lightweight materials and components	0	0	0	0	0
23. Use mechanical connections not chemical	2	2	0	3	4
24. Use modular design	2	2	1	2	4
25. Use prefabricated components and mass production	4	4	2	4	4
Σ weighted score:	67	67	44	69	85

Table 6.1: Multi-criteria analysis of the four commonly used and newly proposed floor system

7

Design Verification

This chapter reviews the verification of the proposed floor system by calculation. The calculations are performed according to codes of practise and/or in line with state-of-the-art research. All results are presented in convenient and organised tables. For the verification of the deflections, occurring bending moments and shear forces, illustrative diagrams are presented as well. It should be noted that only one width is considered for the calculation results presented in this chapter. The width considered in this chapter is $w = 1.2m$. The results for the other building blocks are presented in Appendix A and C.

7.1. Calculation procedure

As an introductory section, the adopted calculation procedure in order to determine all relevant loads, due to self-weight, imposed live load and from the prestressing tendon lay-out, together with the resistance of the system, are outlined here. The general lay-out of the system is presented in section 6.3. The calculation procedure and the related sections in this chapter are summarised in bullet-points.

1. Classification and loading in section 7.2
 - (a) Classification and imposed loading in paragraphs 7.2.1 and 7.2.2
 - (b) Load situations and combinations in paragraphs 7.2.3
 - (c) Cross-sectional and material properties 7.2.4
2. Initial amount of required prestressing tendons in section 7.3
3. Prestressing losses in section 7.4
 - (a) Immediate losses in section 7.4.1
 - (b) Time-dependent losses in section 7.4.2
4. Cross-sectional stress checks in SLS in section 7.4
 - (a) Stresses in section 7.5.1
 - (b) Deformations in section 7.5.2
 - (c) Vibrations in section 7.5.3
5. Bending moment resistance in ULS in section 7.6
6. Shear resistance in ULS in section 7.7

7.2. Classification and imposed loading

7.2.1. Classification

The buildings of the case study have been classified according to NEN-EN 1990 [96] and its national annex [97]. In the case study, two different types of buildings can be distinguished: (i): ground-based housing units and (ii): apartments. The classification is presented in table 7.1. The case study building has been used to provide information regarding structural dimensions and determining the spanning length interval.

In order to make the concrete modules as versatile as possible, the highest reliability class is normative

in the design. The reliability class largely depends on the consequence class. The reliability class affects the multiplication factor k_{F1} for the partial factors. Since the normative consequence class is medium (CC2), the multiplication factor $k_{F1} = 1.0$.

	Ground-based housings units	Apartments
Building stage:	New	New
Consequence Class	CC1	CC2
Design working life class	3	3
Design working life	50 years	50 years

Table 7.1: Classification of residential units of the case study

7.2.2. Imposed vertical loading

Buildings can be subjected to a variety of vertical load actions. NEN-EN 1991 [98] subdivides buildings in different categories with respect to their specific use. Category A represents domestic and residential activities, where as category B represents office areas. A full overview of the different categories and their accompanying imposed vertical loads can be found in NEN-EN 1991 section 6.3. It should be noted that national annexes may define different conditions.

The total vertical load used in this case consists of the following components: **(i)**: the self-weight of the structure (g_k), **(ii)**: additional self-weight of fixed components, such as: installations or a raised floor system ($g_{k,add}$), **(iii)**: imposed loading (q_k) and **(iv)**: additional variable loading, for example: partition walls ($q_{k,add}$). The characteristic values are summarized in table 7.2. For the installations a self-weight of $0.25kN/m^2$ is adopted [99]. Based upon various online resources and Glabbeek [99], an initial self-weight of the floor finishing (either a raised floor or a suspended ceiling) of $0.30kN/m^2$ is considered. According to NEN-EN 1991 [98] clause 6.3.1.2 the value for the movable partition walls with a self-weight of $\leq 2.0kN/m$ is: $q_{i,add} = 0.8kN/m^2$. The imposed variable loading according to NEN-EN 1991/National Annex [100] table NB.1 - 6.2 is: $q_{imp} = 1.75kN/m^2$.

	Characteristic values [kN/m ²]	
Self-weight	q_k	4.46
Concrete modules	3.91	
Installations	0.25	
Floor finishing	0.30	
Variable loading	q_k	2.55
Imposed loading - category A (residential)	1.75	
Partition walls	0.8	

Table 7.2: Vertical loading on the residential units

7.2.3. Load combinations

The vertical load actions are outlined in paragraph 7.2.2. To check whether a structure can be classified as safe, the design should be based on limit states. Two main limit states are: **(i)**: serviceability limit state (SLS), which concerns the functioning of the structure under normal use and **(ii)**: ultimate limit state (ULS), which concerns the safety of the structure and/or people. For both limit states, different combinations of loads may be present. In NEN-EN 1990 [96] this is expressed by applying partial factors for actions. For ultimate limit state, the partial factors are presented in figure 7.2.

From figure 7.2 and the vertical loads defined in 7.2 it is concluded that the governing load combination equations under normal use become:

Equation 6.10a

$$q_{ed,uls} = 1.35 \cdot g_k + 1.5 \cdot \psi_0 \cdot q_k$$

$$q_{ed,uls} = 1.35 \cdot 4.46 + 1.5 \cdot 0.4 \cdot 2.55 = 7.55kN/m^2$$

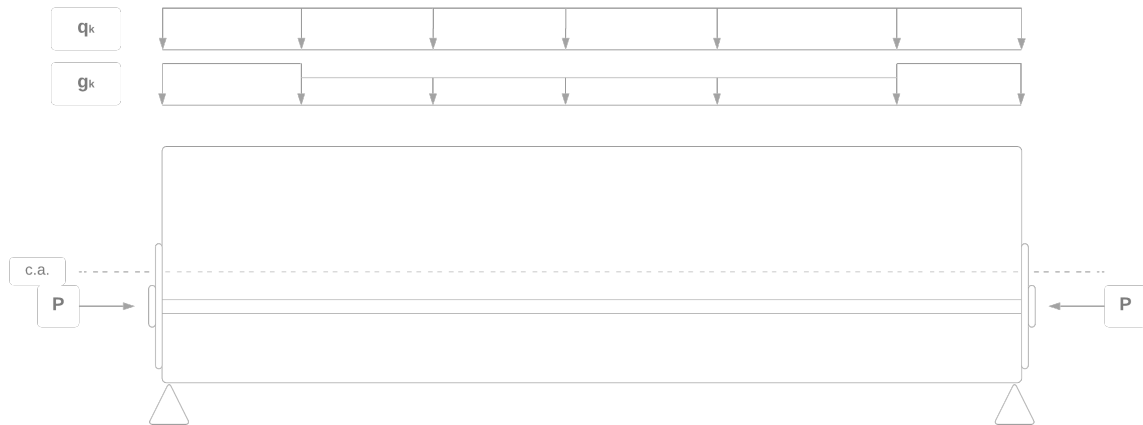


Figure 7.1: Loading scheme system

Tabel NB.4 - A1.2(B) — Rekenwaarden van belastingen (STR/GEO) (groep B)

Blijvende en tijdelijke ontwerpsituaties	Blijvende belastingen		Overheersende veranderlijke belasting	Veranderlijke belastingen gelijktijdig met de overheersende	
	Ongunstig	Gunstig		Belangrijkste (indien aanwezig)	Andere
(Vgl. 6.10a)	1,35 $G_{k,j,sup}$ ^a	0,9 $G_{k,j,inf}$		1,5 $\psi_{0,1} Q_{k,1}$	1,5 $\psi_{0,i} Q_{k,i}$ ($i > 1$)
(Vgl. 6.10b)	1,2 $G_{k,j,sup}$ ^b	0,9 $G_{k,j,inf}$	1,5 $Q_{k,1}$		1,5 $\psi_{0,i} Q_{k,i}$ ($i > 1$)

^a Bij vloeistofdrukken met een fysiek beperkte waarde mag zijn volstaan met 1,2 $G_{k,j,sup}$.

^b Deze waarde is berekend met $\xi = 0,89$.

Figure 7.2: Calculation values for loads (STR/GEO group B) [97]

Equation 6.10b

$$q_{ed,uls} = 1.2 \cdot g_k + 1.5 \cdot q_k$$

$$q_{ed,uls} = 1.2 \cdot 4.46 + 1.5 \cdot 2.55 = 9.12 \text{ kN/m}^2$$

Similar to the variable imposed loading, the combination factors (ψ) differ per category as well. In accordance with NEN-EN 1990/National Annex table NB.2 - A1.1 the combination factors are given in table 7.3.

Imposed load in buildings	ψ_0	ψ_1	ψ_2
Category A: residential	0.4	0.5	0.3

Table 7.3: Combination factors ψ

The partial factors for the load combinations in serviceability limit state are equal to 1.0. To determine the deflections and part of the prestressing losses, the quasi-permanent situation should be considered as well. The quasi-permanent situation consists of the self-weight of the structure, combined with a part of the variable load which is expected to be permanently present. This results in:

$$q_{ed,sls} = 1.0 \cdot g_k + 1.0 \cdot q_k$$

$$q_{ed,sls} = 1.0 \cdot 4.46 + 1.0 \cdot 2.55 = 7.01 \text{ kN/m}^2$$

$$q_{ed,QP} = 1.0 \cdot g_k + 1.0 \cdot \psi_2 \cdot q_k$$

$$q_{ed,QP} = 1.0 \cdot 4.46 + 1.0 \cdot 0.3 \cdot 2.55 = 5.23 \text{ kN/m}^2$$

In order to be able to perform initial checks at different locations in the cross-section, the maximum occurring bending moments should be determined in both serviceability and ultimate limit state. According to figure 7.1 the calculated loads should be multiplied with the width of the system (b). The moment induced by the eccentricity of the tendons should be determined as well. These moments are presented in eq. (7.1).

$$M_{q+g,sls} = \frac{(q_{ed,sls} \cdot b) \cdot l^2}{8} \quad M_{q+g,uls} = \frac{(q_{ed,uls} \cdot b) \cdot l^2}{8} \quad M_{p,0} = P_{m,0} \cdot e_p \quad (7.1)$$

7.2.4. Cross-sectional and material properties

Other geometrical properties of the system are calculated to perform various calculation checks further on, where:

$$b_w = b - n_{holes} \cdot d_{hole} \quad z = \frac{h}{2}$$

$$A = b \cdot h - \frac{n_{holes} \cdot \pi \cdot d_{hole}^2}{4} \quad W = \frac{I}{z}$$

$$I = \frac{b \cdot h^3}{12} - \frac{n_{holes} \cdot \pi \cdot d_{hole}^4}{64} \quad S = \frac{bh^2}{8} - n_{holes} \cdot \frac{\pi \cdot d_{hole}^2}{4} \cdot \frac{4 \cdot r_{hole}}{3\pi}$$

- b_w : width of the cross-section at the centroidal axis
 z : location of the centroidal axis in the cross-section
 W : section modulus
 I : second moment of area
 S : first moment of area above and about the centroidal axis

Geometry properties

$$h = 0.24 \text{ m} \quad b = 1.2 \text{ m} \quad d_{hole} = 0.16 \text{ m}$$

$$n_{holes} = 5 \quad b_w = 0.4 \text{ m} \quad b_{w,out} = 0.068 \text{ m}$$

$$e_p = 0.05 \text{ m} \quad d_{ps} = 0.17 \text{ m} \quad A = 0.187 \text{ m}^2$$

$$W = 0.0102 \text{ m}^3 \quad I = 0.001221 \text{ m}^4 \quad S = 0.00693 \text{ m}^3$$

Concrete properties C45/55 [101]

$$f_{ck} = 45 \text{ MPa} \quad f_{cd} = 30 \text{ MPa} \quad f_{cm} = 53 \text{ MPa}$$

$$f_{ctd} = 1.77 \text{ MPa} \quad E_{cm} = 36000 \text{ MPa} \quad \varepsilon_{cu} = 3.5\text{‰}$$

Tendon properties Y1860S7 [95]

$$\varnothing_{strand} = 15.7 \text{ mm} \quad A_p = 150 \text{ mm}^2 \quad E_p = 195000 \text{ MPa}$$

$$f_{p,0.1k} = 1640 \text{ MPa} \quad f_{pk} = 1860 \text{ MPa} \quad f_{py} = 1522 \text{ MPa}$$

$$\sigma_{pm,0} = 1394 \text{ MPa} \quad \rho_{1000} = 2.5\% \quad \Delta l_s = 5 \text{ mm}$$

7.3. Required amount of prestressing

The required amount of prestressing is depending on several variables. As discussed in section 6.2, the floor system should comply with a fully prestressed situation in serviceability limit state to prevent joint opening between the modules. This is one of the governing principles of the verification. If tensile stresses occur anywhere in the cross-section, the design should be reconsidered. Two critical locations where tensile stresses are most likely to occur are at:

- midspan: due to self weight of the system and the imposed vertical loading
- support location: due to the prestressing moments imposed by the eccentricity of the tendons

From literature, a reasonable first estimation of the total prestressing losses is 15% [102]. In order to calculate the stresses at both locations, an expression for the stresses should be obtained. At midspan location, three factors are affecting the stresses in the cross-section: an axial force due to the prestressing tendons, a moment due to the eccentricity of the tendons and the self-weight plus variable live load on the system. At the support locations, the effect of the self-weight plus variable live load can be neglected. The expression for the stress at midspan is presented in eq. (7.2) and an expression for the stress at support location is presented in eq. (7.3).

$$\begin{aligned}\sigma_{c,top} &= -0.85 \frac{P_{m,0}}{A_c} + 0.85 \frac{P_{m,0} \cdot e_p}{W} - \frac{M_{q+g,sls}}{W} \\ \sigma_{c,bottom} &= -0.85 \frac{P_{m,0}}{A_c} - 0.85 \frac{P_{m,0} \cdot e_p}{W} + \frac{M_{q+g,sls}}{W}\end{aligned}\quad (7.2)$$

$$\begin{aligned}\sigma_{c,top} &= -0.85 \frac{P_{m,0}}{A_c} + 0.85 \frac{P_{m,0} \cdot e_p}{W} \\ \sigma_{c,bottom} &= -0.85 \frac{P_{m,0}}{A_c} - 0.85 \frac{P_{m,0} \cdot e_p}{W}\end{aligned}\quad (7.3)$$

NEN-EN 1992 [101] clause 5.10.2.2 states that the concrete compressive stress in the system, resulting from the prestressing force and other loads at the time of tensioning of prestress, should be limited to (i): $\sigma_c \leq 0.6f_{ck}$. Moreover, to comply with the fully prestressed situation, the maximum allowable tensile stress in the system is (ii): $\sigma_t \leq 0$. Considering the loading scheme, presented in figure 7.1, these two requirements apply to:

- (i) midspan location at top fibre level and support location at bottom fibre level
- (ii) midspan location at bottom fibre level and support location at top fibre level

For the sake of brevity, calculations are presented for one span length only. Substitution of the geometrical parameters and the two requirements into eqs. (7.2) and (7.3), results in a prestressing force at $t = 0$ ($P_{m,0}$), under the assumption of 15% prestressing losses. Next, the minimum required amount of prestressing steel can be calculated ($A_{p,req}$). From the minimum amount of required prestressing steel, the total number of strands can be deduced. To finalise the calculations regarding the (initially) required amount of prestressing steel, the obtained values can be substituted back into eqs. (7.2) and (7.3) as a first cross-sectional check to see whether the requirements are met. For a span length of $l = 7.8m$ the required prestressing force at $t = 0$ is $P_{m,0} = 721.2kN$, resulting in:

$$\begin{aligned}A_{p,required} &= \frac{P_{m,0}}{\sigma_{pm,0}} = \frac{721.2 \cdot 10^3}{1394} = 518mm^2 \\ n_{strands} &= \frac{A_{p,required}}{A_p} = \frac{518}{150} = 3.45 = 4 \\ P_{m,0,total} &= n_{strands} \cdot A_p \cdot \sigma_{pm,0} = \frac{4 \cdot 150 \cdot 1394}{10^3} = 836.4kN \\ M_{p,0,total} &= P_{m,0,total} \cdot e_p = 836.4 \cdot 0.05 = 41.8kNm\end{aligned}$$

Analogous to the calculations for a span length of $l = 7.8m$, the required amount of prestressing steel for the other span lengths can be obtained as well. The results are presented in table 7.4. For a span length of $l = 6.0m$ the amount of prestressing steel is approximately on the limit for two tendons. At this moment, it is yet unknown whether the assumption of 15% is slightly conservative. Therefore, an extra strand is provided in the system. After the detailed analysis in 7.4, it should be verified whether the assumption is too conservative.

Span length [m]	$P_{m,0}$ [kN]	$A_{p,req}$ [mm ²]	$n_{strands}$ [–]	$A_{p,tot}$ [mm ²]	$P_{m,0,tot}$ [kN]	$M_{p,0,tot}$ [kNm]
5.4	345.6	248	2	300	418.2	20.9
6.0	426.7	306	3	450	627.3	31.4
6.6	516.3	370	3	450	627.3	31.4
7.2	614.5	441	3	450	627.3	31.4
7.8	721.2	518	4	600	836.4	41.8

Table 7.4: Required amount of prestressing steel for all span lengths

7.4. Prestressing losses

Properly designed prestressed structures consist of a calculation of the prestressing force exerted by the tendons on the concrete sections. An initial calculation, together with an assumption for the prestressing losses, has been made in section 7.3. The accuracy, precision and conservatism of the prestress loss estimation should be carefully considered. An underestimation of the prestressing losses can lead to service-load cracking and long-term durability concerns, while an overestimation may lead to uneconomical designs, due to a (unnecessarily) larger quantity of required prestressing tendons or, in the case of curved tendon profiles, larger tendon drapes. Therefore, appropriate estimation of all losses is essential for a safe, durable and economical structure.

Appropriate calculation guidelines for prestressing losses is provided in NEN-EN 1992 [101] and the national annex [103]. The total prestressing losses are subdivided into two categories: (i): immediate losses and (ii): time-dependent losses. Immediate losses are related to: friction, anchorage slip or wedge set and elastic deformations. Time-dependent losses are related to: creep, relaxation and shrinkage. The immediate prestressing losses are reviewed and calculated in section 7.4.1 and the time dependent prestressing losses in section 7.4.2

7.4.1. Immediate prestressing losses

In this section the immediate prestressing losses are reviewed and calculated. NEN-EN 1992 [101] provides expressions for the losses due to friction and instantaneous deformation of the system. An analytical expression for the losses due to wedge set is obtained from Walraven and Braam [102]. Relevant parameters in the determination of the losses are obtained from the European Technical Assessment of the applied post-tensioning system [95]. The results for all considered span lengths are summarised in one table at the end of this section.

Friction losses

During the prestressing of post-tensioned steel, a part of the prestressing force is lost due to friction between the tendon and duct. For this reason, the prestressing force is not constant along the length of the tendon. In general, the expression of NEN-EN 1992 [101] clause 5.10.5.2 is used to determine the frictional losses. This expression is presented in eq. (7.4), where:

$$\Delta P_{\mu} = P_{max} (1 - e^{-\mu(\theta+kx)}) \quad (7.4)$$

- P_{max} : maximum force at the active end during tensioning: $P_{max} = P_{m,0,tot}$
- μ : coefficient of friction between the tendon and duct: $\mu = 0.06$ [95]
- θ : sum of angular displacements over a distance x : straight tendons with assumed zero height difference between the anchorages: $\theta \approx 0$
- k : Wobble-effect for internal tendons: $k = 0.9 * 10^{-2}$ [95]
- x : distance along the tendon from the point where the prestressing force is equal to P_{max} : $x = L$

Anchorage slip

When strands are locked off in the anchorage, the wedges move over a small pre-specified distance. This distance is independent of the tendon unit, nominal diameter and strength grade [104]. NEN-EN 1992 [101] states that losses due to wedge draw-in of the anchorage devices should be taken into account during anchoring after tensioning. In general, slip of wedges is in the range of 5 – 15mm [102]. For short tendons lengths, the losses due to wedge set are relatively more severe than for longer tendon lengths. The values of the wedge draw-in of various anchoring systems are provided in the European Technical Assessment [95]. The expression for determining the losses due to anchorage or wedge slip is presented in eq. (7.5), where:

$$\Delta P_{ws} = \frac{\Delta l_s}{L} \cdot E_p \cdot A_p \quad (7.5)$$

L : span length of the system
 Δl_s : draw-in or slip of wedges: $\Delta l_s = 5mm$ [95]

Elastic deformations

If a prestressing force is applied to the system, not only will the concrete shorten, but so will the tendons that were previously tensioned. In other words, the total elastic deformation is governed by shortening of both the slab and the $(n - 1)$ tendons, where n is the total number of tendons. Shortening of the other tendons results in a prestressing force reduction. NEN-EN 1992 [101] clause 5.10.5.1 defines a mean loss per tendon. Summation of each mean tendon loss results in an expression for the total prestressing losses due to elastic deformations and is presented in eq. (7.6), where:

$$\Delta P_{el} = \frac{n(n-1)}{2} \cdot P_{m,0} \cdot \frac{E_p \cdot A_p}{E_c \cdot A_c} \quad (7.6)$$

n : total number of tendons
 E_p : modulus of elasticity of the prestressing steel
 $P_{m,0}$ and A_p : prestressing force and area of prestressing steel per tendon
 E_c and A_c : modulus of elasticity and area of concrete

Summary

For the sake of brevity, intermediate calculation results are not presented throughout the previous sections. Instead, the (immediate) prestressing losses due to friction, wedge set and elastic deformation for all considered span lengths are summarised in table 7.5.

Span length [m]	ΔP_μ [kN]	ΔP_{ws} [kN]	ΔP_{el} [kN]	$\sum \Delta P_0$ kN	$P_{m,0}$ [kN]	Δ_0 [%]
5.4	1.2	54.2	0.9	56.3	418.2	13.5
6.0	2.9	73.1	2.7	78.7	627.3	12.4
6.6	2.2	66.5	2.7	71.4	627.3	11.4
7.2	2.4	60.9	2.7	66.0	627.3	10.5
7.8	3.5	75.0	5.4	83.9	836.4	10.0

Table 7.5: Immediate prestressing losses due to friction, wedge set and elastic deformation

7.4.2. Time dependent prestressing losses

In this section, the time-dependent losses are reviewed and calculated. NEN-EN 1992 [101] and the national annex [103] provide expressions for the time-dependent losses. Relevant parameters in the determination of the losses are obtained from the European Technical Assessment of the applied post-tensioning system [95]. Three time-dependent prestressing losses are considered in this section, namely: relaxation, creep and shrinkage. The results for all considered span lengths are summarised in one table at the end of this section.

Relaxation

Time-dependent deformations occur in steel subjected to high stress levels. Deformations of concrete are usually small compared to the strains of prestressing steel. Therefore a constant time-independent deformation in the tendons can be assumed [102]. Relaxation of the prestressing steel will decrease the (effective) stress under imposed deformation. The relaxation of the prestressing steel primarily depends on three factors: **(i)**: initial stress, where relaxation strongly increases at higher initial stresses, **(ii)**: temperature, where relaxation proceeds faster at elevated temperatures and **(iii)**: manufacturing method and post-treatment of the steel. NEN-EN 1992 [101] distinguishes three classes. For each distinguished class, an expression is proposed to determine the stress reduction due to relaxation losses ($\Delta\sigma_{pr}$). These expressions are presented in eqs. (7.7) to (7.9), where:

- Class 1: wire or strand - ordinary relaxation:

$$\frac{\Delta\sigma_{pr}}{\sigma_{pi}} = 5.39 \cdot \rho_{1000} \cdot e^{6.7\mu} \left(\frac{t}{1000} \right)^{0.75(1-\mu)} \cdot 10^{-5} \quad (7.7)$$

- Class 2: wire or strand - low relaxation:

$$\frac{\Delta\sigma_{pr}}{\sigma_{pi}} = 0.66 \cdot \rho_{1000} \cdot e^{9.1\mu} \left(\frac{t}{1000} \right)^{0.75(1-\mu)} \cdot 10^{-5} \quad (7.8)$$

- Class 3: hot rolled and processed bars:

$$\frac{\Delta\sigma_{pr}}{\sigma_{pi}} = 1.98 \cdot \rho_{1000} \cdot e^{8.0\mu} \left(\frac{t}{1000} \right)^{0.75(1-\mu)} \cdot 10^{-5} \quad (7.9)$$

- σ_{pi} : the absolute value of the initial prestress (for unbonded tendons): $\sigma_{pi} = \sigma_{pm,0}$
 t : time after tensioning in hours: $t = 500000$ hours
 μ : ratio of initial prestress to characteristic strength: $\mu = \frac{\sigma_{pi}}{f_{pk}}$
 ρ_{1000} : value of relaxation loss at 1000 hours after tensioning at a mean temperature of 20 °C

Creep

Concrete structures response to loading is depending on various circumstances, both immediate and time-dependent. Development and magnitude of creep primarily depends on: relative humidity and temperature, development of degree of hydration, concrete strength class, cross-sectional dimensions and duration of loading. The magnitude of creep deformation is directly proportional to the elastic deformation [102]. Therefore, determination of a creep deformation factor ($\phi(t, t_0)$) is important to approximate creep effects present in the concrete. NEN-EN 1992 [101] clause B1 proposes a calculation procedure where the creep deformation factor ($\phi(t, t_0)$) can be calculated. The results are presented in eq. (7.10), where for a concrete strength class of C45/55:

$$\phi(t, t_0) = \phi_0 \cdot \beta_c(t, t_0) = 1.80 \quad (7.10)$$

- ϕ_0 : notional creep coefficient
 $\beta_c(t, t_0)$: coefficient to describe the development of creep with time after loading

$$\phi_0 = \phi_{RH} \cdot \beta(f_{cm}) \cdot \beta(t_0) = 1.80$$

$$\phi_{RH} = 1 + \left[\frac{1 - RH/100}{0.1 \sqrt[3]{h_0}} \cdot \alpha_1 \right] \cdot \alpha_2 = 1.60$$

$$\beta_{fm} = \frac{16.8}{\sqrt{f_{cm}}} = 2.31$$

$$\beta(t_0) = \frac{1}{0.1 + t_0^{0.20}} = 0.49$$

- ϕ_{RH} : factor to allow for the effect of relative humidity on the notional creep coefficient
 $\beta(f_{cm})$: factor to allow for the effect of concrete strength on the notional creep coefficient
 $\beta(t_0)$: factor to allow for the effect of concrete age at loading on the notional
 RH : relative humidity of the ambient environment in %: $RH = 50$
 f_{cm} : mean compressive strength of concrete at the age of 28 days: $f_{cm} = 53 \text{ MPa}$
 h_0 : notional size of the member: $h_0 = \frac{2A_c}{u} = 130 \text{ mm}$
 A_c : cross-sectional area: $A_c = 187 \cdot 10^3 \text{ mm}^2$
 u : perimeter of the member in contact with the atmosphere: $u = 2(b + h) = 2880 \text{ mm}$
 α_i : coefficients to consider the influence of the concrete strength

$$\beta_c(t, t_0) = \left[\frac{t - t_0}{\beta_H + t - t_0} \right]^{0.3} \approx 1.0$$

$$\beta_H = 1.5 \left[1 + (0.012 \cdot RH)^{18} \right] h_0 + 250 \alpha_3 \leq 1500 \alpha_3$$

$$\beta_H = 399 \leq 1215 \Rightarrow \beta_H = 399$$

$$\alpha_1 = \left[\frac{35}{f_{cm}} \right]^{0.7} = 0.75 \quad \alpha_2 = \left[\frac{35}{f_{cm}} \right]^{0.2} = 0.92 \quad \alpha_3 = \left[\frac{35}{f_{cm}} \right]^{0.5} = 0.81$$

- β_H : coefficient depending on the relative humidity and the notional member size
 t : age of concrete in days at the moment considered: $t = 500000 \text{ h} \approx 20833 \text{ days}$
 t_0 : age of concrete at loading in days: $t_0 = 28 \text{ days}$

NEN-EN 1992 [101] also provides expressions for the type of cement and for elevated or reduced temperatures. For cement class N and considering an ambient indoor temperature of 20 °C, no alterations have to be performed. The last consideration is related to the stress levels in the concrete. If the stress under quasi-permanent loads is $\geq 0.45 f_{ck}$, non-linear creep effects should be taken into account. From figure 7.4 and 7.5 it is evident that such stress levels are not reached. Therefore, non-linear creep effects can be disregarded.

Shrinkage

Shrinkage strain is composed of two components: drying shrinkage and autogenous shrinkage. Drying shrinkage develops slowly, since it is a function of the mitigation of water through the hardened concrete and is therefore time-dependent. Autogenous shrinkage develops during the hardening of concrete. Therefore, the main contribution is developed in the early days or weeks after casting [101]. Since the elements are prefabricated and not utilised during the curing stage of (minimum) 28 days, it is plausible to assume that the losses due to autogenous shrinkage are approximately zero. Hence, the value of the total shrinkage strain (ε_{cs}) can be expressed as in eq. (7.11), where:

$$\varepsilon_{cs} = \varepsilon_{cd} + 0 \cdot \varepsilon_{ca} = 3.8 \cdot 10^{-4} \quad (7.11)$$

- ε_{cd} : drying shrinkage strain
 ε_{ca} : autogenous shrinkage strain

$$\varepsilon_{cd} = \beta_{ds}(t, t_s) \cdot k_h \cdot \varepsilon_{cd,0} = 3.8 \cdot 10^{-4}$$

$$\beta_{ds} = \frac{t - t_s}{(t - t_s) + 0.04\sqrt{h_0^3}} \approx 1.0$$

$$\varepsilon_{cd,0} = 0.85 \left[(220 + 110\alpha_{ds1}) e^{-\alpha_{ds2} \frac{f_c}{f_{cm,0}}} \right] \cdot \beta_{RH} = 4.0 \cdot 10^{-4}$$

$$\beta_{RH} = 1.55 \left[1 - \left(\frac{RH}{RH_0} \right)^3 \right] = 1.36$$

k_h :	coefficient depending on the notional size according to table 3.3 from NEN-EN 1992 [101]. Intermediate values for k_h can be linearly interpolated, resulting in $k_h = 0.95$
$\varepsilon_{cd,0}$:	basic drying shrinkage strain
t :	age of concrete at the moment considered in days
t_s :	age of concrete at the beginning of dry shrinkage or swelling, usually this is at the end of the curing phase: $t_s = 28$ days
α_{ds1} and α_{ds2} :	coefficient depending on the cement type: for Class N: $\alpha_{ds1} = 4$ and $\alpha_{ds2} = 0.12$
f_{cm} :	mean compressive strength of concrete at $t = t_s$: $f_{cm} = 53$ MPa
$f_{cm,0}$:	10 MPa
RH :	relative humidity of the ambient environment: $RH = 50\%$
RH_0 :	100%

Summary

In this last section the calculation results are presented. From Annex 11 of the European Technical Assessment of the applied post-tensioning system [95] the relaxation losses after 1000 hours (ρ_{1000}) is $\leq 2.5\%$. Therefore, in accordance with NEN-EN 1992 [101], the post-tensioning tendons can be classified as: Class 2. Substitution of the parameters into eq. (7.8) results in a stress reduction due to relaxation. Furthermore, NEN-EN 1992 [101] states that the other time-dependent losses may be calculated by considering two reductions of stress:

- Reduction of strain, caused by the deformation of concrete due to creep and shrinkage, under permanent loads
- Reduction of stress in the prestressing steel due to relaxation under tension

Therefore, this interaction can approximately be taken into account with a reduction factor of 0.8. The simplified expression of NEN-EN 1992 [101] clause 5.10.6 is given in eq. (7.12), where:

$$\Delta P_{c+s+r} = A_p \frac{\varepsilon_{cs} \cdot E_p + 0.8 \cdot \Delta\sigma_{pr} + \frac{E_p}{E_{cm}} \cdot \phi(t, t_0) \cdot \sigma_{c,QP}}{1 + \frac{E_p}{E_{cm}} \frac{A_p}{A_c} \left(1 + \frac{A_c}{I_c} \cdot z_{cp}^2 \right) [1 + 0.8 \cdot \phi(t, t_0)]} \quad (7.12)$$

$$\sigma_{c,QP} = -\frac{P_{m,0}}{A_c} - \frac{P_{m,0} \cdot e_p}{W} + \frac{M_{ed,QP}}{W} \quad M_{ed,QP} = \frac{1}{8} \cdot q_{ed,QP} \cdot l^2$$

$\Delta\sigma_{pr}$:	absolute value of the stress reduction due to relaxation of the prestressing steel
$\sigma_{c,QP}$:	absolute value of the stress in the concrete under quasi-permanent actions
$M_{ed,QP}$:	moment caused by the loading under quasi-permanent actions
$q_{ed,QP}$:	value of the loading under quasi-permanent actions obtained from section 7.2.3 and to be multiplied with the considered width (w) of the system
I_c :	second moment of area of the concrete cross-section
z_{cp} :	distance between centre of gravity and tendons: $z_{cp} = e_p$

Concluding to this last section, the time-dependent losses can be calculated by substitution of the parameters into eq. (7.12). The time-dependent losses account for the effects of relaxation, creep and

shrinkage. For all considered span lengths, the results are presented in table 7.6. The sixth column represents the total losses due to immediate and time-dependent effects. It can be concluded that the initial estimation of the prestressing losses (15%) proposed in literature [102] is in line with the calculated results, albeit slightly unconservative for small tendon lengths.

Span length [m]	$\sum \Delta P_0$ [kN]	Δ_0 [%]	ΔP_{c+s+r} [kN]	Δ_∞ [%]	Δ_{tot} [%]	$P_{m\infty}$ [kN]	$M_{p\infty}$ [kNm]
5.4	56.3	13.5	21.9	5.2	18.7	340.0	17.0
6.0	78.7	12.4	32.4	5.2	17.6	517.1	25.9
6.6	71.4	11.4	32.4	5.2	16.6	523.5	26.2
7.2	66.0	10.5	32.4	5.2	15.7	528.9	27.9
7.8	83.9	10.0	42.5	5.1	15.1	709.9	35.5

Table 7.6: Total prestressing losses due to immediate and time-dependent effects

7.5. Cross-sectional checks in SLS

In this section, the floor system is verified with respect to the loads in serviceability limit state. This limit state relates to: (i): the functioning of the structure under normal use, (ii): the comfort of the users and (iii): the appearance of the structure or building. In this context, appearance refers to measures such as deflections and crack formation, rather than to aesthetic qualities. Three checks are performed: stresses in the cross-section in paragraph 7.5.1, deformations of the floor system in paragraph 7.5.2 and vibrations in paragraph 7.5.3.

7.5.1. Cross-sectional stresses

One of the cornerstones in the design is that, due to the self-weight and the variable imposed loading, no tensile stresses occur in the cross-section in serviceability limit state. This is referred to as a fully prestressed situation. The maximum tendon eccentricity is depending on several variables. The first one is related to the edge (and center-to-center) distances imposed by the manufacturer of the post-tensioning system. Next, geometrical properties of the system, mainly parameters which are related to the self-weight, should be considered. Examples of these geometrical properties are the height of the system or the diameter of the weight-reducing voids. The last variable is the location of the axial compressive force, imposed by the tendons, to achieve a fully prestressed situation.

When a compression member is loaded by an axial force applied through the centroid, the entire cross-section is uniformly stressed. A combination of axial compression and bending is generated when the member is subjected to an eccentrically applied loading. Therefore, an eccentric load, placed a suitable distance from the centroid, may result in tensile stresses within the cross-section. The design guidelines for many structures, such as prestressed concrete beams, often require that tensile stresses should be prevented from developing in the cross-section. This zone, which defines the location where an axial load may be applied without inducing tensile stresses, is called the kern area. The kern area has also been referred to as the core or the limit zone [105]. An example of the kern area in a T-shaped beam is presented in figure 7.3.

Figures 6.6a and 6.6b present the dimensions of the proposed system. A quick check to verify whether the location of the axial force is within the kern area of the cross-section, is to divide the section modulus over the cross-sectional area. This is valid, because the location of the centroidal axis of the cross-section is at $\frac{h}{2}$, which implies that: $W_{ct} = W_{cb}$. The result is the maximum eccentricity that can be applied without the occurrence of tensile stresses due to the axial force. From the cross-sectional properties, the maximum tendon eccentricity is 54.5mm. The applied eccentricity is 50mm, so it is expected that no tensile stresses occur. However, it should be verified for two locations within the cross-section: (i): top fibre level and (ii): bottom fibre level and for two (fictitious) moments in time:

- $t = 0$: before all immediate and time-dependent losses
- $t = \infty$: after all prestressing losses have occurred

The results are presented in figure 7.4 for a span length of $5.4m$ and in figure 7.5 for span length of $7.8m$. For both span lengths, it can be concluded that no tensile stresses occur in the cross-section and, therefore, comply with the requirement of a fully-prestressed situation in serviceability limit state. Due to the different amount of required tendons for each span length, the absolute values of the stresses differ. However, for intermediate span lengths, the governing requirement is fulfilled.

In figures 7.4b and 7.5b there is almost no noticeable difference in the stresses at the two considered times moments. This can be explained by the fact that the eccentricity of the tendons is chosen such that is close to the lower limit of the kern area of the cross-section: $e_p = 50mm$ and $e_{p,max} = 54.5mm$. Therefore, at top fibre level, the effect of the compressive force and the induced bending moment, due to the tendon eccentricity, (approximately) counterbalance each other. Hence, the main contribution to the increase of stress is from the imposed vertical loading and the self-weight of the system.

7.5.2. Deformations

Structures or structural components are expected to function properly for its entire design life. For most buildings, this is 50 years. According to the Building Decree (in Dutch: 'Bouwbesluit') most requirements are related to the strength and safety of the structure. Additional requirements for deformations, in horizontal and vertical direction, from a user perspective, are desirable and should therefore remain within acceptable limits. NEN-EN 1990/National Annex [97] proposes limit values for conventional situations to ensure that no (significant) damage is caused to all elements supported by the structure and that the users of the building are not hindered by the static deformation. For the proposed floor system, the main contribution to the deformations are in vertical direction.

Therefore, the second check in serviceability limit state is regarding the deflections of the system under imposed loading actions. NEN-EN 1990/National Annex [97] clause A1.4.3 dictates that the governing loads are based on the quasi-permanent combination for short- and long-term properties if the general appearance of the structure is considered. Figure 7.6 defines four different vertical deflections, where:

- w_c : precamber (in Dutch: 'zeeg') of the unloaded structural member
- w_1 : initial deflection under permanent loads from the quasi-permanent combination determined with the short-term properties
- w_2 : additional deflection under permanent loads from the quasi-permanent load combination determined with the long-term properties minus the deflection from the quasi-permanent load combination determined with short-term properties
- w_3 : supplementary deflection induced by the remaining part of the variable actions determined with short-term properties
- w_{tot} : total deflection as the sum of w_1 , w_2 and w_3
- w_{max} : remaining deflection taken into account the precamber of the member (w_c)

If the functioning or damage of the structure to non-structural elements, such as cladding or partitions walls, is considered, the governing loads should be based on the frequent load combination, instead of the quasi-permanent load combination. NEN-EN 1990/National Annex [97] clause A1.4.3 defines maximum deflection limits for three generic cases. These are presented in table 7.7.

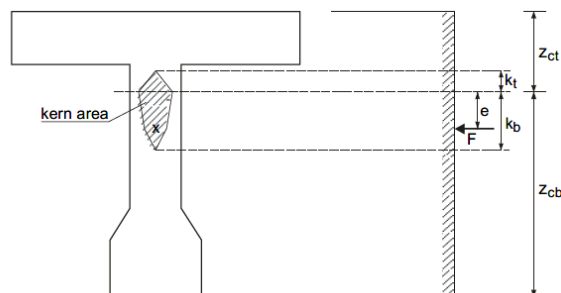
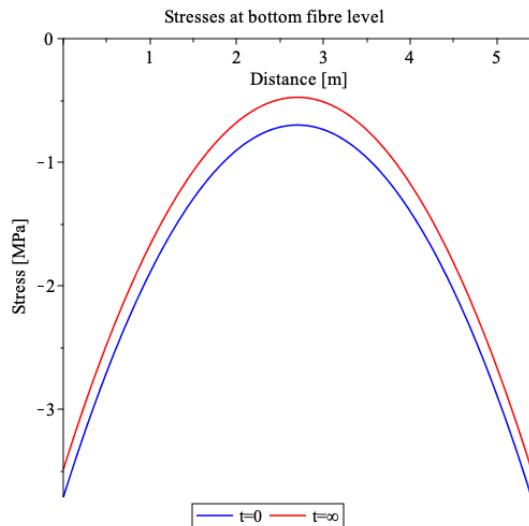
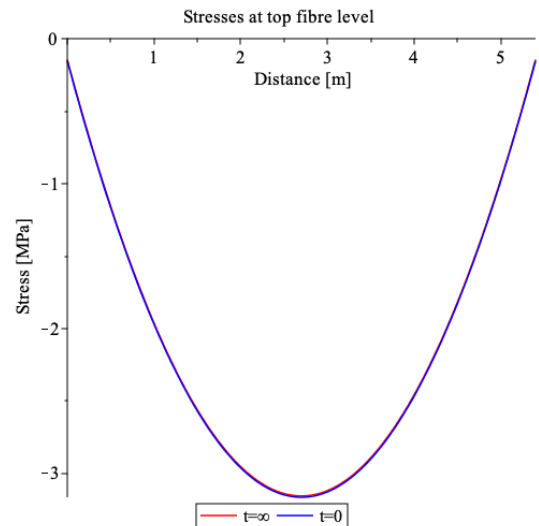


Figure 7.3: Example of the kern area of a T-shaped beam [102]

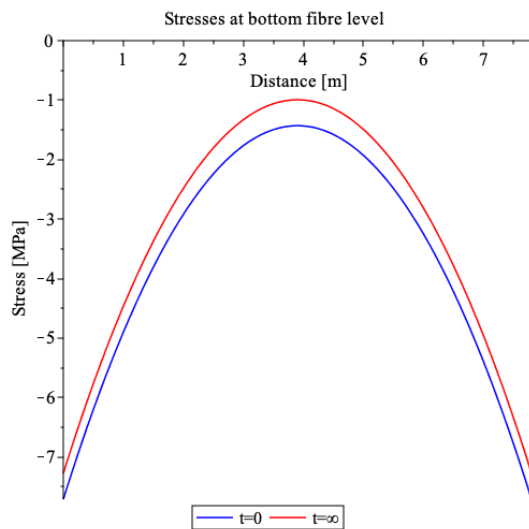


(a) Stresses at bottom fibre level

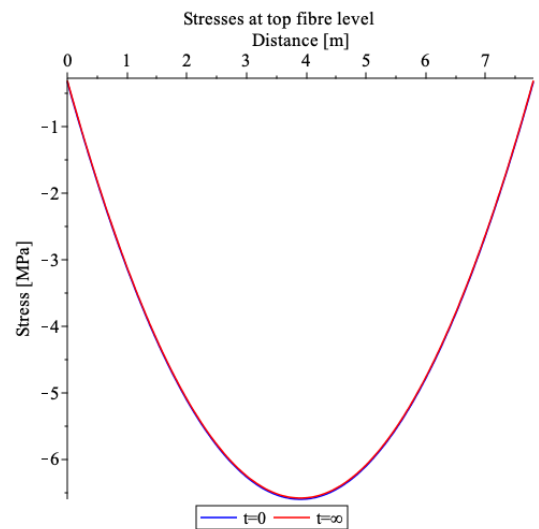


(b) Stresses at top fibre level

Figure 7.4: Stresses in the cross-section for a span length of 5.4 m



(a) Stresses at bottom fibre level



(b) Stresses at top fibre level

Figure 7.5: Stresses in the cross-section for a span length of 7.8 m

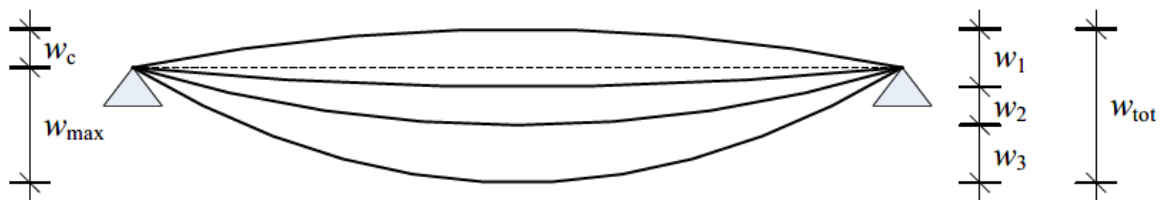


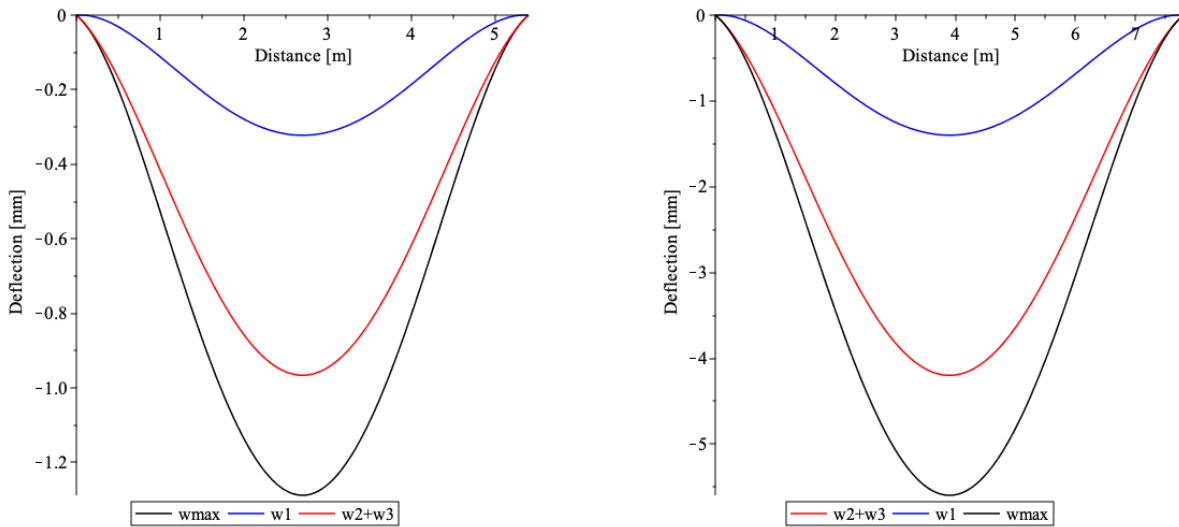
Figure 7.6: Vertical components of the deflections defined by NEN-EN 1990/National Annex [97]

Due to the defined maximum deflection limits, the deflections according to the frequent load combination are more significant than those based upon the quasi-permanent load combination. Therefore, the deflection lines of the system are presented according to the frequent load combination. Figure 7.7 presents the deflection lines for two span lengths: $l = 5.4\text{m}$ and $l = 7.8\text{m}$. The results for all floor

	$w_2 + w_3$	w_{max}
Floors with crack-sensitive partition walls	$\leq l_{rep}/500$	$\leq l_{rep}/250$
Other floors or roofs used extensively by persons	$\leq l_{rep}/333$	$\leq l_{rep}/250$
Other roofs (only accessible for maintenance)	$\leq l_{rep}/250$	$\leq l_{rep}/250$

Table 7.7: Vertical deformation limits for buildings [97]

spans, together with the most stringent limit of table 7.7, floors with crack-sensitive partition walls, are presented and verified in table 7.8.



(a) Deflections for a span length of 5.4m

(b) Deflections for a span length of 7.8m

Figure 7.7: Deflection lines according to the frequent load combination

Span length		Deflections		Check
[m]		[mm]	[mm]	[-]
5.4	$w_2 + w_3$	0.97	\leq 10.8	Satisfied
	w_{max}	1.29	\leq 21.6	Satisfied
6.0	$w_2 + w_3$	0.57	\leq 12.0	Satisfied
	w_{max}	0.57	\leq 24.0	Satisfied
6.6	$w_2 + w_3$	1.98	\leq 13.2	Satisfied
	w_{max}	2.60	\leq 26.4	Satisfied
7.2	$w_2 + w_3$	4.06	\leq 14.4	Satisfied
	w_{max}	5.63	\leq 28.8	Satisfied
7.8	$w_2 + w_3$	4.20	\leq 15.6	Satisfied
	w_{max}	5.60	\leq 31.2	Satisfied

Table 7.8: Results regarding deflections for all span lengths

From table 7.8 it can be concluded that, for all span lengths, the requirements for the deflections are amply met. Prestressing, whether it is bonded or unbonded, fundamentally influences the behaviour of structures under serviceability conditions. The effects of post-tensioning tendons are simulated as equivalent loads that counteract the loads imposed by self-weight and/or applied live loads. For this reason, deflection control is beneficial, especially for long spans or high live loads. Despite the fact that the span lengths adopted in this thesis are not considerably large nor is the live load substantially high, the beneficial effect of the prestressing on the deflections is evident.

An important assumption in determining the deflections of the segmented system is that the deflection behaviour is similar as one of a monolithic slab. The validation of this assumption is illustrated in the stress diagrams of figures 7.4 and 7.5. The fully prestressed situation results in zero tensional stresses in the cross-section and, therefore, the joints or interfaces of the elements remain closed in serviceability limit state. For this reason, it is validated that the segmented slab results in similar deflection behaviour as of a monolithic slab. This assumption is validated for the other span lengths as well.

7.5.3. Vibrations

Under serviceability conditions, the last aspect that should be taken into account is that of the vibrations of a structure or structural component. Satisfactory vibration behaviour should be considered for: **(i)**: the comfort of the user and **(ii)**: functioning of the structure, including prevention of damage to partition walls, cladding or objects within the building due to vibrations. In order for a structure or structural component not to exceed the serviceability limits when exposed to vibrations, the natural frequency of vibration should be determined and should not exceed appropriate limits, which depend on the functioning of the building and on the source of vibration. Clients or relevant authorities may impose these limit values.

In general, for floors that are frequently walked upon, such as floors of residential and office buildings, the limit value for the first eigenfrequency should not be lower than the highest frequency induced by people walking: 3 Hz . NEN-EN 1990/National Annex [97] clause A1.4.4 states that if the sum of all characteristic values of the permanent and ψ_2 times the variable imposed load is at least 5 kN/m^2 , further calculations are not required. Moreover, a maximum deflection for short term behaviour for the quasi-permanent load combination of 34 mm suffices in many cases. Should it be the case that none of the above-standing requirements are satisfied, a detailed analysis can be performed according to *Trillingen van vloeren door lopen: Richtlijn voor het voorspellen, meten en beoordelen* [106]. Especially for light-weight floor systems, a detailed analysis should be performed to prevent complaints regarding vibrations.

One important remark of NEN-EN 1990/National Annex [97] clause A1.4.4 is that, for prestressed structures, the load induced by the prestress as part of the permanent load should not be considered when assessing resonance. However, for the proposed floor system, a detailed analysis can be omitted due to the fact that the characteristic value of the permanent and ψ_2 times the variable imposed load is 6.26 kN/m^2 . Therefore, in accordance with NEN-EN 1990/National Annex [97], satisfactory vibration behaviour is ensured.

7.6. Bending moment resistance in ULS

Unbonded tendons in structures are generally subdivided into two categories: **(i)**: internally embedded inside the concrete, as is the case for most post-tensioned slabs or **(ii)**: external to the concrete, as is the case for post-tensioned box girder bridges for example. The main difference is in the deflected shape of the structure and the tendon. The deflections of internal tendons follow the deflected shape of the slab throughout the entire span, whereas the deflections of external tendons is limited to the deflection at deviator positions in the slab or girder and, therefore, is different for other locations in the span. The proposed floor system has embedded tendons inside the concrete, which are anchored at both ends of the slab and can therefore be classified as internal unbonded post-tensioned tendons.

Analysis of members prestressed with unbonded tendons, during loading and up to their ultimate limit state offers one additional level of complexity in comparison to members prestressed with bonded tendons. This additional complexity is related to the stress increase beyond the effective prestress. The stress increase (Δf_{ps}) is member-dependent rather than section-dependent. Sectional analysis is therefore insufficient. Moreover, the stress in unbonded tendons is assumed to be uniform along the entire length of the tendons between the anchorages. Because the stress at ultimate in internally unbonded (or external) tendons (f_{ps}) cannot be determined directly using conventional strain compatibility and sectional analysis, as is the case with bonded tendons, a deformation analysis for the entire member is required during elastic, inelastic and at ultimate limit state [107].

Previously conducted studies focused on non-linear analysis or numerical techniques to describe the behaviour throughout loading or at ultimate limit state. In a very elaborated literature study, Alqam and

Alkhairi [108] present a detailed chronological review of these previously conducted studies. It also consists of an overview of the prediction equations for the stress at ultimate limit state for internally unbonded and/or external tendons of simply supported beams. The review covers the most relevant factors, such as: span-to-depth ratio, second-order effects, length of the plastic hinge, slip at deviators and experimental verification. In later writing, Alqam et al. [107] argue that, in general, two schools of thought prevail among these studies:

1. The emphasis on the effect of the span-to-depth ratio [109]
2. The equivalent length of the plastic hinge that forms at the critical cross-section [110]

In traditional strength analysis of prestressed concrete members at the section of maximum moment, three equations are required to solve three unknowns. The three unknowns in the analysis are: **(i)**: the depth of the neutral axis (c), **(ii)**: the ultimate stress in the tendon at failure (f_{ps}) and **(iii)**: the ultimate limit state moment (M_u). The three equations that can be used to solve the unknowns are: **(i)**: moment equilibrium equation, **(ii)**: force equilibrium equation and **(iii)**: an equation for the ultimate stress in the tendon. A general approach to determine the ultimate stress in the tendon is presented in eq. (7.13), where:

$$f_{ps} = f_{pe} + \Delta f_{ps} \quad (7.13)$$

f_{ps} : ultimate stress in the tendon
 f_{pe} : effective prestress due to the imposed loading after all losses
 Δf_{ps} : stress increase beyond the effective prestress

Thus it is crucial for the determination of the ultimate limit state moment (M_u) to accurately predict the ultimate stress in the tendons (f_{ps}). This can either be done according to various codes of practice or by proposed equations of various researchers, against available experimental data.

Alqam et al. [107] used extensive statistical analysis techniques to assess the strength, accuracy and degree of conservatism of the variously proposed equations. The coefficient of correlation (CoC) was introduced to assess the strength of predicted versus experimental data relative to a best-fit straight line, but not necessarily relative to the 45°-line, which represents perfect correlation and accuracy. In order to improve the CoC-computations and to confirm the predicted accuracy of the proposed equations, the sum of the least square deviation error, LS method, has been used to measure the statistical accuracy of the results with respect to the 45°-line. The highest accuracy is obtained when the sum of least square deviation error is minimized while the CoC is maximized. The last statistical analysis measure used is consisting of a percentage representing the number of predicted-to-experimental data points that are less than 1.0 divided by the total number of test data. In total, Alqam et al. [107] utilised 227 test data results, originating from previously conducted research. The obtained percentage (%P<E) indicates the conservatism of the proposed equations. A higher percentage indicates a more conservative prediction, based on the test data used [107].

In paragraph 7.6.1, one proposed equation for f_{ps} of each school of thought, so two equations in total, are evaluated based on the accuracy and degree of conservatism. The paragraph is finalised with a recommended equation for code implementation, proposed by Alqam et al. [107]. Paragraph 7.6.2 presents various codes of practice that impose limit values or straightforward closed-form calculation procedures to determine f_{ps} .

7.6.1. Previously conducted research

Since the sixties of the past century, a substantial amount of research projects have been carried out to predict and define closed-form calculation procedures or equations for f_{ps} for the purpose of code implementation. Twenty-five equations are reviewed and discussed in the study of Alqam et al. [107]. As mentioned in the previous section, two of those research projects are evaluated and highlighted in this paragraph. The fundamental basis is different for both studies: the first one is primarily based on the span-to-length ratio and the second study is based on the equivalent length of the plastic hinge. The recommended equation for code implementation, proposed by Alqam et al. [107], is a continuation of

the first study. All studies provide closed-form procedures to determine two of the three unknowns: the height of the neutral axis (c) and the ultimate stress in the tendon (f_{ps}). The ultimate limit state moment (M_u) can be determined based upon the moment equilibrium equation. The results are presented in paragraph 7.6.3.

Naaman and Alkhairi (1991)

Naaman and Alkhairi [109] present a new rational approach for calculating f_{ps} for internally unbonded tendons. Starting from a detailed review for expressions of the stress in the tendons using a bond reduction coefficient, while assuming elastic cracked analysis for different loading situations and tendon profiles. At ultimate limit state, Naaman and Alkhairi [109] propose the concept of a bond reduction coefficient (Ω_u) expressed as a function of the ratio of the strain increment beyond the effective prestress (f_{pe}). The bond reduction coefficient accounts for the most important variables, namely: the loading conditions and the span-to-depth ratio (L/d_{ps}) of the member and is derived using 143 available test beams from previous research. Together with the ratio of the neutral axis at ultimate limit state to the depth of the prestressing steel (c/d_{ps}), Naaman and Alkhairi [109] develop an equation to predict the ultimate stress (f_{ps}). The proposed equation accounts for tendons spanning multiple fields as well. A limitation for the ultimate stress of the tendons (f_{ps}) is introduced to ensure that the tendon stress remains within the linear elastic range. The values for the bond reduction coefficient (Ω_u) are chosen such that the best correlation between experimental and analytical results is obtained. However, Naaman and Alkhairi [109] argue that these values should be calibrated in such a way that the results are more conservative than the experimental results. For one-point loading: 2.6 should be reduced to 1.5 and for two-point or uniform loading: 5.6 should be reduced to 3.0. Nevertheless, the equations and proposed values for Ω_u at ultimate limit state are presented in eq. (7.14), where:

$$f_{ps} = f_{pe} + \Delta f_{ps} = f_{pe} + \Omega_u E_{ps} \varepsilon_{cu} \left(\frac{d_{ps}}{c} - 1 \right) \frac{L1}{L2} \quad (7.14)$$

$$f_{ps} \leq 0.94 f_{py}$$

$$\Omega_u = \frac{2.6}{L/d_{ps}} \quad \text{for one-point loading} \quad \Omega_u = \frac{5.4}{L/d_{ps}} \quad \text{for two-point or uniform loading}$$

- L1: length of loaded span or sum of lengths of loaded spans, affected by the same tendon
- L2: length of the tendon between end anchorages
- ε_{cu} : concrete strain at ultimate loading = 0.003 [109]
- f_{py} : yield strength of prestressing steel
- E_{ps} : modulus of elasticity of prestressing steel
- d_{ps} : depth from the extreme compressed fibre to the centroid of the prestressing steel

In order to calculate the depth of the neutral axis (c), Naaman and Alkhairi [109] propose an equation, based upon force equilibrium, assuming rectangular section behaviour of a T-section. This equation takes into account the presence of non-prestressed reinforcement both in the compression and in the tensile zone. For rectangular cross-sections or rectangular section behaviour of flanged sections: $b_w = b$. The full equation and the reduced equation in case of the proposed floor system, where prestressing reinforcement is present only and the cross-section is rectangular, are presented in eq. (7.15).

$$A_p f_{ps} + A_s f_y - A'_s f'_y = 0.85 \beta_1 f'_c (b - b_w) h_f + 0.85 \beta_1 f'_c b_w c$$

$$A_p f_{ps} = 0.85 \beta_1 f'_c b_w c \quad (7.15)$$

- A_s and A'_s : area of non-prestressed reinforcement in the tensile and compression zone
- f_y and f'_y : yield strength of non-prestressed reinforcement in the tensile and compression zone
- β_1 : ACI code stress block reduction factor
- f'_c : concrete compressive strength
- b : beam width of a rectangular section or flange width of a T-section
- b_w : web width of a T-section
- h_f : flange thickness of a T-section

Equations 7.14 and 7.15 should be solved simultaneously to determine the maximum stress increase (Δf_{ps}) at ultimate limit state. The term bond reduction coefficient can also be interpreted as a strain reduction coefficient for members where primarily unbonded tendons are present. Alqam et al. [107] conclude that the generated scatter of predicted results shows high accuracy with a comparable high correlation (CoC). The results are presented in figure 7.9. The percentage which indicates the degree of conservatism (%P<E) is 63%, indicating that 63% of the predicted results is on the safe side. Moreover, the proposed equations, with the calibrated values for Ω_u , were adopted for implementation in the AASHTO LRFD code [111] in 1994.

He and Liu (2010)

He and Liu [110] propose a simple unified methodology for computation of the ultimate tendon stress (f_{ps}) in internally unbonded and externally prestressed beams under both serviceability and ultimate limit state loading. In total, 89 test beam results with internally unbonded tendons are adopted from previously conducted research. It was found that the AASHTO code [111] specifications were very conservative compared to the experimental results and more consistent and accurate equations should be proposed. In their study, He and Liu [110] specifically considered second-order effects. In the proposed equations, two reduction factors for second-order effects are provided to account for: stress reduction (R_s) and depth reduction (R_d). However, He and Liu [110] argue that second-order effects can be ignored if deviators are placed symmetrically near the third point along the span. The tendon elongation is expressed as a function of the eccentricity and beam curvature, which is primarily based on the formation of a plastic hinge. In an elastic analysis, the results are very similar to Naaman and Alkhairi [109]. At ultimate limit state, the ratio of tendon eccentricity and the neutral axis depth (e_m/c) has significant influence on the maximum stress increase (Δf_{ps}). Analogous to previous studies, He and Liu [110] consider various loading situations, different tendon layouts and continuous beams in their analysis as well. The proposed equations and variables at ultimate limit state are presented in eq. (7.16), where:

$$\begin{aligned} f_{ps} &= f_{pe} + \Delta f_{ps} = f_{pe} + \kappa E_{ps} \frac{e_m}{c} R_s \frac{L_1}{L_2} \\ f_{ps} &\leq 0.8 f_{pu} \end{aligned} \quad (7.16)$$

$$\begin{aligned} \kappa &= 1.26 \cdot 10^{-3} \left(0.3 + \frac{3}{L/d_{ps}} \right) && \text{for one-point loading} \\ \kappa &= 1.62 \cdot 10^{-3} \left(0.78 + \frac{2.35}{L/d_{ps}} \right) && \text{for two-point or uniform loading} \\ R_s &= 1.0 && \text{for internally unbonded tendons} \\ R_s &= 1 - \frac{L/e_m}{83.3} \frac{\phi}{\eta} && \text{for external tendons} \end{aligned}$$

- κ : deflection reduction coefficient with respect to the loading
- e_m : eccentricity of the prestressing steel
- R_s : stress reduction coefficient for second-order effects
- f_{pu} : specified tensile strength of prestressing steel

In the stress reduction coefficient for second order effects two parameters are present: ϕ and η . These parameters are depending on three variables: loading situation, tendon profile and the ratio of end eccentricity to maximum eccentricity. The values of these parameters for several situations are presented in figure 7.8. Moreover, He and Liu [110] propose a closed-form procedure to facilitate hand calculations in order to determine the maximum stress increase (Δf_{ps}) in accordance with the proposed methodology. For more detailed information is referred to the research paper of He and Liu [110].

Alqam et al. [107] conclude that the generated scatter of predicted results shows good accuracy with an excellent correlation (CoC). The results are presented in figure 7.10. The percentage which indicates

the degree of conservatism (%P<E) is 94%, indicating that 94% of the predicted results is on the safe side. It is noted that this resulted in the highest degree of conservatism throughout the twenty-five analysed equations [107].

Load case	Tendon profile	η	ϕ	k_1
		6	4.80	1
		$4-2\beta$	0.80	0
		$\frac{46-8\beta}{9}$	0.45	0.148
		$\frac{144}{23}$	4.95	1
		$\frac{88-56\beta}{23}$	0.94	0
		$\frac{100-24\beta}{23}$	0.41	0.130
		$\frac{32}{5}$	4.97	1
		$4-2.4\beta$	0.97	0
		$\frac{32(22-5\beta)}{135}$	0.43	0.131

Figure 7.8: Values of parameters under typical load situations and tendon profiles [110]

Alqam et al. (2020)

Based on the results from the extensive statistical analysis, adopting a database of 227 simply supported beams from fifteen research groups, presented an understanding of how each proposed equation for the ultimate tendon stress (f_{ps}) fares in terms of accuracy and correlation. Alqam et al. [107] conclude that the equation proposed by Naaman and Alkhairi [109] stood among others for its rational development and accuracy. With a more extended database compared to Naaman and Alkhairi [109], Alqam et al. [107] carried out a separate regression analysis with some trial-and-error approaches to develop a new expression for the bond reduction (or strain reduction) coefficient (Ω_u). To avoid unrealistic high or low tendon stress increases (Δf_{ps}), Alqam et al. [107] introduce upper and lower bound limits. Moreover, Alqam et al. [107] further calibrate the values for the strain reduction coefficient (Ω_u) and more conservative upper and lower bound limits for code implementation. Nevertheless, the proposed equations and parameters at ultimate limit state, with maximised accuracy and correlation, together with the upper and lower bound limits, are presented in eq. (7.17) and in figure 7.11, where:

$$f_{ps} = f_{pe} + \Delta f_{ps} = f_{pe} + \Omega_u E_{ps} \varepsilon_{cu} \left(\frac{d_{ps}}{c} - 1 \right) \frac{L1}{L2} \leq 0.86 f_{pu} \quad (7.17)$$

$$f_{ps} \geq f_{pe} + 0.50 f_{py} \tilde{w}_{pe}$$

$$\Omega_u = 0.05 \left(\frac{d_{ps} - h/2}{0.25 d_{ps}} \right) \left[0.20 + \frac{18}{L/d_{ps}} \right] \quad \text{for one-point loading}$$

$$\Omega_u = 0.09 \left(\frac{d_{ps} - h/2}{0.25 d_{ps}} \right) \left[1.41 + \frac{18}{L/d_{ps}} \right] \quad \text{for two-point or uniform loading}$$

$$\tilde{w}_{pe} = \frac{A_{ps} \cdot f_{pe} + A_s \cdot f_y}{f'_c \cdot b \cdot d_{ps}}$$

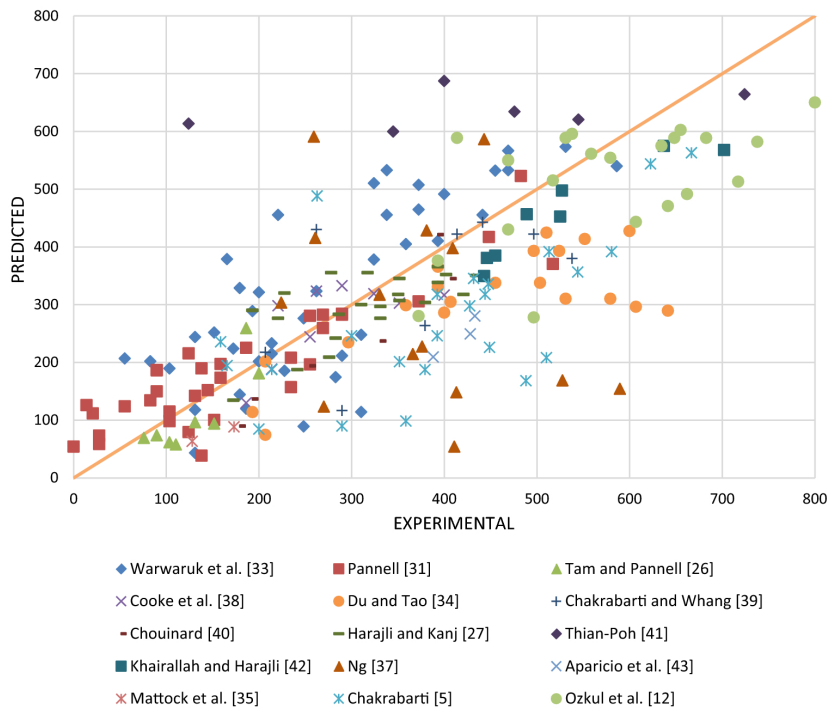


Figure 7.9: Δf_{ps} prediction versus experimental results by Naaman and Alkhairi [109] obtained from [107]

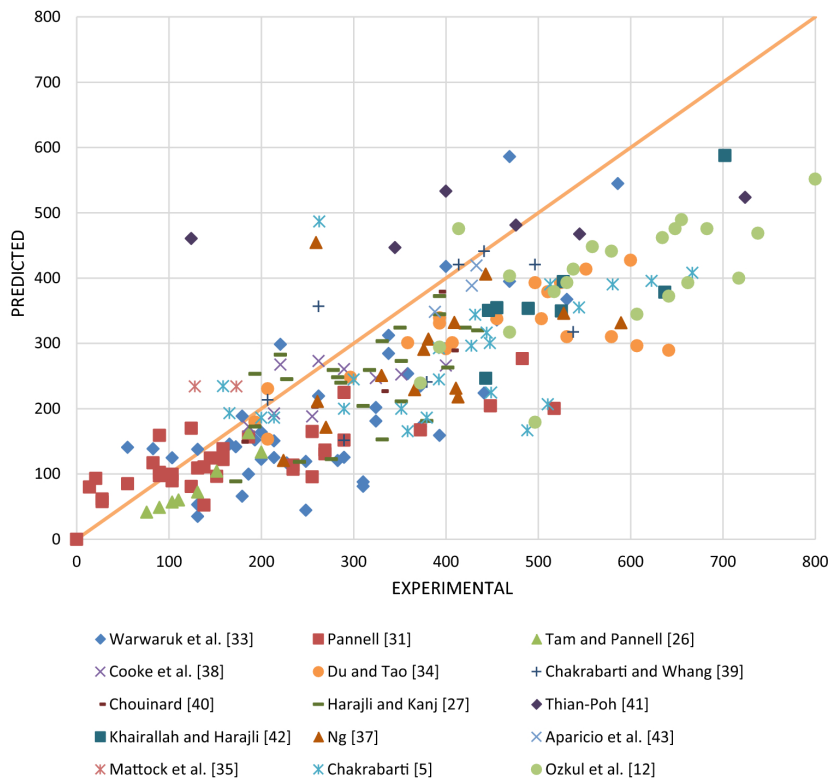


Figure 7.10: Δf_{ps} prediction versus experimental results by He and Liu [110] obtained from [107]

7.6.2. Codes of practice

As has become evident from the foregoing, analysis of structures prestressed with unbonded tendons is more complex than prestress with bonded tendons. Several studies have been conducted to propose

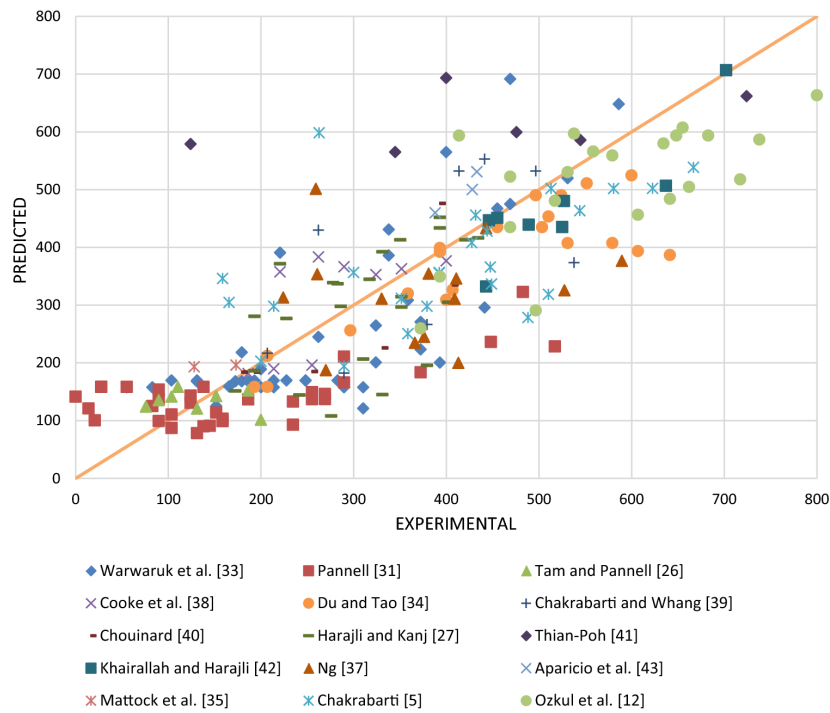


Figure 7.11: Δf_{ps} prediction versus experimental results by Alqam et al. [107] obtained from [107]

analytical equations for application in codes of practise. In this paragraph, several codes of practise are reviewed and the suggested equations to determine the ultimate tendon stress (f_{ps}) are presented.

European code: EN-1992

The Eurocodes are an integrated set of European standards for the design of buildings and other civil engineering works. Related to concrete structures, the governing standard is NEN-EN 1992 [101]. In the Netherlands, a national annex [103] is available with supplementary conditions or regulations that should be obeyed. Regarding structures prestressed with unbonded tendons, NEN-EN 1992 [101] clause 5.10.8 states that: it is generally necessary to take the deformation of the whole member into account when calculating the tendon stress increase (Δf_{ps}). If no detailed calculation is made, the maximum allowable tendon stress increase at ultimate limit state is predefined by an upper bound value. The calculation is presented in eq. (7.18).

$$f_{ps} = f_{pe} + \Delta f_{ps} = f_{pe} + 100 \quad (7.18)$$

The national annex [103] is even more conservative, as represented by the reduced upper bound value at ultimate limit state. The calculation is presented in eq. (7.19).

$$f_{ps} = f_{pe} + \Delta f_{ps} = f_{pe} + 50 \quad (7.19)$$

American code: ACI 318-19

The American code is the American equivalent of the Eurocode. The ACI 318 code [112] includes requirements for design and construction of structural concrete that are necessary to ensure public health and safety. Regarding structures prestressed with unbonded tendons, ACI 318-19 provides simple calculation guidelines for the maximum tendon stress (f_{ps}) at ultimate limit state. The results are only applicable when the effective prestress (f_{pe}) is greater than $0.5f_{pu}$. Moreover, the ACI 318 code [112] prescribes a minimum amount of non-prestressed reinforcement to ensure flexural behaviour at ultimate limit state. The calculation is presented in eqs. (7.20) and (7.21), where:

$$f_{ps} = f_{pe} + 70 + \frac{f'_c}{100\rho_{ps}} \leq f_{pe} + 420 \leq f_{py} \quad \text{for} \quad \frac{L}{d_{ps}} \leq 35 \quad (7.20)$$

$$f_{ps} = f_{pe} + 70 + \frac{f'_c}{300\rho_{ps}} \leq f_{pe} + 200 \leq f_{py} \quad \text{for} \quad \frac{L}{d_{ps}} > 35 \quad (7.21)$$

$$\rho_{ps} = \frac{A_{ps}}{bd_{ps}}$$

f'_c : concrete compressive strength
 A_{ps} : area of unbonded prestressing reinforcement
 ρ_{ps} : ratio of prestressing reinforcement

7.6.3. Results

This paragraph presents the results regarding the bending moment resistance. From section 7.2 the occurring bending moment can be calculated, due to self-weight and variable imposed loading, As mentioned in the previous paragraphs, various parameters have significant influence on the flexural behaviour of the system.

In the study of Le et al. [113], it was found that for precast segmental concrete beams with unbonded tendons, the effective prestress in the tendon (f_{pe}) significantly influences the load-bearing capacity, deflection and failure mode. Beams with a higher effective prestress exhibit greater load-bearing capacity and less deflection at ultimate limit state. Additionally, a change in effective prestress, with the same amount of prestress (A_{ps}), can lead to a change in failure mode from compression to tensile failure. Furthermore, Le et al. [113] considered five other effects in their study, namely: **(i)**: the span-to-depth ratio, **(ii)**: the amount of prestressing steel, **(iii)**: the concrete strength, **(iv)**: the number and location of the joint and **(v)**: the type of loading on the system. Regarding the number of joints, it is concluded that the effect on the load bearing capacity and failure mode is insignificant [113]. However, the effect of the location of the joints is significant. When the load is applied near the vicinity of a joint or when joint is located near mid-span, the joint resistance is reduced and, therefore, reducing the bending moment resistance of the entire system [114].

To determine the bending moment resistance of the proposed floor system, a failure model or mechanism should be adopted. The ratio of effective prestress to the maximum stress (f_{pe}/f_{pk}) is approximately 0.66 for all span lengths. Therefore, concluding from the research of Le et al. [113], it is reasonable to expect compression failure of the system, which will lead to crushing of the concrete before yielding of the prestressing steel. Concluding from the research of Li et al. [114], the joint resistance near or exactly at midspan location is the lowest and, therefore, failure is likely to occur at that critical joint. The adopted failure model is illustrated in figure 7.12.

Paragraphs 7.6.1 and 7.6.2 propose equations to determine the maximum tendon stress (f_{ps}) in the system. The equations from previously conducted research also include the determination of the neutral axis depth (c) in a closed-form procedure. Therefore, two of the three unknowns can be solved simultaneously. For the equations presented in the codes of practise, one intermediate step should be performed in the analysis, with the objective to determine the neutral axis depth. Analogous to the previously conducted research, this can be done based upon force equilibrium. Next, the ultimate limit state moment (M_u) can be determined by solving the moment equilibrium equation.

For the evaluation of the bending moment resistance of the system, the state-of-the-art equations proposed by Alqam et al. [107] are adopted in the analysis. Additionally, the equation proposed by the national annex of NEN-EN 1992 [103] is adopted as well to verify whether the systems fulfils the requirements imposed by the Eurocode. The bending moment diagrams for a span length of $l = 5.4m$ and $l = 7.8m$ are presented in figure 7.13.

According to the NEN-EN 1992 [101] clause 3.1.7, for the design of cross-sections, a bi-linear stress-strain relationship for concrete is adopted, assuming a rectangular stress distribution. Provided that the concrete strength class is C45/55, the values for λ and η are 0.8 and 1.0 respectively. The definition of

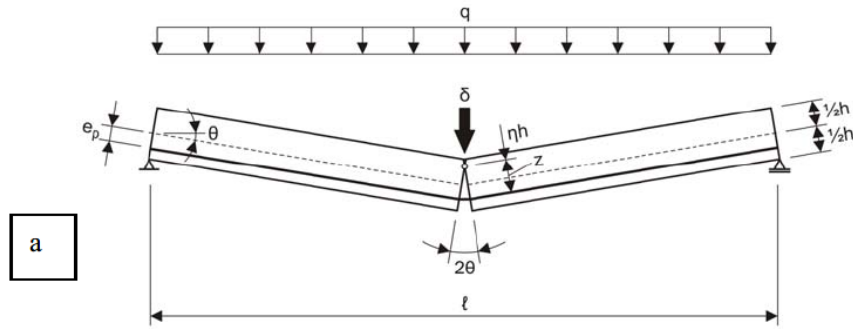
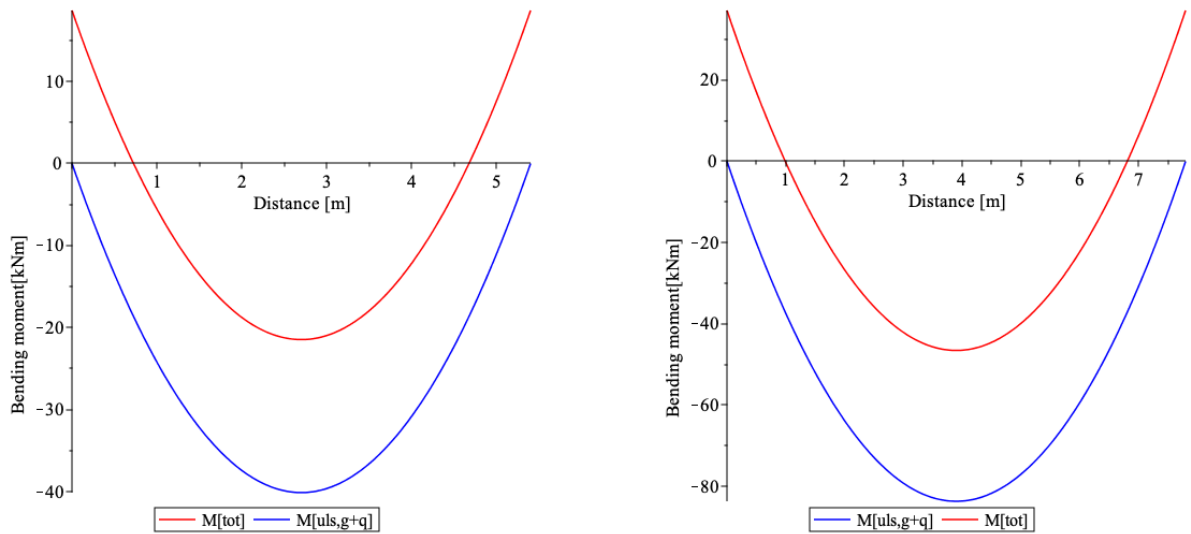


Figure 7.12: Adopted kinematic failure model due to the imposed loading [102]



(a) Bending moment diagram for $l = 5.4m$

(b) Bending moment diagram for $l = 7.8m$

Figure 7.13: Bending moment diagrams due to the imposed loading

these values is illustrated in figure 7.14 together with the cross-sectional forces to determine the force and bending moment equilibrium equations. These equations are presented in eqs. (7.22) and (7.23), where:

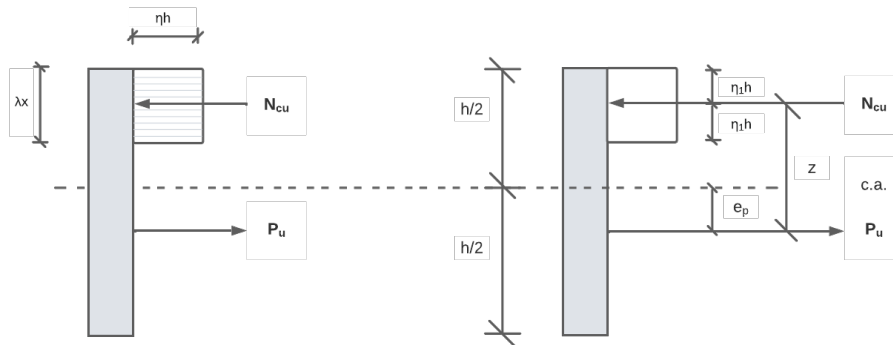


Figure 7.14: Cross-sectional equilibrium at ultimate limit state

$$\text{Force equilibrium equation:} \quad N_{cu} = P_{m\infty} + \Delta P \quad (7.22)$$

$$\text{Moment equilibrium equation:} \quad M_u = (P_{m\infty} + \Delta P) \left(\frac{h}{2} + e_p - \eta_1 h \right) \quad (7.23)$$

- ca : centroidal axis level
 h : height of the cross-section
 e_p : eccentricity of the prestressing steel
 P_u : prestressing force at ultimate limit state: $P_u = P_{m\infty} + \Delta P$
 N_{cu} : concrete compressive force at ultimate limit state
 z : internal lever arm between tensile and compressive force
 $\eta_1 h$: location of the concrete compressive force from the extreme fiber

Substituting the variables and the limit value for the maximum stress increase imposed by the national annex of NEN-EN 1992 [103] clause 5.10.8 into eqs. (7.22) and (7.23) results for a span length of $l = 7.8m$ in:

$$0.8f_{cd} \cdot b \cdot (2\eta_1 h) = P_{m\infty} + A_p \Delta f_{ps} \quad \eta_1 h = \frac{709.9 \cdot 10^3 + 600 \cdot 50}{2 \cdot 1200 \cdot 0.8 \cdot 30} = 12.8mm$$

$$M_u = (P_{m\infty} + \Delta P) \cdot \left(\frac{h}{2} + e_p - \eta_1 h \right) \quad M_u = (709.9 + 30) \cdot \left(\frac{0.240}{2} + 0.05 - 0.0128 \right)$$

$$= 116.3kNm$$

Analogously, substitution of the variables into the closed-form procedure proposed by Alqam et al. [107], presented in eq. (7.17), results in the maximum stress increase and neutral axis depth. With these results, the bending moment equilibrium equation can be solved to determine the ultimate limit state moment (M_u). For a span length of $l = 7.8m$ this results in:

$$\Omega_u = \alpha \left(\frac{d_{ps} - h/2}{0.25d_{ps}} \right) \left[\mu + \frac{18}{L/d_{ps}} \right] \quad \Omega_u = 0.09 \left(\frac{170 - 240/2}{0.25 \cdot 170} \right) \left[1.41 + \frac{18}{7800/170} \right] = 0.19$$

$$\tilde{w}_{pe} = \frac{A_{ps} \cdot f_{pe} + A_s \cdot f_y}{f'_c \cdot b \cdot d_{ps}} \quad \tilde{w}_{pe} = \frac{600 \cdot 1183 + 0}{45 \cdot 1200 \cdot 170} = 0.08$$

$$f_{ps} \geq f_{pe} + 0.50f_{py} \cdot \tilde{w}_{pe} \quad f_{ps} \geq 1183 + 0.50 \cdot 1522 \cdot 0.08 = 1244MPa$$

$$f_{ps} = f_{pe} + \Delta f_{ps} = f_{pe} + \Omega_u E_{ps} \varepsilon_{cu} \left(\frac{d_{ps}}{c} - 1 \right) \frac{L1}{L2} \leq 0.86f_{pu}$$

$$f_{ps} = 1183 + 0.19 \cdot 195000 \cdot 0.003 \cdot \left(\frac{170}{c} - 1 \right) 1.0 \leq 0.86 \cdot 1860$$

$$\Rightarrow c = 36.0mm \Rightarrow \eta_1 h = c/2 = 18.0mm \Rightarrow \Delta f_{ps} = 416.6MPa \Rightarrow \Delta P = 249.9kN$$

$$M_u = (709.9 + 249.9) \cdot \left(\frac{0.240}{2} + 0.05 - 0.018 \right) = 145.9kNm$$

The foregoing calculation presents the results for one specific span length. To verify whether the maximum moment at ultimate limit state is larger than the occurring bending moment, a unity check is performed. The ratio between both should be smaller than 1.0. The unity checks for a span length of $l = 7.8m$ and for other considered span lengths are presented in table 7.9. From table 7.9 can be concluded that all floor spans have a unity check below 1.0 and, therefore, fulfil the safety requirements with respect to (flexural) bending failure. The ultimate moments calculated by using the expressions of Alqam et al. [107] show higher a higher capacity, compared to the conservative approach proposed by the national annex of the Eurocode 2 [103].

Span length [m]		M_{ed} [kNm]	M_{rd} [kNm]	UC [-]	$Check$ [-]
5.4	Eurocode 2 [103]	40.1	58.2	0.69	satisfied
	Alqam et al. [107]	40.1	73.1	0.54	satisfied
6.0	Eurocode 2 [103]	49.5	86.7	0.57	satisfied
	Alqam et al. [107]	49.5	109.6	0.45	satisfied
6.6	Eurocode 2 [103]	59.9	87.6	0.68	satisfied
	Alqam et al. [107]	59.9	109.5	0.55	satisfied
7.2	Eurocode 2 [103]	71.3	88.4	0.81	satisfied
	Alqam et al. [107]	71.3	109.4	0.65	satisfied
7.8	Eurocode 2 [103]	83.7	116.3	0.72	satisfied
	Alqam et al. [107]	83.7	145.9	0.57	satisfied

Table 7.9: Unity checks regarding the bending moment capacity for all span lengths

7.7. Shear resistance in ULS

In this section the resistance to shear of the system is reviewed and calculated according to the European code of practise: NEN-EN 1992 [101] and the national annex [103]. The adopted kinematic failure model, presented in figure 7.12, assumes that two rigid bodies rotate around their intersection point. For segmental beams, this rigid body mechanism localises the bending deformation at the opening of the joints. For monolithic beams, the bending deformation occurs at the location of a flexural crack. From previous research [113], it shows that for segmental beams opening of the (dry) joints occurs prior to potential flexural cracks due to the imposed loading. Therefore, it is expected that the modules of the proposed floor system show similar behaviour and therefore remain uncracked in bending. The shear resistance of the modules of the floor system is reviewed in paragraph 7.7.1. The shear resistance at the interfaces (or joints) of the modules is reviewed in paragraph 7.7.2.

7.7.1. Shear resistance cross-section

NEN-EN 1992 [101] clause 6.2.2 states that for prestressed single span members without shear reinforcement in regions uncracked in bending, the shear resistance should be limited by the tensile strength of the concrete. For these regions, the shear resistance is provided in eq. (7.24), where:

$$V_{rd,c} = \frac{I \cdot b_w}{S} \sqrt{f_{ctd}^2 + \alpha_l \cdot \sigma_{cp} \cdot f_{ctd}} \quad (7.24)$$

- I : second moment of inertia
- b_w : cross-sectional width at the centroidal axis level
- S : first moment of area above and about the centroidal axis
- α_l : 1.0 for unbonded post-tensioned tendons
- f_{ctd} : concrete design tensile strength
- $\sigma_{cp} = \frac{N_{ed}}{A_c}$: concrete compressive stress at centroidal axis level due to axial loading and/or prestressing

Section 7.6 presents various expressions to define the maximum tendon stress increase (Δf_{ps}) and maximum tendon stress (f_{ps}) at ultimate limit state. For the analysis of the bending moment capacity, two expressions are considered. The first one is from NEN-EN 1992 [101] and the second one is from Alqam et al. [107]. The national annex [103] does not impose stricter regulations. The maximum tendon stress also affects the resistance to shear in the interfaces. The concrete compressive stress (σ_{cp}) is depending on the axial force on the system. A higher maximum tendon stress equals a higher prestressing force at ultimate limit state and thus a higher concrete compressive stress. Substitution of the properties presented in section 7.2.4 and the calculated values of maximum tendon force at ultimate limit state, according to NEN-EN 1992, results for a span length of $l = 7.8m$ in:

$$V_{rd,c} = \frac{Ib_w}{S} \sqrt{f_{ctd}^2 + \alpha_l \left(\frac{P_{m\infty} + \Delta P}{A_c} \right) f_{ctd}}$$

$$V_{rd,c,EC2} = \frac{0.001221 \cdot 0.4}{0.00693} \sqrt{(1.77 \cdot 10^3)^2 + 1.0 \cdot \frac{709.9 + 30}{0.187} \cdot (1.77 \cdot 10^3)} = 224.3 \text{ kN}$$

Analogously, the shear resistance at ultimate limit state, considering the maximum tendon stress calculated in accordance with Alqam et al. [107], results for a span length of $l = 7.8\text{m}$ in:

$$V_{rd,c,Alqam} = \frac{0.001221 \cdot 0.4}{0.00693} \sqrt{(1.77 \cdot 10^3)^2 + 1.0 \cdot \frac{709.9 + 249.9}{0.187} \cdot (1.77 \cdot 10^3)} = 246.2 \text{ kN}$$

Due to the increased maximum tendon stress, leading to a higher concrete compressive stress in the cross-sections, results in a higher resistance to shear for a span length of $l = 7.8\text{m}$. This effect is also noticeable for other span lengths. The resulting shear force diagrams for span lengths $l = 5.4\text{m}$ and $l = 7.8\text{m}$ are depicted in figure 7.15. Likewise to the bending moment resistance calculation, a unity check for the shear resistance is calculated. The results for all considered span lengths are presented in table 7.10. From table 7.10 can be concluded that all floor spans have a unity check below 1.0 and, therefore, fulfil the safety requirements with respect to shear failure.

Span length [m]		V_{ed} [kN]	$V_{rd,c}$ [kN]	UC [-]	Check [-]
5.4	Eurocode 2 [101]	29.7	179.6	0.17	satisfied
	Alqam et al. [107]	29.7	195.2	0.15	satisfied
6.0	Eurocode 2 [101]	33.0	202.2	0.16	satisfied
	Alqam et al. [107]	33.0	222.2	0.15	satisfied
6.6	Eurocode 2 [101]	36.3	203.0	0.18	satisfied
	Alqam et al. [107]	36.3	222.2	0.16	satisfied
7.2	Eurocode 2 [101]	39.6	203.6	0.19	satisfied
	Alqam et al. [107]	39.6	222.2	0.18	satisfied
7.8	Eurocode 2 [101]	42.9	224.3	0.19	satisfied
	Alqam et al. [107]	42.9	246.2	0.17	satisfied

Table 7.10: Unity checks regarding the shear force capacity for all span lengths

7.7.2. Shear resistance interfaces

Randl [115] has made significant contributions to improve the accuracy for the assessment of the longitudinal shear stress at concrete-to-concrete interfaces at ultimate limit state. Randl [115] proposes an expression that includes the contributions of: cohesion, friction and dowel action. The cohesion term is related to the contribution of interlocking aggregates. The second term, friction, relates to the contribution of relative slip between two concrete elements and is influenced by the roughness factor and the normal stress present in the interface. The third and final term, dowel action, identifies the contribution of the shear reinforcement crossing the interface. The proposed expression, together with the inclusion of partial safety factors, is presented in eq. (7.25), where:

$$v_u = \tau_{coh} + \mu \cdot \sigma_n + \alpha \cdot \rho \cdot \sqrt{f_c \cdot f_y}$$

$$v_u = c \cdot \frac{f_{ck}^{1/3}}{\gamma_{coh}} + \mu \left(\sigma_n + \rho \cdot k \cdot \frac{f_{yk}}{\gamma_s} \right) + \alpha \cdot \rho \cdot \sqrt{\frac{f_{yk} f_{ck}}{\gamma_s \gamma_c}} \leq \beta \cdot v \cdot \frac{f_{ck}}{\gamma_c} \quad (7.25)$$

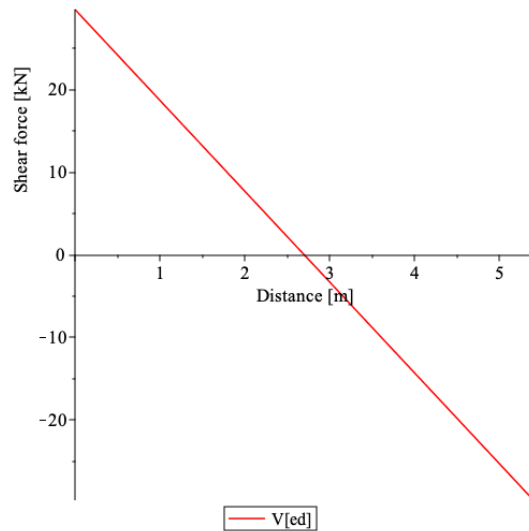
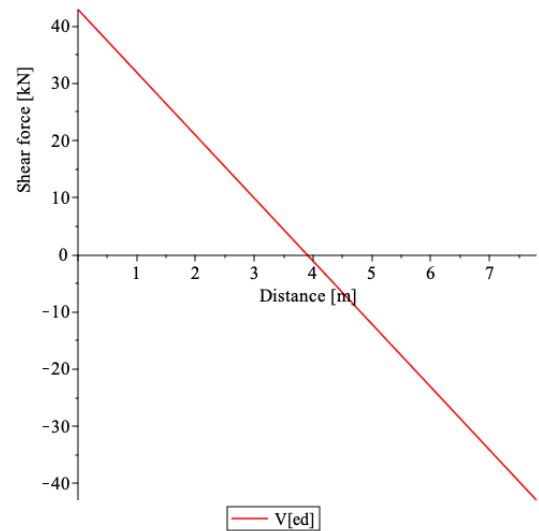
(a) Shear force diagram for $l = 5.4m$ (b) Shear force diagram for $l = 7.8m$

Figure 7.15: Shear force diagrams due to the imposed loading

- v_u : longitudinal shear stress at the interface at ultimate limit state
- c : coefficient of cohesion
- γ_{coh} : partial safety factor for cohesion
- μ : coefficient of friction
- ρ : ratio of reinforcement crossing the interface
- k : coefficient of efficiency for tensile forces transmitted to the shear reinforcement
- α : coefficient for flexural resistance of the reinforcement
- β : coefficient allowing for the angle of concrete diagonal strut
- v : strength reduction factor: $v = 0.6 \cdot \left(1 - \frac{f_{ck}}{250}\right)$
- σ_n : normal stress at the interface due to axial loading

The FIB Model Code 2010 [116] and the Eurocode 2 [101] adopted the design expression proposed by Randl [115]. In order to calculate the shear stress resistance at the interface of the concrete modules, it is necessary to check which of the three components is present in the system. The system consists of prefabricated modules which are connected using unbonded post-tensioned tendons. Since there is no additional (shear) reinforcement between the modules, the only contribution to the shear stress resistance is due to friction. This friction is generated by the roughness of the interfaces and by the axial prestressing force at ultimate limit state. Eurocode 2 [101] clause 6.2.5 proposes a slightly modified expression of Randl [115]. Moreover, the shear stress resistance ($v_{rd,i}$) should be lower or equal to the occurring design shear stress ($v_{ed,i}$). These expressions, together with the reduced expression considering the proposed floor system, is presented in eq. (7.26), where:

$$v_{ed,i} = \frac{\beta \cdot V_{ed}}{z \cdot b_i}$$

$$v_{rd,i} = c \cdot f_{ctd} + \mu \cdot \sigma_n + \rho \cdot f_{yd} (\mu \sin \alpha + \cos \alpha) \leq 0.5 \cdot v \cdot f_{cd} \quad (7.26)$$

$$v_{rd,i} = \mu \cdot \sigma_n \leq 0.5 \cdot v \cdot f_{cd}$$

V_{ed} :	transverse shear force
β :	ratio of longitudinal force in the new concrete and the total longitudinal force either in the compression or tension zone, both calculated for the section considered: $\beta = 1.0$ as a conservative value
z :	internal lever arm of composite section: $z = d_{ps}$
b_i :	width of the interface: $b = b_w$
α :	angle of reinforcement: $45^\circ \leq \alpha \leq 90^\circ$
σ_n :	normal stress at the interface due to axial loading: $\sigma_n \leq 0.6f_{cd}$
$\mu = 0.5$ and $c = 0.25$:	very smooth: a surface cast against steel, plastic or specially prepared wooden moulds
$\mu = 0.6$ and $c = 0.35$:	smooth: a slipformed or extruded surface or a free surface left without further treatment after vibration
$\mu = 0.7$ and $c = 0.45$:	rough: a surface with at least 3mm roughness at about 40mm spacing, achieved by raking, exposing of aggregate or other methods giving an equivalent behaviour
$\mu = 0.9$ and $c = 0.50$:	intended: a surface with indentations of at least 5mm

Table 7.11: Interface roughness factors according to NEN-EN 1992 [101]

Eurocode 2 [101] defines, in absence of more detailed information, four roughness classifications. These four classifications are presented in table 7.11. For the sake of convenience, it is assumed that the concrete elements are cast in properly designed formwork, resulting in very smooth interfaces. For a span length of $l = 7.8m$, the width at centroidal axis level and the concrete compressive stress calculated by the induced maximum tendon stress (f_{ps}) according to Eurocode 2 [101], substitution of the parameters in eq. (7.26), results in:

$$v_{ed,i} = \frac{1.0 \cdot 42.9 \cdot 10^3}{170 \cdot 400} = 0.63MPa$$

$$v_{rd,i} = 0.5 \cdot \frac{709.9 + 30}{0.187 \cdot 10^3} \leq 0.5 \cdot \left[0.6 \cdot \left(1 - \frac{45}{250} \right) \right] \cdot 30 \Rightarrow 1.98MPa \leq 7.38MPa$$

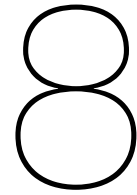
Analogous, for a span length of $l = 7.8m$, the width at centroidal axis level, but now for the concrete compressive stress calculated by the induced maximum tendon stress (f_{ps}) according to Alqam et al. [107], substitution of the parameters in eq. (7.26), results in:

$$v_{rd,i} = 0.5 \cdot \frac{709.9 + 249.9}{0.187 \cdot 10^3} \leq 0.5 \cdot \left[0.6 \cdot \left(1 - \frac{45}{250} \right) \right] \cdot 30 \Rightarrow 2.56MPa \leq 7.38MPa$$

Above standing calculations are performed at the critical interfaces. The critical interfaces are located where the absolute value of the shear force is maximum. Considering the type of loading, presented in figure 7.1, the maximum shear force occurs near the two supports. Now, likewise to the bending moment and shear resistance calculations, a unity check for the shear stress resistance at the interfaces is calculated. The results for all considered span lengths is presented in table 7.12. From table 7.12 can be concluded that all floor spans have a unity check below 1.0 and, therefore, the shear resistance at the interfaces under the imposed loading fulfil the safety requirements.

Span length [m]		v_{ed} [MPa]	$v_{rd,i}$ [MPa]	UC [-]	$Check$ [-]
5.4	Eurocode 2 [101]	0.44	0.95	0.46	satisfied
	Alqam et al. [107]	0.44	1.28	0.34	satisfied
6.0	Eurocode 2 [101]	0.49	1.44	0.34	satisfied
	Alqam et al. [107]	0.49	1.92	0.25	satisfied
6.6	Eurocode 2 [101]	0.53	1.46	0.37	satisfied
	Alqam et al. [107]	0.53	1.92	0.28	satisfied
7.2	Eurocode 2 [101]	0.58	1.47	0.40	satisfied
	Alqam et al. [107]	0.58	1.92	0.30	satisfied
7.8	Eurocode 2 [101]	0.63	1.98	0.32	satisfied
	Alqam et al. [107]	0.63	2.56	0.25	satisfied

Table 7.12: Unity checks regarding the shear stress at the interfaces for all span lengths



Buildability Aspects

In this section, various buildability aspects are assessed. The proposed floor system has been designed according to circular design principles discussed in section 3. The most commonly used concrete floor systems in newly-build buildings are reviewed in section 5. Validation of the proposed floor system, in comparison to the commonly used concrete floor systems, is done in section 6. Verification according to codes of practice and state-of-the-art research is carried out in section 7. Several practical constraints that affect applicability in most buildings should be taken into account in order to achieve implementation of the design in current practice. Moreover, in buildings stability due to horizontal loads, wind for example, should be considered as well.

8.1. Fabrication and Assembly Procedure

The proposed floor system consists of two different element types: anchor or end elements and intermediate elements. The end elements are designed such that the anchor of the post tensioning system is embedded in the concrete with opening for installation of the tendons. The intermediate elements have weight-reduced voids for more efficient load bearing capacity. All element are prefabricated in an environment-controlled factory to guarantee certain quality aspects. Moreover, by prefabricating the concrete elements in the factory, the anchors of the post tensioning system can be installed at the desired and required location with a high accuracy, which is important for the final tendon eccentricity and thus the load bearing capacity of the entire floor system. Additional unbonded reinforcement for the end elements and the practical reinforcement for the intermediate elements can be placed inside the molds to guarantee a prespecified cover distance and thus ensure durability of the elements. The practical reinforcement of the intermediate elements provides more robustness of the elements during transportation and assembly in order to avoid damage to the elements.

After the concrete elements have cured and obtained their desirable and required strength, in this thesis: at least 28 days after casting, the post tensioning tendons can be installed to construct the floor system. Assembly of the elements and of the tendons can, in principle, take place in a factory environment or at the construction site. Handling and installation of the tendons requires special skill, knowledge and equipment. The tensioning of the tendons is achieved by using a hydraulic jack, as presented in figure 8.2. Since the span length of the elements is not of considerable length (<50 meters) and frictional prestressing losses are relatively small, tensioning will take place at one end only, also referred to as the 'live end'. The other end is referred to as the 'dead end'. After installation of the tendons, wedges at both ends are installed prior to tensioning. Now, the stressing operation at the live end can start. At the live end, the initial positions of the tendons are marked in order to measure and record the elongation of each tendon. The measurement should be reviewed to determine and verify that the proper force exists in each tendon. Once the required elongation of the tendons has been reached, the stressing operation is stopped and the tendons are anchored into place. The excessive length of the tendons are cut off just inside the edge of the end elements. A protective cap is installed to prevent water intrusion into the anchors and tendons. Usually, the stressing pocket is filled with non-

shrink grout or concrete. Dywidag [95] recommends at least 25 millimeters of cover for the stressing pockets. However, to improve the demountability and reusability of the end elements, other solutions should be considered and it is recommended for further research.

As mentioned above, the assembly can occur in a factory environment or at the construction site. For assembling the elements it is of importance that the subsurface provides a relatively smooth sliding surface for the elements or, in other words, limited friction between the subsurface and the elements should be present to prevent damage to the elements. However, limited friction is beneficial for the elements to remain within their horizontally aligned location upon stressing. The elements should be placed sufficiently close to the other elements to prevent high dynamic impact forces. Furthermore, a completely flat subsurface enables proper alignment of the elements. If not, the elements do not align perfectly, resulting in a reduced frictional surface between the elements. Because of the dry joints between the elements, imposed by the post tensioning force, reduced frictional surface results in a reduced load bearing capacity as well. One solution could be to apply a layer of grease on each interface surface of the elements and in between a layer of grout. This enables a demountable connection between the segments, as has been demonstrated in the Circular Viaduct project of Rijkswaterstaat in Kampen. It should be noted that this requires additional labour and therefore additional construction time. Therefore, it should only be applied in case of significantly reduced contact surfaces.

Secondly, the stressing operation requires experienced and skilled workers. However, it should be noted that the tendon profile is straight and not curved, which simplifies installation of the tendons. Nevertheless, the forces generated when the tendons are stressed are high enough to damage the structure or cause harm to people working in the vicinity of the assembly site in case of a sudden failure of the tendons. In other words, safety during the stressing operation includes making sure that no one is working in the area where the tendons are stressed, which could be an issue on a construction site where there is limited available space. Assembly of the elements in a factory environment with experienced workers can diminish these two issues and ensures proper assembly of the floor system. The assembly process is illustrated in figure 8.1. Figure 8.3 illustrates a side view of the stressing operation. The hydraulic jack exerts an increasing force on the anchors embedded in concrete end elements during stressing. Due to this exerted force, the concrete elements are compressed and (symmetrically) shift towards each other. This shift is illustrated by a horizontal displacement (u). The movement of the jack is opposite to that of the contact element and is illustrated by a horizontal displacement (δ).

Proper assembly of the floor system in a factory environment also has its drawback. Transportation of a fully assembled floor systems to the construction site is less efficient. Individual elements are easier to load on lorry and result in less transport movements. Moreover, damage during transportation is more severe in case of pre-assembled floor systems than for individual elements. In the latter case, one damaged element results in a rejection or disapproval of that particular element, which can be supplemented with a subsequent transport movement easily. More intrusive interventions are necessary in case of a damaged floor system. A new system should be transported to the construction site or the damaged floor system should be disassembled, where the damaged element(s) are replaced and subsequently re-assembled on the construction site with all of the concerns mentioned previously.

Despite potential transportation issues, it is recommended to assemble the elements in a factory controlled environment if: **(i)**: no experienced and skilled workers are present on the construction site **(ii)**: insufficient available space on the construction site during the stressing operation and **(iii)**: uneven subsurface for the horizontal and vertical alignment of the elements. Regardless of the location of assembly, all assembled floor slabs should be hoisted into allocated positions inside buildings. A detailed design of a hoisting connection is beyond the scope for this research project. However, it is recommended to implement a hoisting connection in the end elements, due to the massive concrete cross-sections and to avoid unfavorable loading situations if applied elsewhere within the floor system.

8.2. Building Services

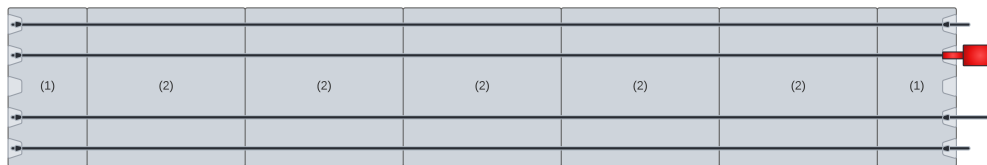
Buildings have to be equipped with a variety of services to increase living comfort. As discussed in section 5 and 3 building services can be implemented into the structural system to reduce the structural height of the floor package. Structural height reduction of the floor package results in a reduced building height, which is favorable regarding financial aspects, such as less required facade cladding surface,



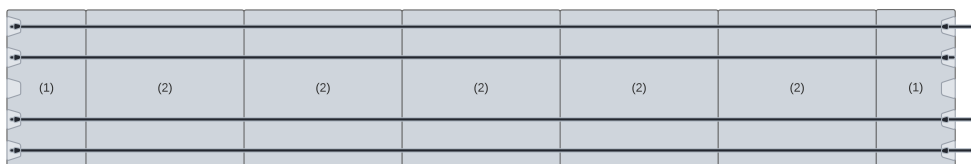
(a) Step I: horizontal and vertical alignment of the elements



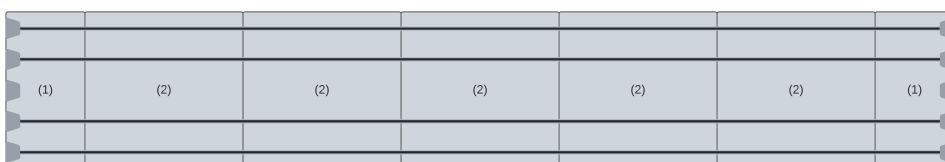
(b) Step II: installation of the tendons and wedges



(c) Step III: stressing operation and measurement of the tendon elongations



(d) Step IV: cutting of the excessive tendon lengths



(e) Step V: covering of the stressing pockets to prevent water intrusion

Figure 8.1: Assembly procedure for the proposed floor system in top view



Figure 8.2: Hydraulic jack from Dywidag for post tensioning tendons [117]

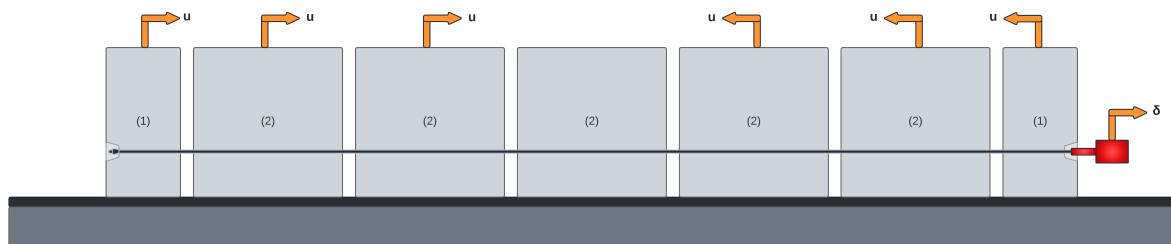


Figure 8.3: Assembly procedure for the proposed floor system in side view

which is known to be one of the biggest cost drivers for buildings or, for medium to high-rise building, an additional storey can be created within the original building height. However, concluding from the theoretical framework, separation of different building layers should be pursued in order to comply with circular principles. Moreover, separation of building services from the structural layer increases the flexibility, reconfigurability and reusability of a floor system for second life cycle. In general, separation of building services from the structural layer can be achieved in two distinct ways: **(i)**: raised floor systems and **(ii)**: suspended ceilings. Both are discussed in the following sections.

8.2.1. Raised floor systems

Raised floor systems are widely used in office buildings and data centers. A raised floor system is a demountable floor at a specified vertical distance from the structural floor, which generates an under-floor space for the distribution of building services. An example of a raised floor system is presented in figure 8.4. The systems consists of load-bearing floor panels which are supported by height-adjustable steel supports or pedestals. The floor panels are placed in a horizontal grid and have common dimensions of 600mm by 600mm [118]. The floor panels are normally composed of particle board, plywood, aluminium, steel or a combination of metal and non-metal. Particle board or plywood panels are usually covered with thin sheet steel or aluminium in order to increase safety under fire loading [118]. As mentioned, the underfloor space, where the building services can be placed, generates a high degree of flexibility for the layout of piping and cables. Changing future demands of the users can easily be facilitated in this way. Moreover, small differential settlements between the (structural) floor slabs can be compensated due to the adjustable height of the pedestals. Therefore, a raised floor system imposes a better alternative than integrated building services in the structural floor system. Raised floor systems have the disadvantage that the total building height of the floor package is increased. This can be taken into account in the context of this thesis, since this thesis focuses on the design phase of buildings, where decisions of this kind are usually taken.

8.2.2. Suspended ceilings

Suspended ceilings systems are a non-structural component installed below the structural floor to serve as an aesthetic barrier between electrical, mechanical and piping systems [120]. Suspended ceilings are commonly used in utility and residential buildings. The grid system of suspended ceilings consists

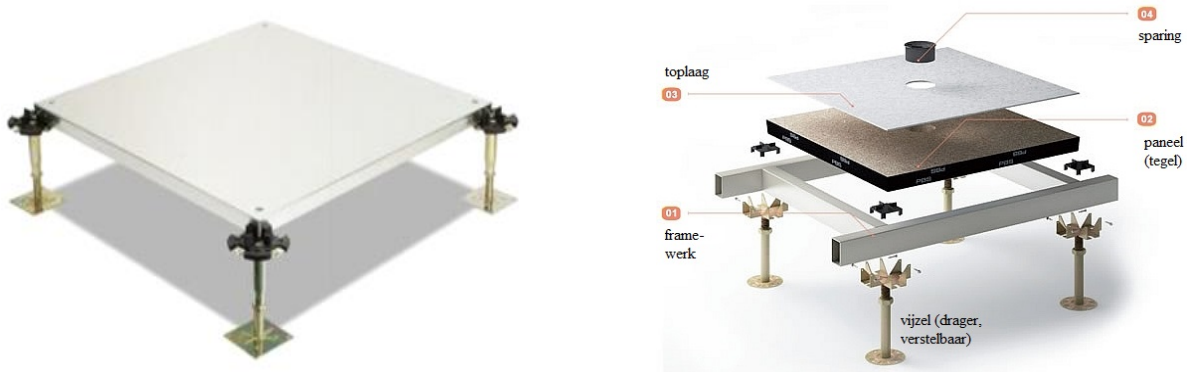


Figure 8.4: Examples of raised floor systems [118] [119]

of interlocking inverted tee beams in two directions, which are suspended from the structural floor. The inverted tee beams are usually made of light-weight metals, such as aluminium or light gauge steel [120]. On top of the inverted tee beams, ceiling tiles are placed. As with raised floor systems, a space for building services between the structural floor and ceiling tiles is realised. This space is referred to as the plenum space. The ceiling tiles do not necessarily have to be locked into place, or in other words, the ceiling tiles are simply resting on the inverted tee beams, so that maximum reconfigurability and accessibility for the building services can be guaranteed. However, there are also ceiling tiles available on the market that can be altered to give a smooth finish. This is particularly the case for application in residential buildings, where aesthetics are more important compared to utility buildings. Moreover, in the plenum space, acoustic, fire and/or thermal insulation can be installed to increase safety and comfort of the building. An example of suspended ceilings is presented in figure 8.5.

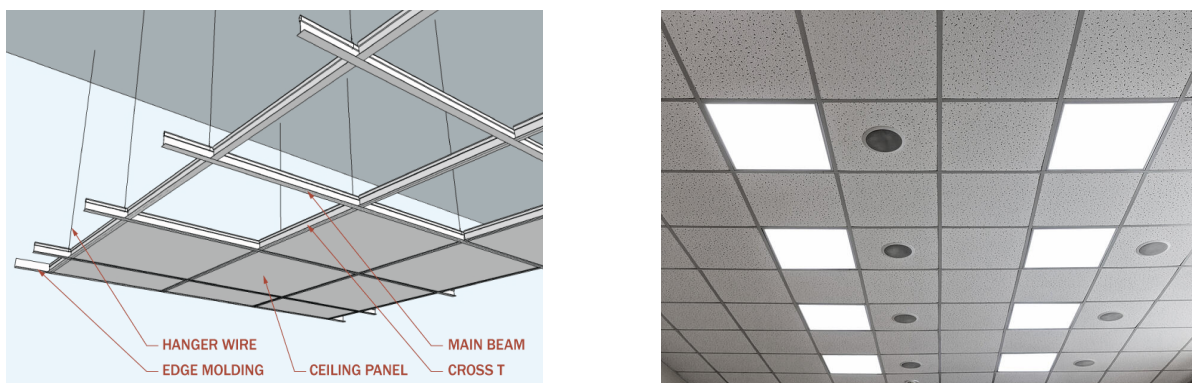


Figure 8.5: Examples of suspended ceilings [121] [122]

Concluding from this section, two systems are proposed to achieve separation of building services from the structural floor system. These two systems are already commonly used in utility and residential buildings and are, therefore, applicable for the newly proposed floor system. However, as with most buildings, (small) recesses should be made in the floor system for numerous reasons. The number of recesses, however, should be kept to a minimum. Section 8.3 elaborates on this and discussed the impact on the load bearing capacity of the newly proposed floor system.

8.3. Recesses

From the foregoing sections, separation of building services and structural systems should be pursued at all times. Maximum reconfigurability and thus reusability of the concrete modules is achieved when the least amount of modifications are made to the modules. However, sometimes it is inevitable to make small recesses in the floor for electrical or water supply for example. Small recesses can be drilled into the considered modules within the floor system at the location of an empty void. Or, in other words, the voids where zero prestressing reinforcement is present. Moreover, it is not recommended to drill holes:

- into the concrete between the weight-reducing voids
- close to the module interfaces (or joints), due to weakening of the interface
- at the location of the anchorage blocks, due to the presence of additional non-prestressed reinforcement

For a span length of $l = 7.8m$ four prestressing tendons are required to ensure safety in serviceability and ultimate limit state. In the design, proposed in section 6.3, this means that the centre void could remain without prestressing reinforcement. The suggested location of recesses is illustrated and indicated in figures 8.6 and 8.7 in the area shaded in red. Note that the practical reinforcement is not depicted in figure 8.6.

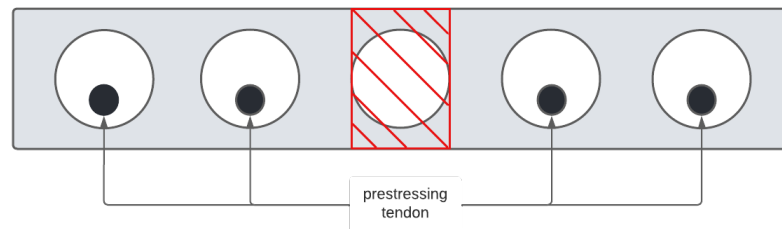


Figure 8.6: Location of recesses for a span length of $l = 7.8m$ in illustrative cross-sectional view

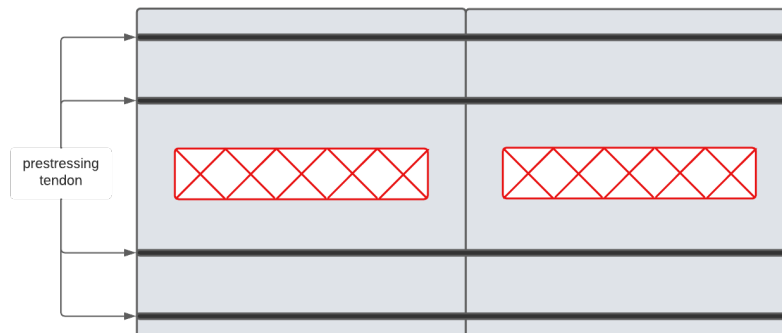


Figure 8.7: Location of recesses for a span length of $l = 7.8m$ in illustrative top view

When larger recesses in the floor field are required, a trimmer beam (in Dutch: 'raveelijzer') can be used. Trimmer beams act as a support for a predetermined number of plates. Trimmer beams are generally used at the intended location of staircases. Additionally, trimmer beams can also be used when a large pipes have to cross several floor levels that can or should not be integrated in vertical walls. For example: large condensation drainage pipes for central heating boilers or ventilation shafts in apartment buildings. Utilisation of trimmer beams is very common when hollow core slabs are used and in timber constructions.

Application of a trimmer beam affects the structural system. An additional point load, next to the uniform loading, is introduced at the plates adjacent to the slabs supported by the trimmer beam. This additional

point load generates an supplementary shear force on the adjacent slabs. The loading scheme of 7.1 is revised to the loading scheme depicted in figure 8.8. Moreover, a torsional moment is imposed as well, due to the location of the point load close to the edges. The number of plates that are supported by the trimmer beam can vary according to customer requirements. For most common staircases, the required longitudinal gap does not exceed three plate widths ($3a = 3.6m$) and a depth of one plate width ($a = 1.2m$) is usually sufficient. Therefore, these dimensions are adopted in the design. Figure 8.9a illustrates the implementation of a trimmer beam in a floor field. The loading and the adopted dimensions are indicated. For the sake of illustration, only five slabs are presented here, whereas a general floor field consists of more slabs. Figure 8.9b depicts the effect of a trimmer beam on the adjacent slab. Again, the adopted dimensions and uniform loading, additional shear force and torsional moment are indicated.



Figure 8.8: Loading scheme with an additional trimmer beam

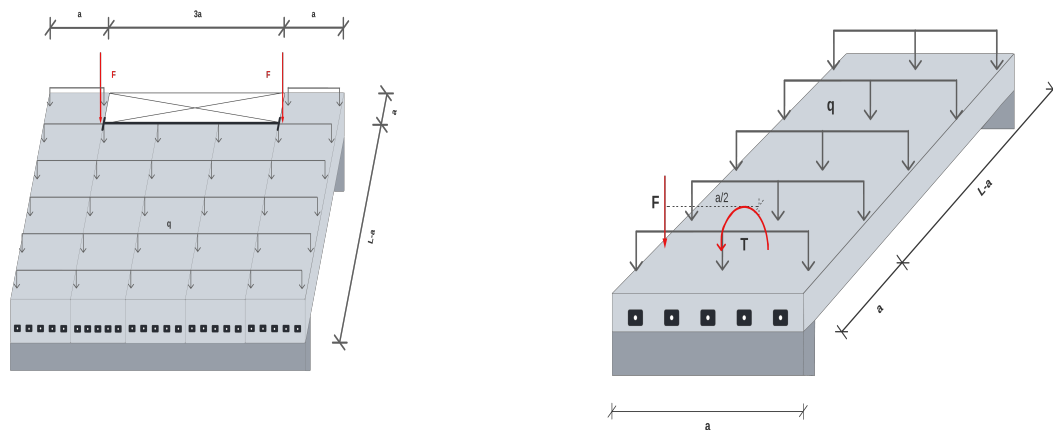
Verification related to serviceability and ultimate limit state should be performed to incorporate the effects of a trimmer beam. Analogous to section 7, the calculations are conducted with respect to the loading scheme depicted in figure 8.8 and figure 8.9b. In order to fulfil the requirements in serviceability and ultimate limit, the minimum number of tendons, specified in table 7.4 is increased to: $n_{strands} + 1$. Immediate and time-dependent prestressing losses are redetermined, but are approximately in the same order of magnitude as calculated for slabs without a trimmer beam. Analysis for a span length of $l = 7.2m$ resulted in unsatisfactory stress values in serviceability limit state. Therefore the minimum amount of required tendons is: $n_{strands} + 2$. All newly obtained results are presented in table 8.1.

Span length [m]	$n_{strands}$ [-]	$A_{p,tot}$ [mm ²]	$P_{m,0,tot}$ [kN]	$M_{p,0,tot}$ [kNm]	$P_{m,\infty}$ [kN]	$M_{p,\infty}$ [kNm]
5.4	3	450	627.3	31.4	509.2	25.5
6.0	4	600	836.4	41.4	688.2	34.4
6.6	4	600	836.4	41.4	696.8	34.8
7.2	5	750	1045.5	52.3	878.4	43.9
7.8	5	750	1045.5	52.3	885.8	44.3

Table 8.1: Required amount of prestressing steel for all span lengths with a trimmer beam

Under serviceability conditions, satisfactory vibration behaviour is ensured, since the uniform loading is equal to the uniform loading discussed in section 7.5.3. The last serviceability check is related to the deflections of the system, with respect to the frequent load combination. Analogous to section 7.5.2, the same criteria (or limit values) for the deflections are adopted, resulting in the deflections for all floor spans as presented in table 8.2. It can be concluded from table 8.2 that the requirements with respect to deflections are satisfactory for slabs with a trimmer beam as well.

For ultimate limit state verification the resistance against occurring bending moments, shear forces



(a) System overview of a trimmer beam

(b) Adjacent slab where the trimmer beam is located

Figure 8.9: System and local slab overviews with the application of a trimmer beam

Span length [m]		Deflections		Check [-]
		[mm]	[mm]	
5.4	$w_2 + w_3$	1.77	\leq 10.8	Satisfied
	w_{max}	2.42	\leq 21.6	Satisfied
6.0	$w_2 + w_3$	1.97	\leq 12.0	Satisfied
	w_{max}	2.56	\leq 24.0	Satisfied
6.6	$w_2 + w_3$	4.12	\leq 13.2	Satisfied
	w_{max}	5.68	\leq 26.4	Satisfied
7.2	$w_2 + w_3$	4.84	\leq 14.4	Satisfied
	w_{max}	6.53	\leq 28.8	Satisfied
7.8	$w_2 + w_3$	8.48	\leq 15.6	Satisfied
	w_{max}	11.48	\leq 31.2	Satisfied

Table 8.2: Results regarding deflections for all span lengths with a trimmer beam

and the shear stress at the interfaces should be determined. The calculation procedure is analogous to that in sections 7.6 and 7.7, with an additional computation for the shear force resistance. The effect of the torsional moment is modelled in accordance with NEN-EN 1168 [123] clause 4.3.3.2.2.4, where sections that are subjected simultaneously to shear and torsion, the shear force capacity should be reduced with an equivalent shear force, imposed by the torsional moment. This reasoning is illustrated in figure 8.10. Note that the torsional stresses are not necessarily representative for the actual torsional moment in the cross-section. The shear capacity of the system can therefore be calculated with eq. (8.1), where:

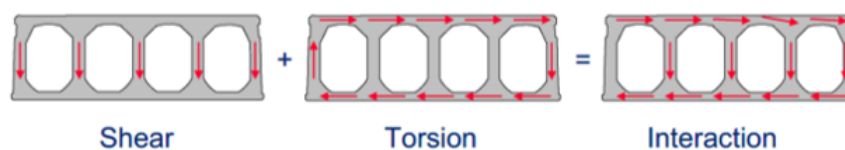


Figure 8.10: Representation of the interaction between shear and torsion [124]

$$V_{rd,n} = V_{rd,c} - V_{et,d} \quad (8.1)$$

$$V_{et,d} = \frac{T_{ed}}{2b_{w,out}} \cdot \frac{\sum b_w}{b - b_{w,out}} \quad \text{for hollow core elements}$$

$$V_{et,d} = T_{ed} \cdot \frac{3 + 1.8 \cdot b/h}{b} \quad \text{for solid elements}$$

- T_{ed} : design value of the torsional moment in the considered cross-section
 $b_{w,out}$: width of the outermost web at the level of centroidal axis: $b_w = 68mm$
 $\sum b_w$: sum of widths of the webs at the level of centroidal axis: $\sum b_w = 400mm$
 b : total width of the cross-section
 h : height of the cross-section

The maximum moment at ultimate limit state (M_u) can be calculated according to two expressions: the national annex of Eurocode 2 [103] and Alqam et al. [107]. Both results, together with accompanying unity checks, for all considered span lengths are presented in table 8.3. As discussed in section 7.7 and expressed in eq. (7.24), the maximum tendon stress (f_{ps}) affects the concrete stress at ultimate limit state and, therefore, the shear force capacity ($V_{rd,c}$) of the cross-section as well. Together with the reduction due to the torsional moment, the shear force capacity of the system can be calculated ($V_{rd,n}$). The results for all considered span lengths are presented in table 8.4. Regarding the shear stress at the location of the interfaces, the calculation procedure of section 7.7.2 is adopted. The results are presented in table 8.5.

Span length [m]		M_{ed} [kNm]	M_{rd} [kNm]	UC [-]	Check [-]
5.4	Eurocode 2 [103]	63.6	85.5	0.74	satisfied
	Alqam et al. [107]	63.6	109.7	0.58	satisfied
6.0	Eurocode 2 [103]	76.1	113.1	0.67	satisfied
	Alqam et al. [107]	76.1	146.2	0.52	satisfied
6.6	Eurocode 2 [103]	89.7	114.4	0.78	satisfied
	Alqam et al. [107]	89.7	146.0	0.61	satisfied
7.2	Eurocode 2 [103]	104.2	141.1	0.74	satisfied
	Alqam et al. [107]	104.2	182.6	0.57	satisfied
7.8	Eurocode 2 [103]	119.6	142.2	0.84	satisfied
	Alqam et al. [107]	119.6	182.4	0.65	satisfied

Table 8.3: Unity checks regarding the bending moment capacity for all span lengths with a trimmer beam

8.4. Stability

Analysis and designing of the proposed floor system has been conducted for vertical loading, due to self-weight and imposed variable loading. However, structures and in this specific case floor systems, should be designed according to horizontal loading as well. Buildings are subjected to horizontal loads caused by: wind, earthquakes and geometrical imperfections. Earthquakes are disregarded in the analysis, due to the fact that earthquakes are only present in a small part of the Netherlands and, therefore, not representative for the majority of the Netherlands. Geometrical imperfections are primarily of interest when assessing stability of walls. For this thesis project, it is assumed that due care has been taken into consideration with respect to geometrical imperfections. However, horizontal loading due to wind loads should be analysed in order to ensure stability and safety of the building.

Horizontal forces are transferred through diaphragm action in floor system. The horizontal loads are transmitted to vertical resisting elements, usually the separation walls (in Dutch: 'woningscheidende

Span length [m]		V_{ed} [kN]	$V_{et,d}$ [kN]	$V_{rd,c}$ [kN]	$V_{rd,n}$ [kN]	UC [-]	Check [-]
5.4	Eurocode 2 [101]	56.7	54.0	201.3	147.3	0.38	satisfied
	Alqam et al. [107]	56.7	54.0	222.2	168.1	0.34	satisfied
6.0	Eurocode 2 [101]	64.7	61.8	222.0	160.2	0.40	satisfied
	Alqam et al. [107]	64.7	61.8	246.2	184.4	0.35	satisfied
6.6	Eurocode 2 [101]	72.8	69.5	222.9	153.4	0.47	satisfied
	Alqam et al. [107]	72.8	69.5	246.2	176.7	0.41	satisfied
7.2	Eurocode 2 [101]	80.9	77.2	242.0	164.8	0.49	satisfied
	Alqam et al. [107]	80.9	77.2	268.1	190.9	0.42	satisfied
7.8	Eurocode 2 [101]	89.0	84.9	242.7	157.8	0.56	satisfied
	Alqam et al. [107]	89.0	84.9	268.1	183.2	0.49	satisfied

Table 8.4: Unity checks regarding the shear force capacity for all span lengths with a trimmer beam

Span length [m]		v_{ed} [MPa]	$v_{rd,i}$ [MPa]	UC [-]	Check [-]
5.4	Eurocode 2 [101]	0.83	1.42	0.59	satisfied
	Alqam et al. [107]	0.83	1.92	0.43	satisfied
6.0	Eurocode 2 [101]	0.95	2.56	0.50	satisfied
	Alqam et al. [107]	0.95	2.56	0.37	satisfied
6.6	Eurocode 2 [101]	1.07	1.94	0.55	satisfied
	Alqam et al. [107]	1.07	2.56	0.42	satisfied
7.2	Eurocode 2 [101]	1.19	2.44	0.49	satisfied
	Alqam et al. [107]	1.19	3.20	0.37	satisfied
7.8	Eurocode 2 [101]	1.31	2.46	0.53	satisfied
	Alqam et al. [107]	1.31	3.20	0.41	satisfied

Table 8.5: Unity checks regarding the shear stress at the interfaces for all span lengths with a trimmer beam

wanden') in residential buildings. Sound insulation is an important aspect in designing residential buildings and the most effective way to ensure sound insulation in both floors and walls is by increasing the mass density. For this reason, properly designed residential buildings, and specifically for low- to medium-rise buildings, the separation walls are considered as stability walls as well. Stability walls are only effective for in-plane loading. Therefore, the stability walls should be chosen such that for various wind directions stability can be guaranteed. Regarding the case study building, the stability walls are indicated in blue, orange and green, together with the various wind directions in figure 8.11. The span direction of the floor slabs is indicated in red for part A1.

For the analysis of the horizontal wind loads, the largest span length of the system is considered. This is in part A1 of figure 8.11, where the span length is 7.8m. At the same time, this means that the stability walls in this area have a centre-to-centre distance of 7.8m as well. In order to determine the wind load on the structure, several variables have to be determined. NEN-EN 1991-1-4 [125] defines these variables and calculation procedures. For the sake of brevity, only the representative value for the distributed wind load ($q_{w,ed}$) is presented in eq. (8.2), where:

$$\begin{aligned}
 q_w &= c_s c_d \cdot c_{pe,10} \cdot c_{corr} \cdot q_p \cdot A_{ref} \\
 q_w &= 1.0 \cdot 1.3 \cdot 0.85 \cdot 0.99 \cdot 3.0 = 3.3 \text{ kN/m} \\
 q_{w,ed} &= \gamma_Q \cdot q_w = 1.5 \cdot 3.3 = 4.95 \text{ kN/m}
 \end{aligned}
 \tag{8.2}$$

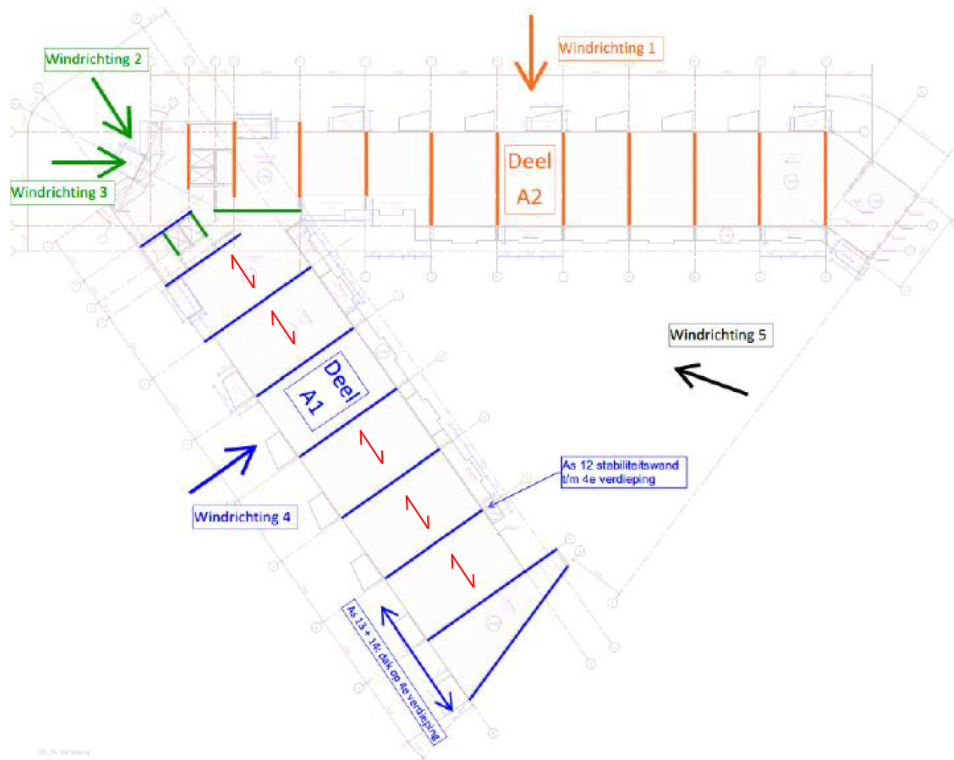


Figure 8.11: Stability walls of the case study building and various wind directions

- $c_s c_d$: structural factor, taken as a conservative value: $c_s c_d = 1.0$
 $c_{pe,10}$: external pressure coefficients for combined the windward and leeward zone: $c_{pe,10} = 0.8 + 0.5 = 1.3$
 c_{corr} : correlation factor for wind pressures between the windward and the leeward side: $c_{corr} = 0.85$
 q_p : peak velocity pressure at reference height: obtained from the national annex of NEN-EN 1991-1-4 [126] table NB.5 for a reference height of 27 meters and terrain category II within the built environment: $q_p = 0.99 \text{ kN/m}^2$
 A_{ref} : reference area per meter width: $A_{ref} = 1.0 \cdot h = 3.0 \text{ m}^2/\text{m}$
 h : height of the considered storey floor: 3.0 m

Since the floor slab is simply supported by the stability walls, the loading scheme of a single field is depicted in figure 8.12a. The stability walls are indicated as two thick black lines, which simulate the continuous support on both edges. The wind loading imposes a bending moment and shear force in the floor slab. In order to verify whether diaphragm action is required, or in other words, collaboration of multiple floor slabs to transmit the horizontal forces to the stability walls. As a starting point, one slab is assumed to take up the forces generated by the wind loading. The loading generates tension on the top side and compression on the bottom side, as illustrated in figure 8.12b. Note that the deformations are exaggerated for illustration purposes. Due to this loading, it is expected that tendon 1 and tendon 2 (marked in red) are elongated and therefore an additional stress increase in the tendons (Δf_{ps}) is generated. Whereas tendon 3 and tendon 4 are in compression (marked in blue). This results in additional tendon forces with internal lever arms of $z_1 = 1052 \text{ mm}$ and $z_2 = 826 \text{ mm}$ from the outermost compressed fibre, since the exact locations of the tendons within the cross-section are known. The tendon forces should be in equilibrium with the imposed bending moment, as expressed in eq. (8.3).

$$\begin{aligned}
 F_1 \cdot z_1 + F_2 \cdot z_2 &= M_{ed} \\
 F_1 \cdot z_1 + F_2 \cdot z_2 &= \frac{1}{8} \cdot q_{w,ed} \cdot l^2
 \end{aligned}
 \tag{8.3}$$

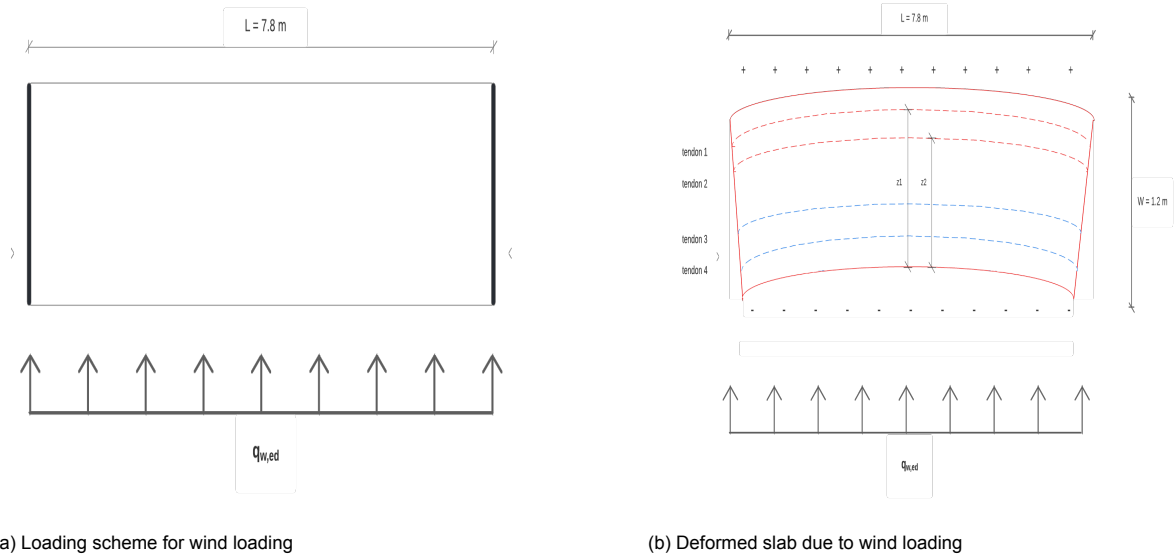


Figure 8.12: Wind loading on the considered floor system

In eq. (8.3), the magnitude of the forces are still unknown and therefore an addition expression should be adopted to solve the equation. It is assumed that the distribution of forces is approximately equal to the ratio of internal lever arms, as expressed in eq. (8.4).

$$\begin{aligned} z_1/z_2 &= 1052/826 \Rightarrow z_1 = 1.27 \cdot z_2 \\ F_1/F_2 &\approx z_1/z_2 \Rightarrow F_1 = 1.27 \cdot F_2 \end{aligned} \quad (8.4)$$

Substitution of eq. (8.4) into eq. (8.3) results in:

$$\begin{aligned} 1.27F_2 \cdot 1.27z_2 + F_2 \cdot z_2 &= \frac{1}{8} \cdot q_{w,ed} \cdot l^2 \\ 2.54F_2 \cdot 0.826 &= 37.7 \text{ kNm} \\ F_2 &= 18.0 \text{ kN} \qquad \qquad \qquad \Rightarrow F_1 = 22.9 \text{ kN} \end{aligned}$$

Analogous to section 7.6, the maximum tendon stress increase (Δf_{ps}) can be calculated according to expressions of the national annex of Eurocode 2 [103] or Alqam et al. [107]. The tendon stress increases of tendon 1 and tendon 2 are presented in eq. (8.5).

$$\begin{aligned} \Delta f_{ps,1} &= \frac{F_1}{A_p} = \frac{22.9 \cdot 10^3}{150} = 152.7 \text{ MPa} \\ \Delta f_{ps,2} &= \frac{F_2}{A_p} = \frac{18.0 \cdot 10^3}{150} = 120.0 \text{ MPa} \end{aligned} \quad (8.5)$$

It is assumed that the maximum horizontal wind load on the system occurs in serviceability limit state for the vertically imposed loading. Therefore, maximum stress increase in the tendons can be generated for wind loading. According to the national annex of Eurocode 2 [103], the maximum tendon stress increase is limited to: $\Delta f_{ps} = 50 \text{ MPa}$, whereas according to Alqam et al. [107]: $\Delta f_{ps} = 361.7 \text{ MPa}$ for a span length of $l = 7.8 \text{ m}$. Therefore, it can be concluded that, for the maximum tendon stress increase calculated in accordance with Alqam et al. [107], one slab has sufficient capacity to resist the horizontal wind load. However, in accordance with the national annex of Eurocode 2 [103], additional measures should be taken. Therefore, it is suggested to connect two adjacent slabs in order to increase the load bearing capacity of the system for horizontal wind loads. Connecting two slabs changes the behaviour

of the system, depending on the degree of cooperation. Basically, two mechanisms can occur: (i): full composite action or (ii): no composite action. In reality, it is expected that the mechanism will be somewhere in between both situations, that is partial composite action. However, in the analysis performed in this section, only these two mechanisms are considered.

Figure 8.13 illustrated both mechanisms. For simply supported beams where there is no connection between the elements, the slip at the interface is free and the two elements independently resist the transverse loading, where each beam has a compression and tension zone. The global bending stiffness is the sum of each elementary stiffness. When a perfect connection is established, the two elements act together without slip at the interface, where one element is primarily under compression and the other element under tension. The global bending stiffness is much higher than the sum of each elementary stiffness [127].

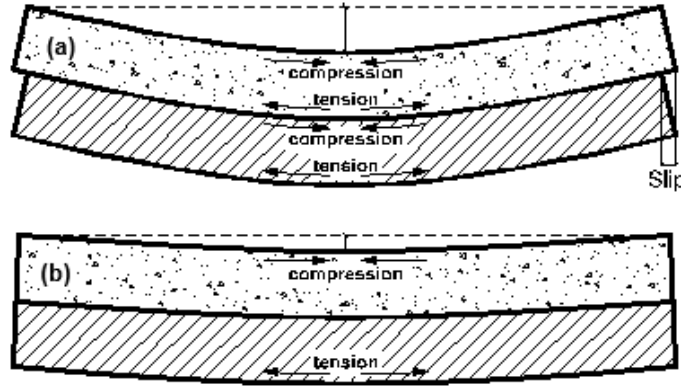


Figure 8.13: Composite action for beams: (a) no composite action; (b) full composite action [127]

Following this analogy, both mechanisms are considered for the proposed floor system. The mechanisms illustrated in figure 8.13 are translated to the floor slab in figure 8.14. In figure 8.14a both floor slabs consist of a tension and a compression zone. Similar to figure 8.12, tendons 1 and tendon 2 are elongated and an additional stress increase in the tendons (Δf_{ps}) is generated. The internal lever arms for both slabs is the same: $z_1 = 1052\text{mm}$ and $z_2 = 826\text{mm}$. Substitution of these parameters into eq. (8.3), under the assumption that the ratio of forces is approximately equal to the ratio of internal lever arms, as expressed in eq. (8.4), results in:

$$\begin{aligned}
 F_1 \cdot z_1 + F_2 \cdot z_2 &= \frac{1}{2} \cdot M_{ed} \\
 1.27F_2 \cdot 1.27z_2 + F_2 \cdot z_2 &= \frac{1}{2} \left(\frac{1}{8} \cdot q_{w,ed} \cdot l^2 \right) \\
 2.61F_2 \cdot 0.826 &= \frac{1}{2} \cdot 37.7 \\
 F_2 &= 8.7\text{kN} & \Rightarrow F_1 &= 11.1\text{kN}
 \end{aligned}$$

With the calculated tendon forces, the stress increase in the tendons can be calculated as well. The tendon stress increases are presented in eq. (8.6). Concluding from eq. (8.6), the tendon stress increases are still too high with respect to the requirements imposed by the national annex of Eurocode 2 [103]. Therefore, zero composite action is not sufficient to ensure safety of the structure and, in the case of two slabs, composite action of the slabs should be enabled.

$$\begin{aligned}
 \Delta f_{ps,1} &= \frac{F_1}{A_p} = \frac{11.1 \cdot 10^3}{150} = 74\text{MPa} \\
 \Delta f_{ps,2} &= \frac{F_2}{A_p} = \frac{8.7 \cdot 10^3}{150} = 58\text{MPa}
 \end{aligned} \tag{8.6}$$

Starting from the assumption that full composite action of the two floor slabs is guaranteed, results in the mechanism illustrated in figure 8.14b. In line with the reasoning presented in figure 8.13, the top

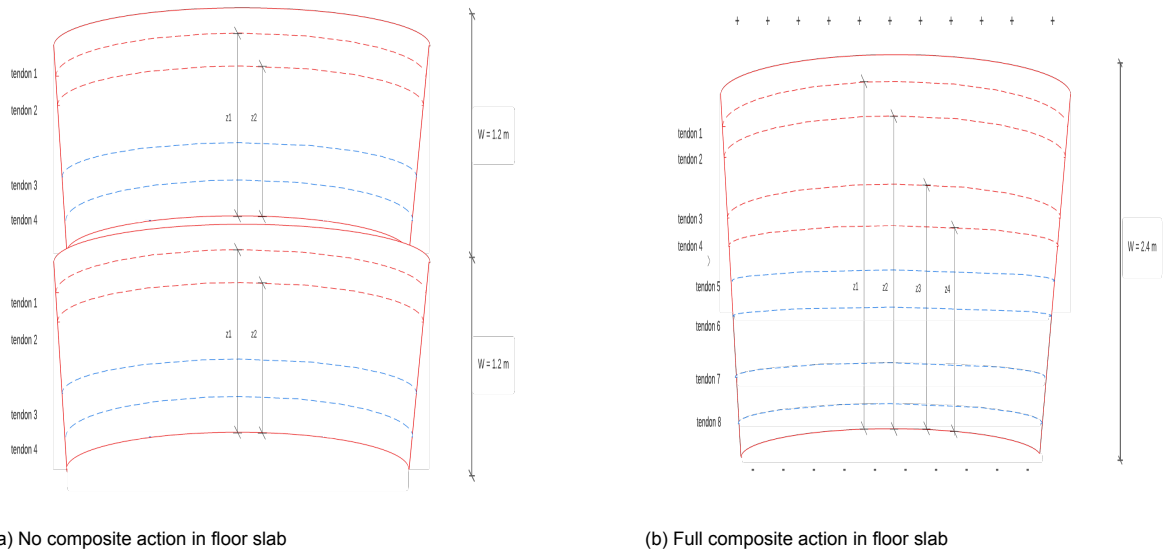


Figure 8.14: Two mechanisms for determination of tendon forces under wind loading

slab is in tension and the bottom slab is in compression. Again, tendon 1 to tendon 4 are elongated and additional stress increases are generated. The internal lever arms of the considered tendons are changed, since the two slabs are assumed to fully cooperate. The internal lever arms are: $z_1 = 2252\text{mm}$, $z_2 = 2026\text{mm}$, $z_3 = 1574\text{mm}$ and $z_4 = 1348\text{mm}$, since the exact locations of the tendons in the cross-sections are known. The ratios of internal lever arms is presented in eq. (8.7). Analogous to the previous calculations, substitution of the parameters into eq. (8.3), under the assumption that the ratios of forces is approximately equal to the ratios of internal lever arms, results in:

$$\begin{aligned} z_1/z_2 &= 2252/2026 \Rightarrow z_1 = 1.11 \cdot z_2 \\ z_3/z_2 &= 1574/2026 \Rightarrow z_3 = 0.78 \cdot z_2 \\ z_4/z_2 &= 1348/2026 \Rightarrow z_4 = 0.67 \cdot z_2 \end{aligned} \quad (8.7)$$

$$\begin{aligned} F_1 \cdot z_1 + F_2 \cdot z_2 + F_3 \cdot z_3 + F_4 \cdot z_4 &= M_{ed} \\ (1.11^2) F_2 \cdot z_2 + (1.0^2) F_2 \cdot z_2 + (0.78^2) F_2 \cdot z_2 + (0.67^2) F_2 \cdot z_2 &= 37.7 \\ \Rightarrow F_1 = 5.8\text{kN} \quad F_2 = 5.2\text{kN} \quad F_3 = 4.1\text{kN} \quad F_4 = 3.5\text{kN} \end{aligned}$$

Concluding from eqs. (8.8) and (8.9), the tendon stresses comply with the maximum limit value imposed by national annex of the Eurocode 2 [103]. Therefore, when full composite action between two adjacent slabs is realised, safety of the floor system regarding horizontal wind loads is ensured.

$$\Delta f_{ps,1} = \frac{F_1}{A_p} = \frac{5.8 \cdot 10^3}{150} = 38.7\text{MPa} \quad \Delta f_{ps,2} = \frac{F_2}{A_p} = \frac{5.2 \cdot 10^3}{150} = 34.7\text{MPa} \quad (8.8)$$

$$\Delta f_{ps,3} = \frac{F_3}{A_p} = \frac{4.1 \cdot 10^3}{150} = 27.3\text{MPa} \quad \Delta f_{ps,4} = \frac{F_4}{A_p} = \frac{3.5 \cdot 10^3}{150} = 23.3\text{MPa} \quad (8.9)$$

Several conclusions can be drawn from the analyses presented in this section. First, diaphragm action of multiple slabs is not necessarily required for the horizontal wind loads if the tendon stress increase, calculated in accordance with Alqam et al. [107], is used. The tendons in one slab have sufficient capacity to resist the horizontal uniformly distributed load. However, in accordance with the national annex of Eurocode 2 [103], at least two slabs have to be connected in such a way to achieve full composite action, in order to resist the horizontal wind loads. One of the frequently used methods is the application of a concrete topping (in Dutch: 'druklaag') on top of floor systems. A concrete topping

enables proper diaphragm action of all individual floor slabs. However, applying a concrete topping has a detrimental effect on the demountability of the floor system and, therefore, should not be used if a building is designed according to the framework presented in section 3.

Dry connections should be preferred over wet connections such as concrete toppings. Establishing a dry connection between two slabs can be done with bolts. One example of a dry connection between two slabs is proposed by Glabbeek [99], where bolt anchors are cast into the concrete, covered with a steel plate and on top four bolt nuts can be fastened. This is illustrated in figure 8.15a. Another option is suggested by Volkov [128], which utilises bolts and steel plates as well. However, contradictory to the design suggested by Glabbeek [99], bolt anchors are not used, but the bolts penetrate through the concrete and are anchored using anchor nut and heads. The suggested connection is depicted in figure 8.15b. Note that Volkov [128] proposed the solution for connecting hollow core slabs, so with respect to the proposed floor system of this thesis, grouted cores and V-gaps are not present.



(a) Dry connection proposed by Glabbeek [99]

(b) Dry connection proposed by Volkov [128]

Figure 8.15: Dry connections with a bolt anchor embedded in the concrete (left) and bolts penetrating through the concrete

Both suggested dry connections are considered applicable in the proposed floor system. For implementation of the solution of Glabbeek [99], the proposed design should be reconsidered and additional reinforcement should be installed to anchor the embedded bolt anchors. Implementation of this kind of solution is recommended for future research. The advantage of the solution proposed by Volkov [128] is that the holes for the bolts can be drilled on site. However, tolerances for bolt diameters and edge distances should be taken into consideration to avoid local spalling of the concrete. Additionally, this is not an aesthetically attractive solution, due to the penetration at both sides of the concrete. Both a raised floor system and a suspended ceiling are required to conceal this type of connection.

The most effective location for the slab connections is near the vertical supports of the floor slab, due to highest transverse shear force induced by the horizontal wind loading. In case of larger distances between stability walls or higher horizontal wind loads, the moment generated in the floor system will increase as well. This is particularly the case when designing for utility or high-rise apartment buildings. Moreover, for earthquake induced loading, stricter requirements regarding diaphragm action of the floor slab could be necessary. It is therefore suggested to change the design of the proposed floor system to install unbonded post-tensioning in the transverse direction as well.

IV

Conclusion

9

Discussion

The impetus for this research originated from two personal interest directions. The first one is related to the residential housing market in the Netherlands. At this moment, there is a distressing housing shortage. The best possible solution to overcome this issue is by investing in newly built houses. The majority of the Dutch housing stock is subdivided into ground-based housing units and low to medium-rise apartment buildings and therefore the most interesting target group to invest in. However, the construction sector is known for its conservative character, while circular thinking is gaining momentum in society and natural resources are becoming increasingly scarce. Hence, the way buildings are designed should fundamentally change. This is related to the second personal interest direction. Implementation of circular principles in the design phase of buildings is only a matter of time. Stricter legislation and regulations from the European Commission and national governments are expected in the near future. Changing to circular design approaches generates more comprehensive and robust structures for generations to come.

Related to this research, several outcomes of the analysis can be discussed. This can be done on a global scale of this research, for example the adopted circular principles or framework or on a more subject orientated scale, such as structural parameters or assumption in the performed analyses. In this section both will be discussed.

Based on literature review, various circular principles have been gathered. Numerous principles or strategies have been proposed throughout scientific literature in order to achieve circular designs in a broad economic perspective. Munaro et al. concluded that only a handful of combined strategies in a comprehensive framework are available for the built environment. Cheshire extensively focuses on design principles. However, buildings that meet circular design principles are not necessarily appealing to the market. Due care has to be taken into consideration regarding the analysis of new business models and services. Consultations with clients for implementation of these new business models, together with financial or contractual agreements is of the utmost importance for the success rate of buildings designed according to circular principles.

Zooming in on the various principles and strategies highlighted in this thesis project, a lot of overlap between strategies is noticeable. Open building systems can both be categorised as a strategy for adaptability or for disassembly. Therefore, subdividing different strategies under design principles has some degree of subjectivity. Moreover, between some strategies, conflicting situations can occur. Increasing the floor-to-floor heights of buildings generates additional space for building services that should be separated from the load bearing structure. Accessibility and reconfigurability of building service is considered as an important circular design criteria. However, increasing the floor-to-floor height of buildings increases the total building height as well, resulting in higher costs for facade cladding, which is known to be one of the biggest cost drivers in buildings. Therefore, combining the circular design principles with the financial aspects of buildings is a delicate procedure and may vary for different buildings and clients. In other words, there is no one holistic solution for all situations.

Within the context of the framework, the multi-criteria analysis that has been performed is based on 25 criteria relating to the adaptability and demountability of buildings. In this research, criteria relating to designing out waste and material selection have not been implemented in the multi-criteria analysis. Strict legislation and insufficient scientific consensus hamper the application of technological advancements in the design phase. This reasoning reveals a limitation of the performed multi-criteria analysis. Moreover, the multi-criteria analysis can be adjusted by changing the assumed starting points for building services for example. Furthermore, the multi-criteria analysis for the five floor systems may be different when performed by someone else, that is: some degree of subjectivity in the results. However, all design criteria are fully objective for every analysis performed by whomever.

The second to last discussion point of the research is related to the verification section of the newly proposed floor system. The bending moment capacity is calculated according to equilibrium equations at the critical cross-sections in two ways: based on the Eurocode and on state-of-the-art research. Without further analysis, the Eurocode imposes limit values for the maximum tendon stress increase. Due to the conservative nature of the Eurocode, it is questionable if the limit value truly represents the behaviour of the system at ultimate limit state. For this reason, the state-of-the-art expressions of Alqam et al. have been used to analytically approximate the bending moment capacity at ultimate limit state. These expressions are validated for span-to-depth ratios in the range between 7.8 and 55.2 for monolithic beams and slabs, including both internal and external tendons. The span-to-depth ratios of the newly proposed floor system are within the validated domain. However, for application of these expressions, the proposed floor system is modelled as a monolithic slab. Therefore revealing an consequential assumption in the calculation and analysis model.

In the analysis of horizontal loading, only the effects of wind are considered for the stability of the system and within the context of the reference case study. Diaphragm action is an important consideration in the design of floor systems. Usually, diaphragm action is ensured by application of a concrete top layer. Based on the performed analysis, two connected floor slabs provide sufficient strength capacity to resist the horizontal wind loading under the maximum tendon stress increase limit values prescribed by the national annex of the Eurocode 2. Moreover, the connections are assumed to enable full composite action of both slabs.

10

Conclusions

In order to answer the central research question, sub-questions have been defined in section 2.3 and answers to these sub-questions are gathered throughout this research. For the final conclusion, the answers to each sub-question are given first. Next, the conclusions are combined to answer the central research question. The central research question is repeated first.

Central research question

To what extent can a modular floor system, consisting of prefabricated concrete elements, be designed to meet the structural, circular and stakeholder requirements for application in residential buildings?

10.1. Sub-questions

This first section repeats the five sub-questions and formulates answers to those sub-questions.

- i What are the state-of-the-art frameworks and principles for a circular economy?*
 - (a) How can circular principles be implemented in the design phase for the built environment?*
 - (b) What criteria can be distinguished in order to evaluate the design?*
 - (c) Are there any barriers or limitations to implementing circular design criteria?*

From literature review, it can be concluded that substantial amounts of scientific information and approaches can be gathered regarding frameworks and principles for a circular economy. One example is the large variety of nuances in the different R-strategies. The circular concept of material conservation has already been successfully implemented in several industries. The commonality in all proposed frameworks is that smarter product design and extended lifespans of products should be pursued. Regarding the built environment, only a handful of combined strategies into a framework are proposed. The most comprehensive framework for the built environment is proposed by Cheshire.

Cheshire developed his framework specifically for the design phase of buildings. The framework consists of six nested circles that define the hierarchy of the framework, in which retaining buildings or building components is the least invasive measure and therefore the most favorable solution. Recycling of buildings or building components requires the most effort and invasive measures and is considered the least favorable option. Overlapping these nested circles, Cheshire proposes five principles for implementing in the design phase. These five design principles are: **(i)**: building in layers, **(ii)**: designing out waste, **(iii)**: design for adaptability, **(iv)**: design for disassembly and **(v)**: selecting materials. This

research project expanded the design principles of Cheshire, by defining and providing hands-on criteria for each design principle. In total, 42 criteria are proposed for transposition into a comprehensive framework for application in practice.

At the time of writing, it is not possible to implement all 42 proposed criteria into design practice. Several barriers and/or limitations are found, especially for the circular principles of designing out waste and selecting materials. For the latter case, integration of by-products or material recycling is still at an early stage of development for application in current practice. Moreover, strict legislation hamper the application of novel technologies as well. Regarding designing out-waste, despite the fact that BIM is widely available and utilised in practice, the end-of-life management of buildings is still not an integral part of buildings yet.

ii How and to what extent are circular principles recently applied in building projects?

Recent building projects are considered in this research project with the intention to investigate which circular principles or strategies are applied. Two different types of buildings are considered, namely: utility and residential buildings. Park 20|20 is one of the first utility building projects with circular principles taken into account. The project is based on the Cradle-to-Cradle principle. Sustainable material use and energy consumption are key characteristics of the project. The 'People's Pavilion' in Eindhoven and the 'ABN Amro Pavilion' in Amsterdam are two projects that specifically focused on demountability and enabling reuse of building components after the allocated service life. Moreover, only second-hand materials or building components have been used in the 'People's Pavilion' project. The last considered utility building project is the 'Temporary Courthouse' in Amsterdam. This project is characterised as a pioneering project which is focused on full demountability of the structure and investigation of residual value of such buildings.

Regarding residential buildings, two projects are considered in this research. The first project is 'Superlocal' in Kerkrade. This project is characterised by the recycling and, where applicable, reuse of structural components. The newly built ground based housing units can be completely deconstructed afterwards. The second project is 'Te Veld' in Eindhoven. The housing units (yet to be built) maximize usage of sustainable building materials and enable complete deconstruction after the project duration, initially set at 30 years.

iii Which concrete floor systems are currently widely used in the built environment, both for residential and utility buildings and why?

Several concrete floor systems are widely used in residential and utility buildings. Concrete floor systems have favorable characteristics in terms of: strength, rigidity, acoustic and thermal insulation, fire resistance and span lengths. For residential and utility buildings, the Dutch Building Decree impose strict requirements regarding acoustic insulation of separating floors in buildings. The most efficient way to improve acoustic insulation is to add mass to the system. Additionally, concrete floor systems are generally well available and offer a variety of suppliers. Standardisation of the production processes result in cost-efficient options as well. The most commonly used concrete floor systems in practice are: **(i)**: hollow core slabs, **(ii)**: service-integrated floor systems, **(iii)**: reinforced plank floors and **(iv)**: Bestcon floor systems.

iv What are other requirements for a floor system, apart from circular principles?

- (a) Which structural aspects are of importance to ensure safe buildings?*
- (b) Does the Dutch Building Decree set certain requirements?*
- (c) What are stakeholder prerequisites for a floor system?*

The first sub-question elaborated circular principles in the design phase of buildings. However, in order to determine the functionality of floor systems, other aspects should be taken into consideration as well. Structural aspects affect the load bearing capacity of floor systems. Several codes of practice, for example the Eurocodes and their national annexes, provide calculation procedures to determine structural parameters. Codes of practice can be consulted for most general cases. However, these codes of practice are known for their degree of conservatism. Extensive research projects, such as Alqam et al. [107], develop calculation procedures in conjunction with a large database of test results.

However, unlike the codes of practice, the proposed calculation procedures do not provide a legal basis for verification of the results.

For the structural design of buildings and civil engineering works the Eurocodes provide a variety of reference material regarding safety, serviceability and durability of these structures. In this thesis project reference is made to: EN 1990, EN 1991 and EN 1992 as the main sources. The aspects considered in the verification of the proposed floor system are in serviceability and ultimate limit state. In serviceability limit state the cross-sectional stresses, deflections and vibrations are verified. In ultimate limit state the bending moment, shear force and shear stress resistance in the interfaces of the elements are verified. Horizontal loading due to wind is considered as well. All obtained results are satisfactory under normal loading conditions. However, it should be noted that accidental load situations, such as fire loading or seismic activity are not considered in this thesis project. Robustness of the proposed floor system is discussed in section 11.

Additional requirements, imposed by the Dutch Building Decree or stakeholders, should be considered as well in order to increase the applicability of the floor system in practice. The Dutch Building Decree impose regulations regarding floor-to-floor heights and acoustic insulation. Stakeholders and the users of the building impose requirements related to the installation of building services to increase living comfort. For the proposed floor system, it is recommended to incorporate building services into the plenum of either a suspended ceiling, a raised floor system or a combination of both. Maximum accessibility and reconfigurability of building services is guaranteed in this way and separation of building layers is well accomplished. Small recesses can be applied in the empty voids of the weight-reduced elements and larger recesses can be made using a conventional trimmer beam.

v How does the newly proposed floor system compare to the current market offer?

In order to compare the newly proposed floor system with the four commonly used concrete floor systems, a multi-criteria analysis has been performed. The starting point of the multi-criteria analysis is based on 25 criteria of the circular design framework. A weighted rating scale from zero to four has been used, where zero is the lowest and four is the highest attainable score per criterion. The weight of each criterion is equal. Therefore, a theoretical score of one hundred can be obtained. The calculated results show that the four commonly used concrete floor systems score average/fair to good in the multi-criteria analysis. The newly proposed floor systems scores excellent. The main differences compared to the other floor systems are related to the reconfigurability, scalability and modularity of the newly proposed floor system. Therefore, it can be concluded that the newly proposed floor system is a better alternative than the commonly used concrete floor systems, from a circular design perspective.

10.2. Central research question

A final conclusive answer to the central research question can be provided now that the research sub-questions have been answered.

To what extent can a modular floor system, consisting of prefabricated concrete elements, be designed to meet the structural, circular and stakeholder requirements for application in residential buildings?

After an iterative design process, the geometrical dimensions and the adopted post-tensioning system of the newly proposed floor system are presented. The newly proposed floor system fulfills the requirements under normal loading conditions according to analytical expressions imposed by the various Eurocodes and, under the predefined assumptions, according to analytical expressions proposed by state-of-the-art research. Stakeholder requirements with regard to recesses and building services are met as well. The newly proposed floor system is suitable for using common tools and equipment and is sized to suit the means of handling. As the multi-criteria analysis has shown, the newly proposed floor system translates valuable dimensions and design criteria into the design to a higher extent compared to the most commonly used concrete floor systems. Nevertheless, the proposed floor system still facilitates sufficient room for improvements. As a conclusive statement to the central research question: the proposed system, but most importantly: the analogy of designing buildings and load bearing floor systems in this way, provides a more comprehensive, future-orientated and yet practical alternative for application in residential buildings.

Recommendations

This section includes recommendations for future research and developments of the newly proposed floor system for use in practice. Some aspects have not been considered throughout this thesis project, but deserve additional attention. A dichotomy is proposed: **(i)**: expansion of the analogy or analyses of the system and **(ii)**: developments of the proposed design.

11.1. Expansion of the analogy or analysis of the system

- *Feedback from an expert panel*

The current version of the multi-criteria analysis consists of a weighted rating system from zero to four, in which each criterion is equal in weight. Allocation of the ratings or scores consists, per definition, of a certain degree of subjectivity. More input data from experienced engineers increases the reliability of the scoring. Moreover, the multi-criteria analysis can be expanded in the future with more criteria when the other design principles are included as well.

- *Business models*

Literature review has revealed that the applicability of circular design principles not necessarily results in appealing buildings. New business models should be developed in conjunction with clients and governmental institutions in order to make cost-effective buildings. Demountable buildings are more expensive in the design and construction phase, but including the residual value of buildings or building components may offset the difference compared with traditionally constructed buildings.

- *Cost analysis*

Financial considerations are one of the decisive factors that determine the applicability of various building components in current practice. This research is performed from an academic perspective and therefore lack an analysis related to the costs of the newly proposed floor system. Cost analysis is comprehensive and is not solely related to the components only. For instance, costs related to transportation, labour or the production process should be included. Moreover, since this system is designed to be fully demountable and reusable, storage costs of the elements for a certain period of time should be taken into consideration as well. Together with a residual value calculation of the elements, as mentioned in the previous recommendation point, offer interesting subjects for further research.

11.2. Developments of the proposed design

- *Optimisation*

After an iterative design process, the geometrical dimensions and the adopted post-tensioning systems of the newly proposed floor system are presented. Parametric study of the geometric properties of the system, however, can result in more optimised cross-sections. The weight reduced voids in the proposed design are circular and located at centroidal axis level. Adopting

other shapes, such as oval voids, may result in a larger number of voids and therefore more self-weight reduction. Additionally, different post-tensioning systems can be considered, such as unbonded multi-strand systems. In the course of this research, it was found that post-tensioning bars could be applied as well. However, imposed edge and center-to-center distances from the manufacturer of the system did not result in a feasible design.

- *Balconies*

The prerequisites of stakeholders regarding building services and recesses are considered in this research. For residential buildings and primarily apartment buildings, balconies are a commonality. The integration of balconies into the load-bearing structure of buildings is a highly complex design aspect and varies according to a multitude of customer requirements. Due to this variation and complexity, this prerequisite is not covered in this research. A starting point for the configuration of balconies, in the current design, is suggested. The demountable and modular character of the proposed floor system limit the available options for balconies. It is therefore suggested to further explore the possibilities for balconies that are supported by additional columns or by consoles in combination with tension rods (in Dutch: 'trekstangen').

- *Utility buildings*

Residential buildings have been the main focus of this thesis. For application of the proposed floor system in utility buildings, different imposed loading configurations and/or span lengths should be considered. Span lengths of utility buildings are generally larger than those of residential buildings. Moreover, the imposed vertical loading may be of a different magnitude as well. Therefore, the proposed dimensions may not fulfill the requirements in serviceability and ultimate limit state under normal loading conditions. Adjustments to the proposed floor system are conceivable and require further research.

- *Robustness*

Robustness of the system is an important aspect when the proposed system is taken into service. Degradation of the concrete quality for frequent dis- and reassembly, together with resistance against wear and tear under normal use should be considered as well. Regarding the post-tensioning tendons, the minimum required amount of tendons is calculated in the analysis. However, in case of unexpected failure of one of the tendons, it is recommended to use a larger amount of prestressing tendons, but with a lower initial amount of prestressing force. For example, for a span length of 5.4 meters, the minimum required amount of tendons is two. Increasing the amount of tendons to four, but with half of the initial prestressing force, increases the robustness of the floor system. However, it is recommended to repeat the calculation procedure in order to determine the new resistance of the floor system. The last recommendation regarding robustness is related to addition of practical (non-prestressed) reinforcement in the elements to ensure more robustness in, for example, the assembly process or during hoisting operations.

Bibliography

- [1] F. Bonviu. “The European economy: From a linear to a circular economy”. In: *Romanian J. Eur. Aff.* 14 (2014), p. 78.
- [2] B. Suárez-Eiroa et al. “Operational principles of circular economy for sustainable development: Linking theory and practice”. In: *Journal of Cleaner Production* 214 (2019), pp. 952–961. DOI: <https://doi.org/10.1016/j.jclepro.2018.12.271>.
- [3] European Commission. *Towards a circular economy: A zero waste programme for Europe*. Brussels, 2014.
- [4] A. Murray et al. “The Circular Economy: An Interdisciplinary Exploration of the Concept and Application in a Global Context”. In: *Journal of Business Ethics* 140 (3 Feb. 2017), pp. 369–380. DOI: [10.1007/s10551-015-2693-2](https://doi.org/10.1007/s10551-015-2693-2).
- [5] K.E. Boulding. “The economics of the coming spaceship earth”. In: *New York* (1966).
- [6] J. Kirchherr et al. “Barriers to the Circular Economy: Evidence From the European Union (EU)”. In: *Ecological Economics* 150 (2018), pp. 264–272. ISSN: 0921-8009. DOI: <https://doi.org/10.1016/j.ecolecon.2018.04.028>.
- [7] J. Kirchherr et al. “Conceptualizing the circular economy: An analysis of 114 definitions”. In: *Resources, Conservation and Recycling* 127 (2017), pp. 221–232. DOI: [10.1016/j.resconrec.2017.09.005](https://doi.org/10.1016/j.resconrec.2017.09.005).
- [8] Ellen MacArthur Foundation. *Delivering the circular economy - a toolkit for policymakers*. June 2015.
- [9] S. Sauvé et al. “Environmental sciences, sustainable development and circular economy: Alternative concepts for trans-disciplinary research”. In: *Environmental Development* 17 (2016), pp. 48–56. DOI: <https://doi.org/10.1016/j.envdev.2015.09.002>.
- [10] M. Geissdoerfer et al. “The Circular Economy – A new sustainability paradigm?” In: *Journal of Cleaner Production* 143 (2017), pp. 757–768. DOI: <https://doi.org/10.1016/j.jclepro.2016.12.048>.
- [11] J. Korhonen et al. “Circular economy as an essentially contested concept”. In: *Journal of Cleaner Production* 175 (2018), pp. 544–552. DOI: <https://doi.org/10.1016/j.jclepro.2017.12.111>.
- [12] Raad voor de Leefomgeving en Infrastructuur. *Circulaire economie: van wens naar uitvoering*. June 2015.
- [13] K. Winans et al. “The history and current applications of the circular economy concept”. In: *Renewable and Sustainable Energy Reviews* 68 (2017), pp. 825–833. DOI: <https://doi.org/10.1016/j.rser.2016.09.123>.
- [14] Sociaal Economische Raad. *Werken aan een circulaire economie: geen tijd te verliezen*. June 2016.
- [15] United Nations, Department of Economic and Social Affairs, Population Division. *World Population Prospects 2019: Highlights (ST/ESA/SER.A)*. June 2019.
- [16] European Commission. *Europe 2020: A strategy for smart, sustainable and inclusive growth*. Brussels, 2010.
- [17] European Commission. *Closing the loop: An EU action plan for the circular economy*. Brussels, 2015.

- [18] European Commission. *Monitoring framework for the circular economy*. Brussels, 2018.
- [19] European Commission. *The European Green Deal*. Brussels, 2019.
- [20] European Commission. *A new Circular Economy Action Plan: For a cleaner and more competitive Europe*. Brussels, 2020.
- [21] Ministerie van Infrastructuur en Waterstaat. *Circular Dutch Economy by 2050*. Nov. 2019.
- [22] Ministerie van Infrastructuur en Milieu & Ministerie van Economische Zaken. *Nederland circulair in 2050*. Sept. 2016.
- [23] Ministerie van Infrastructuur en Waterstaat. *Grondstoffenakkoord: Intentieovereenkomst om te komen tot transitieagenda's voor de circulaire economie*. Jan. 2017.
- [24] Rijksoverheid. *Nederland circulair in 2050*. URL: <https://www.rijksoverheid.nl/onderwerpen/circulaire-economie/nederland-circulair-in-2050> (visited on 09/29/2021).
- [25] Ministerie van Infrastructuur en Waterstaat. *Uitvoeringsprogramma circulaire economie 2019-2023*. Feb. 2019.
- [26] M. Kamali et al. "Conventional versus modular construction methods: A comparative cradle-to-gate LCA for residential buildings". In: *Energy and Buildings* 204 (2019), p. 109479. DOI: <https://doi.org/10.1016/j.enbuild.2019.109479>.
- [27] United Nations Environment Programme. *2020 global status report for buildings and construction: Towards a zero-emission, efficient and resilient buildings and construction sector*. Nairobi, 2020.
- [28] A. Marino and P. Pariso. "Comparing European countries' performances in the transition towards the Circular Economy". In: *Science of The Total Environment* 729 (2020), p. 138142. DOI: <https://doi.org/10.1016/j.scitotenv.2020.138142>.
- [29] A. Bonoli et al. *Sustainability in building and construction within the framework of circular cities and European new green deal. The contribution of concrete recycling*. Feb. 2021, pp. 1–16. DOI: [10.3390/su13042139](https://doi.org/10.3390/su13042139).
- [30] Ministerie van Infrastructuur en Waterstaat. *De transitieagenda circulaire bouwconomie*. Jan. 2018.
- [31] MVO Netwerk Beton. *Betonakkoord voor duurzame groei*. July 2018. URL: <https://www.betonakkoord.nl/betonakkoord/> (visited on 09/01/2021).
- [32] NOS. *Schreeuwend tekort aan woningen, wat moet eraan gedaan worden?* Feb. 2021. URL: <https://nos.nl/artikel/2369109-schreeuwend-tekort-aan-woningen-wat-moet-eraan-gedaan-worden> (visited on 10/05/2021).
- [33] Centraal Bureau voor de Statistiek. *Prijsstijging koopwoningen opnieuw hoger*. June 2021. URL: <https://www.cbs.nl/nl-nl/nieuws/2021/25/prijsstijging-koopwoningen-opnieuw-hoger> (visited on 05/06/2022).
- [34] Centraal Bureau voor de Statistiek. *12.5 duizend woningen door transformatie van gebouwen in 2019*. Oct. 2020. URL: <https://www.cbs.nl/nl-nl/nieuws/2020/44/12-5-duizend-woningen-door-transformatie-van-gebouwen-in-2019> (visited on 10/05/2021).
- [35] NOS. *Grote werkgevers gaan na corona kantoorruimte schrappen*. Jan. 2021. URL: <https://nos.nl/nieuwsuur/artikel/2366749-grote-werkgevers-gaan-na-corona-kantoorruimte-schrappen> (visited on 10/05/2021).
- [36] NOS. *Wat doen deze bedrijven met hun kantoorruimte?* Jan. 2021. URL: <https://nos.nl/nieuwsuur/artikel/2366750-wat-doen-deze-bedrijven-met-hun-kantoorruimte.html> (visited on 10/05/2021).

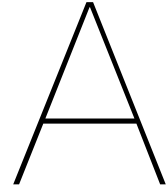
- [37] Trouw. *Kunnen tijdelijke woningen de wooncrisis oplossen?* Mar. 2021. URL: <https://www.trouw.nl/economie/kunnen-tijdelijke-woningen-de-wooncrisis-oplossen-eindhoven-neemt-het-voortouw~b0b306b2/> (visited on 10/05/2021).
- [38] E. Durmisevic. “Transformable building structures: design for disassembly as a way to introduce sustainable engineering to building design & construction”. PhD thesis. Delft University of Technology, 2006.
- [39] S. Ortlepp et al. *Demountable construction for sustainable buildings*. June 2015. URL: https://www.researchgate.net/publication/278675186_Demountable_construction_for_sustainable_buildings.
- [40] R. Merli et al. “How do scholars approach the circular economy? A systematic literature review”. In: *Journal of Cleaner Production* 178 (2018), pp. 703–722. ISSN: 0959-6526. DOI: <https://doi.org/10.1016/j.jclepro.2017.12.112>.
- [41] R. Minunno et al. “Strategies for Applying the Circular Economy to Prefabricated Buildings”. In: *Buildings* 8.9 (2018). DOI: [10.3390/buildings8090125](https://doi.org/10.3390/buildings8090125).
- [42] W. McDonough and M. Braungart. *Remaking the way we make things: Cradle to cradle*. New York: North Point Press, 2002. ISBN: 9780865475878.
- [43] M.E. Toxopeus et al. “Cradle to cradle: Effective vision vs. efficient practice?” In: *Procedia cirp* 29 (2015), pp. 384–389. DOI: [10.1016/j.procir.2015.02.068](https://doi.org/10.1016/j.procir.2015.02.068).
- [44] K.M. Rahla et al. “Implementing Circular Economy Strategies in Buildings—From Theory to Practice”. In: *Applied System Innovation* 4.2 (2021). DOI: [10.3390/asi4020026](https://doi.org/10.3390/asi4020026).
- [45] A. Lansink. *Report of parliamentary debates 1979-1980*. The Hague: SDU, 1979.
- [46] J. Potting et al. *Circular economy: Measuring innovation in the product chain*. The Hague: PBL Netherlands Environmental Assessment Agency, 2017.
- [47] European Commission. *Directive 2008/92/EC of the European Parliament and of the council of 19 november 2008 on waste and repealing certain directives*. Brussels, 2008.
- [48] S. Sihvonen and T. Ritola. “Conceptualizing ReX for Aggregating End-of-life Strategies in Product Development”. In: *Procedia CIRP* 29 (2015). The 22nd CIRP Conference on Life Cycle Engineering, pp. 639–644. DOI: <https://doi.org/10.1016/j.procir.2015.01.026>.
- [49] A. Campbell. “Mass timber in the circular economy: paradigm in practice?” In: *Proceedings of the Institution of Civil Engineers - Engineering Sustainability* 172.3 (2019), pp. 141–152. DOI: [10.1680/jensu.17.00069](https://doi.org/10.1680/jensu.17.00069).
- [50] Arup. *The circular economy in the built environment*. Sept. 2016. URL: <https://www.arup.com/perspectives/publications/research/section/circular-economy-in-the-built-environment> (visited on 10/20/2021).
- [51] D. Cheshire. *Building revolutions: Applying the circular economy to the built environment*. 1st ed. London: RIBA Publishing, 2016. DOI: <https://doi.org/10.4324/9780429346712>.
- [52] K. Van den Berghe and M. Vos. “Circular area design or circular area functioning? A discourse-institutional analysis of circular area developments in Amsterdam and Utrecht, The Netherlands”. In: *Sustainability* 11.18 (2019). DOI: [10.3390/su11184875](https://doi.org/10.3390/su11184875).
- [53] P. Crowther. “Developing an inclusive model for design for deconstruction”. In: *Proceedings of the CIB Task Group 39 - Deconstruction Meeting*. Rotterdam: CIB, Int Council for Research and Innovation in Bd, 2001, pp. 1–26. URL: <https://eprints.qut.edu.au/2884/> (visited on 10/12/2021).
- [54] N.J. Habraken. *The structure of the ordinary*. Cambridge: MIT Press, 1998.
- [55] F. Duffy and A. Henny. *The changing city*. London: Bulstrode Press, 1989.
- [56] S. Brand. *How buildings learn: What happens after they're built*. New York: Viking, 1994.

- [57] R. Schmidt III and S. Austin. *Adaptable architecture: Theory and practice*. Abingdon: Routledge, 2016. ISBN: 9780415522588.
- [58] E. Schut et al. *Circular economy in the Dutch construction sector: A perspective for the market and government*. 2016.
- [59] S.O. Ajayi and L.O. Oyedele. "Critical design factors for minimising waste in construction projects: A structural equation modelling approach". In: *Resources, conservation and Recycling* 137 (2018), pp. 302–313. DOI: <https://doi.org/10.1016/j.resconrec.2018.06.005>.
- [60] J. Won and J.C.P. Cheng. "Identifying potential opportunities of building information modeling for construction and demolition waste management and minimization". In: *Automation in Construction* 79 (2017), pp. 3–18. DOI: <https://doi.org/10.1016/j.autcon.2017.02.002>.
- [61] O.O. Akinade et al. "Design for Deconstruction: Critical success factors for diverting end-of-life waste from landfills". In: *Waste management* 60 (2017), pp. 3–13. DOI: <https://doi.org/10.1016/j.wasman.2016.08.017>.
- [62] J. Kanters. "Design for Deconstruction in the Design Process: State of the Art". In: *Buildings* 8.11 (2018). DOI: [10.3390/buildings8110150](https://doi.org/10.3390/buildings8110150).
- [63] International Organization for Standardization (ISO). *Sustainability in buildings and civil engineering works — Design for disassembly and adaptability — Principles, requirements and guidance (ISO 20887:2020(E))*. Geneva, 2020.
- [64] M.R. Munaro et al. "The ecodesign methodologies to achieve buildings' deconstruction: A review and framework". In: *Sustainable Production and Consumption* (2021). DOI: <https://doi.org/10.1016/j.spc.2021.12.032>.
- [65] B.E. Ross et al. "Enabling adaptable buildings: Results of a preliminary expert survey". In: *Procedia Engineering* 145 (2016), pp. 420–427. DOI: <https://doi.org/10.1016/j.proeng.2016.04.009>.
- [66] Z.R. Rockow. "Qualitative & quantitative analyses of existing buildings' adaptability". PhD thesis. Clemson University, 2020. URL: https://tigerprints.clemson.edu/all_dissertations/2670.
- [67] Rijksoverheid. *Bouwbesluit 2012*. URL: <https://rijksoverheid.bouwbesluit.com/Inhoud/docs/wet/bb2012> (visited on 01/26/2022).
- [68] R. Askar et al. "Adaptability of Buildings: A Critical Review on the Concept Evolution". In: *Applied Sciences* 11.10 (2021). DOI: [10.3390/app11104483](https://doi.org/10.3390/app11104483).
- [69] O. Heidrich et al. "A critical review of the developments in building adaptability". In: *International Journal of Building Pathology and Adaptation* (2017). DOI: <https://doi.org/10.1108/IJBPA-03-2017-0018>.
- [70] L.I. van Iperen. "Flexible floor systems - The effectiveness of flexibility measures in improving the circularity of building components". MA thesis. Delft University of Technology, 2021. URL: <https://repository.tudelft.nl/islandora/search/?collection=education>.
- [71] P. Crowther. "Design for disassembly - Themes and principles". In: *Environment Design Guide* (2005). URL: <http://www.jstor.org/stable/26149108>.
- [72] C.J. Kibert. "Establishing principles and a model for sustainable construction". In: *Sustainable Construction - Proceedings of the First International Conference of CIB TIG 16* (1994). URL: https://www.irbnet.de/daten/iconda/CIB_DC24773.pdf.
- [73] F.C. Rios et al. "Design for disassembly and deconstruction - Challenges and opportunities". In: *Procedia engineering* 118 (2015), pp. 1296–1304. DOI: <https://doi.org/10.1016/j.proeng.2015.08.485>.
- [74] L.C.M. Eberhardt et al. "Potential of Circular Economy in Sustainable Buildings". In: *IOP Conference Series: Materials Science and Engineering* 471 (2019), p. 092051. DOI: [10.1088/1757-899x/471/9/092051](https://doi.org/10.1088/1757-899x/471/9/092051).

- [75] A. Ojha and P. Aggarwal. "Fly ash based geopolymer concrete: a comprehensive review". In: *Silicon* (2021), pp. 1–20. DOI: <https://doi.org/10.1007/s12633-021-01044-0>.
- [76] M.F. Nuruddin et al. "Geopolymer concrete for structural use: Recent findings and limitations". In: *IOP Conference Series: Materials Science and Engineering* 133 (2016). DOI: [10.1088/1757-899x/133/1/012021](https://doi.org/10.1088/1757-899x/133/1/012021).
- [77] N. Tošić et al. "Towards a codified design of recycled aggregate concrete structures: Background for the new fib Model Code 2020 and Eurocode 2". In: *Structural Concrete* 22.5 (2021), pp. 2916–2938. DOI: <https://doi.org/10.1002/suco.202000512>.
- [78] M. Heinrich and W. Lang. *Materials passports - Best practice*. Munich: Technical University of Munich, in association with BAMB, 2019. URL: <https://www.bamb2020.eu/news/publication-materials-passports/>.
- [79] L. Luscuere. "Materials Passports: Providing Insights in the Circularity of Materials, Products and Systems". In: *Proceedings of the Sustainable Innovation* (2016), pp. 176–179. URL: <https://www.bamb2020.eu/wp-content/uploads/2016/11/lars-sustainable-innovation-paper.pdf>.
- [80] T. Zwart. *PARK 2020 A Circular Economy Business Model Case*. 2018. URL: <http://hdl.handle.net/10347/20253> (visited on 05/16/2022).
- [81] Circular Glasgow. *Park 2020 - A working environment with people and the material world at its core*. URL: <https://www.circularglasgow.com/story/park-2020/> (visited on 05/16/2022).
- [82] I Amsterdam. *Rob van den Broek, director at the Delta Development Group and a co-creator of Park 20|20, believes in the power of people-centric design*. URL: <https://www.iamsterdam.com/en/business/why-amsterdam/who-is-here/park-2020> (visited on 05/16/2022).
- [83] M. de Danschutter et al. "Tijdelijke rechtbank met permanent karakter". In: *Bouwen met Staal* 257 (June 2017).
- [84] de Architecten Cie. *Circl - De circulaire filosofie in praktijk gebracht*. URL: <https://cie.nl/circl?lang=nl> (visited on 05/19/2022).
- [85] Archdaily. *People's Pavilion / Bureau SLA + Overtreders W*. Apr. 2019. URL: <https://www.archdaily.com/915977/peoples-pavilion-bureau-sla-plus-overtreders-w> (visited on 05/18/2022).
- [86] N. Heidinga. *Pionieren op vlak van circulair en demontabel bouwen*. June 2021. URL: <https://betonhuis.nl/demontabel-flats> (visited on 05/18/2022).
- [87] VBI. *Product data sheets*. URL: <https://vbi.nl/downloads/> (visited on 12/01/2021).
- [88] TU Delft. *Concrete Building structures - reader CIE3340/CIE4281*. 2016. URL: <https://www.webedu.nl/bestellen/tudelft/?action=order&og=3010> (visited on 12/10/2021).
- [89] Betonson. *Wing plaatvloer - Productgegevens*. 2003. URL: <https://www.joostdevree.nl/shtmls/wing-vloer.shtml> (visited on 05/01/2022).
- [90] P. Diersen. *Flexibel bouwen met leidingvloeren*. 2012. URL: <https://www.bouwwereld.nl/producten/flexibel-bouwen-met-leidingvloeren/> (visited on 12/09/2021).
- [91] Dycore. *Breedplaatvloer*. URL: <https://www.dycore.nl/producten/breedplaatvloeren> (visited on 12/01/2021).
- [92] Bouwwereld. *Richtlijnen leidingen in breedplaatvloeren*. 2018. URL: <https://www.bouwwereld.nl/bouwkennis/richtlijnen-leidingen-in-breedplaatvloeren/> (visited on 05/03/2022).
- [93] Bestcon. *Bestcon MPV140 en MPV160 vloerplaten & Bestcon-60 vloersysteem*. URL: <https://www.bestcon.nl/producten/> (visited on 12/01/2021).

- [94] A. Glias. "The Donor Skelet: Designing with reused structural concrete elements". MA thesis. Delft University of Technology, 2013. URL: <https://repository.tudelft.nl/islandora/search/?collection=education>.
- [95] Dywidag-Systems International GmbH. *SUSPA/DSI - Unbonded Monostrand System with 1 to 5 Monostrands - ETA 03/0036*. Tech. rep. European Organisation for Technical Assessment, 2021. URL: <https://dywidag.com/downloads> (visited on 12/13/2021).
- [96] *NEN-EN 1990+A1+A1/C2. Eurocode 0: Grondslagen voor het constructief ontwerp*. CEN, 2019.
- [97] *NEN-EN 1990+A1+A1/C2/NB. Nationale bijlage bij Eurocode 0: Grondslagen voor het constructief ontwerp*. CEN, 2019.
- [98] *NEN-EN 1991-1-1+C1+C11. Eurocode 1: Belastingen op constructies - Deel 1-1: Algemene belastingen - Volumieke gewichten, eigen gewicht en gebruiksbelastingen voor gebouwen*. CEN, 2019.
- [99] L. van Glabbeek. "Development of an innovative demountable floor system - Structural design and verification". MA thesis. Delft University of Technology, 2019. URL: <https://repository.tudelft.nl/islandora/search/?collection=education>.
- [100] *NEN-EN 1991-1-1+C1+C11/NB. Nationale bijlage bij Eurocode 1: Belastingen op constructies - Deel 1-1: Algemene belastingen - Volumieke gewichten, eigen gewicht en gebruiksbelastingen voor gebouwen*. CEN, 2019.
- [101] *NEN-EN 1992-1-1+C2. Eurocode 2: Ontwerp en berekening van betonconstructies - Deel 1-1: Algemene regels en regels voor gebouwen*. CEN, 2020.
- [102] J.C. Walraven and C.R. Braam. *CIE3150/4160 - Prestressed Concrete*. 2019.
- [103] *NEN-EN 1992-1-1+C2/NB+A1. Nationale bijlage bij Eurocode 2: Ontwerp en berekening van betonconstructies - Deel 1-1: Algemene regels en regels voor gebouwen*. CEN, 2020.
- [104] VSL. *Strand post-tensioning systems*. Tech. rep. 2019. URL: <https://vsl.com/home/technologies/post-tensioning-systems/> (visited on 12/13/2021).
- [105] H.B. Wilson and L.H. Turcotte. "Determining the kern for a compression member of general cross-section". In: *Advances in Engineering Software* 17.2 (1993), pp. 113–123. DOI: [https://doi.org/10.1016/0965-9978\(93\)90048-X](https://doi.org/10.1016/0965-9978(93)90048-X).
- [106] P. Waarts. *Trillingen van vloeren door lopen: Richtlijn voor het voorspellen, meten en beoordelen*. Den Haag, 2005.
- [107] M. Alqam et al. "An Improved Methodology for the Prediction of the Stress at Ultimate in Unbonded Internal and External Steel Tendons". In: *Arabian Journal for Science and Engineering* 45 (2020). DOI: [10.1007/s13369-020-04475-w](https://doi.org/10.1007/s13369-020-04475-w).
- [108] M. Alqam and F.M. Alkhairi. "Numerical and analytical behavior of beams prestressed with unbonded internal or external steel tendons: a state-of-the-art review". In: *Arabian Journal for Science and Engineering* 44.10 (2019). DOI: <https://doi.org/10.1007/s13369-019-03934-3>.
- [109] A.E. Naaman and F.M. Alkhairi. "Stress at ultimate in unbonded post-tensioning tendons: Part 2—proposed methodology". In: *Structural Journal* 88.6 (1991), pp. 683–692.
- [110] Z-Q. He and Z. Liu. "Stresses in External and Internal Unbonded Tendons: Unified Methodology and Design Equations". In: *Journal of Structural Engineering* 136.9 (2010), pp. 1055–1065. DOI: [10.1061/\(ASCE\)ST.1943-541X.0000202](https://doi.org/10.1061/(ASCE)ST.1943-541X.0000202).
- [111] AASHTO (American Association of State Highway and Transportation Officials). *LFRD Bridge Design Specifications*. 1st edition. Washington, 1994.
- [112] ACI (American Concrete Institute). *ACI 318-19: Building code requirements for structural concrete and commentary*. Farmington Hills, 2019.

- [113] T.D. Le et al. "Numerical study on the flexural performance of precast segmental concrete beams with unbonded internal steel tendons". In: *Construction and Building Materials* 248 (2020), p. 118362. DOI: <https://doi.org/10.1016/j.conbuildmat.2020.118362>.
- [114] Q. Li et al. "Experimental study on shear behavior in negative moment regions of segmental externally prestressed concrete continuous beams". In: *Journal of Bridge Engineering* 18.4 (2013), pp. 328–338. DOI: [https://doi.org/10.1061/\(ASCE\)BE.1943-5592.0000351](https://doi.org/10.1061/(ASCE)BE.1943-5592.0000351).
- [115] N Randl. "Investigations on transfer of forces between old and new concrete at different joint roughness". PhD thesis. University of Innsbruck, 1997.
- [116] FIB (Federation Internationale du Beton). *FIB Model Code for Concrete Structures 2010*. Wilhelm Ernst & Sohn Verlag fur Architektur und Technische, 2013. DOI: [10.1002/9783433604090](https://doi.org/10.1002/9783433604090).
- [117] C. W. Dolan and H. R. Hamilton. "Materials". In: *Prestressed Concrete: Building, Design, and Construction*. Cham: Springer International Publishing, 2019, pp. 63–84. DOI: https://doi.org/10.1007/978-3-319-97882-6_3.
- [118] Y. Wu et al. "Application of lifecycle assessment and finite element analysis in the design of raised access floor products". In: *Proceedings of the XIV International Conference on Computational Plasticity - Fundamentals and Applications*. Barcelona: International Center for Numerical Methods in Engineering (CIMNE), 2017, pp. 806–814. URL: <http://irep.ntu.ac.uk/id/eprint/31652/>.
- [119] PBS Holland. *Verhoogde vloeren*. 2022. URL: <https://pbsholland.com/> (visited on 04/30/2022).
- [120] S. Soroushian et al. "Numerical Simulation of Integrated Suspended Ceiling-Sprinkler Systems". In: Apr. 2015, pp. 1879–1890. DOI: [10.1061/9780784479117.162](https://doi.org/10.1061/9780784479117.162).
- [121] Archtoolbox. *Suspended ceilings - Acoustic ceiling tiles/panels*. 2022. URL: <https://www.archtoolbox.com/acoustic-ceiling-tiles/> (visited on 04/30/2022).
- [122] F. Muresan. *Exposed ceilings vs suspended ceilings: how do they compare?* 2021. URL: <https://www.ny-engineers.com/blog/exposed-ceilings-vs-suspended-ceilings> (visited on 04/30/2022).
- [123] NEN-EN 1168+A3. *Vooraf vervaardigde betonproducten - Kanaalplaatvloeren*. CEN, 2011.
- [124] K. Lundgren et al. *Shear and torsion in hollow core slabs: How advanced modelling can be used in design*. 2019. URL: https://usercontent.one/wp/hollowcore.org/wp-content/uploads/2019/03/10_Holcotors-results-b.pdf (visited on 04/10/2022).
- [125] NEN-EN 1991-1-4. *Eurocode 1: Belastingen op constructies - Deel 1-4: Algemene belastingen - Windbelasting*. CEN, 2005.
- [126] NEN-EN 1991-1-4/NB Nationale bijlage bij Eurocode 1-1-4: *Belastingen op constructies - Deel 1-4: Algemene belastingen - Windbelasting*. CEN, 2005.
- [127] J.N. Rodrigues et al. "Timber-Concrete Composite Bridges: State-of-the-Art Review". In: *Biore-sources* 8 (2013), pp. 6630–6649. URL: <https://bioresources.cnr.ncsu.edu/resources/timber-concrete-composite-bridges-state-of-the-art-review/>.
- [128] M. Volkov. "Structural connections in circular concrete - A study about the jointing methods for "second-hand" concrete elements". MA thesis. Delft University of Technology, 2019. URL: <https://repository.tudelft.nl/islandora/search/?collection=education>.



Calculation results for Group I

The calculation results for element Group I are presented in this section. The elements are illustrated in figure 6.3. The width of the elements is 600 millimeters. These elements are designed to serve as a fitting plate or slab for the other element groups, in order to accommodate for a larger variety of grid sizes in generic floor fields. However, the elements of Group I are not designed to be used with a trimmer beam. Therefore, only the results of the general loading situation are presented. For all the span lengths considered, the same method of presentation is used as in the main report.

Span length [m]	$P_{m,0}$ [kN]	$A_{p,req}$ [mm ²]	$n_{strands}$ [-]	$A_{p,tot}$ [mm ²]	$P_{m,0,tot}$ [kN]	$M_{p,0,tot}$ [kNm]
5.4	190.4	137	1	150	209.1	10.5
6.0	235.1	169	2	300	418.2	20.9
6.6	284.4	204	2	300	418.2	20.9
7.2	338.5	243	2	300	418.2	20.9
7.8	397.2	285	2	300	418.2	20.9

Table A.1: Required amount of prestressing steel for all span lengths

Span length [m]	ΔP_{μ} [kN]	ΔP_{ws} [kN]	ΔP_{el} [kN]	$\sum \Delta P_0$ kN	$P_{m,0}$ [kN]	Δ_0 [%]
5.4	0.6	27.1	0.8	28.5	209.1	13.6
6.0	1.4	48.8	1.6	51.8	418.2	12.4
6.6	1.5	44.3	1.6	47.4	418.2	11.4
7.2	1.6	40.6	1.6	43.8	418.2	10.5
7.8	1.8	37.5	1.6	40.9	418.2	9.8

Table A.2: Immediate prestressing losses due to friction, wedge set and elastic deformation

Span length [m]	$\sum \Delta P_0$ [kN]	Δ_0 [%]	ΔP_{c+s+r} [kN]	Δ_∞ [%]	Δ_{tot} [%]	$P_{m\infty}$ [kN]	$M_{p\infty}$ [kNm]
5.4	28.5	13.6	11.1	5.3	18.9	169.5	17.0
6.0	51.8	12.4	21.6	5.2	17.6	349.9	17.2
6.6	47.4	11.3	21.6	5.2	16.5	349.2	17.5
7.2	43.8	10.5	21.6	5.2	15.7	352.7	17.6
7.8	40.9	9.8	21.6	5.2	15.0	355.7	17.8

Table A.3: Total prestressing losses due to immediate and time-dependent effects

Span length [m]		Deflections		Check [-]
		[mm]	[mm]	
5.4	$w_2 + w_3$	1.18	\leq 10.8	Satisfied
	w_{max}	1.62	\leq 21.6	Satisfied
6.0	$w_2 + w_3$	(-)0.73	\leq 12.0	Satisfied
	w_{max}	(-)1.36	\leq 24.0	Satisfied
6.6	$w_2 + w_3$	0.35	\leq 13.2	Satisfied
	w_{max}	0.52	\leq 26.4	Satisfied
7.2	$w_2 + w_3$	2.38	\leq 14.4	Satisfied
	w_{max}	3.04	\leq 28.8	Satisfied
7.8	$w_2 + w_3$	5.06	\leq 15.6	Satisfied
	w_{max}	6.95	\leq 31.2	Satisfied

Table A.4: Results regarding deflections for all span lengths

Span length [m]		M_{ed} [kNm]	M_{rd} [kNm]	UC [-]	Check [-]
5.4	Eurocode 2 [103]	21.2	29.0	0.73	satisfied
	Alqam et al. [107]	21.2	36.6	0.58	satisfied
6.0	Eurocode 2 [103]	26.1	56.7	0.46	satisfied
	Alqam et al. [107]	26.1	73.1	0.36	satisfied
6.6	Eurocode 2 [103]	31.6	57.3	0.55	satisfied
	Alqam et al. [107]	31.6	73.0	0.43	satisfied
7.2	Eurocode 2 [103]	37.6	57.8	0.65	satisfied
	Alqam et al. [107]	37.6	72.9	0.52	satisfied
7.8	Eurocode 2 [103]	44.1	58.3	0.76	satisfied
	Alqam et al. [107]	44.1	72.9	0.61	satisfied

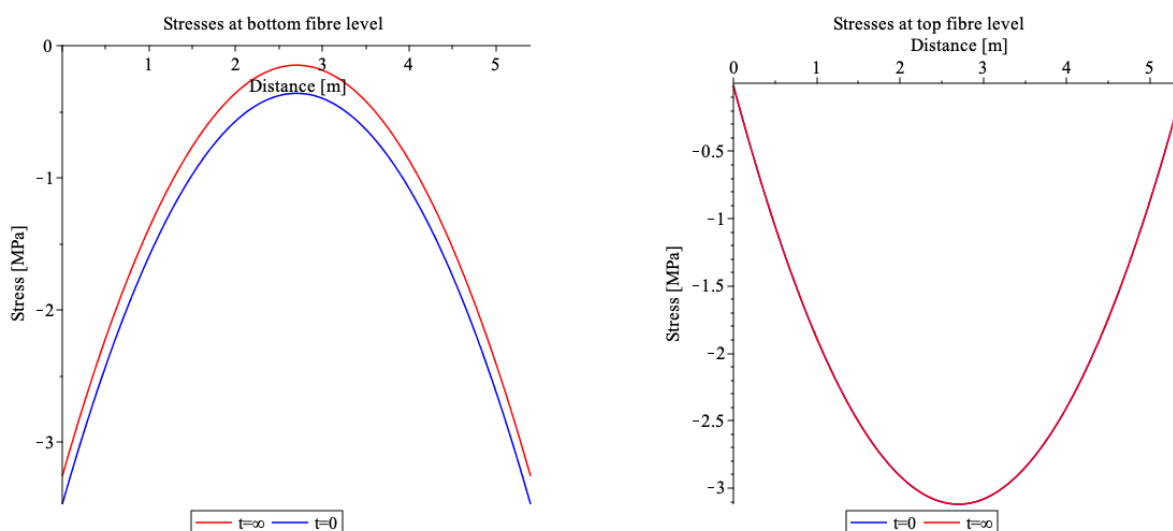
Table A.5: Unity checks regarding the bending moment capacity for all span lengths

Span length [m]		V_{ed} [kN]	$V_{rd,c}$ [kN]	UC [-]	$Check$ [-]
5.4	Eurocode 2 [101]	15.7	119.7	0.13	satisfied
	Alqam et al. [107]	15.7	129.8	0.12	satisfied
6.0	Eurocode 2 [101]	17.4	147.0	0.11	satisfied
	Alqam et al. [107]	17.4	162.4	0.11	satisfied
6.6	Eurocode 2 [101]	19.2	147.6	0.13	satisfied
	Alqam et al. [107]	19.2	162.4	0.12	satisfied
7.2	Eurocode 2 [101]	20.9	148.1	0.14	satisfied
	Alqam et al. [107]	20.9	162.4	0.13	satisfied
7.8	Eurocode 2 [101]	22.6	148.5	0.15	satisfied
	Alqam et al. [107]	22.6	162.4	0.14	satisfied

Table A.6: Unity checks regarding the shear force capacity for all span lengths

Span length [m]		v_{ed} [MPa]	$v_{rd,i}$ [MPa]	UC [-]	$Check$ [-]
5.4	Eurocode 2 [101]	0.33	0.85	0.39	satisfied
	Alqam et al. [107]	0.33	1.16	0.29	satisfied
6.0	Eurocode 2 [101]	0.37	1.73	0.12	satisfied
	Alqam et al. [107]	0.37	2.31	0.16	satisfied
6.6	Eurocode 2 [101]	0.40	1.75	0.23	satisfied
	Alqam et al. [107]	0.40	2.31	0.17	satisfied
7.2	Eurocode 2 [101]	0.44	1.77	0.25	satisfied
	Alqam et al. [107]	0.44	2.31	0.19	satisfied
7.8	Eurocode 2 [101]	0.48	1.79	0.27	satisfied
	Alqam et al. [107]	0.48	2.31	0.21	satisfied

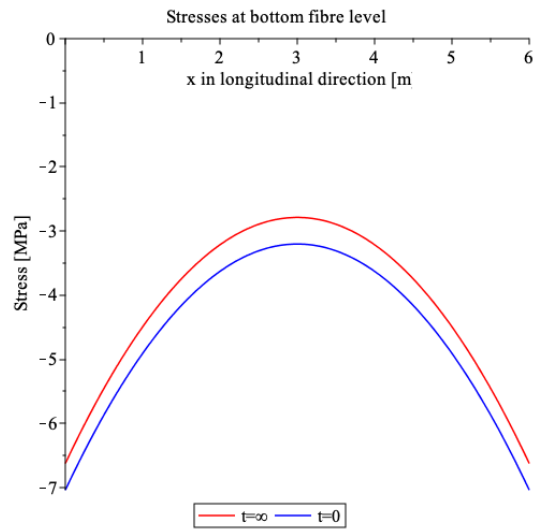
Table A.7: Unity checks regarding the shear stress at the interfaces for all span lengths



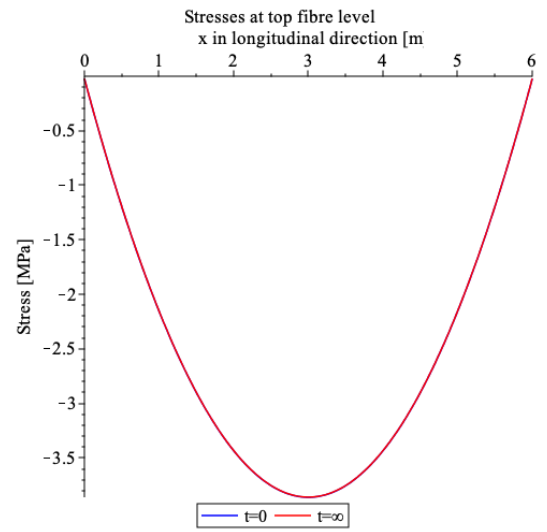
(a) Stresses at bottom fibre level

(b) Stresses at top fibre level

Figure A.1: Stresses in the cross-section for a span length of 5.4 m

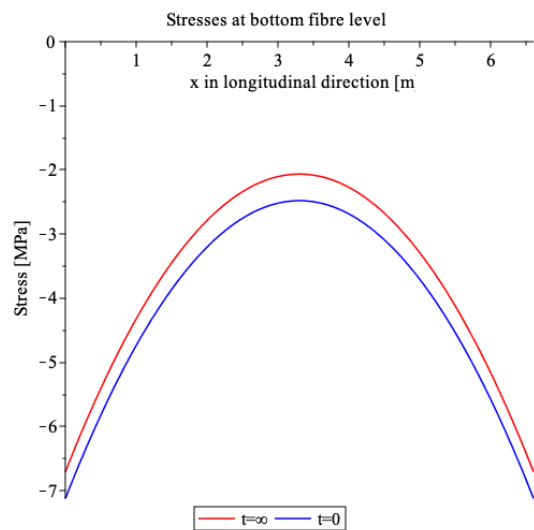


(a) Stresses at bottom fibre level

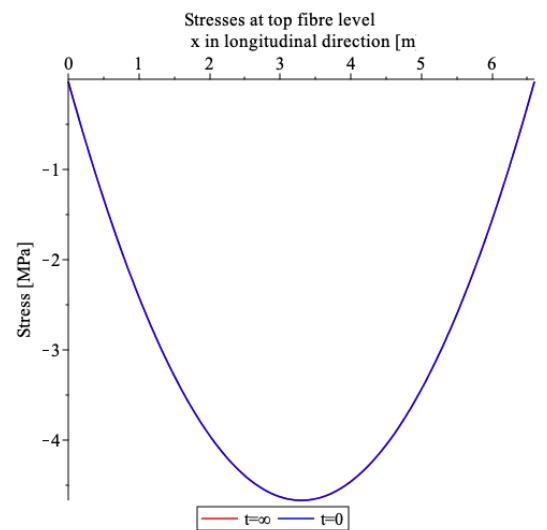


(b) Stresses at top fibre level

Figure A.2: Stresses in the cross-section for a span length of 6.0 m

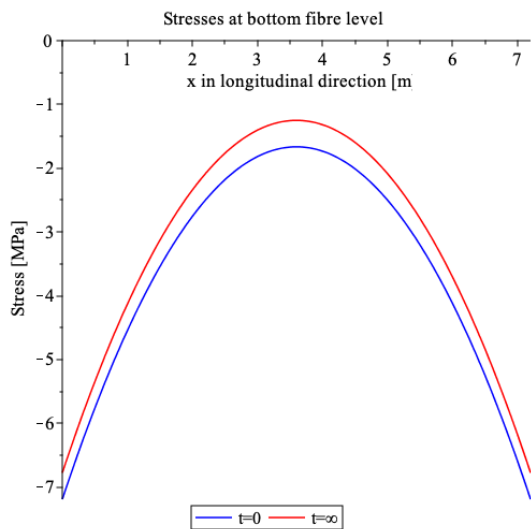


(a) Stresses at bottom fibre level

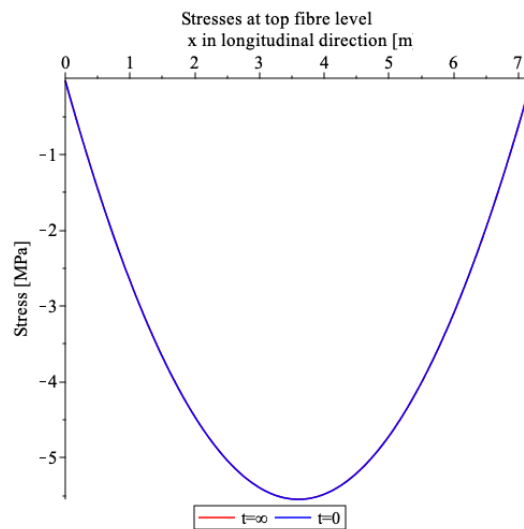


(b) Stresses at top fibre level

Figure A.3: Stresses in the cross-section for a span length of 6.6 m

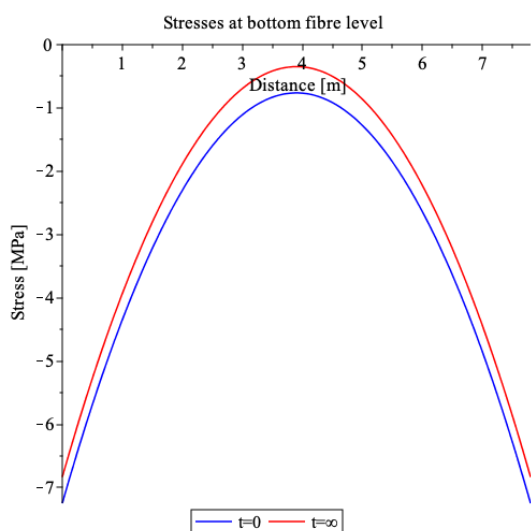


(a) Stresses at bottom fibre level

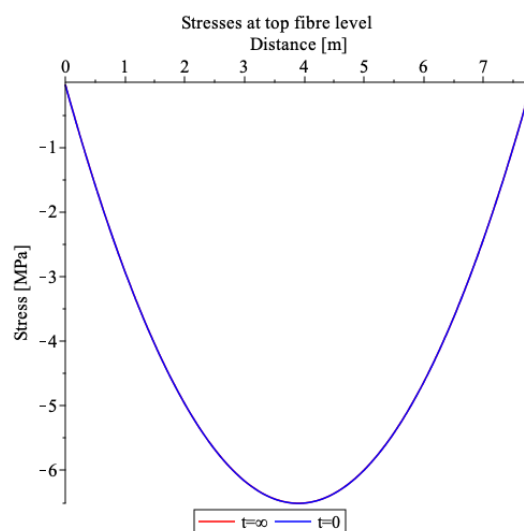


(b) Stresses at top fibre level

Figure A.4: Stresses in the cross-section for a span length of 7.2 m



(a) Stresses at bottom fibre level



(b) Stresses at top fibre level

Figure A.5: Stresses in the cross-section for a span length of 7.8 m

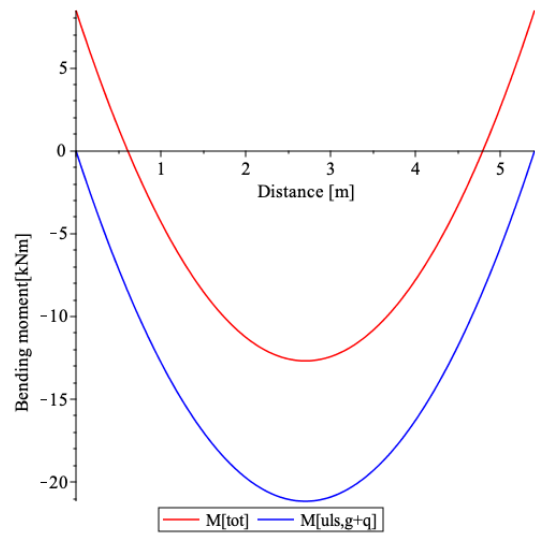
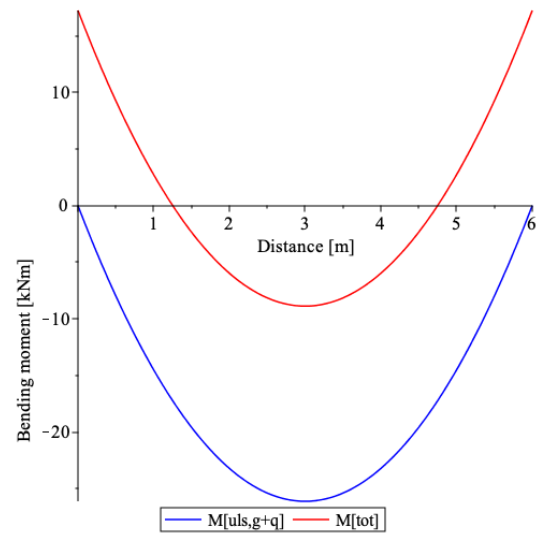
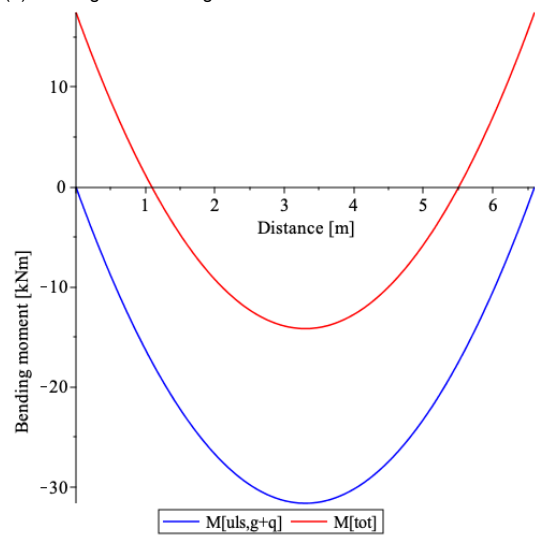
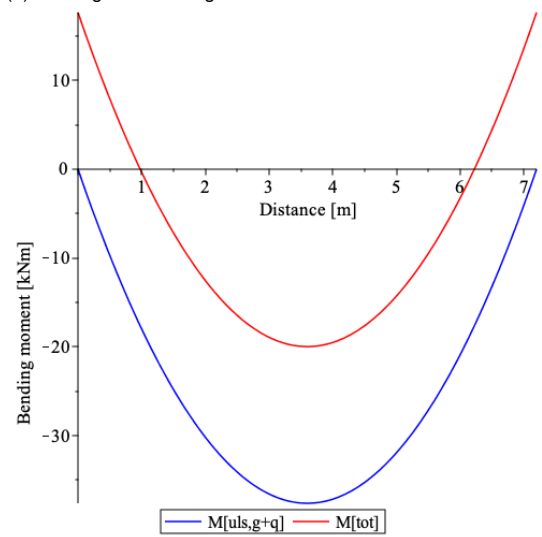
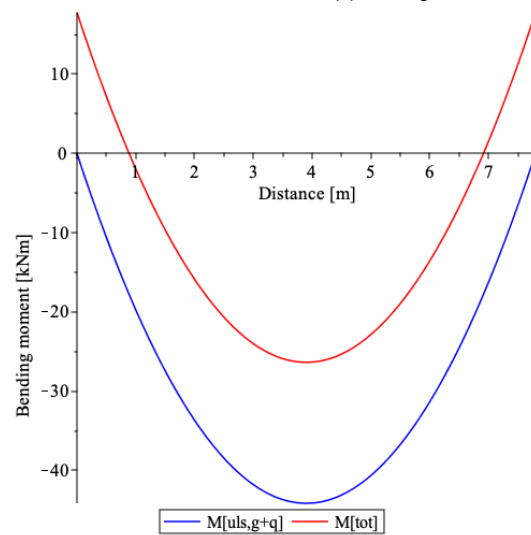
(a) Bending moment diagram for $l = 5.4$ m(b) Bending moment diagram for $l = 6.0$ m(c) Bending moment diagram for $l = 6.6$ m(d) Bending moment diagram for $l = 7.2$ m(e) Bending moment diagram for $l = 7.8$ m

Figure A.6: Bending moment diagrams due to the imposed loading

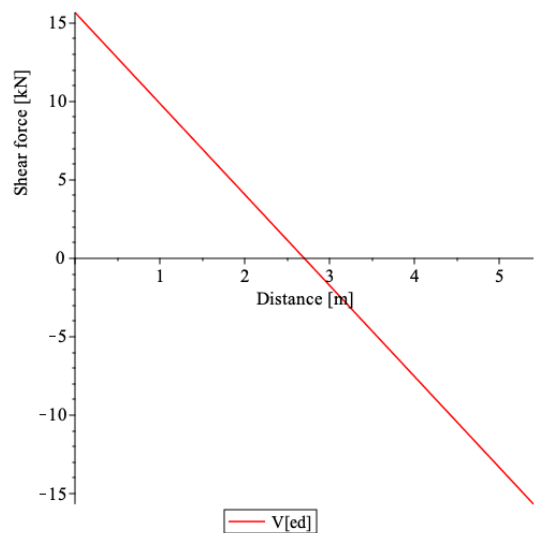
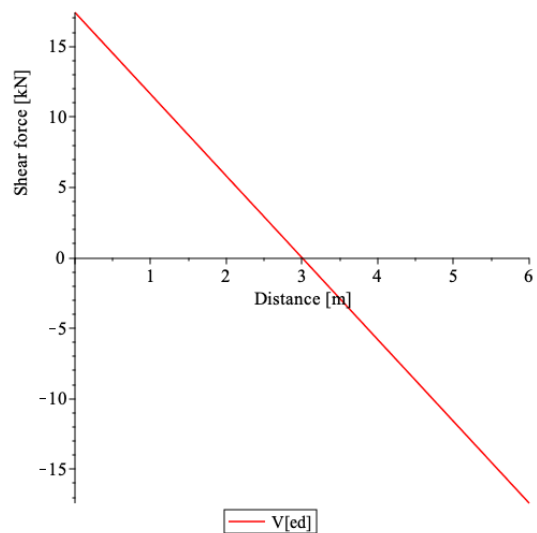
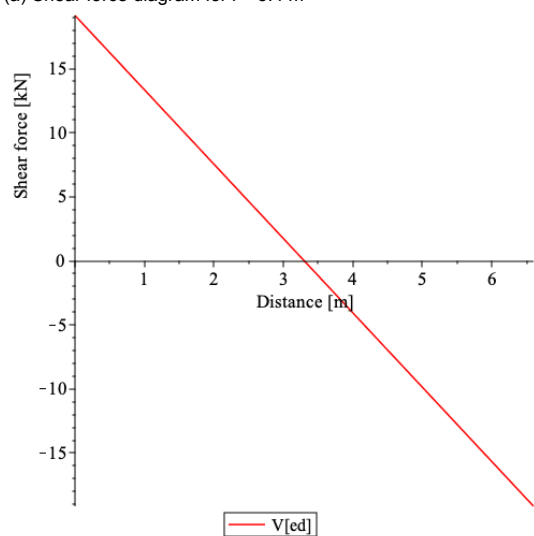
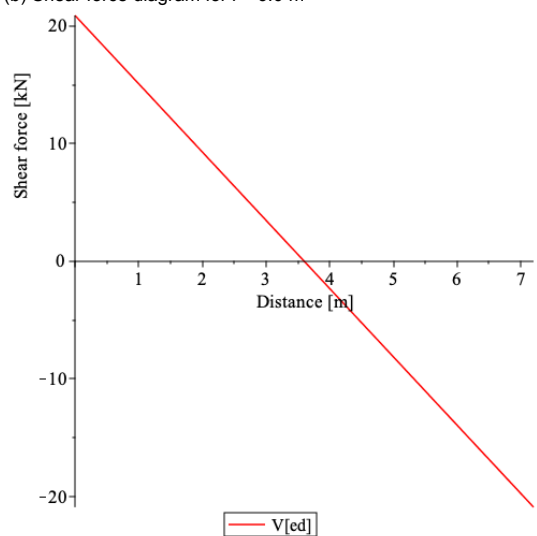
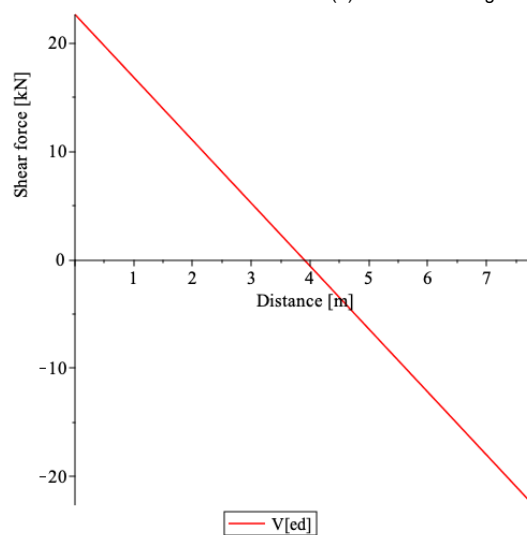
(a) Shear force diagram for $l = 5.4$ m(b) Shear force diagram for $l = 6.0$ m(c) Shear force diagram for $l = 6.6$ m(d) Shear force diagram for $l = 7.2$ m(e) Shear force diagram for $l = 7.8$ m

Figure A.7: Shear force diagrams due to the imposed loading

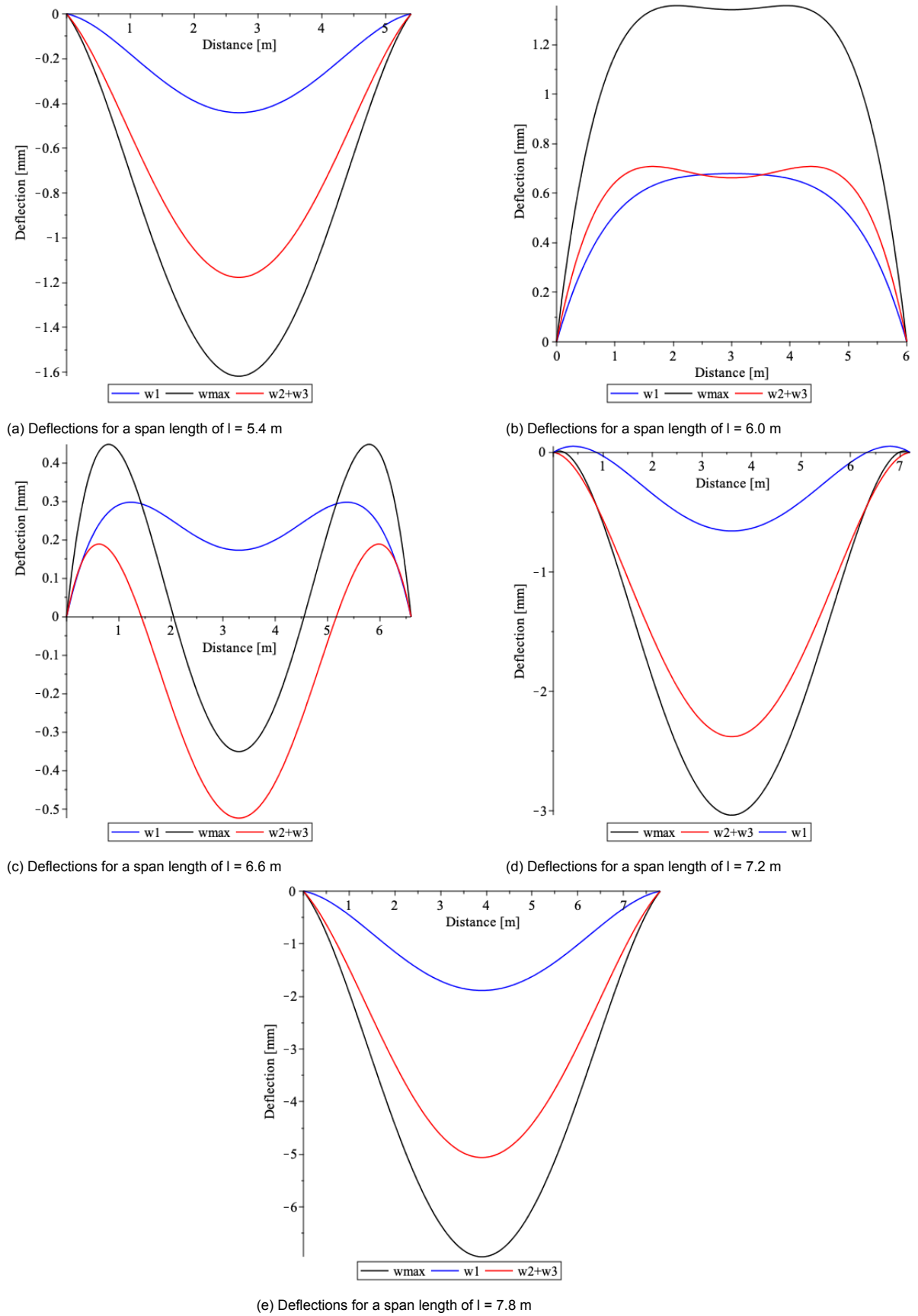


Figure A.8: Deflection lines according to the frequent load combination

B

Calculation results for Group II

This section presents the calculation results for element Group II, including the results that are previously presented in the report. The width of the elements is 1200 millimeters. The elements are designed to be used with a trimmer beam. The maximum recess length is equal to 3.6 meters. This means that a maximum of three slabs are supported by a trimmer beam. The calculation results and diagrams are presented for both loading situations: with and without the use of a trimmer beam.

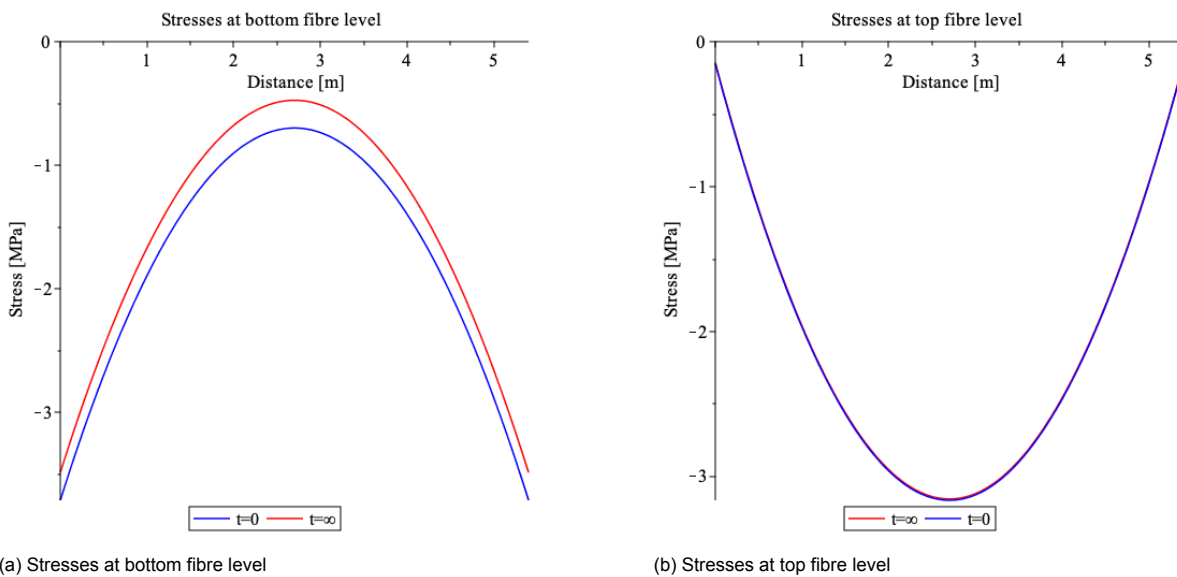
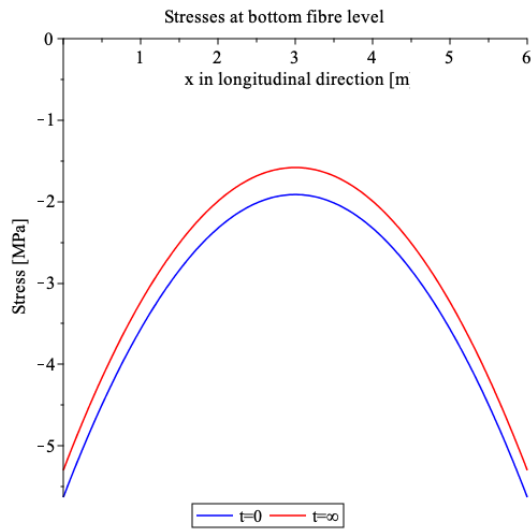
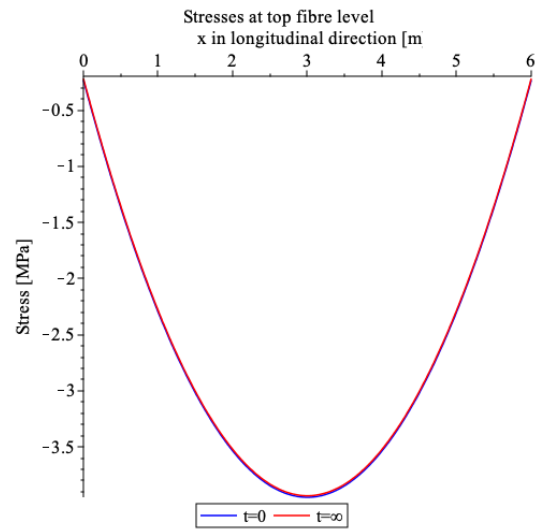


Figure B.1: Stresses in the cross-section for a span length of 5.4 m

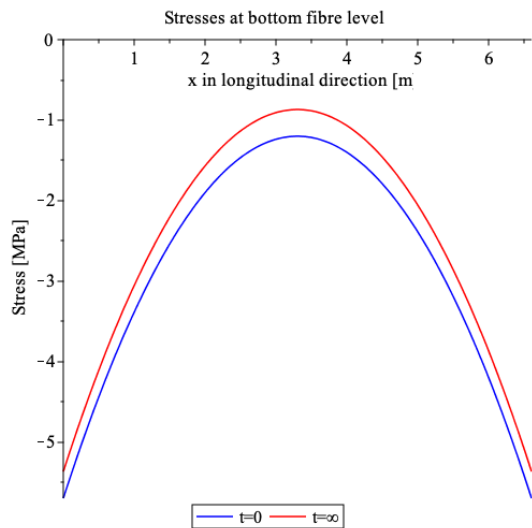


(a) Stresses at bottom fibre level

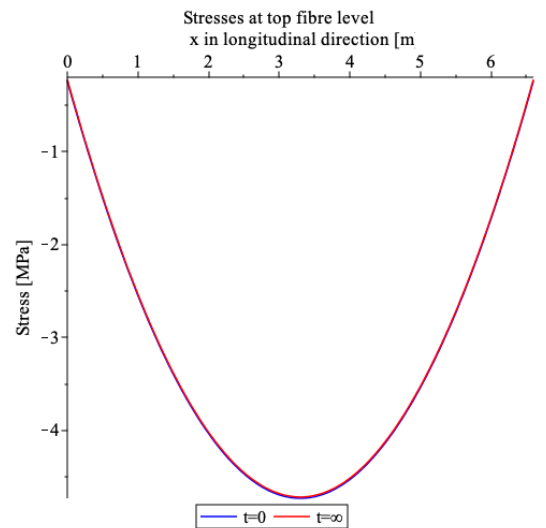


(b) Stresses at top fibre level

Figure B.2: Stresses in the cross-section for a span length of 6.0 m

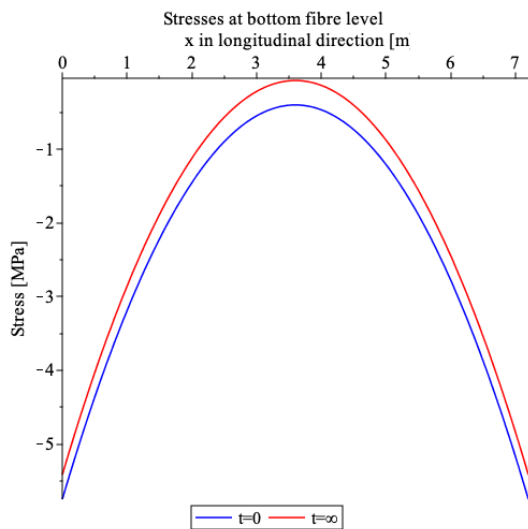


(a) Stresses at bottom fibre level

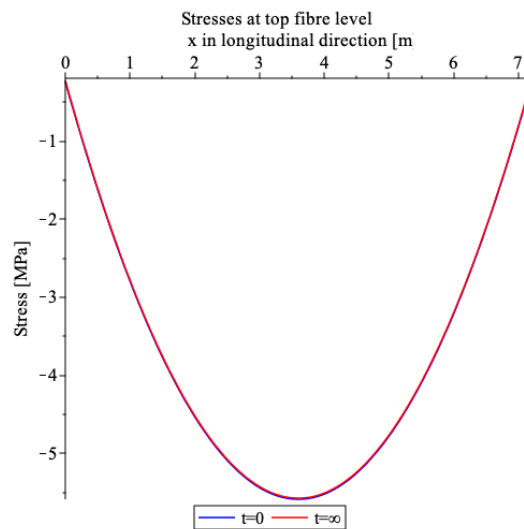


(b) Stresses at top fibre level

Figure B.3: Stresses in the cross-section for a span length of 6.6 m

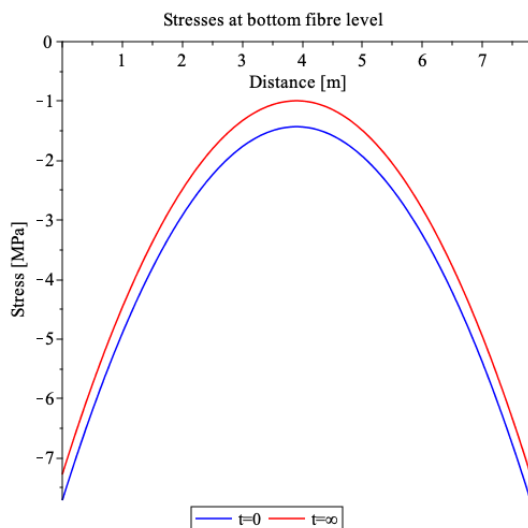


(a) Stresses at bottom fibre level

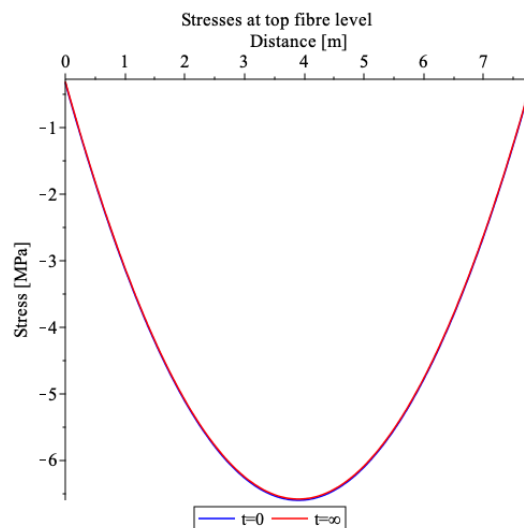


(b) Stresses at top fibre level

Figure B.4: Stresses in the cross-section for a span length of 7.2 m

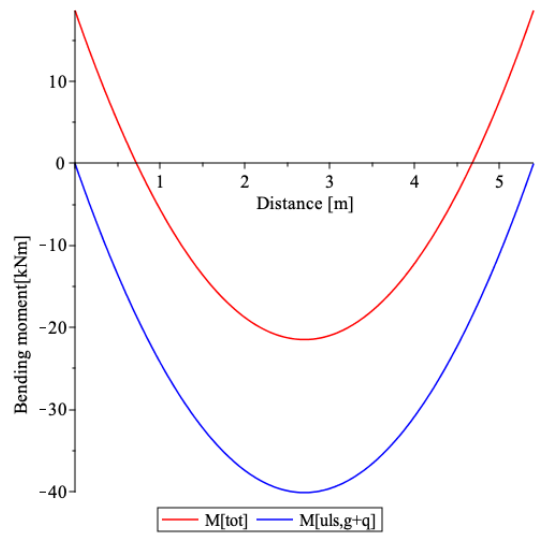


(a) Stresses at bottom fibre level

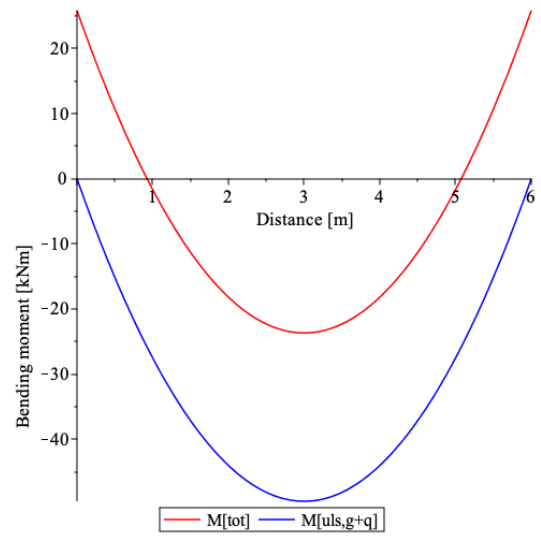


(b) Stresses at top fibre level

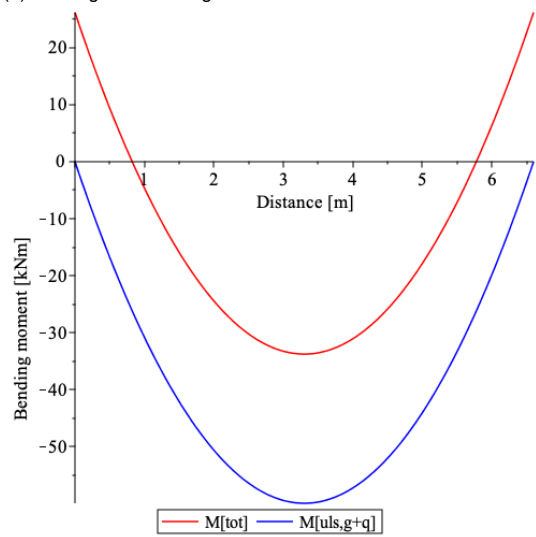
Figure B.5: Stresses in the cross-section for a span length of 7.8 m



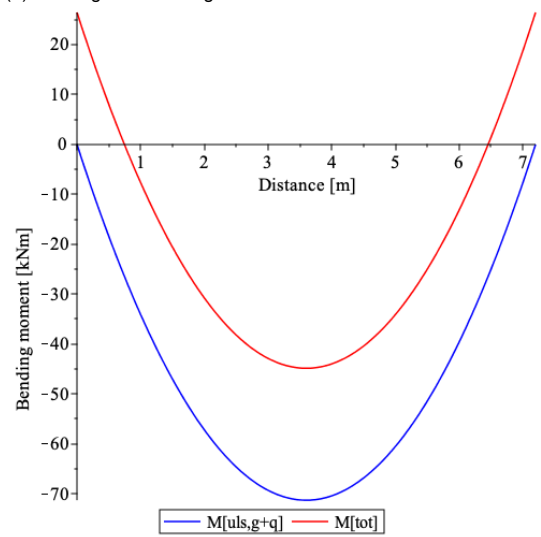
(a) Bending moment diagram for $l = 5.4$ m



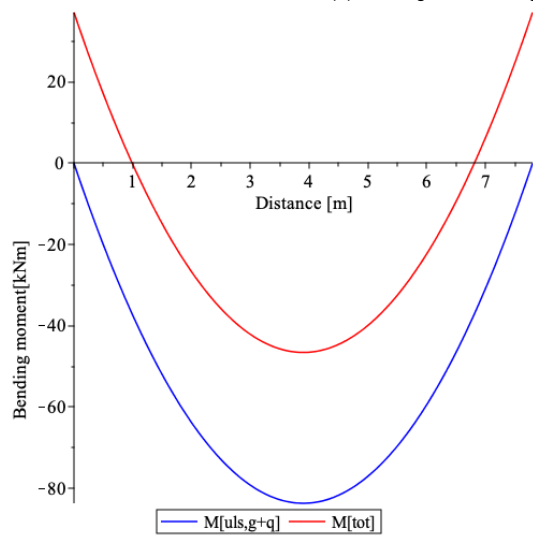
(b) Bending moment diagram for $l = 6.0$ m



(c) Bending moment diagram for $l = 6.6$ m



(d) Bending moment diagram for $l = 7.2$ m



(e) Bending moment diagram for $l = 7.8$ m

Figure B.6: Bending moment diagrams due to the imposed loading

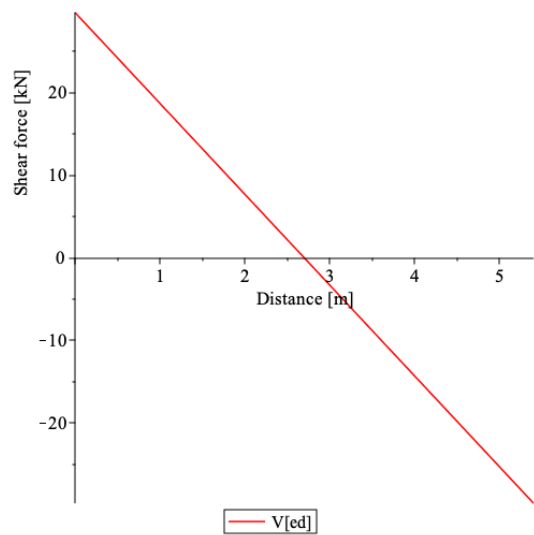
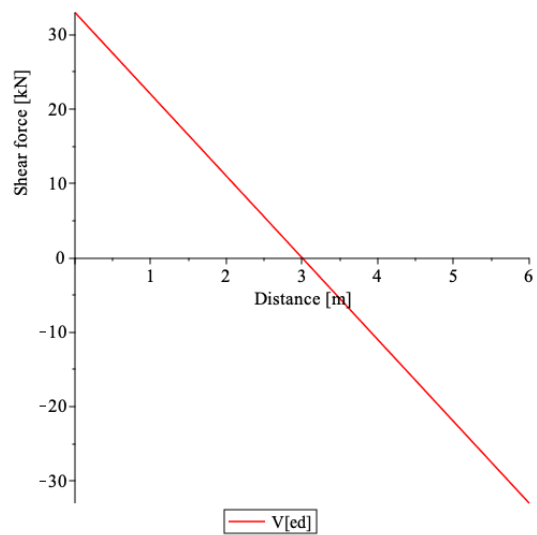
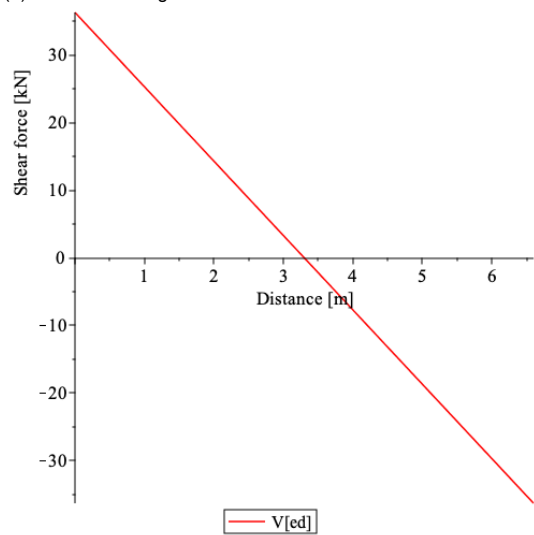
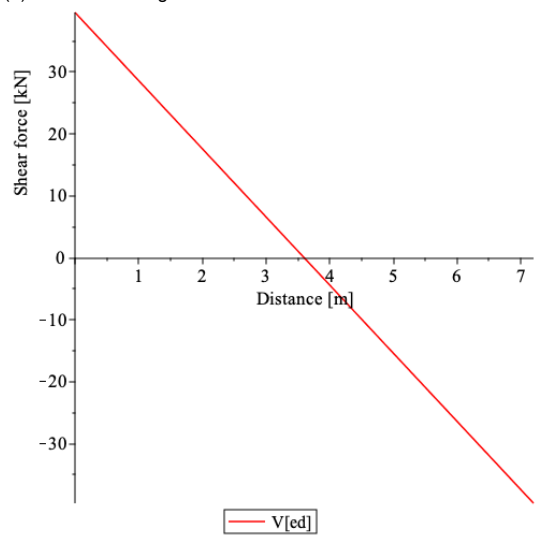
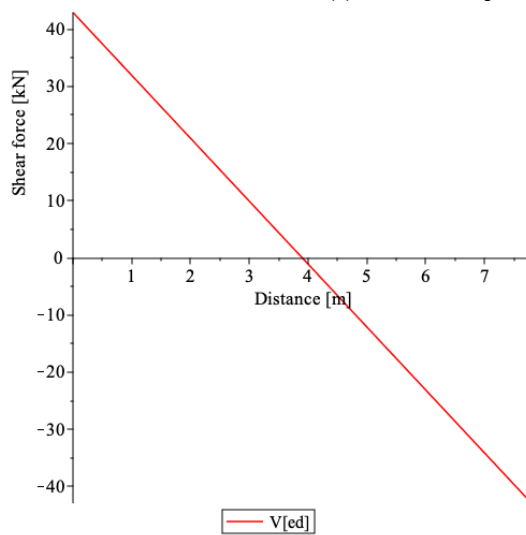
(a) Shear force diagram for $l = 5.4$ m(b) Shear force diagram for $l = 6.0$ m(c) Shear force diagram for $l = 6.6$ m(d) Shear force diagram for $l = 7.2$ m(e) Shear force diagram for $l = 7.8$ m

Figure B.7: Shear force diagrams due to the imposed loading

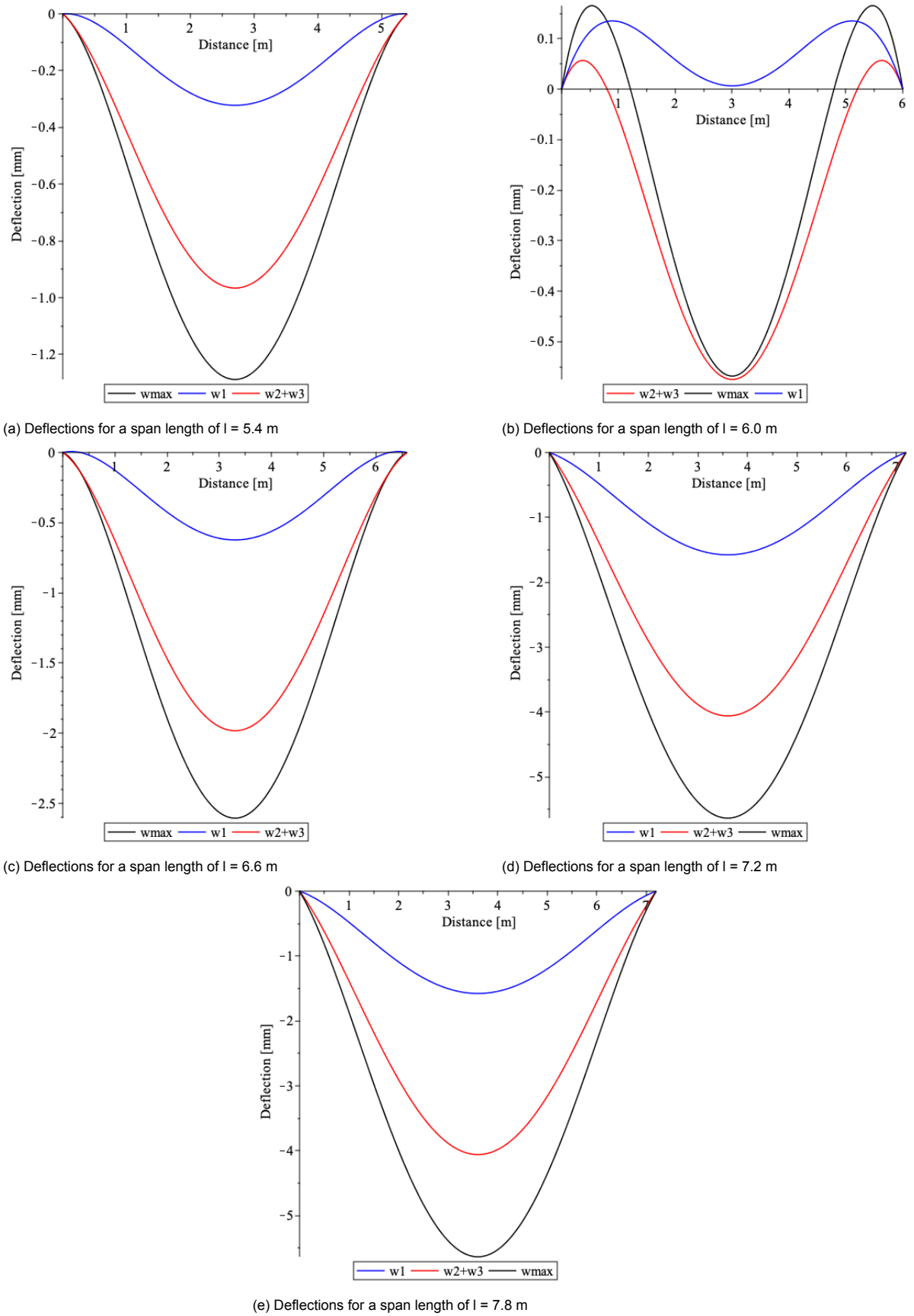
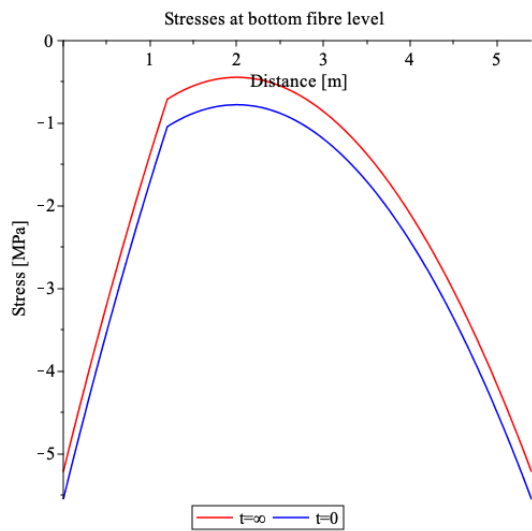
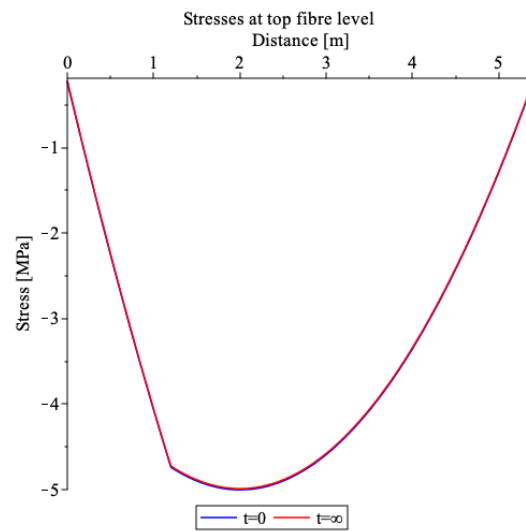


Figure B.8: Deflection lines according to the frequent load combination

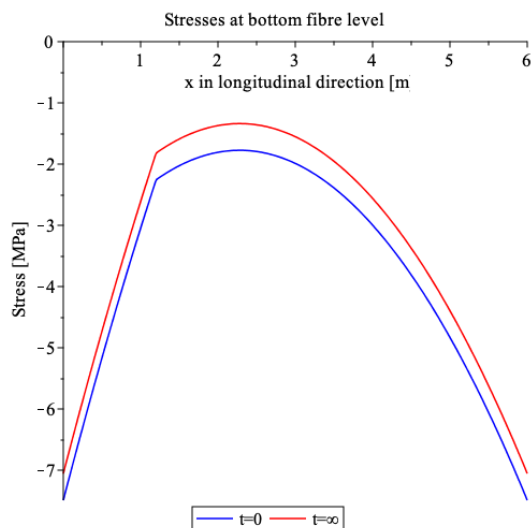


(a) Stresses at bottom fibre level

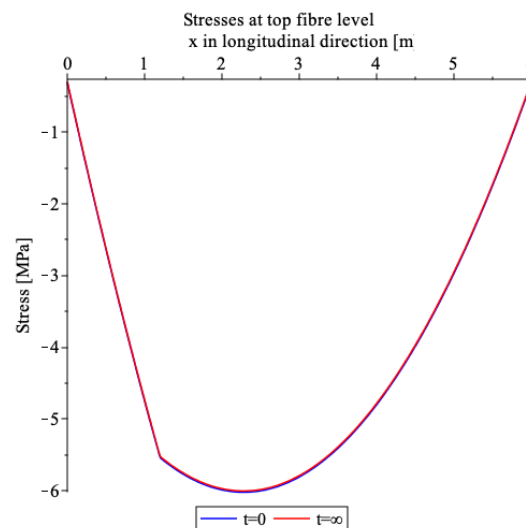


(b) Stresses at top fibre level

Figure B.9: Stresses in the cross-section for a span length of 5.4 m with a trimmer beam

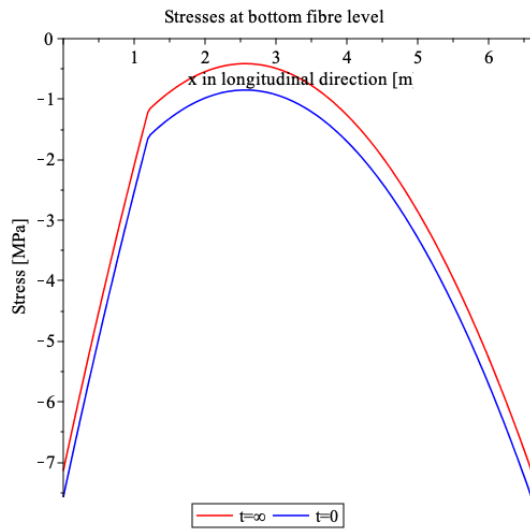


(a) Stresses at bottom fibre level

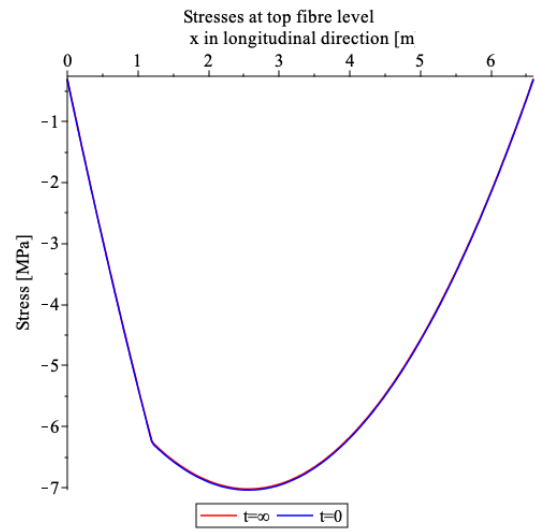


(b) Stresses at top fibre level

Figure B.10: Stresses in the cross-section for a span length of 6.0 m with a trimmer beam

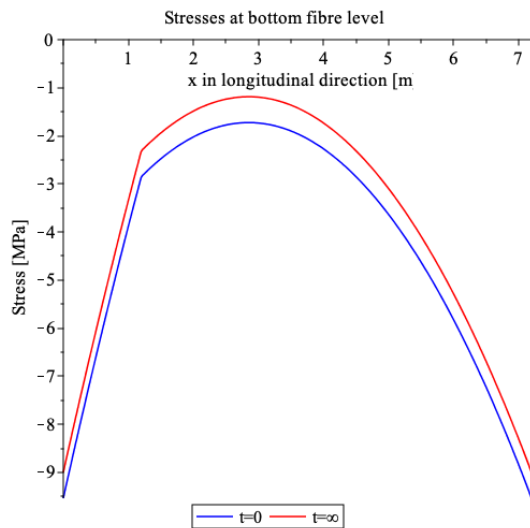


(a) Stresses at bottom fibre level

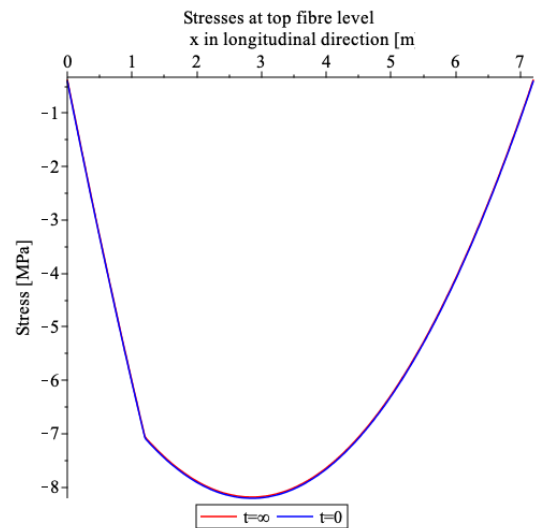


(b) Stresses at top fibre level

Figure B.11: Stresses in the cross-section for a span length of 6.6 m with a trimmer beam

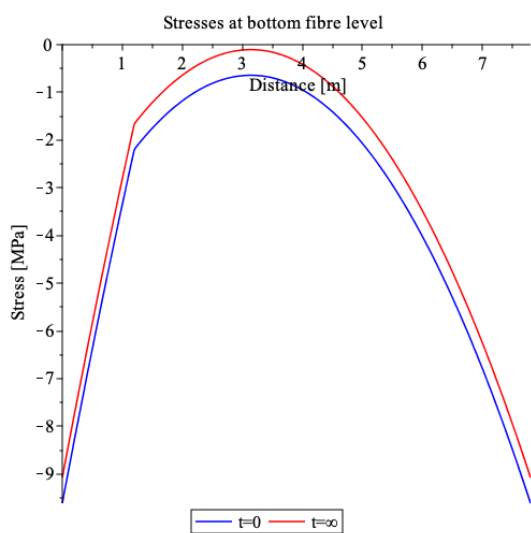


(a) Stresses at bottom fibre level

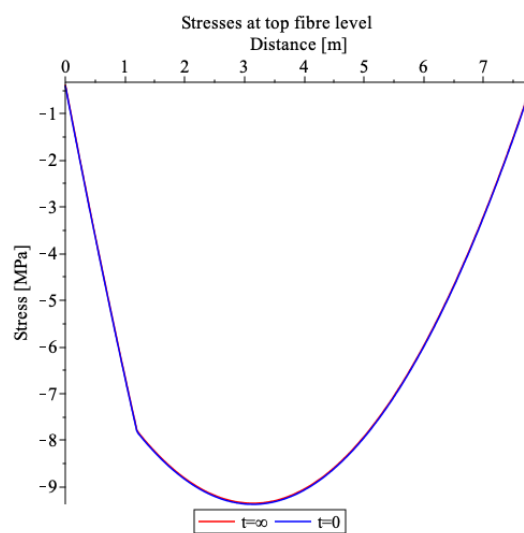


(b) Stresses at top fibre level

Figure B.12: Stresses in the cross-section for a span length of 7.2 m with a trimmer beam



(a) Stresses at bottom fibre level



(b) Stresses at top fibre level

Figure B.13: Stresses in the cross-section for a span length of 7.8 m with a trimmer beam

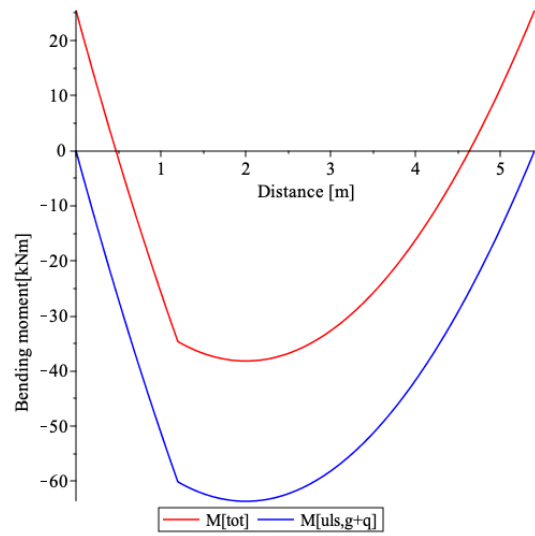
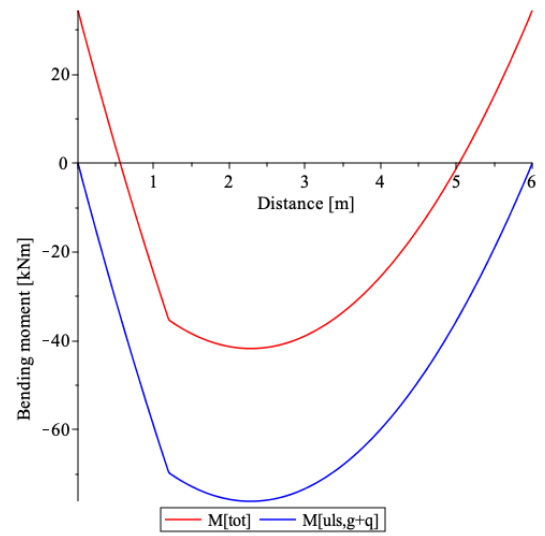
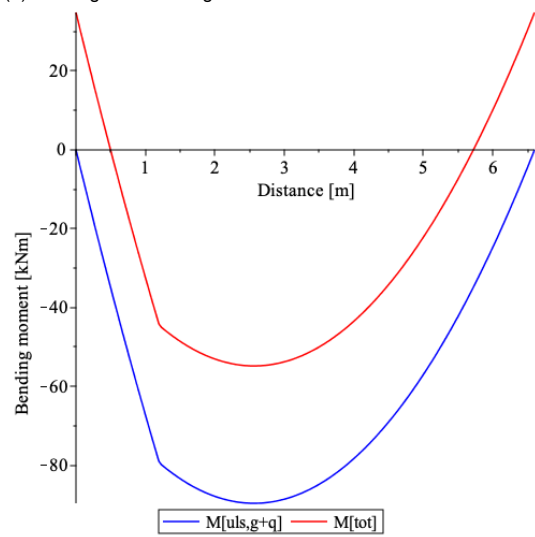
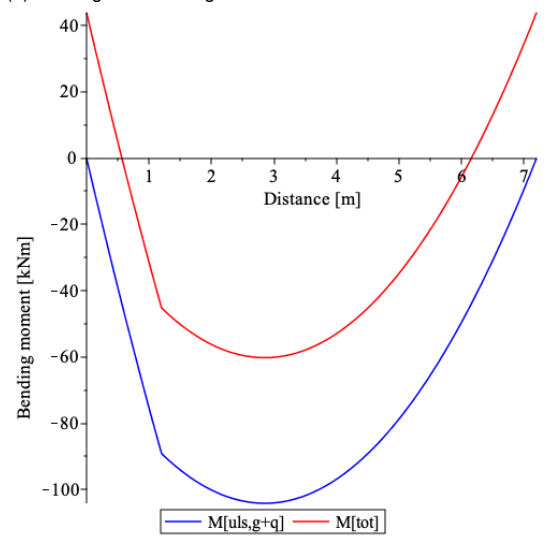
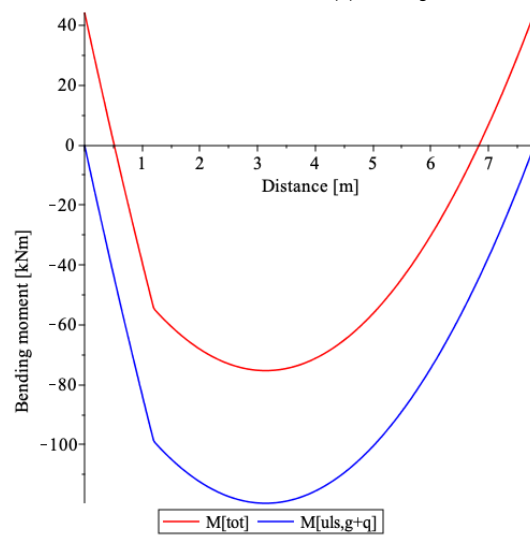
(a) Bending moment diagram for $l = 5.4$ m(b) Bending moment diagram for $l = 6.0$ m(c) Bending moment diagram for $l = 6.6$ m(d) Bending moment diagram for $l = 7.2$ m(e) Bending moment diagram for $l = 7.8$ m

Figure B.14: Bending moment diagrams due to the imposed loading with a trimmer beam

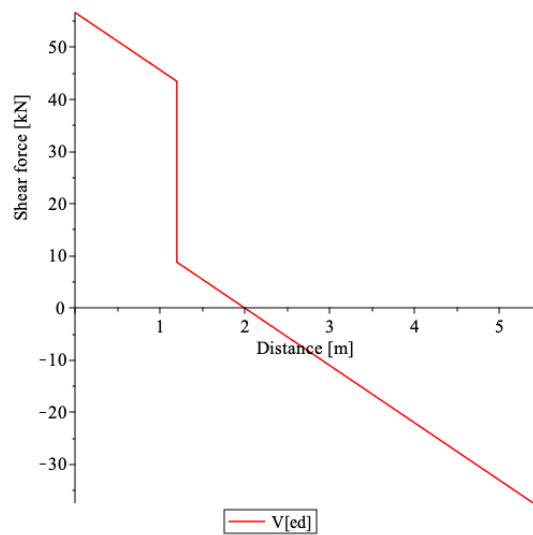
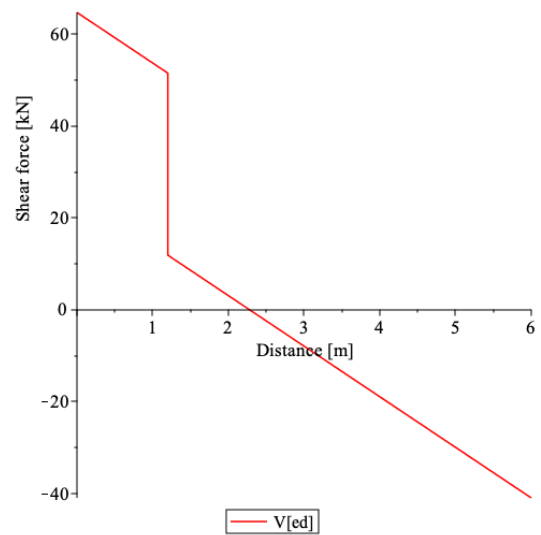
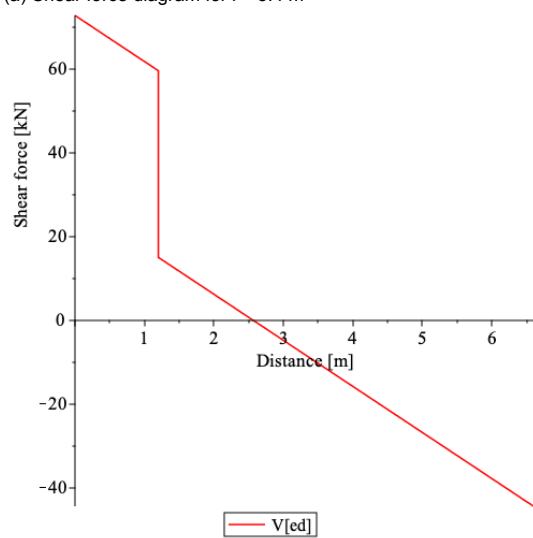
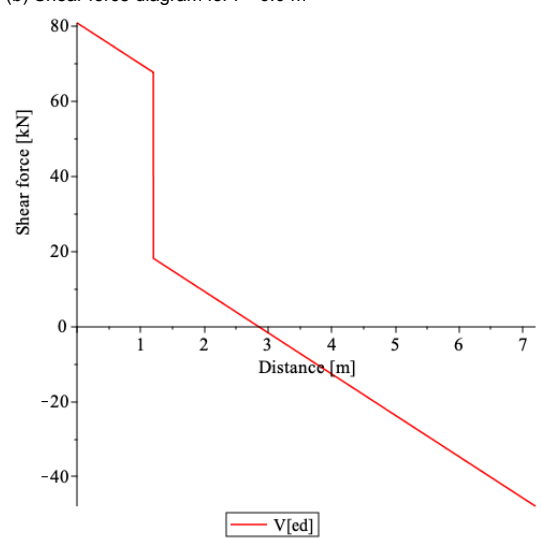
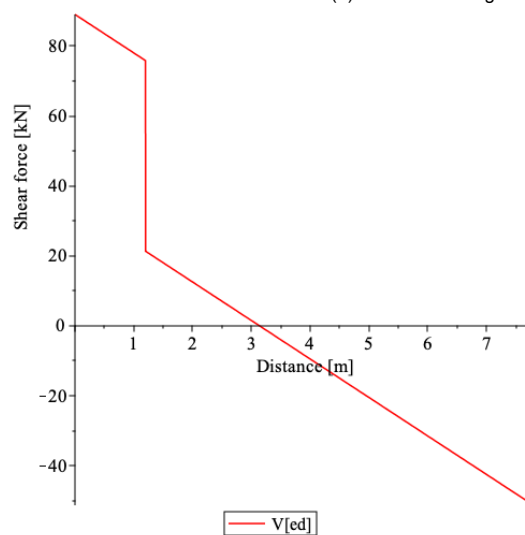
(a) Shear force diagram for $l = 5.4$ m(b) Shear force diagram for $l = 6.0$ m(c) Shear force diagram for $l = 6.6$ m(d) Shear force diagram for $l = 7.2$ m(e) Shear force diagram for $l = 7.8$ m

Figure B.15: Shear force diagrams due to the imposed loading with a trimmer beam

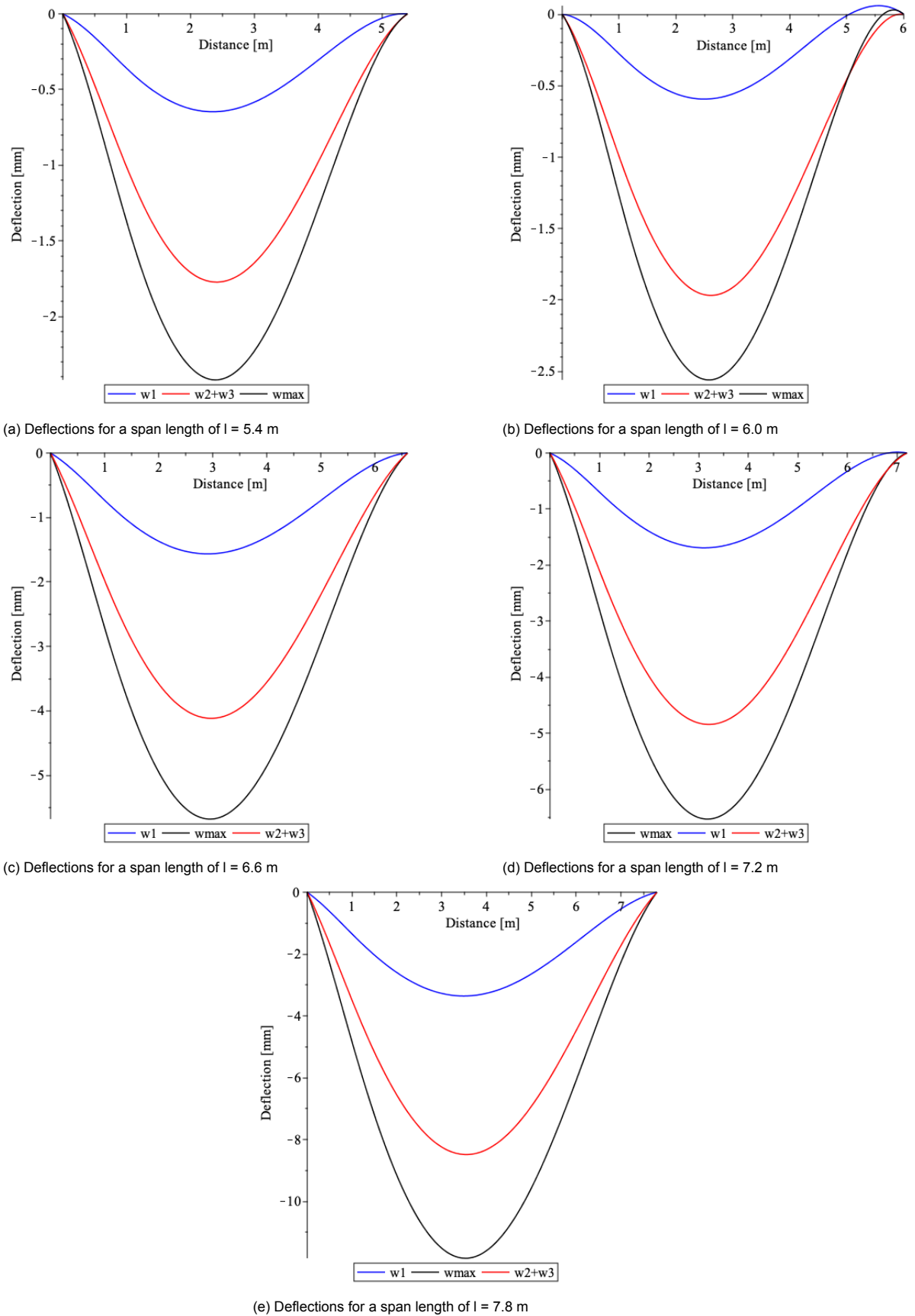
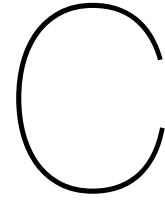


Figure B.16: Deflection lines according to the frequent load combination with a trimmer beam



Calculation results for Group III

The calculation results for element Group III are presented in this section. The elements are illustrated in figure 6.5. The width of the elements is 1800 millimeters. These elements are designed to accommodate a larger variety of grid sizes in generic floor fields. Since the widths of this element group are greater, fewer lifting movements are required, thus reducing the construction time. Likewise as the elements of Group II, where the width is 1200 millimeters, the elements are designed to be used with a trimmer beam. The maximum recess length is again equal to 3.6 meters. This means that a maximum of two slabs are supported by a trimmer beam. The calculation results and diagrams are presented for both loading situations: with and without the use of a trimmer beam.

Span length [m]	$P_{m,0}$ [kN]	$A_{p,req}$ [mm ²]	$n_{strands}$ [-]	$A_{p,tot}$ [mm ²]	$P_{m,0,tot}$ [kN]	$M_{p,0,tot}$ [kNm]
5.4	536.1	385	3	450	627.3	31.4
6.0	661.8	475	4	600	836.4	41.8
6.6	800.8	575	4	600	836.4	41.8
7.2	953.0	684	5	750	1045.5	52.3
7.8	1118.4	803	6	900	1254.6	62.7

Table C.1: Required amount of prestressing steel for all span lengths

Span length [m]	ΔP_{μ} [kN]	ΔP_{ws} [kN]	ΔP_{el} [kN]	$\Sigma \Delta P_0$ kN	$P_{m,0}$ [kN]	Δ_0 [%]
5.4	1.8	81.3	1.8	84.9	627.3	13.5
6.0	2.7	97.5	3.5	103.7	836.4	12.4
6.6	3.0	88.6	3.5	95.1	836.4	11.4
7.2	4.1	101.6	5.8	111.5	1045.5	10.7
7.8	5.3	112.5	8.8	126.6	1254.6	10.1

Table C.2: Immediate prestressing losses due to friction, wedge set and elastic deformation

Span length [m]	$\sum \Delta P_0$ [kN]	Δ_0 [%]	ΔP_{c+s+r} [kN]	Δ_∞ [%]	Δ_{tot} [%]	$P_{m\infty}$ [kN]	$M_{p\infty}$ [kNm]
5.4	84.9	13.5	32.2	5.1	18.6	510.3	25.5
6.0	103.7	12.4	42.5	5.1	17.5	690.1	34.5
6.6	95.1	11.4	42.5	5.1	16.5	698.1	34.9
7.2	111.5	10.7	52.7	5.0	15.7	881.3	44.1
7.8	126.6	10.1	62.7	5.0	15.1	1065.4	53.3

Table C.3: Total prestressing losses due to immediate and time-dependent effects

Span length [m]		Deflections		Check	
		[mm]		[-]	
5.4	$w_2 + w_3$	1.02	\leq	10.8	Satisfied
	w_{max}	1.38	\leq	21.6	Satisfied
6.0	$w_2 + w_3$	1.20	\leq	12.0	Satisfied
	w_{max}	1.54	\leq	24.0	Satisfied
6.6	$w_2 + w_3$	2.75	\leq	13.2	Satisfied
	w_{max}	3.81	\leq	26.4	Satisfied
7.2	$w_2 + w_3$	3.46	\leq	14.4	Satisfied
	w_{max}	4.72	\leq	28.8	Satisfied
7.8	$w_2 + w_3$	4.45	\leq	15.6	Satisfied
	w_{max}	6.01	\leq	31.2	Satisfied

Table C.4: Results regarding deflections for all span lengths

Span length [m]		M_{ed} [kNm]	M_{rd} [kNm]	UC [-]	Check [-]
5.4	Eurocode 2 [103]	61.3	87.3	0.70	satisfied
	Alqam et al. [107]	61.3	109.6	0.56	satisfied
6.0	Eurocode 2 [103]	75.7	116.4	0.65	satisfied
	Alqam et al. [107]	75.7	146.1	0.52	satisfied
6.6	Eurocode 2 [103]	91.5	117.7	0.78	satisfied
	Alqam et al. [107]	91.5	146.0	0.63	satisfied
7.2	Eurocode 2 [103]	108.9	146.4	0.74	satisfied
	Alqam et al. [107]	108.9	182.4	0.60	satisfied
7.8	Eurocode 2 [103]	127.9	174.5	0.73	satisfied
	Alqam et al. [107]	127.9	218.8	0.58	satisfied

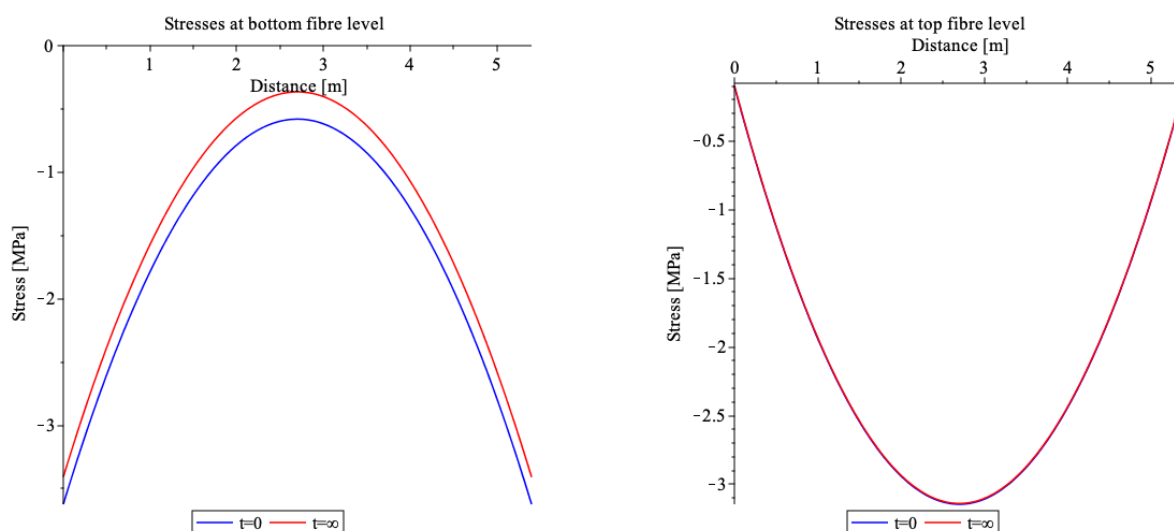
Table C.5: Unity checks regarding the bending moment capacity for all span lengths

Span length [m]		V_{ed} [kN]	$V_{rd,c}$ [kN]	UC [-]	$Check$ [-]
5.4	Eurocode 2 [101]	45.4	300.3	0.15	satisfied
	Alqam et al. [107]	45.5	326.0	0.14	satisfied
6.0	Eurocode 2 [101]	50.4	326.0	0.15	satisfied
	Alqam et al. [107]	50.4	356.2	0.14	satisfied
6.6	Eurocode 2 [101]	55.5	327.1	0.17	satisfied
	Alqam et al. [107]	55.5	356.2	0.16	satisfied
7.2	Eurocode 2 [101]	60.5	351.2	0.17	satisfied
	Alqam et al. [107]	60.5	384.1	0.16	satisfied
7.8	Eurocode 2 [101]	65.6	373.9	0.18	satisfied
	Alqam et al. [107]	65.6	410.0	0.16	satisfied

Table C.6: Unity checks regarding the shear force capacity for all span lengths

Span length [m]		v_{ed} [MPa]	$v_{rd,i}$ [MPa]	UC [-]	$Check$ [-]
5.4	Eurocode 2 [101]	0.39	0.92	0.43	satisfied
	Alqam et al. [107]	0.39	1.24	0.32	satisfied
6.0	Eurocode 2 [101]	0.44	1.24	0.35	satisfied
	Alqam et al. [107]	0.44	1.65	0.26	satisfied
6.6	Eurocode 2 [101]	0.48	1.25	0.38	satisfied
	Alqam et al. [107]	0.48	1.65	0.29	satisfied
7.2	Eurocode 2 [101]	0.52	1.58	0.33	satisfied
	Alqam et al. [107]	0.52	2.06	0.25	satisfied
7.8	Eurocode 2 [101]	0.57	1.91	0.30	satisfied
	Alqam et al. [107]	0.57	2.47	0.23	satisfied

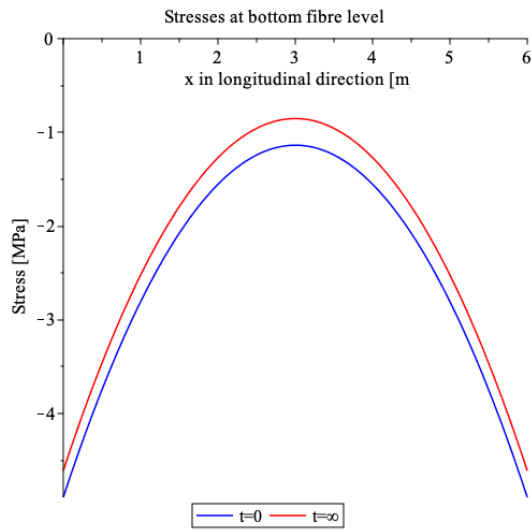
Table C.7: Unity checks regarding the shear stress at the interfaces for all span lengths



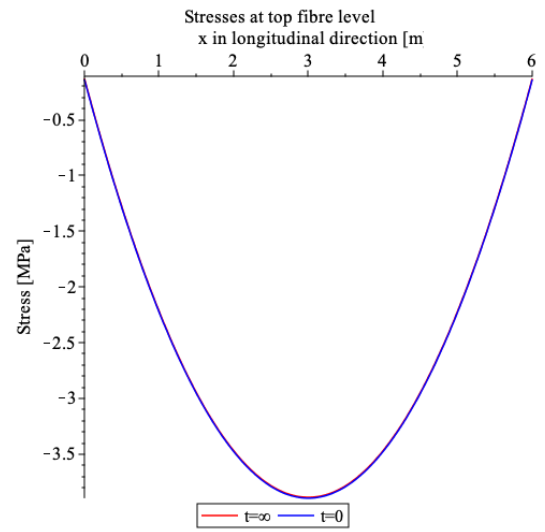
(a) Stresses at bottom fibre level

(b) Stresses at top fibre level

Figure C.1: Stresses in the cross-section for a span length of 5.4 m

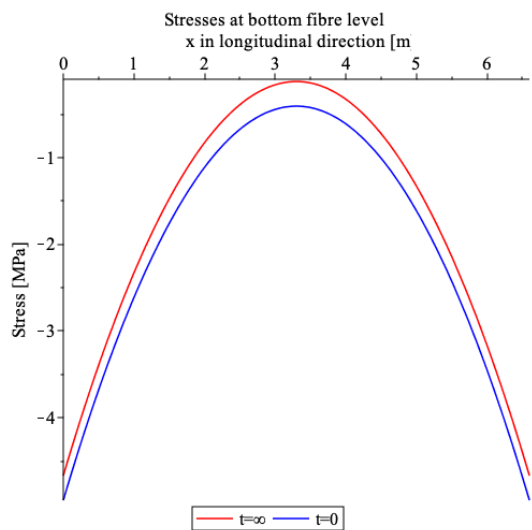


(a) Stresses at bottom fibre level

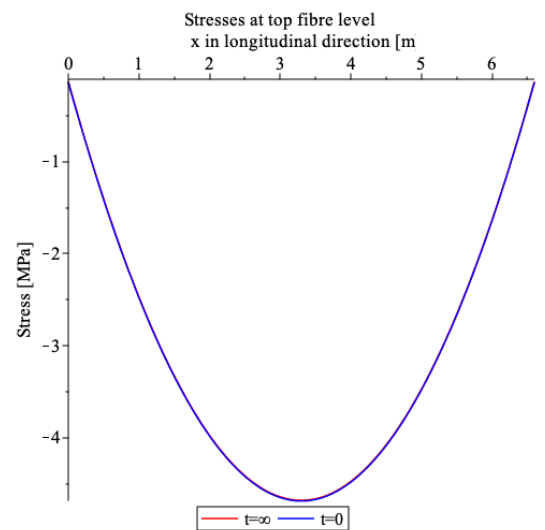


(b) Stresses at top fibre level

Figure C.2: Stresses in the cross-section for a span length of 6.0 m

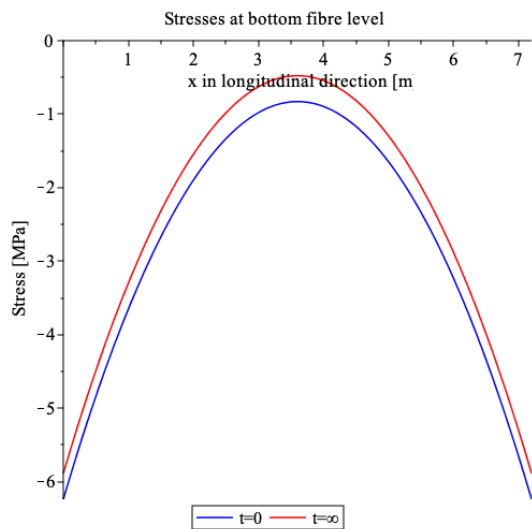


(a) Stresses at bottom fibre level

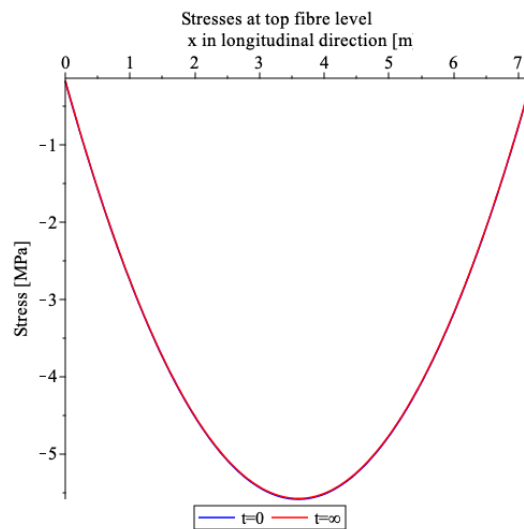


(b) Stresses at top fibre level

Figure C.3: Stresses in the cross-section for a span length of 6.6 m

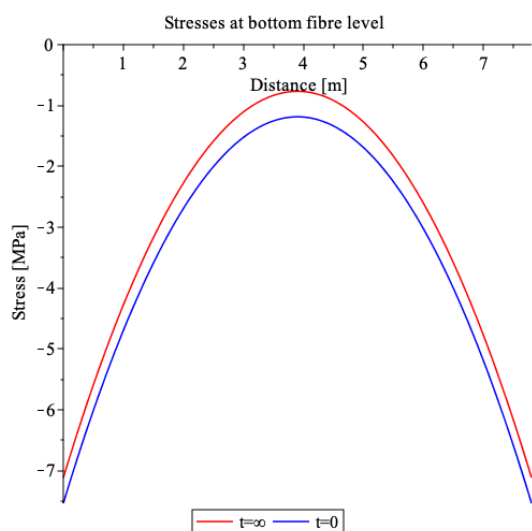


(a) Stresses at bottom fibre level

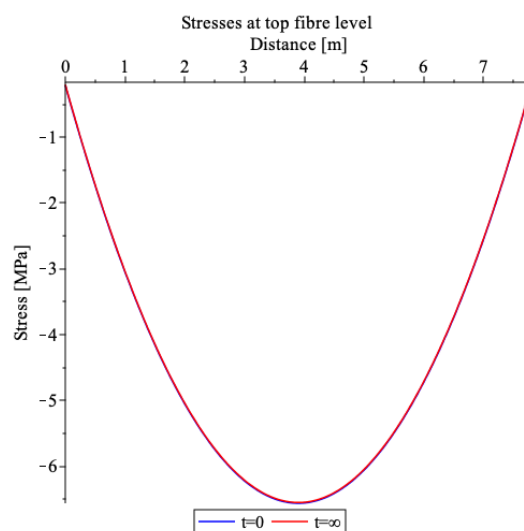


(b) Stresses at top fibre level

Figure C.4: Stresses in the cross-section for a span length of 7.2 m



(a) Stresses at bottom fibre level



(b) Stresses at top fibre level

Figure C.5: Stresses in the cross-section for a span length of 7.8 m

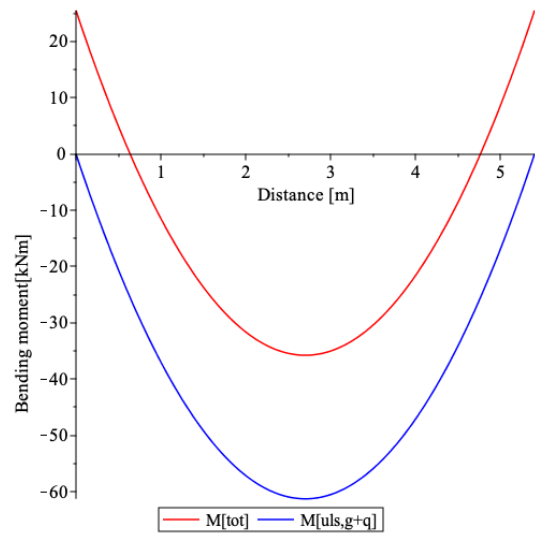
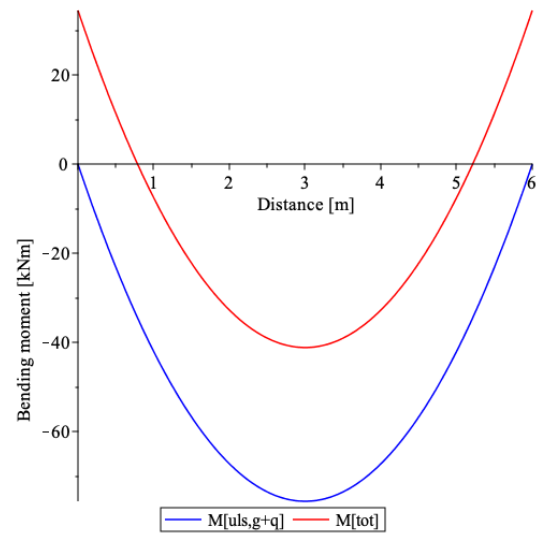
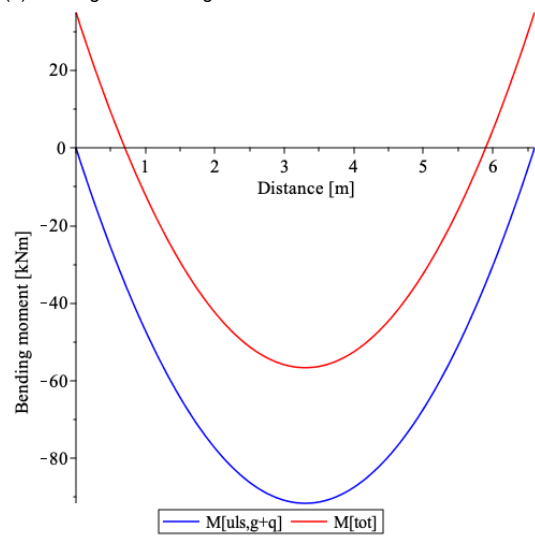
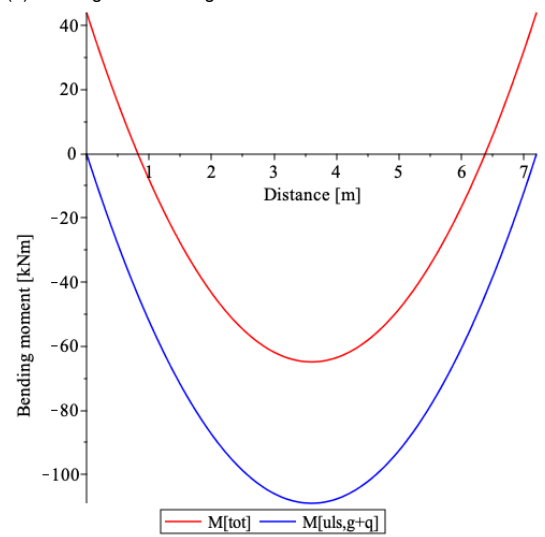
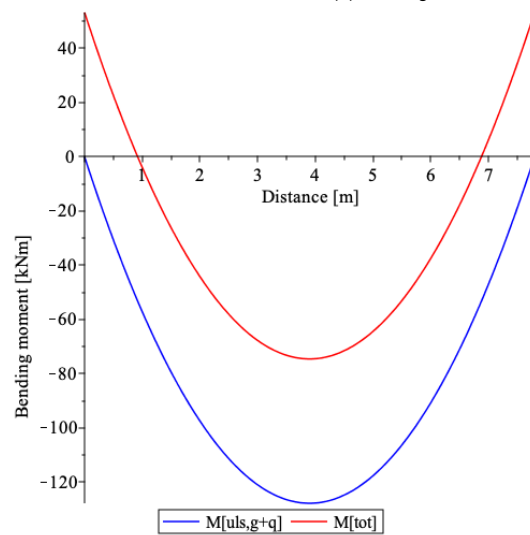
(a) Bending moment diagram for $l = 5.4$ m(b) Bending moment diagram for $l = 6.0$ m(c) Bending moment diagram for $l = 6.6$ m(d) Bending moment diagram for $l = 7.2$ m(e) Bending moment diagram for $l = 7.8$ m

Figure C.6: Bending moment diagrams due to the imposed loading

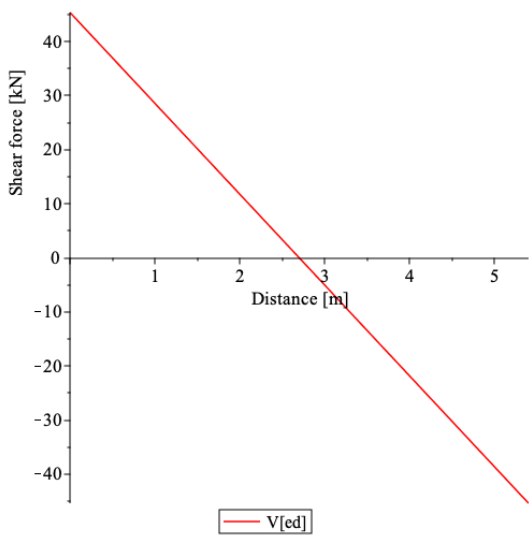
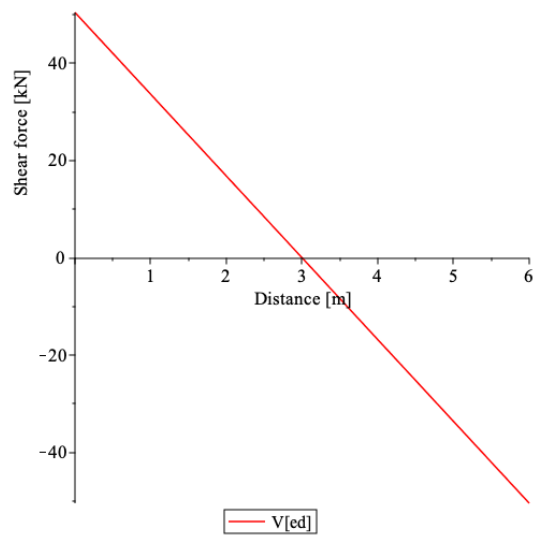
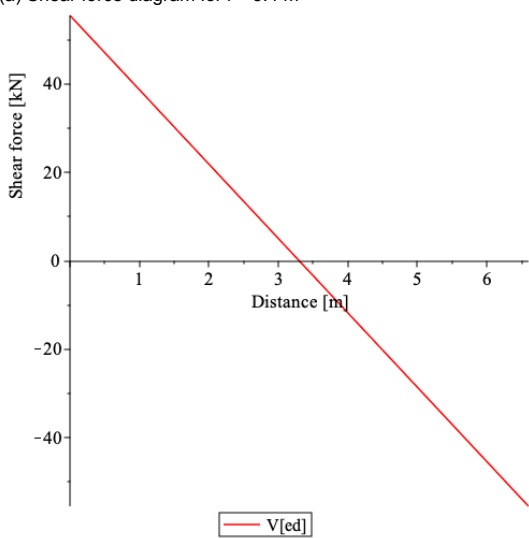
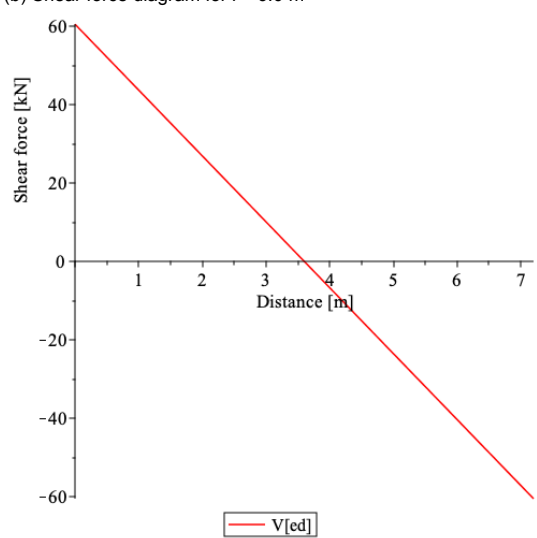
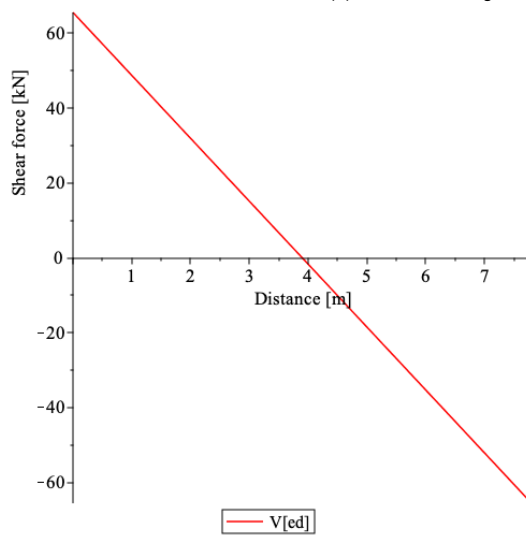
(a) Shear force diagram for $l = 5.4$ m(b) Shear force diagram for $l = 6.0$ m(c) Shear force diagram for $l = 6.6$ m(d) Shear force diagram for $l = 7.2$ m(e) Shear force diagram for $l = 7.8$ m

Figure C.7: Shear force diagrams due to the imposed loading

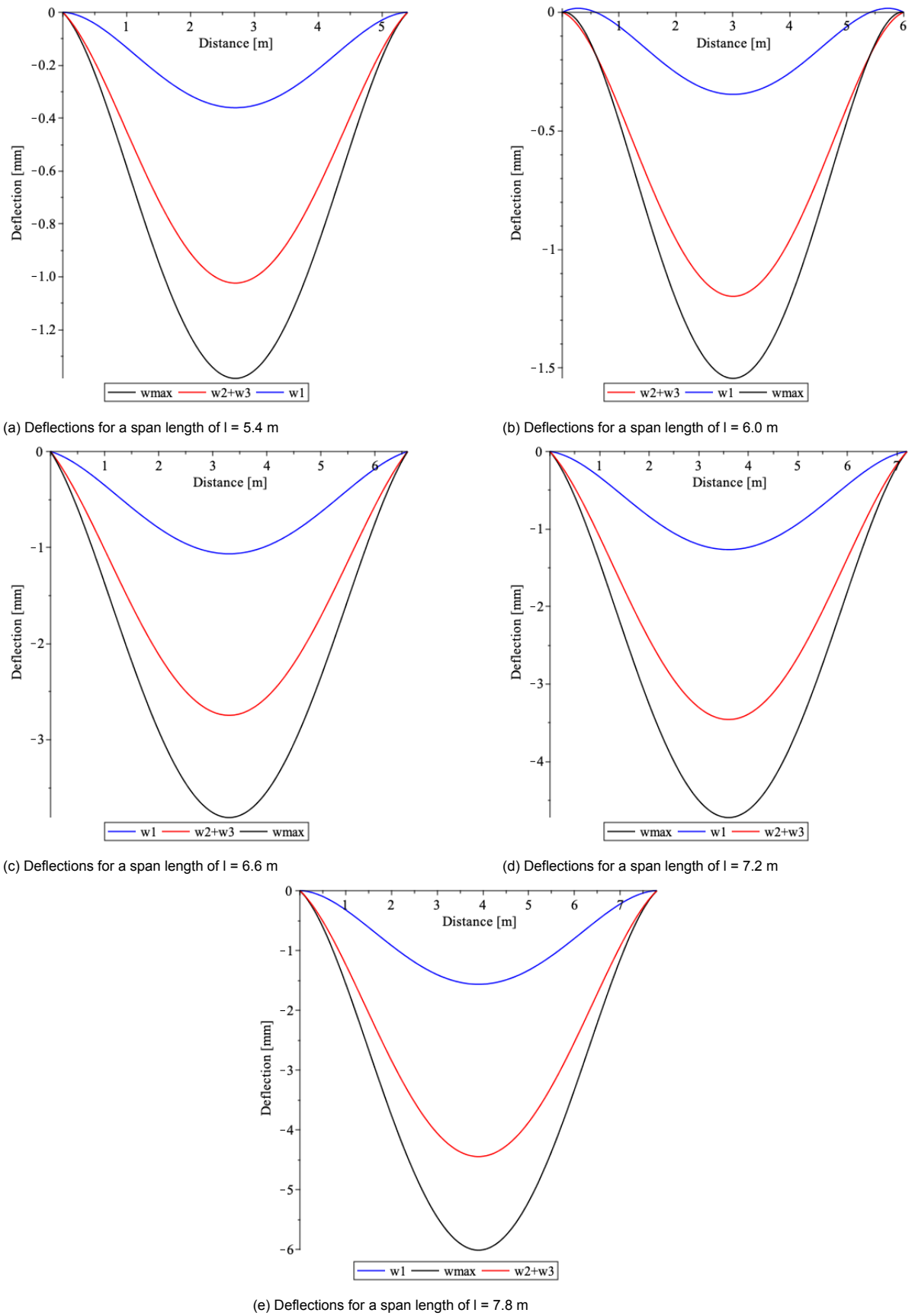


Figure C.8: Deflection lines according to the frequent load combination

Span length [m]	$n_{strands}$ [-]	$A_{p,tot}$ [mm ²]	$P_{m,0,tot}$ [kN]	$M_{p,0,tot}$ [kNm]	$P_{m,\infty}$ [kN]	$M_{p,\infty}$ [kNm]
5.4	4	600	836.4	41.8	679.6	34.0
6.0	5	750	1045.5	52.3	861.7	43.1
6.6	6	900	1254.6	62.7	1045.8	52.3
7.2	6	900	1254.6	62.7	1056.4	52.8
7.8	7	1050	1463.7	73.2	1241.6	62.1

Table C.8: Required amount of prestressing steel for all span lengths with a trimmer beam

Span length [m]		Deflections			Check
		[mm]		[mm]	[-]
5.4	$w_2 + w_3$	1.57	≤	10.8	Satisfied
	w_{max}	2.16	≤	21.6	Satisfied
6.0	$w_2 + w_3$	2.14	≤	12.0	Satisfied
	w_{max}	2.89	≤	24.0	Satisfied
6.6	$w_2 + w_3$	2.93	≤	13.2	Satisfied
	w_{max}	3.93	≤	26.4	Satisfied
7.2	$w_2 + w_3$	5.54	≤	14.4	Satisfied
	w_{max}	7.76	≤	28.8	Satisfied
7.8	$w_2 + w_3$	7.33	≤	15.6	Satisfied
	w_{max}	10.23	≤	31.2	Satisfied

Table C.9: Results regarding deflections for all span lengths with a trimmer beam

Span length [m]		M_{ed} [kNm]	M_{rd} [kNm]	UC [-]	Check [-]
5.4	Eurocode 2 [103]	84.3	114.8	0.73	satisfied
	Alqam et al. [107]	84.3	146.2	0.58	satisfied
6.0	Eurocode 2 [103]	101.8	143.5	0.71	satisfied
	Alqam et al. [107]	101.8	182.7	0.56	satisfied
6.6	Eurocode 2 [103]	120.8	171.7	0.70	satisfied
	Alqam et al. [107]	120.8	219.1	0.55	satisfied
7.2	Eurocode 2 [103]	141.3	173.2	0.82	satisfied
	Alqam et al. [107]	141.3	219.0	0.65	satisfied
7.8	Eurocode 2 [103]	163.3	200.6	0.81	satisfied
	Alqam et al. [107]	163.3	255.4	0.64	satisfied

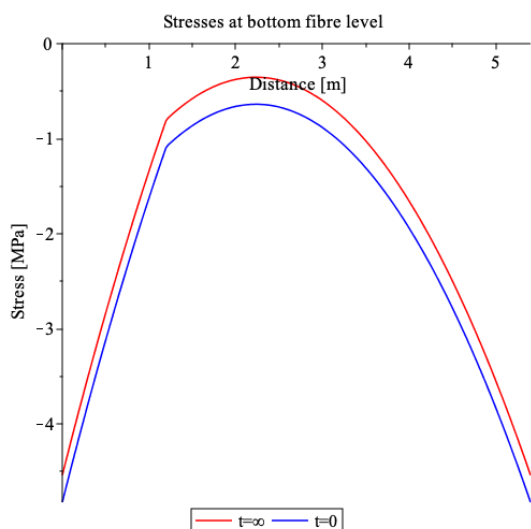
Table C.10: Unity checks regarding the bending moment capacity for all span lengths with a trimmer beam

Span length [m]		V_{ed} [kN]	$V_{et,d}$ [kN]	$V_{rd,c}$ [kN]	$V_{rd,n}$ [kN]	UC [-]	<i>Check</i> [-]
5.4	Eurocode 2 [101]	72.9	91.7	324.6	232.9	0.31	satisfied
	Alqam et al. [107]	72.9	91.7	356.2	264.5	0.28	satisfied
6.0	Eurocode 2 [101]	82.7	104.8	348.8	244.0	0.34	satisfied
	Alqam et al. [107]	82.7	104.8	384.1	279.2	0.30	satisfied
6.6	Eurocode 2 [101]	92.6	117.9	371.7	253.7	0.37	satisfied
	Alqam et al. [107]	92.6	117.9	410.0	292.1	0.32	satisfied
7.2	Eurocode 2 [101]	102.6	131.0	372.9	241.9	0.42	satisfied
	Alqam et al. [107]	102.6	131.0	410.0	279.0	0.37	satisfied
7.8	Eurocode 2 [101]	112.5	144.1	394.5	250.4	0.45	satisfied
	Alqam et al. [107]	112.5	144.1	434.5	290.3	0.39	satisfied

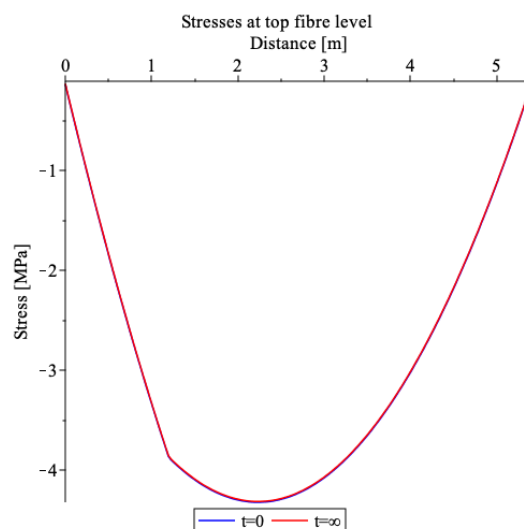
Table C.11: Unity checks regarding the shear force capacity for all span lengths with a trimmer beam

Span length [m]		v_{ed} [MPa]	$v_{rd,i}$ [MPa]	UC [-]	<i>Check</i> [-]
5.4	Eurocode 2 [101]	0.63	1.22	0.52	satisfied
	Alqam et al. [107]	0.63	1.65	0.38	satisfied
6.0	Eurocode 2 [101]	0.72	1.54	0.46	satisfied
	Alqam et al. [107]	0.72	2.06	0.35	satisfied
6.6	Eurocode 2 [101]	0.80	1.87	0.43	satisfied
	Alqam et al. [107]	0.80	2.47	0.32	satisfied
7.2	Eurocode 2 [101]	0.89	1.89	0.47	satisfied
	Alqam et al. [107]	0.89	2.47	0.36	satisfied
7.8	Eurocode 2 [101]	0.97	2.22	0.44	satisfied
	Alqam et al. [107]	0.97	2.88	0.34	satisfied

Table C.12: Unity checks regarding the shear stress at the interfaces for all span lengths with a trimmer beam

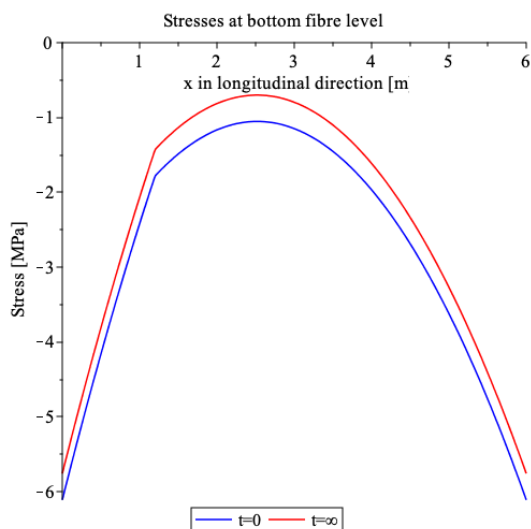


(a) Stresses at bottom fibre level

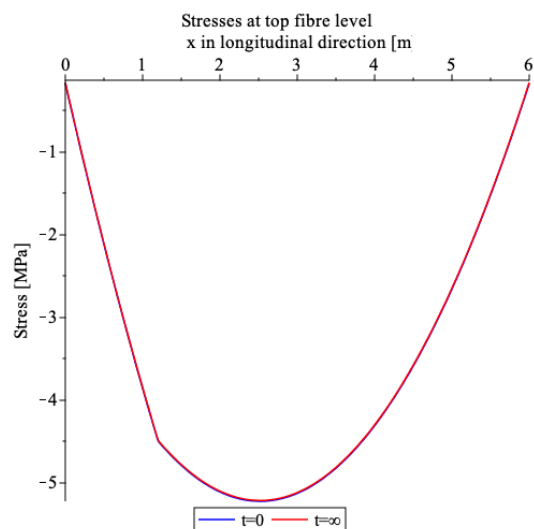


(b) Stresses at top fibre level

Figure C.9: Stresses in the cross-section for a span length of 5.4 m with a trimmer beam

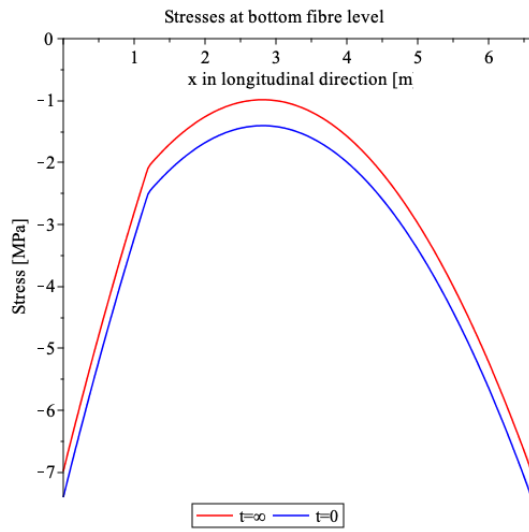


(a) Stresses at bottom fibre level

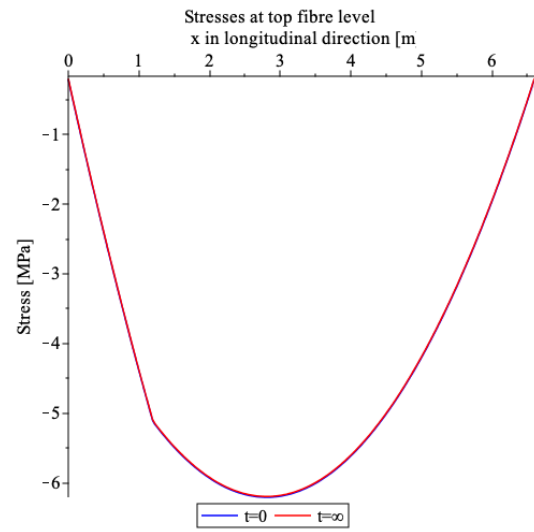


(b) Stresses at top fibre level

Figure C.10: Stresses in the cross-section for a span length of 6.0 m with a trimmer beam

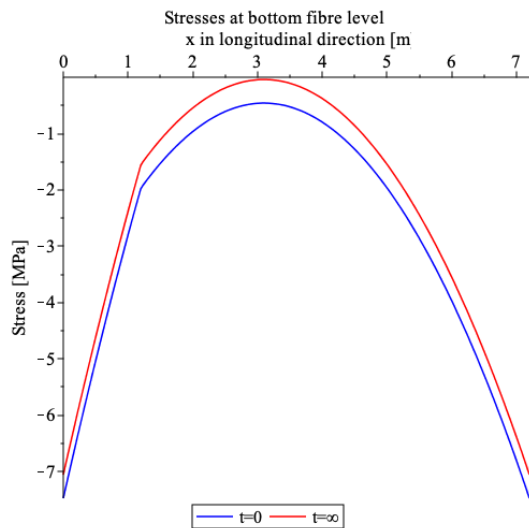


(a) Stresses at bottom fibre level

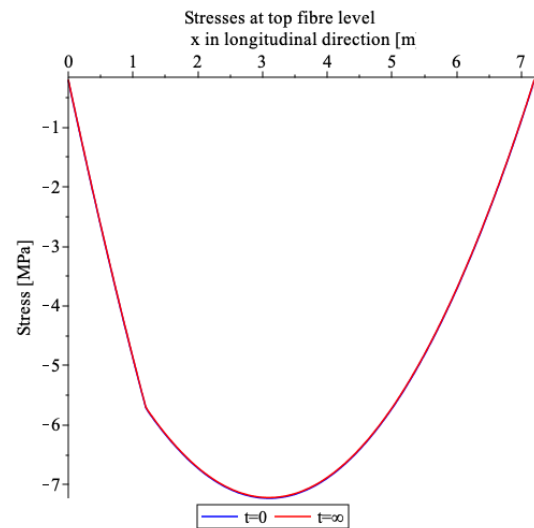


(b) Stresses at top fibre level

Figure C.11: Stresses in the cross-section for a span length of 6.6 m with a trimmer beam

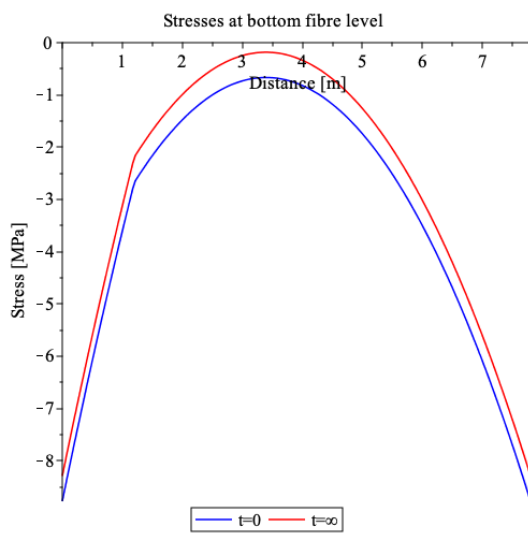


(a) Stresses at bottom fibre level

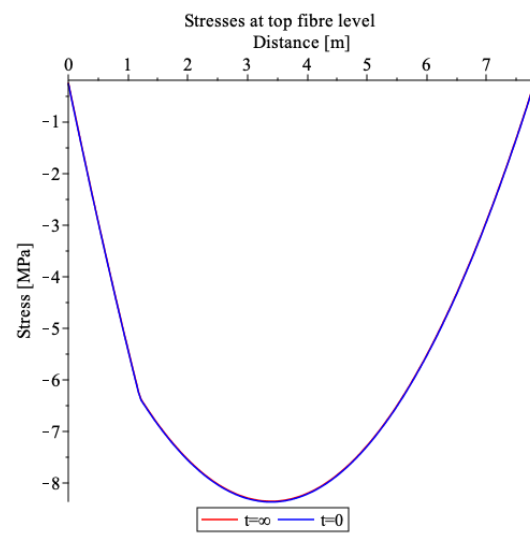


(b) Stresses at top fibre level

Figure C.12: Stresses in the cross-section for a span length of 7.2 m with a trimmer beam



(a) Stresses at bottom fibre level



(b) Stresses at top fibre level

Figure C.13: Stresses in the cross-section for a span length of 7.8 m with a trimmer beam

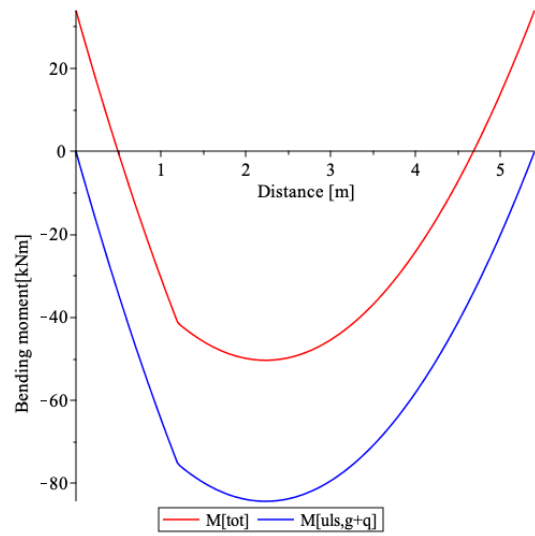
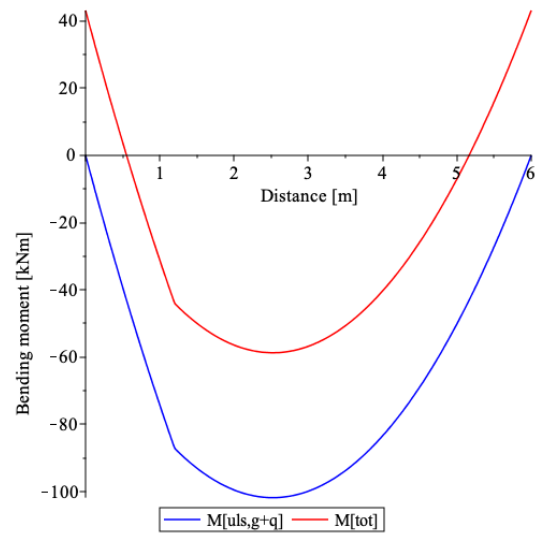
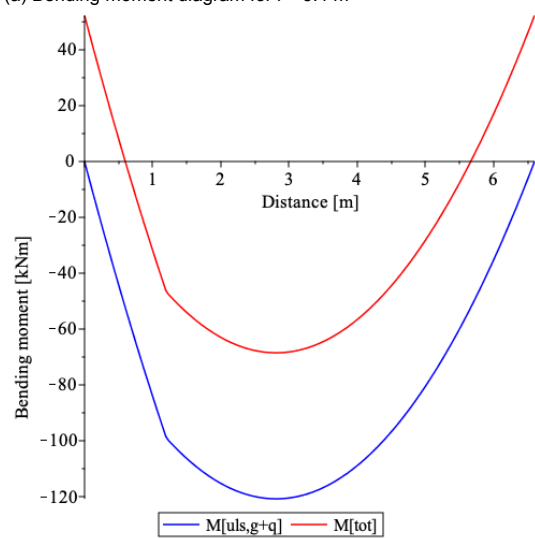
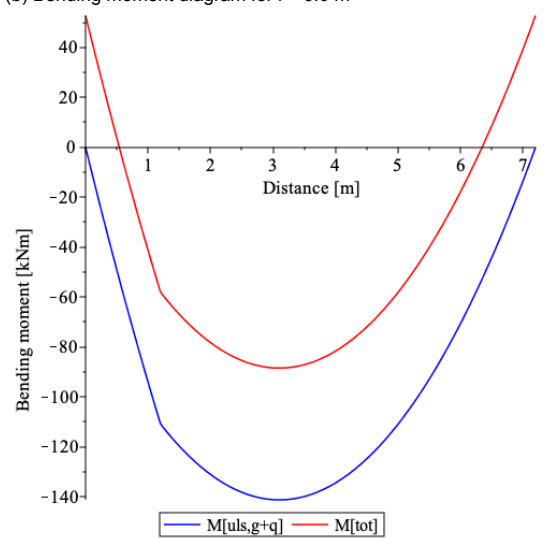
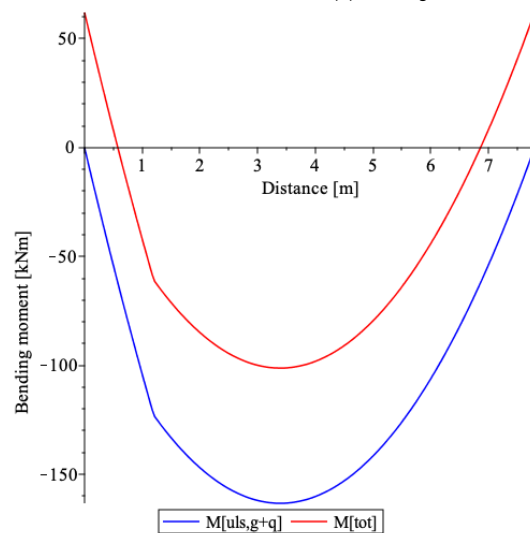
(a) Bending moment diagram for $l = 5.4$ m(b) Bending moment diagram for $l = 6.0$ m(c) Bending moment diagram for $l = 6.6$ m(d) Bending moment diagram for $l = 7.2$ m(e) Bending moment diagram for $l = 7.8$ m

Figure C.14: Bending moment diagrams due to the imposed loading with a trimmer beam

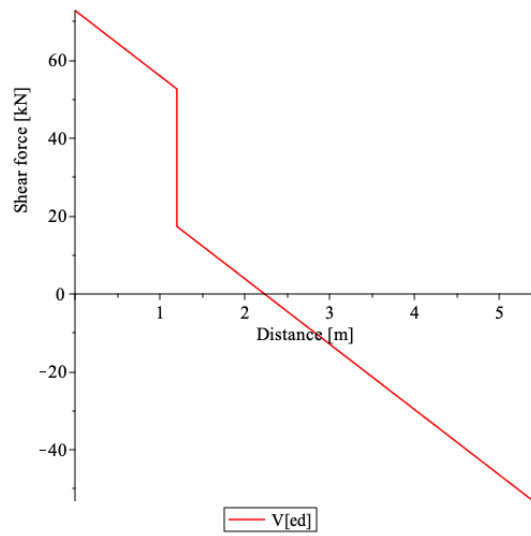
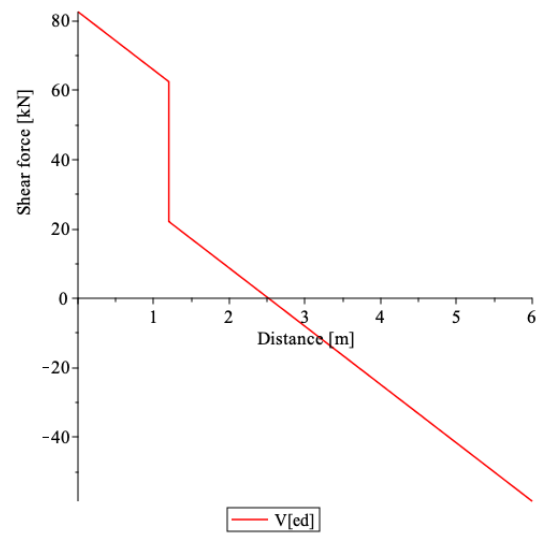
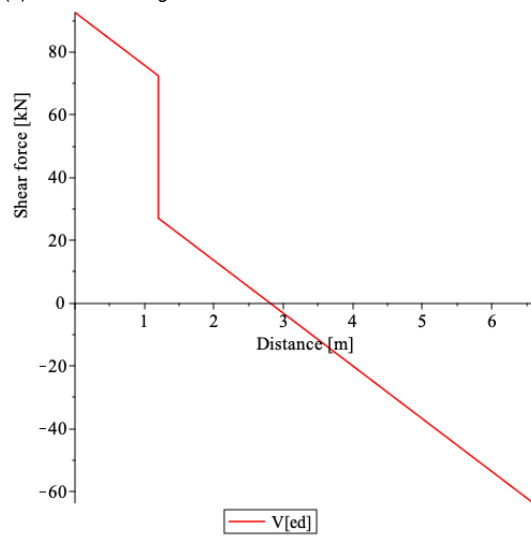
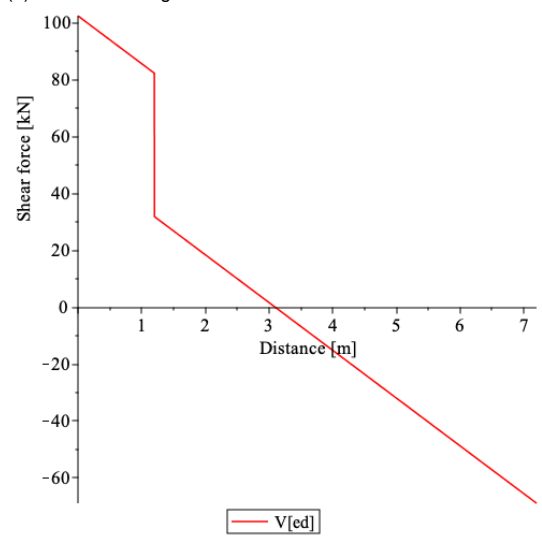
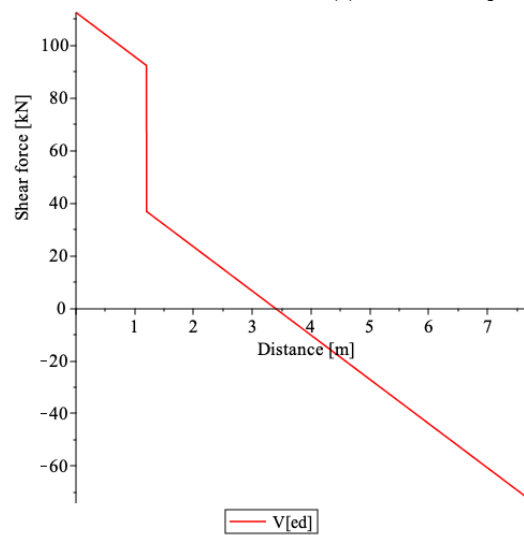
(a) Shear force diagram for $l = 5.4$ m(b) Shear force diagram for $l = 6.0$ m(c) Shear force diagram for $l = 6.6$ m(d) Shear force diagram for $l = 7.2$ m(e) Shear force diagram for $l = 7.8$ m

Figure C.15: Shear force diagrams due to the imposed loading with a trimmer beam

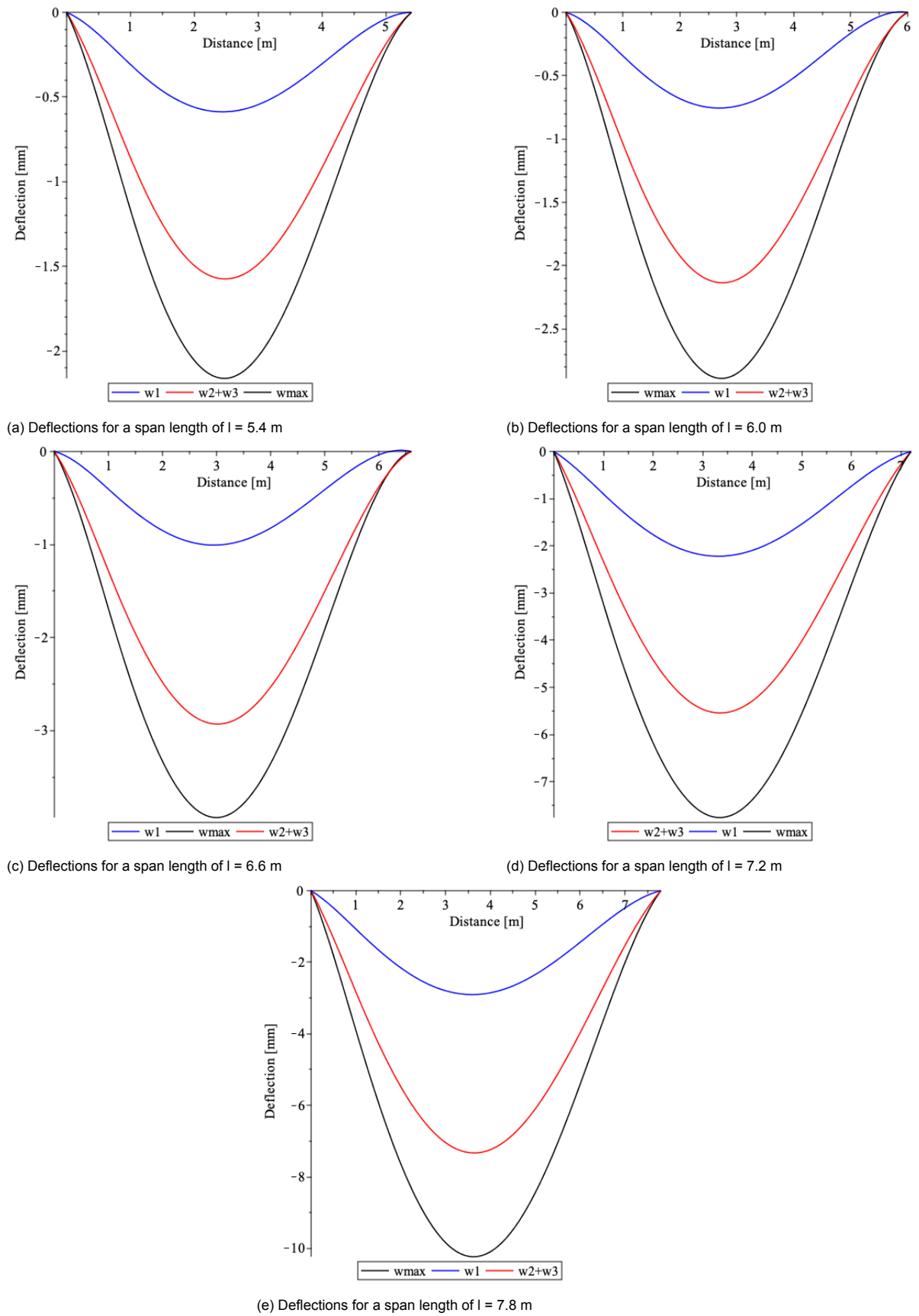
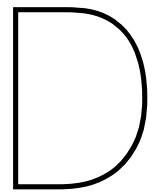


Figure C.16: Deflection lines according to the frequent load combination with a trimmer beam



European Technical Assessment Post Tensioning system

DYWIDAG 



European Organisation for Technical Approvals
Europäische Organisation für Technische Zulassungen
Organisation Européenne pour l'Agrément Technique



POST-TENSIONING

**SUSPA/DYWIDAG –
Unbonded Monostrand System
with 1 to 5 Monostrands**

ETA-03/0036

140

29. June 2021



Austrian Institute of Construction Engineering
Schenkenstrasse 4 | T+43 1 533 65 50
1010 Vienna | Austria | F+43 1 533 64 23
www.oib.or.at | mail@oib.or.at



European Technical Assessment

ETA-03/0036
of 29.01.2021

General part

Technical Assessment Body issuing the European Technical Assessment

Österreichisches Institut für Bautechnik (OIB)
Austrian Institute of Construction Engineering

Trade name of the construction product

SUSPA/DSI – Unbonded Monostrand System
with 1 to 5 Monostrands

Product family to which the construction product belongs

Unbonded post-tensioning kits for prestressing of
structures with monostrands

Manufacturer

DYWIDAG-Systems International GmbH
Neuhofweg 5
85716 Unterschleissheim
Germany

Manufacturing plants

DYWIDAG-Systems International GmbH
Max-Planck-Ring 1
40764 Langenfeld
Germany

DYWIDAG-Systems International GmbH
ul. Hallera 78
41-709 Ruda Śląska
Poland

This European Technical Assessment contains

38 pages including Annexes 1 to 15, which form
an integral part of this assessment.

This European Technical Assessment is issued in accordance with Regulation (EU) № 305/2011, on the basis of

European Assessment Document
(EAD) 160004-00-0301 – Post-Tensioning Kits
for Prestressing of Structures.

This European Technical Assessment replaces

European Technical Assessment ETA-03/0036 of
15.06.2018.

Table of contents

EUROPEAN TECHNICAL ASSESSMENT ETA-03/0036 OF 29.01.2021 1

GENERAL PART 1

TABLE OF CONTENTS 2

REMARKS 6

SPECIFIC PARTS 6

1 TECHNICAL DESCRIPTION OF THE PRODUCT 6

1.1 General 6

PT SYSTEM 7

1.2 Designation and range of anchorages and couplings 7

 1.2.1 Designation 7

 1.2.2 Single anchorages SK6 and SF6 and couplings KS6-SK6 and K6-K6 7

 1.2.2.1 General 7

 1.2.2.2 Stressing anchor SK6 7

 1.2.2.3 Fixed anchor SF6 7

 1.2.2.4 Fixed coupling KS6-SK6 7

 1.2.2.5 Movable coupling K6-K6 7

 1.2.3 Multistrand anchorages MER6 and MEF6 7

 1.2.3.1 Stressing anchor MER6 7

 1.2.3.2 Fixed anchor MEF6 8

 1.2.4 Centre and edge distances of anchorages, concrete cover 8

 1.2.5 Strength of concrete 8

 1.2.6 Reinforcement in the anchorage zone 8

1.3 Designation and range of tendons 8

 1.3.1 Designation 8

 1.3.2 Range of tendons 9

 1.3.3 Maximum stressing forces 9

1.4 Slip at anchorages 9

1.5 Friction losses 10

1.6 Support of monostrands 10

1.7 Radii of curvature of internal tendons 10

COMPONENTS 11

1.8 Monostrand 11

 1.8.1 Specification of prestressing steel strand 11

 1.8.2 Specification of monostrand 11

electronic copy

1.9	Anchorage components.....	11
1.9.1	General	11
1.9.2	Anchor and coupling heads	11
1.9.3	Wedges.....	12
1.9.4	Helix	12
1.10	Permanent corrosion protection.....	12
1.11	Material specifications of the components	12
2	SPECIFICATION OF THE INTENDED USE IN ACCORDANCE WITH THE APPLICABLE EUROPEAN ASSESSMENT DOCUMENT (HEREINAFTER EAD).....	12
2.1	Intended use	12
2.2	Assumptions.....	12
2.2.1	General	12
2.2.2	Packaging, transport and storage.....	12
2.2.3	Design.....	13
2.2.4	Installation.....	13
2.2.4.1	General.....	13
2.2.4.2	De-sheathing of monostrands	13
2.2.4.3	Examination of tendons and possible repairs of the corrosion protection system	14
2.2.4.4	Stressing anchor SK6	14
2.2.4.5	Fixed anchor SF6.....	14
2.2.4.6	Fixed coupling KS6-SK6	15
2.2.4.7	Movable coupling K6-K6	15
2.2.4.8	Stressing anchor MER6	16
2.2.4.9	Fixed anchor MEF6.....	17
2.2.4.10	Checking of tendons	17
2.2.4.11	Stressing and stressing records	17
2.2.4.11.1	General	17
2.2.4.11.2	Stressing	17
2.2.4.11.3	Restressing	18
2.2.4.11.4	Stressing records	18
2.2.4.11.5	Stressing equipment, clearance requirements, and safety-at-work.....	18
2.2.4.12	Welding at anchorages	18
2.3	Assumed working life	18
3	PERFORMANCE OF THE PRODUCT AND REFERENCES TO THE METHODS USED FOR ITS ASSESSMENT	19
3.1	Essential characteristics	19
3.2	Product performance.....	20
3.2.1	Mechanical resistance and stability	20
3.2.1.1	Resistance to static load	20
3.2.1.2	Resistance to fatigue	20

electronic copy

3.2.1.3	Load transfer to the structure	20
3.2.1.4	Friction coefficient	20
3.2.1.5	Deviation, deflection (limits) for internal bonded and unbonded tendon.....	20
3.2.1.6	Assessment of assembly	20
3.2.1.7	Corrosion protection.....	20
3.2.2	Safety in case of fire.....	20
3.2.2.1	Reaction to fire.....	20
3.2.3	Hygiene, health, and the environment	20
3.2.3.1	Content, emission and/or release of dangerous substances	20
3.3	Assessment methods	21
3.4	Identification	21
4	ASSESSMENT AND VERIFICATION OF CONSTANCY OF PERFORMANCE (HEREINAFTER AVCP) SYSTEM APPLIED, WITH REFERENCE TO ITS LEGAL BASE	21
4.1	System of assessment and verification of constancy of performance	21
4.2	AVCP for construction products for which a European Technical Assessment has been issued.....	22
5	TECHNICAL DETAILS NECESSARY FOR THE IMPLEMENTATION OF THE AVCP SYSTEM, AS PROVIDED FOR IN THE APPLICABLE EAD	22
5.1	Tasks for the manufacturer.....	22
5.1.1	Factory production control	22
5.1.2	Declaration of performance	23
5.2	Tasks for the notified product certification body.....	23
5.2.1	Initial inspection of the manufacturing plant and of factory production control.....	23
5.2.2	Continuing surveillance, assessment and evaluation of factory production control	23
5.2.3	Audit-testing of samples taken by the notified product certification body at the manufacturing plant or at the manufacturer's storage facilities	23
ANNEXES	24
ANNEX 1	ANCHORAGES AND COUPLINGS – OVERVIEW	24
ANNEX 2	BASIC COMPONENTS OF ANCHORAGES – CAST-IRON ANCHORS SK6 AND SF6.....	25
ANNEX 3	STRESSING ANCHOR SK6 AND FIXED ANCHOR SF6.....	26
ANNEX 4	STRESSING ANCHOR SK6 AND FIXED ANCHOR SF6 – MINIMUM CENTRE AND EDGE DISTANCES.....	27
ANNEX 5	FIXED COUPLING KS6-SK6	28
ANNEX 6	MOVABLE COUPLING K6-K6	29
ANNEX 7	STRESSING ANCHOR MER6 AND FIXED ANCHOR MEF6	30
ANNEX 8	STRESSING ANCHOR MER6 AND FIXED ANCHOR MEF6 – SIZE 6-2 TO 6-5	31

electronic copy

ANNEX 9	TENDON INSTALLATION INSTRUCTIONS – FREE TENDON LAYOUT	32
ANNEX 10	MAXIMUM PRESTRESSING AND OVERSTRESSING FORCES	33
ANNEX 11	PRESTRESSING STEEL STRANDS – CHARACTERISTIC MAXIMUM FORCE OF TENDON	34
ANNEX 12	MATERIAL SPECIFICATIONS.....	35
ANNEX 13	CONTENTS OF THE PRESCRIBED TEST PLAN.....	36
ANNEX 14	AUDIT TESTING	37
ANNEX 15	REFERENCE DOCUMENTS.....	38

electronic copy electronic copy electronic copy electronic copy electronic copy electronic copy electronic copy

Remarks

Translations of the European Technical Assessment in other languages shall fully correspond to the original issued document and should be identified as such.

Communication of the European Technical Assessment, including transmission by electronic means, shall be in full. However, partial reproduction may be made with the written consent of Österreichisches Institut für Bautechnik. Any partial reproduction has to be identified as such.

Specific parts

1 Technical description of the product

1.1 General

The European Technical Assessment¹ – ETA – applies to a kit, the unbonded PT system

SUSPA/DSI – Unbonded Monostrand System with 1 to 5 Monostrands,

comprising the following components.

– Tendon

Unbonded monostrand tendon with one to five tensile elements

– Tensile element

7-wire prestressing steel strand with nominal diameter and nominal tensile strengths as given in Table 1, factory provided with a corrosion protection system, comprising corrosion protection filling material and PE-sheathing

Table 1 Tensile elements

Nominal diameter		Designation according to prEN 10138-3 ²	Nominal tensile strength
mm	inch	—	N/mm ²
15.7	0.62	Y1770S7	1 770
15.7	0.62	Y1860S7	1 860

NOTE 1 N/mm² = 1 MPa

– Anchorage and coupling

Monostrand anchored by 2-piece wedge

Stressing and fixed anchors SK6 and SF6 for tendons with one single monostrand

Fixed coupling KS6-SK6 and movable coupling K6-K6 for tendons with one single monostrand

Stressing and fixed anchors MER6 and MEF6 for tendons with 2 to 5 monostrands

¹ ETA-03/0036 was firstly issued in 2004 as European technical approval with validity from 01.04.2004, amended in 2009 with validity from 01.04.2009 and 2013 with validity from 30.06.2013, converted 2018 to European Technical Assessment ETA-03/0036 of 15.06.2018 and amended in 2021 to European Technical Assessment ETA-03/0036 of 29.01.2021.

² Standards and other documents referred to in the European Technical Assessment are listed in Annex 15.

For monostrands with a nominal tensile strength of either 1 860 N/mm² or 1 770 N/mm², the same anchorages and couplings are used.

- Helix and additional reinforcement in the anchorage zone
- Corrosion protection for tensile elements, anchorages, and couplings

PT system

1.2 Designation and range of anchorages and couplings

1.2.1 Designation

Anchorage and coupling are designated according to their function in the structure, by the nominal diameter of the prestressing steel strand, and the number of required prestressing steel strands with 6-n. The first number indicates the nominal diameter of prestressing steel strand (6 = 15.7 mm (0.62")), followed by the maximum number n of prestressing steel strands per anchorage or coupling. The available anchorages and couplings are shown in Annex 1.

1.2.2 Single anchorages SK6 and SF6 and couplings KS6-SK6 and K6-K6

1.2.2.1 General

With these anchorages and couplings only one single monostrand is anchored or coupled. If installed with additional reinforcement, the minimum centre and edge distances can be attained with these anchorages, see Annex 4.

1.2.2.2 Stressing anchor SK6

The stressing anchor SK6, see Annex 2, is fastened to the formwork on site and connected to the monostrand, see Annex 3. A PE-sleeve covers the transition from monostrand to anchorage and completes the corrosion protection. The stressing anchor can also be used as a fixed anchor. In that case, access is given to the fixed anchor during stressing.

The stressing anchor SK6 is designed to allow, after stressing, the anchor to be connected to the coupling head KS6 to form a fixed coupling, see Annex 5.

1.2.2.3 Fixed anchor SF6

The outward appearance of the fixed anchor SF6, see Annex 2, is identical to the stressing anchor SK6. In the factory, the fixed anchor is attached to the monostrand, which is cut to the required length. The wedges of the fixed anchor are secured by spring and protective cap, see Annex 3. A PE-sleeve covers the transition from monostrand to anchorage and completes the corrosion protection.

1.2.2.4 Fixed coupling KS6-SK6

This coupling allows the joining of a second tendon with an already stressed first tendon, see Annex 5. This is achieved by screwing coupling head KS6 with coupling sleeve S into the already stressed stressing anchor SK6. Subsequently, the monostrand is inserted into the self-acting anchorage of the coupling head KS6. A PE-sleeve covers the transition from monostrand to coupling head KS6 and completes the corrosion protection.

1.2.2.5 Movable coupling K6-K6

The movable coupling is used to join two monostrands, which subsequently are stressed at the same time, see Annex 6. The corrosion protection is completed by two overlapping PE-protective tubes, filled with corrosion protection filling material.

1.2.3 Multistrand anchorages MER6 and MEF6

1.2.3.1 Stressing anchor MER6

2 to 5 monostrands are anchored in one anchorage, with bore hole distances of 33 mm. A rectangular bearing plate is used, see Annex 7 and Annex 8, to which PE-transition tubes have already been attached in the factory. The bearing plate is fastened to the formwork on site and

connected to the monostrands. PE-transition tubes cover the transition from monostrands to anchorage and complete the corrosion protection. The stressing anchor can also be used as a fixed anchor. In that case, access is given to the fixed anchor during stressing.

1.2.3.2 Fixed anchor MEF6

In the factory, the anchor head is tack welded to the bearing plate and the PE-transition tubes are attached to the bearing plate, see Annex 7. The anchorage can be connected to the monostrands either in the factory or on site. PE-transition tubes cover the transition from monostrands to anchorage and complete the corrosion protection.

1.2.4 Centre and edge distances of anchorages, concrete cover

All centre and edge distances have been determined with regard to requirements on load-bearing capacity. Centre and edge distances of anchorages conform to the values specified in Annex 4 and Annex 8. However, the values specified in Annex 4 and Annex 8 for centre distance between anchorages may be reduced in one direction by 15 % but are not lower than the outside diameter of the helix. In case of a reduction of the distances in one direction, the centre and edge distances in the perpendicular direction are increased by the same percentage in order to keep an equal concrete area in the anchorage zone.

The concrete cover of tendons is neither smaller than 20 mm nor smaller than the concrete cover of reinforcement installed in the same cross section. The anchorage has a concrete cover of at least 20 mm. Standards and regulations on concrete cover in force at the place of use are observed.

1.2.5 Strength of concrete

Concrete according to EN 206 is used.

For stressing, the mean compressive strength of concrete is at least $f_{cm,0}$ as given in Annex 4 and Annex 8. The actual mean compressive strength, $f_{cm,0,cube}$ or $f_{cm,0,cyl}$, is verified by means of at least three specimens, cube of size 150 mm or cylinder with diameter of 150 mm and height of 300 mm, which are cured under the same conditions as the structure.

For partial prestressing with 30 % of the full prestressing force, the actual mean value of the concrete compressive strength is at least $0.5 \cdot f_{cm,0,cube}$ or $0.5 \cdot f_{cm,0,cyl}$. Intermediate values may be interpolated linearly according to Eurocode 2.

1.2.6 Reinforcement in the anchorage zone

In any case, steel grades and dimensions of helix and additional reinforcement specified in Annex 4 and Annex 8 are conformed to.

The centric position of the helix is secured by welding the end ring onto the bearing plate or by means of holding devices braced against the tendon.

If required for a specific project design, the reinforcement given in Annex 4 and Annex 8 may be modified in accordance with the respective regulations in force at the place of use as well as with the relevant approval of the local authority and of the ETA holder to provide equivalent performance.

1.3 Designation and range of tendons

1.3.1 Designation

The tendon is designated by the nominal diameter of the prestressing steel strand and the number of prestressing steel strands with 6-n. The first number indicates the nominal diameter of the prestressing steel strand $6 = 15.7 \text{ mm (0.62")}$, followed by the number "n" of prestressing steel strands.

1.3.2 Range of tendons

SUSPA/DSI – Unbonded Monostrand System with 1 to 5 Monostrands includes tendons with 1, 2, 3, 4, and 5 monostrands according to Clause 1.1 and Annex 11. The monostrands of each tendon are anchored in stressing and fixed anchors according to Clause 1.2.2 and 1.2.3.

Characteristic values of maximum force of the tendons are listed in Annex 11.

1.3.3 Maximum stressing forces

Prestressing and overstressing forces are specified in the respective standards and regulations in force at the place of use. Annex 10 lists the maximum prestressing and overstressing forces of the tendons according to Eurocode 2. I.e., the maximum prestressing force applied to a tendon does not exceed $0.90 \cdot A_p \cdot f_{p0.1k}$. Overstressing with up to $0.95 \cdot A_p \cdot f_{p0.1}$ is only permitted, if the force in the jack can be measured to an accuracy of $\pm 5\%$ of the final value of the overstressing force.

Initial prestressing force, P_{m0} , immediately after stressing and anchoring does not exceed the forces as specified in Eurocode 2.

Where

- A_p mm² Cross-sectional area of prestressing steel, i.e. $A_p = n \cdot S_0$
- $f_{p0.1}$N/mm²..... Characteristic 0.1 % proof stress of prestressing steel, i.e.
 $F_{p0.1} = f_{p0.1k} \cdot S_0$
- n — Number of prestressing steel strands, i.e. $n = 1$ to 5
- S_0 mm² Nominal cross-sectional area of one single prestressing steel strand, see Annex 11
- $F_{p0.1}$ kN..... Characteristic value of 0.1 % proof force, see Annex 11
- P_{m0} kN..... Initial prestressing force immediately after stressing and anchoring

1.4 Slip at anchorages

Slip at anchorages is taken into consideration in design and for determining tendon elongation. Table 2 specifies the slip values that are taken into consideration in calculations of tendon elongation and tendon force, as well as the required locking measures of wedges at anchorages and couplings that are passive during stressing.

Table 2 Slip values and wedge locking for anchorages and couplings

Anchorage, coupling	Slip	Wedge locking
—	mm	—
Stressing anchor ¹⁾ SK6	5	Protective cap
Stressing anchor ¹⁾ MER6	6	Locking plate
Fixed anchor SF6	5	Washer, compression spring, protective cap
Fixed anchor MEF6	5	Locking plate
Fixed coupling 2 nd tendon KS6-SK6	5	Washer, compression spring
Movable coupling K6-K6, total	10	Washer, compression spring

NOTE

¹⁾ Slip at transfer of prestressing force from jack to anchorage.

electronic copy

1.5 Friction losses

The tendon layout should not feature abrupt changes of the tendon axis, since this may lead to significant additional friction losses. For calculation of losses of prestressing forces due to friction, Coulomb's friction law applies. Due to the corrosion protection filling material within the PE-sheathing of monostrands, the friction coefficient μ is very low. Calculation of friction loss is by the equation

$$P_x = P_0 \cdot e^{-\mu \cdot (\alpha + k \cdot x)}$$

Where

- P_xkN.....Prestressing force at distance x from the stressing anchor along the tendon
- P_0kN.....Prestressing force at the distance x = 0 m
- μ rad⁻¹.....Friction coefficient, $\mu = 0.06 \text{ rad}^{-1}$
- α rad.....Sum of angular deviations over a distance x, irrespective of direction and sign
- k rad/m.....Wobble coefficient, $k = 0.9 \cdot 10^{-2} \text{ rad/m} (= 0.5 \text{ }^\circ/\text{m})$
- x m.....Distance along the tendon from the point where the prestressing force is equal to P_0

NOTE 1 rad = 1 m/m = 1

Friction losses in the anchorages are low and are not taken into consideration in design and execution.

1.6 Support of monostrands

Monostrands are installed with high accuracy and are secured in their position. Spacing of tendon support is.

- 1 Normally 1.00–1.30 m
 For radius of curvature in normal cases see Clause 1.7.
- 2 Free tendon layout, see Annex 9, in maximum 45 cm thick slabs
 In the transition zone between
 - a) high tendon position and anchorage (e.g. cantilever) 1.50 m
 - b) low and high tendon position or low tendon position and anchorage 3.00 m

At high and low tendon position, the tendons are connected in an appropriate way to the rebar mesh, at least at two points with a spacing of 0.3 m to 1.0 m. The rebar mesh is fixed in its position. Therefore, special spacers for tendons are not required. For details see Annex 9.

1.7 Radii of curvature of internal tendons

The minimum allowable radius of curvature for internal tendons with prestressing steel strands of nominal diameter of 15.7 mm is 2.5 m. If this radius is adhered to, verification of prestressing steel outer fibre stresses in curvatures is not required. The minimum allowable radius of curvature for deviation of a tendon with multistrand anchors in the anchorage zone outside PE-sleeve or PE-transition tube is 3.5 m.

Components

1.8 Monostrand

1.8.1 Specification of prestressing steel strand

7-wire prestressing steel strand with plain surfaces of the individual wires, a nominal diameter of 15.7 mm and tensile strengths of 1 770 N/mm² or 1 860 N/mm² is used. Dimensions and specifications of prestressing steel strand are according to prEN 10138-3 and are given in Clause 1.1, Table 1, and Annex 11.

1.8.2 Specification of monostrand

The monostrand is a 7-wire prestressing steel strand according to Clause 1.8.1, factory provided with a corrosion protection system comprising corrosion protection filling material and PE-sheathing, see Table 3.

Within one structure, prestressing steel strands with one characteristic tensile strength should be used. If tendons with prestressing steel strands of different tensile strengths are to be installed, appropriate measures to prevent confusion are implemented.

In the course of preparing the European Technical Assessment, no characteristic has been assessed for the monostrand. In execution, a suitable monostrand that conforms to Annex 11 and is according to the standards and regulations in force at the place of use is taken.

Table 3 Monostrand

7-wire prestressing steel strand	—	Y1770S7 ¹⁾	Y1860S7 ¹⁾
Nominal diameter	mm	15.7 ²⁾	15.7 ²⁾
Nominal cross-sectional area	mm ²	150	150
Characteristic tensile strength	N/mm ²	1 770	1 860
Mass of prestressing steel	kg/m	1.17	1.17
Monostrand			
External diameter of monostrand	mm	≥ 20	≥ 20
Mass of monostrand	kg/m	1.30	1.30

¹⁾ Designation according to prEN 10138-3

²⁾ Corresponding to 0.62 inches

1.9 Anchorage components

1.9.1 General

Specification of anchorage components are given in the Annexes and the technical file³ of the European Technical Assessment. Therein the components' dimensions, materials, and material identification data with tolerances are specified.

For prestressing steel strands with nominal tensile strength of 1 860 N/mm² as well as 1 770 N/mm² the same anchorages and couplings are used.

1.9.2 Anchor and coupling heads

The exits of the conical bores of anchor and coupling heads are countersunk and deburred. For installation, they are clean, free from rust, and provided with corrosion protection oil.

³ The technical file of the European Technical Assessment is deposited at Österreichisches Institut für Bautechnik.

1.9.3 Wedges

Only wedges as specified in Annex 2 are used. The wedges feature an annular groove.

1.9.4 Helix

Steel grades and dimensions of helixes conform to the values specified in Annex 8 and Annex 12.

In general, both ends of each helix are welded to closed rings. Welding of one end, the inner end, may be omitted. Details on welding of helix are given in Annex 8.

1.10 Permanent corrosion protection

In the course of preparing the European Technical Assessment, no characteristic has been assessed for components and materials of the corrosion protection system. In execution, all components and materials are selected according to the standards and regulations in force at the place of use.

The prestressing steel strand is provided in the factory with corrosion protection comprising corrosion protection filling material and extruded PE-sheathing – monostrand. Application of corrosion protection in the anchorage zone is described in the assembly instructions in Clause 2.2.4. The void in the anchorage zone is completely filled with a corrosion protection filling material.

If PE-protective tubes with a length of more than 1.5 m are installed with the movable couplings K6-K6, handling tests for injection of the corrosion protection filling material are performed prior to injection.

1.11 Material specifications of the components

Material specifications of the components are given in Annex 12.

2 Specification of the intended use in accordance with the applicable European Assessment Document (hereinafter EAD)

2.1 Intended use

The PT system SUSPA/DSI – Unbonded Monostrand System with 1 to 5 Monostrands is intended to be used for the prestressing of structures. The use category according to tendon configuration and material of structure is

- Internal unbonded tendon for concrete and composite structures

2.2 Assumptions

2.2.1 General

Concerning product packaging, transport, storage, maintenance, replacement, and repair it is the responsibility of the manufacturer to undertake the appropriate measures and to advise his clients on transport, storage, maintenance, replacement, and repair of the product as he considers necessary.

2.2.2 Packaging, transport and storage

Tendons and anchorages may be assembled on site or at the factory, i.e. pre-assembled tendons. During transport, the tendons may be wound to a coil with a minimum internal diameter of 1.5 m or as specified by the manufacturer of the monostrand.

Advice on packaging, transport, and storage includes

- Temporary protection of prestressing steels and components in order to prevent corrosion during transportation from the production site to the job site.

- Transportation, storage, and handling of prestressing steel and other components in a manner as to avoid damage by mechanical or chemical impact.
- Protection of tensile elements and other components from moisture.
- Keeping tensile elements away from zones where welding operations are performed.

2.2.3 Design

Advice on design includes

- Design of the structure permits correct installation and stressing of tendon and design and reinforcement of the anchorage zone permits correct placing and compacting of concrete.
- Verification of transfer of stressing forces to the structural concrete is not required, if centre and edge distances of the tendons, strength of concrete, as well as grade and dimensions of helix and additional reinforcement, see Clause 1.2.4, Clause 1.2.5, Clause 1.2.6, Annex 4, and Annex 8 are conformed to. The forces outside the area of helix and additional reinforcement are verified and, if necessary, covered by appropriate, in general transverse reinforcement. The reinforcement of the structure is not employed as additional reinforcement. Reinforcement exceeding the required reinforcement of the structure may be used as additional reinforcement if appropriate placing is possible.
- The anchorage recess is designed as to ensure a concrete cover of at least 25 mm at the caps in the final stage.
- Bursting out of prestressing steels in case of failure is prevented. Sufficient protection is provided by e.g. a cover of reinforced concrete.
- The initial stressing force applied to the stressing anchor will decrease especially as a result of slip, see Clause 1.4, friction along the tendon, see Clause 1.5, and of the elastic shortening of the structure, and in the course of time because of relaxation of the prestressing steel, and creep and shrinkage of concrete. The stressing instructions prepared by the ETA holder should be consulted.
- Under all possible load combinations, the stressing force at the 2nd construction stage of the fixed coupler is at no time higher than at the 1st construction stage, neither during construction nor in the final stage.
- The length of the PE-protective tube and its position relative to the coupler ensures unimpeded movement of the coupler in the PE-protective tube along a length of minimum $1.15 \cdot \Delta l + 30$ mm, where Δl in mm as the expected displacement of the coupler during stressing.

2.2.4 Installation

2.2.4.1 General

It is assumed that the product will be installed according to the manufacturer's instructions or – in absence of such instructions – according to the usual practice of the building professionals.

Assembly and installation of tendons are only carried out by qualified PT specialist companies with the required resources and experience in the use of the SUSPA/DSI – Unbonded Monostrand System with 1 to 5 Monostrands, see CWA 14646. The company's PT site manager has a certificate, stating that she or he has been trained by the ETA holder and that she or he possesses the necessary qualification and experience with the SUSPA/DSI – Unbonded Monostrand System with 1 to 5 Monostrands.

The centric position of the additional reinforcement is secured by tying or by means of spacers braced against the tendon.

2.2.4.2 De-sheathing of monostrands

The length of the PE-sleeves, see Annex 2, and the tube connections of the PE-protective tubes, see Annex 6, as well as the length along which the monostrand sheathing is removed are

determined by the PT specialist company depending on the expected variations in temperature between installation and concreting. The monostrand sheathing overlaps the PE-sleeve, the tube connections of the PE-protective tubes, or the PE-transition tube by at least 150 mm and does not press against the anchorage. This is checked by application of markings before concreting.

2.2.4.3 Examination of tendons and possible repairs of the corrosion protection system

During installation careful handling of tendons is ensured. Before concreting the PT site manager carries out a final examination of the installed tendons. Damages to PE-sheathings, which cause or may cause leaking of corrosion protection filling material, are repaired. Repair is in accordance with the respective load requirements and suitable for operating temperatures up to 30 °C.

The fixed anchor MEF6, see Annex 7, is only installed if all tack welding seams between the bearing plate and anchor head are intact, ensuring a safe and joint free connection between bearing plate and anchor head.

2.2.4.4 Stressing anchor SK6

The stressing anchor SK6 is designed that, after stressing, it can be connected to the coupling head KS6 to form a fixed coupling, see Annex 5.

The anchor SK6 is fastened to the formwork on site and connected to the monostrand. It can also be used as a fixed anchor. In that case, access is given to the fixed anchor during stressing.

Site assembly comprises the following working steps, see Annex 3.

- Fastening the cast-iron anchor using the sealing washer and installation spindle that is pushed through the hole in the formwork.
- Placing PE-sleeve and sealing sleeve onto the monostrand.
- Placing the monostrand against the anchorage to mark the cutting point on the PE-sheathing.
- Cutting and pulling off the PE-sheathing in the anchorage zone of the prestressing steel strand.
- Inserting the monostrand through the cast-iron anchor.
- Filling corrosion protection filling material into the expanded section of the PE-sleeve and screwing the PE-sleeve onto the cast-iron anchor.
- Sealing the transition zone PE-sleeve to monostrand with the sealing sleeve. The two parts overlap by at least 3 cm.

Alternatively, the transition zone PE-sleeve to monostrand may be sealed by means of an adhesive tape with an overlap of at least 5 cm.

- Place the previously removed PE sheathing onto the prestressing steel strand ends in order to protect the prestressing steel strand protrusions.

2.2.4.5 Fixed anchor SF6

As a rule, this anchorage is factory-assembled. Factory assembly comprises the following working steps.

- Filling a sufficient quantity of corrosion protection filling material into the expanded section of the PE-sleeve.
- Screwing PE-sleeve and sealing sleeve onto the cast-iron anchor.
- Placing the wedge into the conical bore.
- Mounting compression spring and washer.¹⁵⁴

- Filling in a measured quantity of corrosion protection filling material.
- Screwing on the protective cap.
- Removing a 5 to 6 cm long piece of the PE-sheathing from the monostrand.
- Applying a marking on the sheathing of the monostrand.
- Inserting the de-sheathed monostrand through the PE-sleeve until it pushes against the protective cap of the cast-iron anchor.
- Checking the insertion depth by means of the marking on the monostrand sheathing.
- Wiping off corrosion protection filling material that has leaked from the PE-sleeve.
- Sealing the transition zone PE-sleeve to monostrand with the sealing sleeve. The two parts overlap by at least 3 cm.
Alternatively, the transition zone PE-sleeve to monostrand may be sealed by means of an adhesive tape with an overlap of at least 5 cm.
- Cut the monostrand from the coil.

2.2.4.6 Fixed coupling KS6-SK6

Fixed coupling is used for joining non-stressed tendon to already stressed tendon by means of a factory-prepared coupling head KS6, see Annex 5.

Site assembly comprises the following working steps.

- Removing the protective cap from the stressing anchor SK6.
- Removing the PE-cap and the PE-plug from the coupling head KS6 and screwing the coupling head KS6 into the internal thread of the stressing anchor SK6.
- Fill a sufficient quantity of corrosion protection filling material into the expanded section of the PE-sleeve.
- Pushing PE-sleeve and sealing sleeve onto the monostrand.
- Removing approximately 12 cm of the monostrand PE-sheathing.
- Apply a coloured marking on the monostrand.
- Placing the de-sheathed prestressing steel strand into the coupling head KS6. The wedge pushed forwards by the compression spring secure the position of the monostrands.
- Check the insertion depth by means of the coloured marking.
- Sealing the transition zone PE-sleeve to monostrand by the sealing sleeve. The two parts overlap by at least 3 cm.
Alternatively, the transition zone PE-sleeve to monostrand may be sealed by means of an adhesive tape with an overlap of at least 5 cm.

2.2.4.7 Movable coupling K6-K6

The movable coupling is used for joining two tendons that are subsequently stressed at the same time, see Annex 6.

Site assembly comprises the following working steps.

Tendon № 1

- Removing approximately 12 cm of the monostrand PE-sheathing.
- Applying a coloured marking on the monostrand.
- Placing PE-protective tube section 1 and sealing sleeve onto the monostrand.
- Filling a sufficient quantity of corrosion protection filling material into the expanded section of the PE-protective tube section 1.

Tendon № 2

- Removing the PE-sheathing of the monostrand along a length equal to that of the PE-protective tube minus 10 cm.
- Applying a coloured marking on the monostrand.
- Placing the PE-protective tube section 2 with the sealing sleeve onto the monostrand.

Coupling

- Removing the PE-protective caps from the prefabricated coupling filled with corrosion protection filling material.
- Placing the coupling onto the de-sheathed prestressing steel strand of tendon № 1 up to the steel locking pin.
- Inserting the de-sheathed prestressing steel strand of tendon № 2 into the coupling up to the steel locking pin.
- Check the insertion depth of the monostrands by means of the coloured marking on both sides of the coupling.

Corrosion protection

- Push forward the PE-protective tube over the coupling and ensure corrosion protection filling material leaks out between PE-protective tube and PE-sheathing of the monostrand of tendon №. 1.
- Press the securing pin into the PE-protective tube section 1 to secure the position of the coupling.
- Push forward the PE-protective tube section 2 to approximately 2 cm before the end of the expanded section of the PE-protective tube section 1.
- Sealing the transition zone of PE-protective tube section 2 to tendon № 2 with the sealing sleeve with an overlap of at least 3 cm.

Alternatively, the transition zone PE-protective tube to monostrand may be sealed by means of an adhesive tape with an overlap of at least 5 cm.

- Inject corrosion protection filling material through the injection nipple of the PE-protective tube section 2 until the corrosion protection filling material begins to spill out at the annular gap between PE-protective tube section 1 and PE-protective tube section 2.
- Clean the PE-components from the excess corrosion protection filling material.
- Sealing the transition zone PE-protective tube section 1 to PE-protective tube section 2 with adhesive tape and sealing of the transition zone PE-protective tube section 1 to tendon № 1 with the sealing sleeve with an overlap of at least 3 cm.

Alternatively, the transition zone PE-protective tube to monostrand may be sealed by means of an adhesive tape with an overlap of at least 5 cm.

2.2.4.8 Stressing anchor MER6

2 to 5 monostrands are anchored in one anchorage. Rectangular bearing plates are used, see Annex 7 and Annex 8, which have already been provided with PE-transition tubes in the factory. The bearing plate is fastened to the formwork on site and connected to the monostrands. The stressing anchor can also be used as a fixed anchor. In that case, access is given to the fixed anchor during stressing.

Site assembly comprises the following working steps.

- Fastening the bearing plate to the formwork with screws.
- Placing the monostrands against the anchor to mark the cutting point on the PE-sheathings.
- Cutting the PE-sheathings.

- Inserting the wedges into the conical bore of the stressing anchor.
- Stressing with prestressing jack.
- Measure tendon elongation during stressing.
- Cutting off the prestressing steel strand protrusion with a cutting disk or cutting tool.
- Screwing on the cap filled with corrosion protection filling material.
- Filling the anchorage recess with concrete.

2.2.4.11.3 Restressing

Restressing of tendons before final cutting of prestressing steel strand protrusions in combination with release and reuse of wedges is permitted. After restressing, the wedges bite into a least 15 mm of virgin prestressing steel strand surface and no wedge marks remain on the tendon between the anchorages.

2.2.4.11.4 Stressing records

All stressing operations are recorded for each tendon. Primarily, stressing is performed up to the required force. For control, the elongation is measured and compared with the prior calculated value.

2.2.4.11.5 Stressing equipment, clearance requirements, and safety-at-work

For stressing, hydraulic jacks are used. Information about the stressing equipment has been submitted to Österreichisches Institut für Bautechnik.

Stressing of single and multistrand anchorages requires approximately 1 m of free space directly behind the anchorages. The ETA holder keeps available more detailed information on the jacks used and the required space for handling and stressing.

The safety-at-work and health protection regulations are observed.

2.2.4.12 Welding at anchorages

Welding is not permitted at anchorages, except welding the end turns of the helix and welding the helix and tack welding the anchor head onto the bearing plate.

In case of welding operations near tendons, precautionary measures are required to avoid damage to the corrosion protection system.

2.3 Assumed working life

The European Technical Assessment is based on an assumed working life of SUSPA/DSI – Unbonded Monostrand System with 1 to 5 Monostrands of 100 years, provided that SUSPA/DSI – Unbonded Monostrand System with 1 to 5 Monostrands is subject to appropriate installation, use, and maintenance, see Clause 2.2.

In normal use conditions, the real working life may be considerably longer without major degradation affecting the basic requirements for construction works⁴.

The indications given as to the working life of the construction product cannot be interpreted as a guarantee, neither given by the product manufacturer or his representative nor by EOTA nor by the Technical Assessment Body, but are regarded only as a means for expressing the expected economically reasonable working life of the product.

⁴ The real working life of a product incorporated in a specific works depends on the environmental conditions to which that works are subject, as well as on the particular conditions of design, execution, use, and maintenance of that works. Therefore, it cannot be excluded that in certain cases the real working life of the product may also be shorter than the assumed working life.

3 Performance of the product and references to the methods used for its assessment

3.1 Essential characteristics

The performances of SUSPA/DSI – Unbonded Monostrand System with 1 to 5 Monostrands for the essential characteristics are given in Table 4.

Table 4 Essential characteristics and performances of the product

No	Essential characteristic	Product performance
Basic requirement for construction works 1: Mechanical resistance and stability		
1	Resistance to static load	See Clause 3.2.1.1.
2	Resistance to fatigue	See Clause 3.2.1.2.
3	Load transfer to the structure	See Clause 3.2.1.3.
4	Friction coefficient	See Clause 3.2.1.4.
5	Deviation, deflection (limits) for internal bonded and unbonded tendon	See Clause 3.2.1.5.
6	Assessment of assembly	See Clause 3.2.1.6.
7	Corrosion protection	See Clause 3.2.1.7.
Basic requirement for construction works 2: Safety in case of fire		
8	Reaction to fire	See Clause 3.2.2.1.
Basic requirement for construction works 3: Hygiene, health, and the environment		
9	Content, emission, and/or release of dangerous substances	See Clause 3.2.3.1.
Basic requirement for construction works 4: Safety and accessibility in use		
—	Not relevant. No characteristic assessed.	—
Basic requirement for construction works 5: Protection against noise		
—	Not relevant. No characteristic assessed.	—
Basic requirement for construction works 6: Energy economy and heat retention		
—	Not relevant. No characteristic assessed.	—
Basic requirement for construction works 7: Sustainable use of natural resources		
—	No characteristic assessed.	—

3.2 Product performance

3.2.1 Mechanical resistance and stability

3.2.1.1 Resistance to static load

The PT system as described in the ETA meets the acceptance criteria of EAD 160004-00-0301, Clause 2.2.1. The characteristic values of maximum force, F_{pk} , of the tendon with prestressing steel strands according to Annex 11 are listed in Annex 11.

3.2.1.2 Resistance to fatigue

The PT system as described in the ETA meets the acceptance criteria of EAD 160004-00-0301, Clause 2.2.2. The characteristic values of maximum force, F_{pk} , of the tendon with prestressing steel strands according to Annex 11 are listed in Annex 11.

Fatigue resistance of anchorages and couplings was tested and verified with an upper force of $0.65 \cdot F_{pk}$, a fatigue stress range of 80 N/mm^2 and $2 \cdot 10^6$ load cycles.

3.2.1.3 Load transfer to the structure

The PT system as described in the ETA meets the acceptance criteria of EAD 160004-00-0301, Clause 2.2.3. The characteristic values of maximum force, F_{pk} , of the tendon with prestressing steel strands according to Annex 11 are listed in Annex 11.

Conformity with the stabilisation and crack width criteria specified for the load transfer test was verified to a force level of $0.80 \cdot F_{pk}$.

3.2.1.4 Friction coefficient

For friction losses including friction coefficient see Clause 1.5.

3.2.1.5 Deviation, deflection (limits) for internal bonded and unbonded tendon

For minimum radii of curvature see Clause 1.7.

3.2.1.6 Assessment of assembly

The PT system as described in the ETA meets the acceptance criteria of EAD 160004-00-0301, Clause 2.2.7.

3.2.1.7 Corrosion protection

The PT system as described in the ETA meets the acceptance criteria of EAD 160004-00-0301, Clause 2.2.13.

3.2.2 Safety in case of fire

3.2.2.1 Reaction to fire

The performance of components made of steel or cast iron is Class A1 without testing.

The performance of components of other materials has not been assessed.

3.2.3 Hygiene, health, and the environment

3.2.3.1 Content, emission and/or release of dangerous substances

According to the manufacturer's declaration, the PT system does not contain dangerous substances.

– SVOC and VOC

The performance of components made of steel or cast iron that are free of coating with organic material is no emission of SVOC and VOC.

The performance of components of other materials has not been assessed.

– Leachable substances

The product is not intended to be in direct contact to soil, ground water, and surface water.

3.3 Assessment methods

The assessment of the essential characteristics in Clause 3.1 of SUSPA/DSI – Unbonded Monostrand System with 1 to 5 Monostrands, for the intended use, and in relation to the requirements for mechanical resistance and stability, safety in case of fire, and for hygiene, health, and the environment, in the sense of the basic requirements for construction works № 1, 2, and 3 of Regulation (EU) № 305/2011, has been made in accordance with Annex A of EAD 160004-00-0301, Post-tensioning kits for prestressing of structures, for Item 2, Internal unbonded tendon.

3.4 Identification

The European Technical Assessment for SUSPA/DSI – Unbonded Monostrand System with 1 to 5 Monostrands is issued on the basis of agreed data that identify the assessed product⁵. Changes to materials, to composition, or to characteristics of the product, or to the production process could result in these deposited data being incorrect. Österreichisches Institut für Bautechnik should be notified before the changes are introduced, as an amendment of the European Technical Assessment is possibly necessary.

4 Assessment and verification of constancy of performance (hereinafter AVCP) system applied, with reference to its legal base

4.1 System of assessment and verification of constancy of performance

According to Commission Decision 98/456/EC, the system of assessment and verification of constancy of performance to be applied to SUSPA/DSI – Unbonded Monostrand System with 1 to 5 Monostrands is System 1+. System 1+ is detailed in Commission Delegated Regulation (EU) № 568/2014 of 18 February 2014, Annex, point 1.1., and provides for the following items.

- (a) The manufacturer shall carry out
 - (i) factory production control;
 - (ii) further testing of samples taken at the manufacturing plant by the manufacturer in accordance with the prescribed test plan⁶.
- (b) The notified product certification body shall decide on the issuing, restriction, suspension or withdrawal of the certificate of constancy of performance of the construction product on the basis of the outcome of the following assessments and verifications carried out by that body
 - (i) an assessment of the performance of the construction product carried out on the basis of testing (including sampling), calculation, tabulated values or descriptive documentation of the product;
 - (ii) initial inspection of the manufacturing plant and of factory production control;
 - (iii) continuing surveillance, assessment, and evaluation of factory production control;
 - (iv) audit-testing of samples taken by the notified product certification body at the manufacturing plant or at the manufacturer's storage facilities.

⁵ The technical file of the European Technical Assessment is deposited at Österreichisches Institut für Bautechnik.

⁶ The prescribed test plan has been deposited with Österreichisches Institut für Bautechnik and is handed over only to the notified product certification body involved in the procedure for the assessment and verification of constancy of performance. The prescribed test plan is also referred to as control plan.

5.1.2 Declaration of performance

The manufacturer is responsible for preparing the declaration of performance. When all the criteria of the assessment and verification of constancy of performance are met, including the certificate of constancy of performance issued by the notified product certification body, the manufacturer draws up the declaration of performance. Essential characteristics to be included in the declaration of performance for the corresponding intended use are given in Table 4.

5.2 Tasks for the notified product certification body

5.2.1 Initial inspection of the manufacturing plant and of factory production control

The notified product certification body establishes that, in accordance with the prescribed test plan, the manufacturing plant, in particular personnel and equipment, and the factory production control are suitable to ensure a continuous manufacturing of the PT system according to the given technical specifications. For the most important activities, EAD 160004-00-0301, Table 4 summarises the minimum procedure.

5.2.2 Continuing surveillance, assessment and evaluation of factory production control

The activities are conducted by the notified product certification body and include surveillance inspections. The kit manufacturer is inspected at least once a year. Factory production control is inspected, and samples are taken for independent single tensile element tests.

For the most important activities, the control plan according to EAD 160004-00-0301, Table 4 summarises the minimum procedure. It is verified that the system of factory production control and the specified manufacturing process are maintained, taking account of the control plan.

Each manufacturer of the components given in Annex 14 is audited at least once in five years. It is verified that the system of factory production control and the specified manufacturing process are maintained, taking account of the prescribed test plan.

The results of continuous surveillance are made available on request by the notified product certification body to Österreichisches Institut für Bautechnik. When the provisions of the European Technical Assessment and the prescribed test plan are no longer fulfilled, the certificate of constancy of performance is withdrawn by the notified product certification body.

5.2.3 Audit-testing of samples taken by the notified product certification body at the manufacturing plant or at the manufacturer's storage facilities

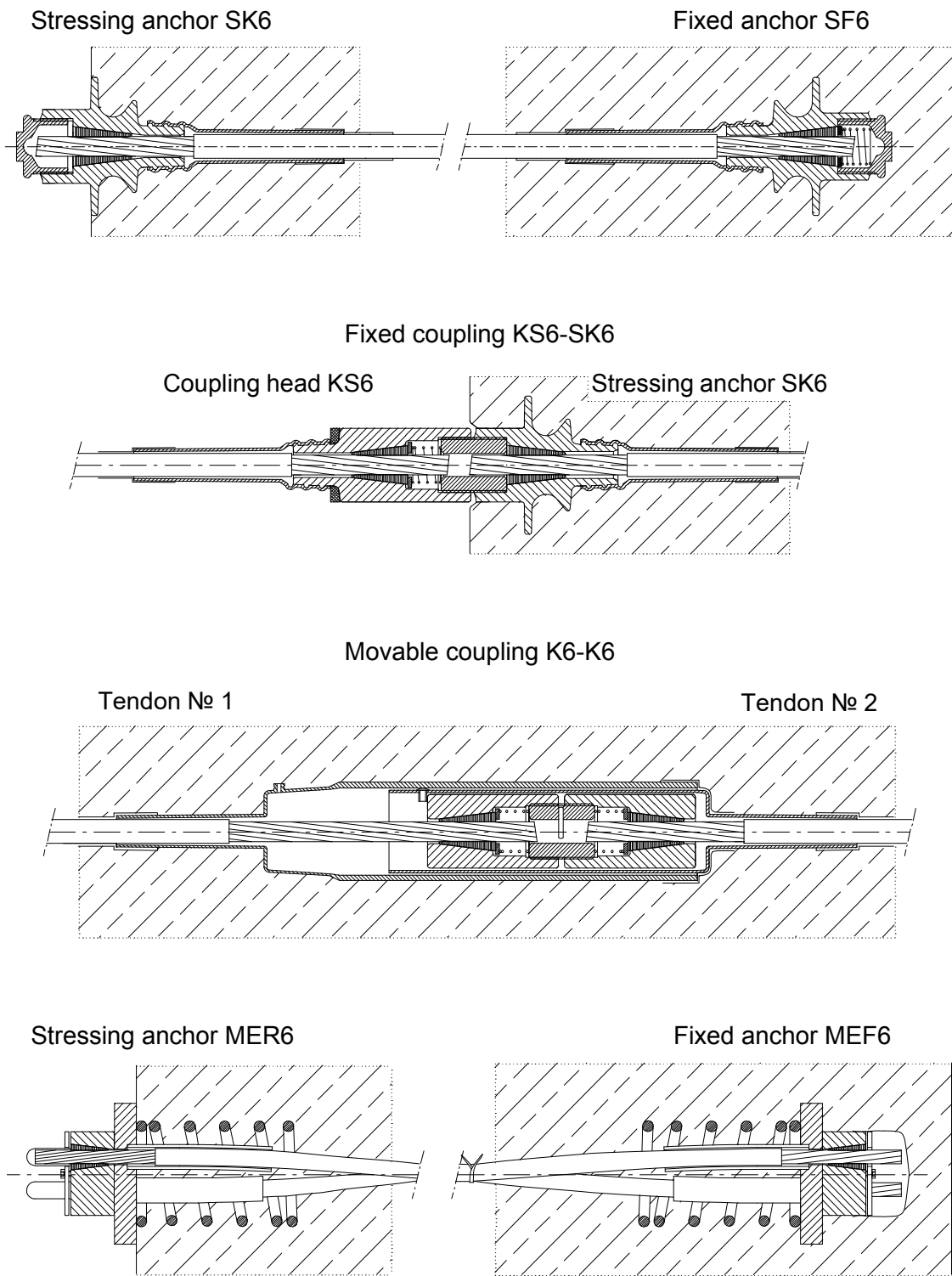
During surveillance inspection, the notified product certification body takes samples of components of the PT system for independent testing. Audit-testing is conducted at least once a year by the notified product certification body. For the most important components, Annex 14 summarises the minimum procedures. Annex 14 conforms to EAD 160004-00-0301, Table 4. In particular, at least once a year, the notified product certification body also carries out one single tensile element test series according to EAD 160004-00-0301, Annex C.7 and Clause 3.3.4 on specimens taken from the manufacturing plant or at the manufacturer's storage facility.

Issued in Vienna on 29 January 2021
by Österreichisches Institut für Bautechnik

The original document is signed by

Rainer Mikulits
Managing Director

electronic copy

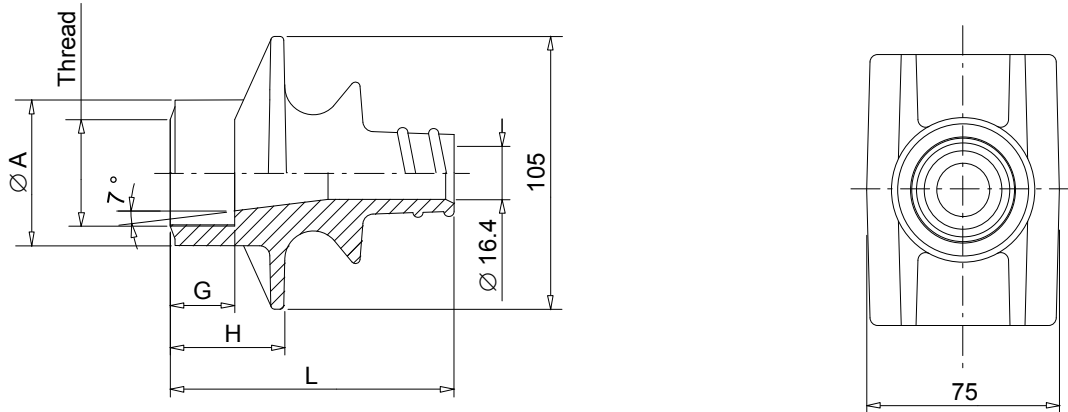


DYWIDAG 
 DYWIDAG-Systems International GmbH
 Phone: +49/89/309050-100
 E-Mail: dsihv@dywidag-systems.com

SUSPA/DSI
Unbonded Monostrand System
 164
 Anchorages and couplings – Overview

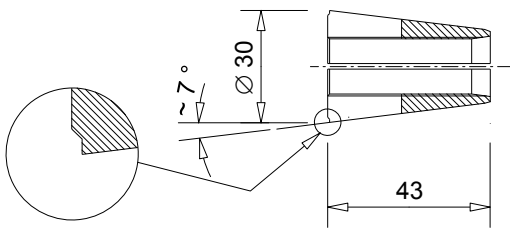
Annex 1
 of European Technical Assessment
ETA-03/0036 of 29.01.2021

Cast iron anchor SK6 and SF6



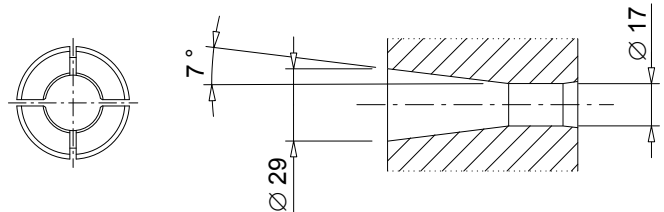
Anchor	Ø A	G	H	L
—	mm	mm	mm	mm
SK6	56	25	45	110
SF6	51	10	30	95

Wedge

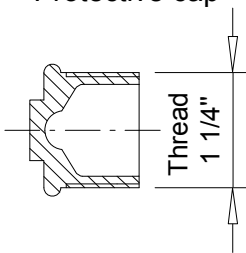


Wedges for prestressing steel strands with nominal diameter 15.7 mm feature an annular groove on the front face.

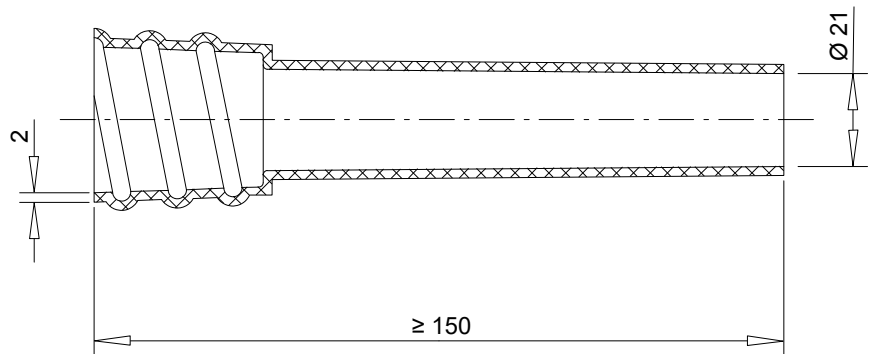
Hole geometry



Protective cap



PE-sleeve



Dimensions in mm



DYWIDAG-Systems International GmbH
 Phone: +49/89/309050-100
 E-Mail: dsihv@dywidag-systems.com

SUSPA/DSI
 Unbonded Monostrand System

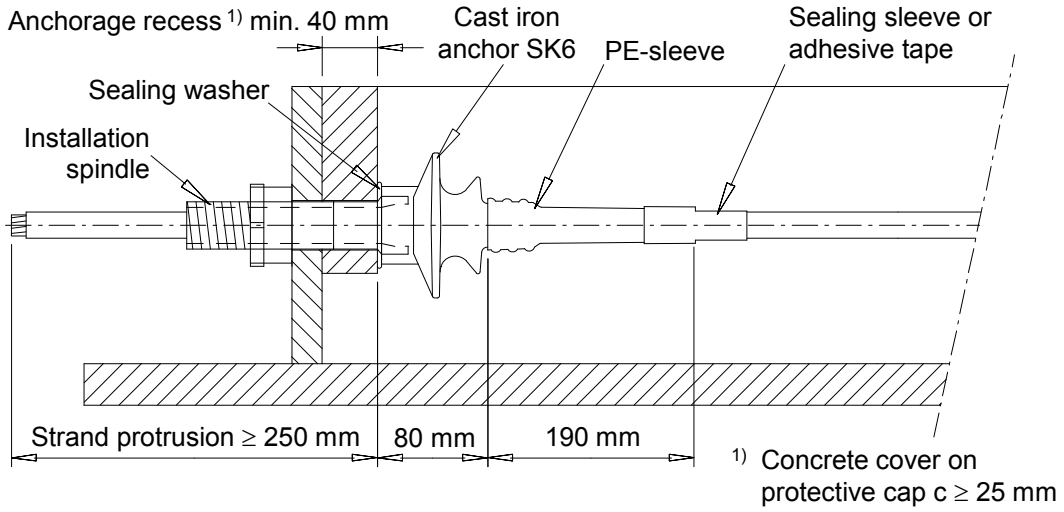
Basic components of anchorages
 Cast-iron anchors SK6 and SF6

Annex 2

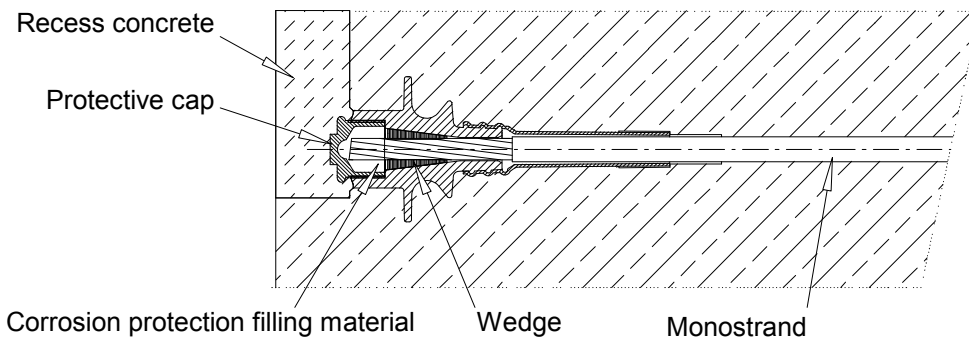
of European Technical Assessment
ETA-03/0036 of 29.01.2021

electronic copy electronic copy electronic copy electronic copy electronic copy electronic copy electronic copy electronic copy electronic copy electronic copy

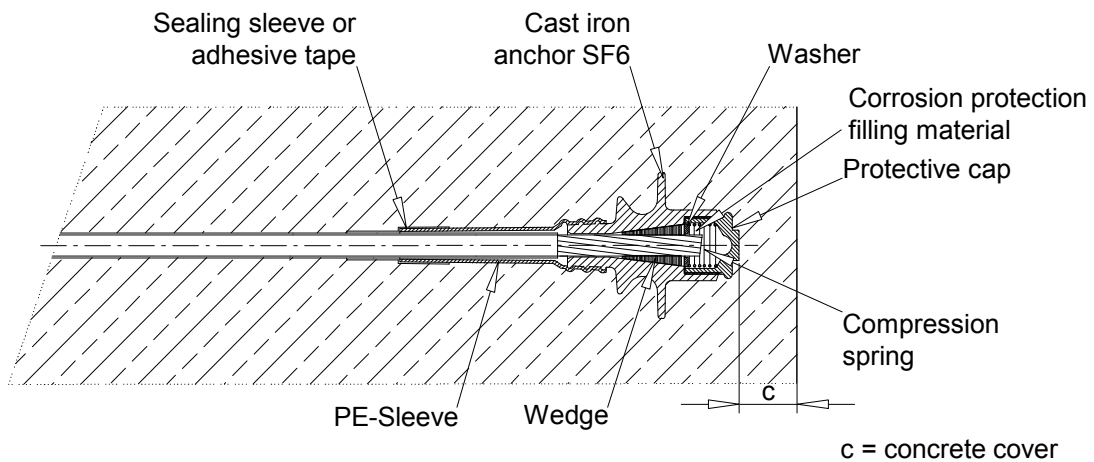
Assembly state of stressing anchor SK6



Stressing anchor SK6, final state



Fixed anchor SF6, final state



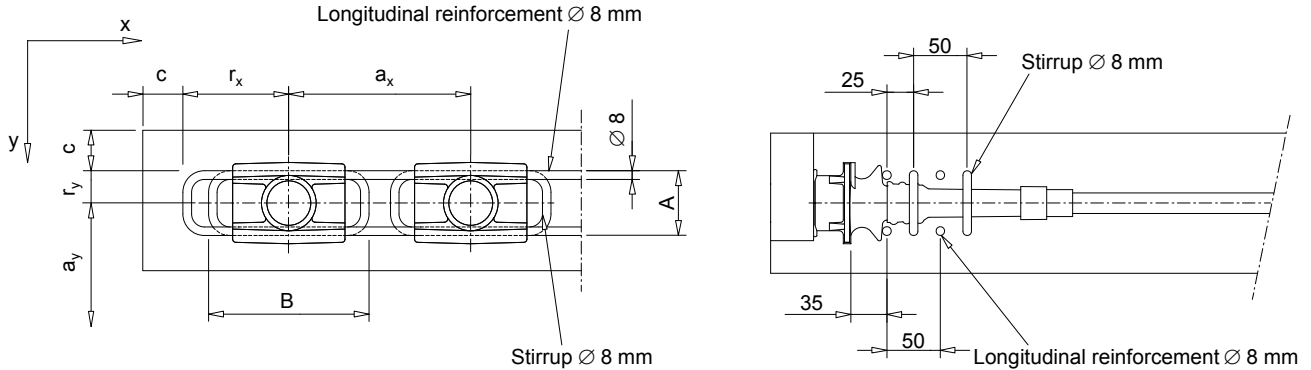
DYWIDAG 
 DYWIDAG-Systems International GmbH
 Phone: +49/89/309050-100
 E-Mail: dsihv@dywidag-systems.com

SUSPA/DSI
Unbonded Monostrand System
 Stressing anchor SK6 and
 fixed anchor SF6

Annex 3
 of European Technical Assessment
ETA-03/0036 of 29.01.2021

**Stressing anchor SK6 and fixed anchor SF6
 Minimum centre and edge distances**

With additional reinforcement



a_x } Minimum centre distance
 a_y }
 $r_x + c$ } Minimum edge distance
 $r_y + c$ }
 c Concrete cover

Concrete strength at time of stressing	$f_{cm, 0, cube 150}$	20 N/mm ²	28 N/mm ²	36 N/mm ²
	$f_{cm, 0, cyl}$	16 N/mm ²	23 N/mm ²	29 N/mm ²
Minimum centre distance	a_x	210	190	170
	a_y	120	105	90
Minimum edge distance, plus c	r_x	120	110	100
	r_y	50	45	35
Additional reinforcement	$R_e \geq 500 \text{ N/mm}^2$			
Number of longitudinal reinforcement	$\varnothing 8 \text{ mm per side}$	2	2	2
Number of stirrups	$\varnothing 8 \text{ mm}$	2	2	1
	Length min. A	100	85	70
	Width min. B	190	170	150

Without additional reinforcement

Concrete strength at time of stressing	$f_{cm, 0, cube 150}$	20 N/mm ²	28 N/mm ²	36 N/mm ²
	$f_{cm, 0, cyl}$	16 N/mm ²	23 N/mm ²	29 N/mm ²
Minimum centre distance	a_x	260	240	220
	a_y	170	150	130
Minimum edge distance, plus c ¹⁾	r_x	120	110	100
	r_y	75	65	55

¹⁾ c as concrete cover of reinforcement in the same cross section, at least 20 mm

Dimensions in mm

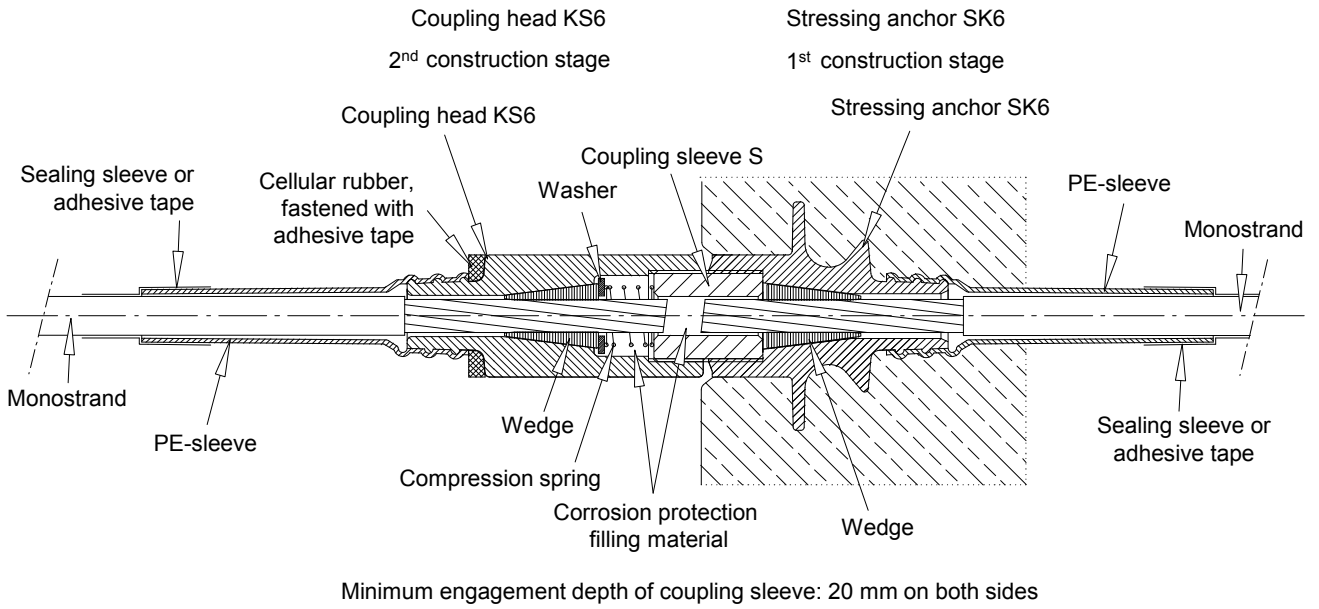
DYWIDAG-Systems International GmbH
 Phone: +49/89/309050-100
 E-Mail: dsihv@dywidag-systems.com

SUSPA/DSI
Unbonded Monostrand System
 Stressing anchor SK6 and
 fixed anchor SF6
 Minimum centre and edge distances

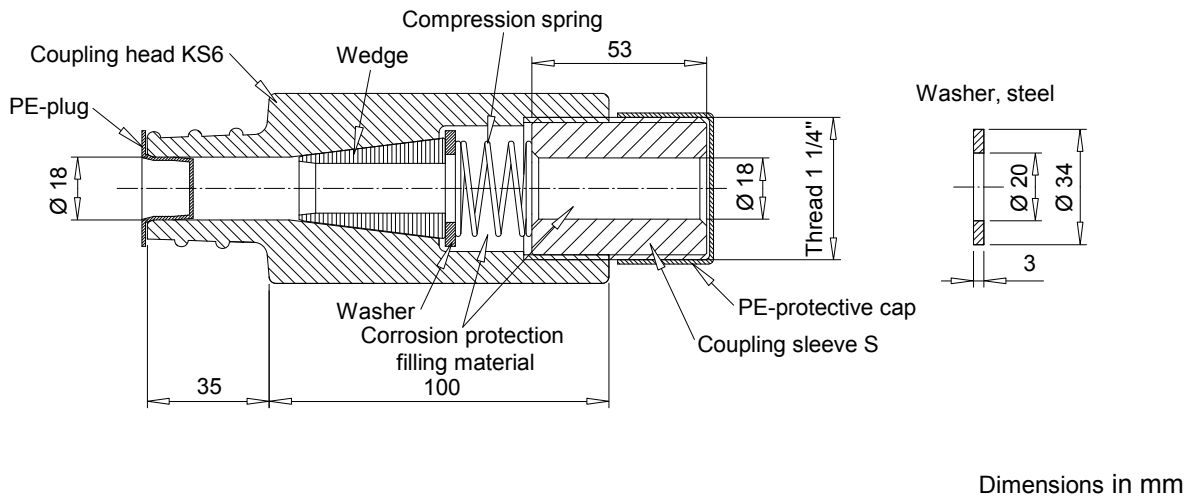
Annex 4
 of European Technical Assessment
ETA-03/0036 of 29.01.2021

electronic copy electronic copy electronic copy electronic copy electronic copy electronic copy electronic copy electronic copy electronic copy electronic copy

Fixed coupling KS6-SK6



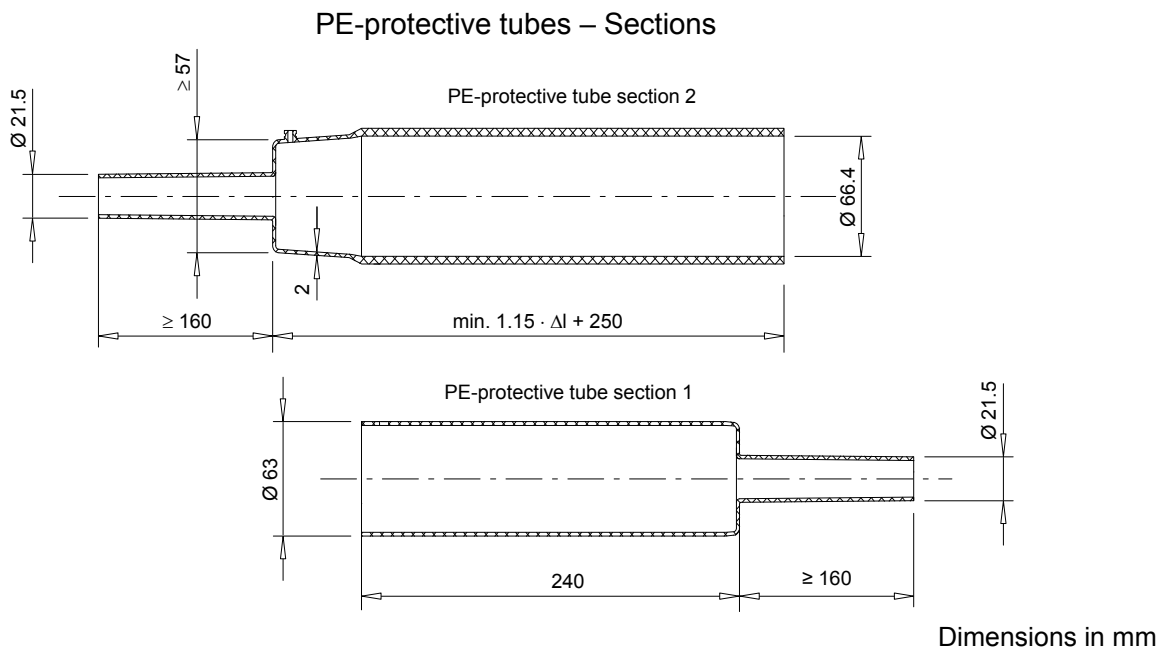
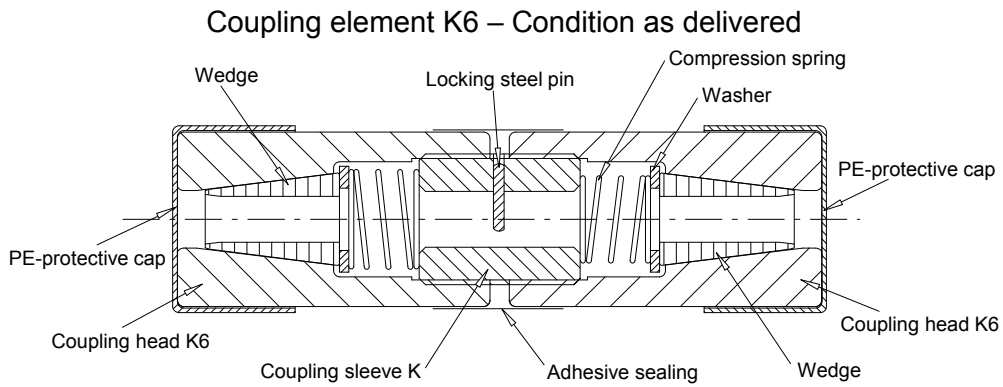
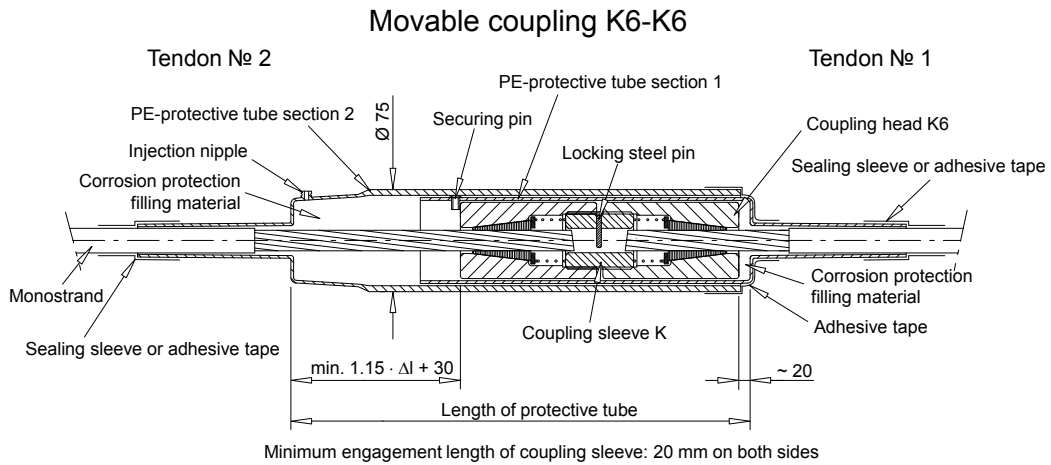
Coupling element KS6 – Condition as delivered



DYWIDAG
 DYWIDAG-Systems International GmbH
 Phone: +49/89/309050-100
 E-Mail: dsihv@dywidag-systems.com

SUSPA/DSI
Unbonded Monostrand System
 Fixed coupling KS6-SK6

Annex 5
 of European Technical Assessment
ETA-03/0036 of 29.01.2021



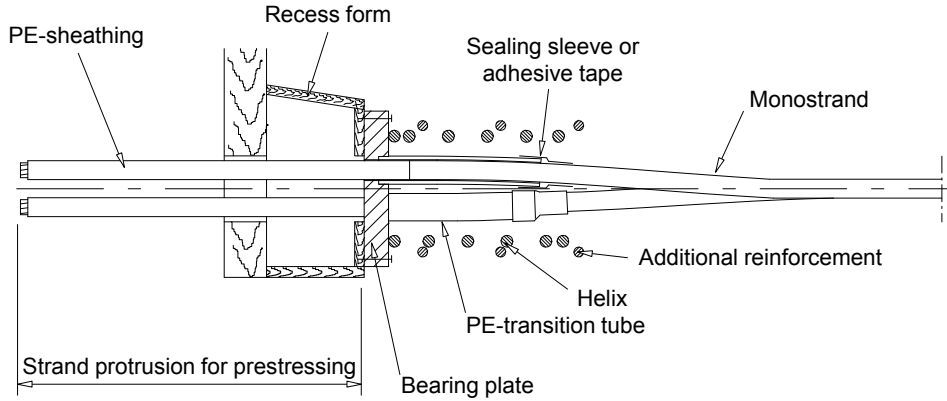
DYWIDAG
 DYWIDAG-Systems International GmbH
 Phone: +49/89/309050-100
 E-Mail: dsihv@dywidag-systems.com

SUSPA/DSI
Unbonded Monostrand System
 Movable coupling K6-K6

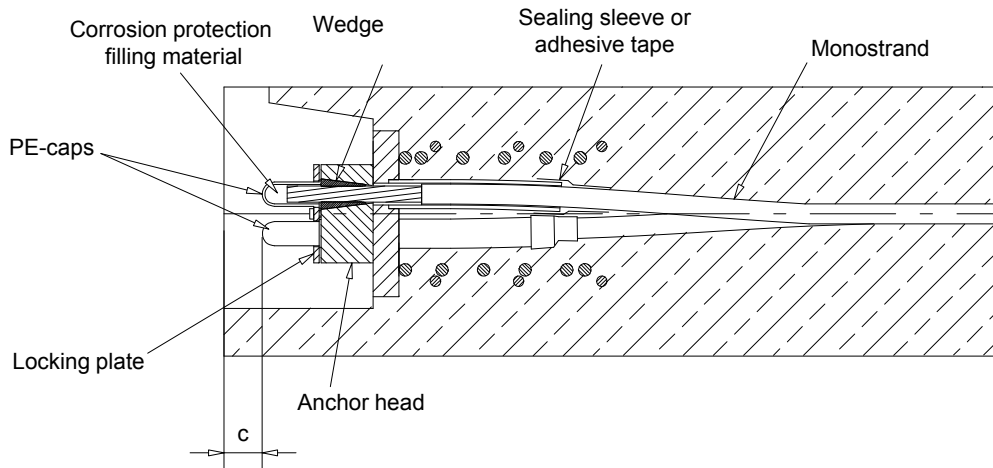
Annex 6
 of European Technical Assessment
ETA-03/0036 of 29.01.2021

electronic copy electronic copy electronic copy electronic copy electronic copy electronic copy electronic copy electronic copy electronic copy electronic copy

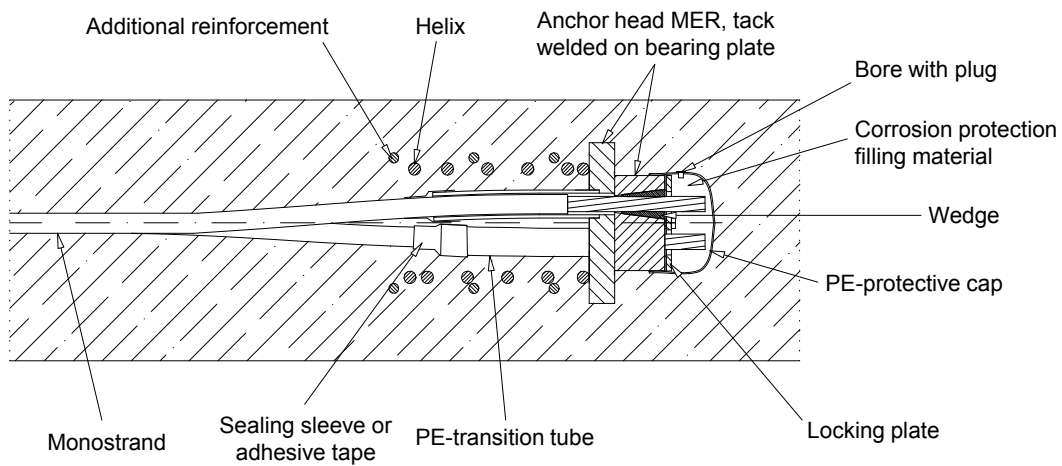
Assembly state of stressing anchor MER6



Stressing anchor MER6 after stressing



Fixed anchor MEF6, final state



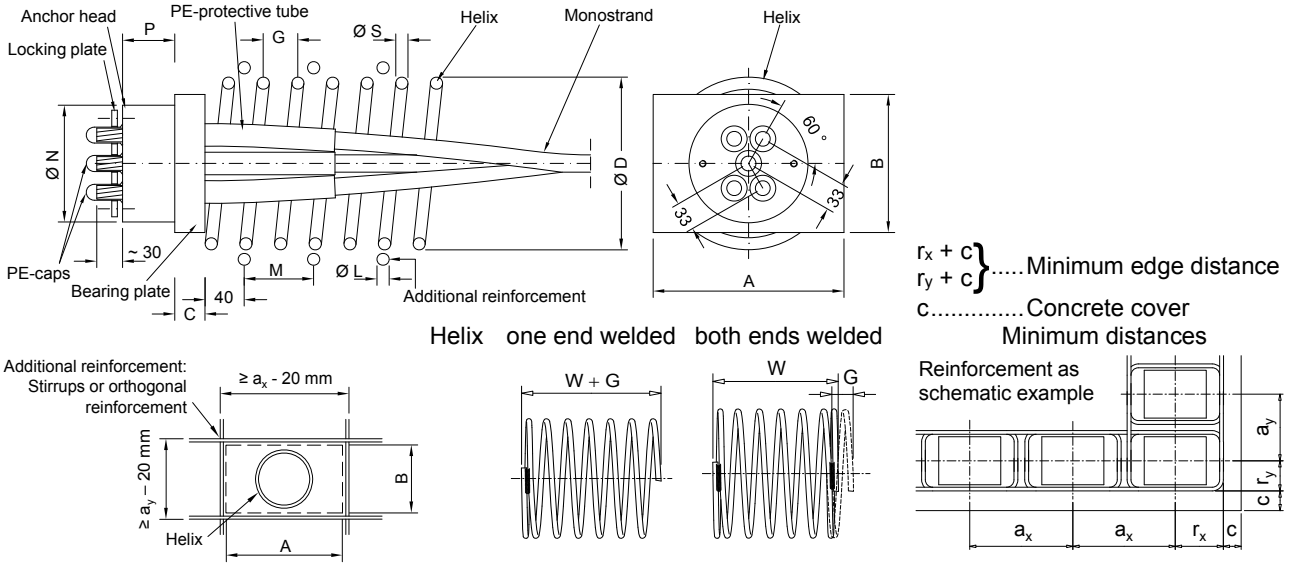
c = concrete cover

DYWIDAG-Systems International GmbH
 Phone: +49/89/309050-100
 E-Mail: dsihv@dywidag-systems.com

SUSPA/DSI
Unbonded Monostrand System
 Stressing anchor MER6 and
 Fixed anchor MEF6

Annex 7
 of European Technical Assessment
ETA-03/0036 of 29.01.2021

Stressing anchor MER6 and fixed anchor MEF6 with rectangular bearing plate



Concrete strength $f_{cm, 0}$, cube 150 at time of stressing		20 N/mm ²				28 N/mm ²				36 N/mm ²				
Designation		6-2	6-3	6-4	6-5	6-2	6-3	6-4	6-5	6-2	6-3	6-4	6-5	
Number of strands		2	3	4	5	2	3	4	5	2	3	4	5	
Strand arrangement														
Anchor head	$\varnothing N$	90	95	110	135	90	95	110	135	90	95	110	135	
	P	50	50	55	60	50	50	55	60	50	50	55	60	
Bearing plate	A	125	150	180	200	125	150	180	200	125	150	180	200	
	B	100	115	135	155	100	115	135	155	100	115	135	155	
	C	25	30	35	35	25	30	35	35	25	30	35	35	
Helix	Min. external diameter	$\varnothing D$	110	140	160	180	100	120	120	140	75	90	110	130
	Min. wire diameter	$\varnothing S$	12	12	12	12	12	12	12	12	10	12	12	12
	Maximum pitch	G	40	50	50	60	40	40	40	40	40	45	45	60
	Minimum length	W	195	285	285	335	195	235	235	235	190	215	215	275
	Min. number of turns	n	5	6	6	6	5	6	6	6	5	5	5	5
Minimum centre distance	a_x	220	280	335	380	200	250	290	330	180	215	250	280	
	a_y	170	195	215	245	145	170	190	215	120	140	165	190	
Minimum edge distance, plus c	r_x	100	130	160	180	90	115	135	155	80	100	115	130	
	r_y	75	90	100	115	65	75	85	100	50	60	75	85	
Additional reinforcement, $R_e \geq 500$ N/mm ²	No of layers	K	3	3	4	5	3	3	4	4	3	3	4	4
	Bar $\varnothing L$		10	12	12	12	10	10	10	12	10	10	10	12
	Spacing M		60	70	75	70	60	70	70	75	55	70	55	75

Dimensions in mm

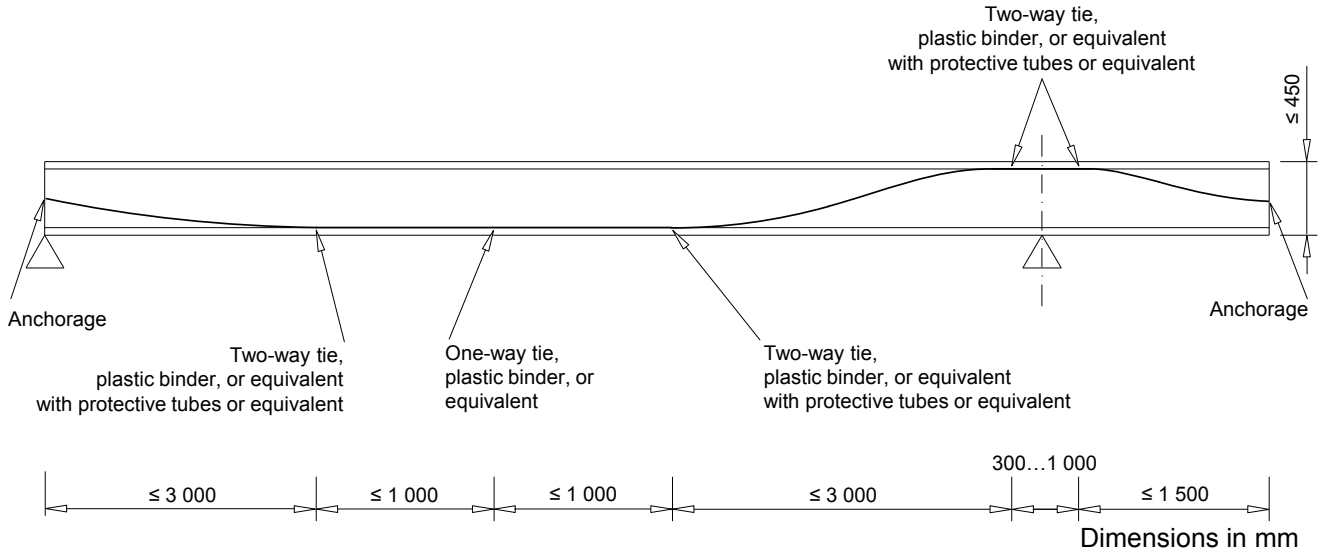
DYWIDAG
DYWIDAG-Systems International GmbH
Phone: +49/89/309050-100
E-Mail: dsihv@dywidag-systems.com

SUSPA/DSI
Unbonded Monostrand System

Stressing anchor MER6 and
Fixed anchor MEF6
Size 6-2 to 6-5

Annex 8
of European Technical Assessment
ETA-03/0036 of 29.01.2021

Free tendon layout, plate thickness ≤ 450 mm



- 1 Installing the bottom layer of reinforcement on spacers
- 2 Installing the spacers for the top layer of reinforcement taking account of tendon installation
- 3 Installing the tendon anchorages, fastening onto the framework
- 4 Placing the tendons on the lower reinforcement and on the spacers for tendon top layer
- 5 Cutting the PE-sheathing to the required length
- 6 Inserting the tendons through the anchorages
- 7 Placing protective tubes (e.g. cut PE-sheathings) in the region of the connections with the reinforcement for protection of the tendons
- 8 Installing the upper reinforcement
- 9 Lifting up and connecting the tendons to the upper reinforcement
- 10 Connecting the tendons with the lower reinforcement
- 11 Connecting and sealing the tendons with tape at the PE-sleeves of the anchors
- 12 Checking correct seat of anchors and of PE-sleeves before concreting

Maximum prestressing and overstressing force

Designation	Number of strands	Mass of mono-strands	Cross-sectional area of strands	$f_{pk} = 1\,770\text{ N/mm}^2$		$f_{pk} = 1\,860\text{ N/mm}^2$	
				Maximum prestressing force	Maximum overstressing force	Maximum prestressing force	Maximum overstressing force
—	—	kg/m	A_p mm ²	$0.90 \cdot A_p \cdot f_{p0.1}$ kN	$0.95 \cdot A_p \cdot f_{p0.1}$ kN	$0.90 \cdot A_p \cdot f_{p0.1}$ kN	$0.95 \cdot A_p \cdot f_{p0.1}$ kN
6-1	1	1.30	150	211	222	221	234
6-2	2	2.60	300	421	445	443	467
6-3	3	3.90	450	632	667	664	701
6-4	4	5.20	600	842	889	886	935
6-5	5	6.50	750	1 053	1 112	1 107	1 169

NOTES
 $0.90 \cdot A_p \cdot f_{p0.1} = 0.90 \cdot F_{p0.1}$ Maximum prestressing force
 $0.95 \cdot A_p \cdot f_{p0.1} = 0.95 \cdot F_{p0.1}$ Maximum overstressing force
 For $F_{p0.1} = A_p \cdot f_{p0.1}$ see Annex 11.



DYWIDAG-Systems International GmbH
 Phone: +49/89/309050-100
 E-Mail: dsihv@dywidag-systems.com

SUSPA/DSI
Unbonded Monostrand System
 Maximum prestressing and overstressing forces

Annex 10
 of European Technical Assessment
ETA-03/0036 of 29.01.2021

Prestressing steel strand

Characteristic	Symbol	Unit	Y1770S7 15.7	Y1860S7 15.7
Tensile strength	R_m, f_{pk}	N/mm ²	1 770	1 860
Nominal diameter of strand	d	mm	15.7 (0.62 ")	
Nominal diameter of outer wire	d_o	mm	5.2	
Diameter of core wire	d'	mm	$\geq 1.03 \cdot d_o$	
Nominal mass per metre of prestressing steel	M	kg/m	1.172	
Allowable deviation from nominal mass	—	%	± 2	
Nominal cross-sectional area	S_0	mm ²	150	
Characteristic value of maximum force	F_{pk}	kN	266	279
Maximum value of maximum force	$F_{m, max}$	kN	306	321
Characteristic value of 0.1 % proof force	$F_{p0.1}$	kN	234	246
Minimum elongation at maximum force, $L_0 \geq 500$ mm	A_{gt}	%	3.5	
Modulus of elasticity	E	N/mm ²	195 000 ¹⁾	
Relaxation after 1 000 h, for an initial force of $0.70 \cdot F_{ma}$	—	%	≤ 2.5	
	—	%	≤ 4.5	

¹⁾ Standard value

Characteristic maximum force of tendon

Number of strands	n	—	01	02	03	04	05
Nominal cross-sectional area of prestressing steel	A_p	mm ²	150	300	450	600	750
Characteristic tensile strength $f_{pk} = 1\,770$ N/mm ²							
Characteristic value of maximum force of tendon	F_{pk}	kN	266	532	798	1 064	1 330
Characteristic tensile strength $f_{pk} = 1\,860$ N/mm ²							
Characteristic value of maximum force of tendon	F_{pk}	kN	279	558	837	1 116	1 395

DYWIDAG 
DYWIDAG-Systems International GmbH
Phone: +49/89/309050-100
E-Mail: dsihv@dywidag-systems.com

SUSPA/DSI
Unbonded Monostrand System
Prestressing steel strands
Characteristic maximum force of tendon

Annex 11
of European Technical Assessment
ETA-03/0036 of 29.01.2021

electronic copy electronic copy electronic copy electronic copy electronic copy electronic copy electronic copy electronic copy electronic copy electronic copy

Designation	Standard	Material ¹⁾
Anchor SK6, SF6	EN 1562 EN 1563	Ductile cast iron
Anchor head	EN ISO 683-1 EN ISO 683-2	Steel
Coupling heads	EN ISO 683-1 EN ISO 683-2	Steel
Bearing plate	EN 10025-2	Steel
Coupling sleeves	EN 10025-2	Steel
Wedge	EN 10277	Steel
Washer	EN ISO 7089	Steel
Locking plate	EN 10025-2	Steel
Helix	EN 10025-2 —	Steel Ribbed reinforcing steel, $R_e \geq 500 \text{ N/mm}^2$
Stirrup and additional reinforcement	Ribbed reinforcing steel, $R_e \geq 500 \text{ N/mm}^2$	
Compression spring	DIN 2098-2	Steel
Protective cap	EN 1562	Cast iron
PE-cap and PE-protective cap PE-plug PE-transition tube PE-installation spindle and PE-nut PE-sleeve PE-protective tube sections 1 and 2	EN ISO 17855-1	PE
Sealing sleeve	Synthetic rubber	

¹⁾ Detailed material specifications are deposited at Österreichisches Institut für Bautechnik

electronic copy

Subject / type of control		Test of control method	Criteria, if any	Minimum number of samples	Minimum frequency of control
Bearing plate MER6, MEF6	Material	Checking ¹⁾	2)	100 %	continuous
	Detailed dimensions	Testing	2)	3 %, ≥ 2 specimens	continuous
	Visual inspection ³⁾	Checking	2)	100 %	continuous
	Traceability	bulk			
Anchor head SK6, SF6, MER6, MEF6 Coupling head KS6, K6 Coupling sleeve S, K	Material	Checking ⁴⁾	2)	100 %	continuous
	Detailed dimensions	Testing	2)	5 %, ≥ 2 specimens	continuous
	Visual inspection ³⁾	Checking	2)	100 %	continuous
	Traceability	full			
Wedge	Material	Checking ⁴⁾	2)	100 %	continuous
	Treatment, hardness	Testing	2)	0.5 %, ≥ 2 specimens	continuous
	Detailed dimensions	Testing	2)	5 %, ≥ 2 specimens	continuous
	Visual inspection ³⁾	Checking	2)	100 %	continuous
	Traceability	full			
Monostrand	Material	Checking	2), 5)	100 %	continuous
	Diameter	Testing	2), 5)	1 sample	each coil or every 7 tons ⁶⁾
	Visual inspection	Checking	2), 5)	1 sample	
Helix in plain round steel EN 10025	Material	Checking ¹⁾	2)	100 %	continuous
	Visual inspection ³⁾	Checking	2)	100 %	continuous
	Traceability	full			

- 1) Checking by means of at least a test report 2.2 according to EN 10204.
- 2) Conformity with the specifications of the component
- 3) Successful visual inspection does not need to be documented.
- 4) Checking by means of an inspection certificate 3.1 according to EN 10204.
- 5) Checking of relevant certificate as long as the basis of "CE"-marking is not available.
- 6) Maximum between a coil and 7 tons has to be taken into account


Traceability full Full traceability of each component to its raw material
 bulk Traceability of each delivery of components to a defined point

Material Defined according to technical specification deposited by the supplier

Detailed dimensions Measuring of all dimensions and angles according to the specification given in the test plan

Visual inspection Main dimensions, correct marking and labelling, surface, corrosion, coating, etc.

Treatment, hardness Surface hardness, core hardness, and treatment depth

 <p>DYWIDAG-Systems International GmbH Phone: +49/89/309050-100 E-Mail: dsihv@dywidag-systems.com</p>	<p>SUSPA/DSI Unbonded Monostrand System</p> <p>176 Contents of the prescribed test plan</p>	<p>Annex 13 of European Technical Assessment ETA-03/0036 of 29.01.2021</p>
--	---	--

Subject / type of control		Test of control method	Criteria, if any	Minimum number of samples ¹⁾	Minimum frequency of control
Bearing plate MER6, MEF6	Material	Checking and testing, hardness and chemical ²⁾	³⁾	1	1/year
	Detailed dimensions	Testing	³⁾	1	1/year
	Visual inspection	Checking	³⁾	1	1/year
Anchor head SK6, SF6, MER6, MEF6 Coupling head KS6, K6 Coupling sleeve S, K	Material	Checking and testing, hardness and chemical ²⁾	³⁾	1	1/year
	Detailed dimensions	Testing	³⁾	1	1/year
	Visual inspection	Checking	³⁾	1	1/year
Wedge	Material	Checking and testing, hardness and chemical ²⁾	³⁾	2	1/year
	Treatment, hardness	Checking and testing, hardness profile	³⁾	2	1/year
	Detailed dimensions	Testing	³⁾	1	1/year
	Main dimensions, surface hardness	Testing	³⁾	5	1/year
	Visual inspection	Checking	³⁾	5	1/year
Single tensile element test		According to EAD 160004-00-0301, Annex C.7		9	1/year

1) If the kit comprises different kinds of anchor heads e.g. with different materials, different shape, different wedges, etc., then the number of samples are understood as per kind of anchor head.

2) Testing of hardness and checking of chemical composition by means of an inspection certificate 3.1 according to EN 10204.

3) Conformity with the specifications of the components

Material Defined according to technical specification deposited by the ETA holder at the Notified body

Detailed dimensions Measuring of all dimensions and angles according to the specification given in the test plan

Visual inspection Main dimensions, correct marking and labelling, surface, corrosion, coating, etc.

Treatment, hardness Surface hardness, core hardness, and treatment depth



DYWIDAG-Systems International GmbH
Phone: +49/89/309050-100
E-Mail: dsihv@dywidag-systems.com

SUSPA/DSI
Unbonded Monostrand System

177
Audit testing

Annex 14
of European Technical Assessment
ETA-03/0036 of 29.01.2021

electronic copy

European Assessment Document

EAD 160004-00-0301 Post-Tensioning Kits for Prestressing of Structures

Standards

Eurocode 2	Eurocode 2 – Design of concrete structures
EN 206+A1 (11.2016)	Concrete – Specification, performance, production and conformity
EN 1562 (03.2019)	Founding - Malleable cast irons
EN 1563 (08.2018)	Founding - Spheroidal graphite cast irons
EN 10025-2 (08.2019)	Hot rolled products of structural steels - Part 2: Technical delivery conditions for non-alloy structural steels
EN 10204 (10.2004)	Metallic products – Types of inspection documents
EN 10277 (06.2018)	Bright steel products - Technical delivery conditions
prEN 10138-3 (08.2009)	Prestressing steels – Part 3: Strands
EN ISO 683-1 (06.2018)	Heat-treatable steels, alloy steels and free-cutting steels - Part 1: Non-alloy steels for quenching and tempering
EN ISO 683-2 (06.2018)	Heat-treatable steels, alloy steels and free-cutting steels - Part 2: Alloy steels for quenching and tempering
EN ISO 7089 (06.2000)	Plain washers – Normal series, Product grade A
EN ISO 17855-1 (10.2014)	Plastics – Polyethylene (PE) moulding and extrusion materials – Part 1: Designation system and basis for specifications
DIN 2098-2 (08.1970)	Helical springs made of round wire – Dimensions for cold-coiled compression springs of less than 0.5 mm wire diameter
CWA 14646 (01.2003)	Requirements for the installation of post-tensioning kits for prestressing of structures and qualification of the specialist company and its personnel

Other documents

98/456/EC	Commission decision 98/456/EC of 3 July 1998 on the procedure for attesting the conformity of construction products pursuant to Article 20 (2) of Council Directive 89/106/EEC as regards posttensioning kits for the prestressing of structures, OJ L 201 of 17.07.1998, p. 112
305/2011	Regulation (EU) № 305/2011 of the European Parliament and of the Council of 9 March 2011 laying down harmonised conditions for the marketing of construction products and repealing Council Directive 89/106/EEC, OJ L 088 of 04.04.2011, p. 5, amended by Commission Delegated Regulation (EU) № 568/2014 of 18 February 2014, OJ L 157 of 27.05.2014, p. 76, Commission Delegated Regulation (EU) № 574/2014 of 21 February 2014, OJ L 159 of 28.05.2014, p. 41, and Regulation (EU) 2019/1020 of the European Parliament and of the Council of 20 June 2019, OJ L 169 of 25.06.2019, p. 1
568/2014	Commission Delegated Regulation (EU) № 568/2014 of 18 February 2014 amending Annex V to Regulation (EU) № 305/2011 of the European Parliament and of the Council as regards the assessment and verification of constancy of performance of construction products, OJ L 157 of 27.05.2014, p. 76



DYWIDAG-Systems International GmbH
Phone: +49/89/309050-100
E-Mail: dsihv@dywidag-systems.com

SUSPA/DSI
Unbonded Monostrand System
Reference documents

Annex 15
of European Technical Assessment
ETA-03/0036 of 29.01.2021

**DYWIDAG-SYSTEMS
INTERNATIONAL GMBH
SPANntechnik NORD**

Tel +49 3321 4418-0
E-mail pt.deutschland@dywidag-systems.com

**DYWIDAG-SYSTEMS
INTERNATIONAL GMBH
SPANntechnik SÜD**

Tel +49 8231 9607-0
E-mail pt.deutschland@dywidag-systems.com



www.dywidag.com

E

Calculation sheet


```

> restart,
> with(plots) :
> General parameters inserted here in [m] and [kN]:

> N[raveel] := 0.0 :
> n[holes] := 5 : N[plates] := 3 : a[raveel] := 1.2 :
> d[hole] := 0.16; R[hole] :=  $\frac{d[hole]}{2}$ ; A[holes] := n[holes]·0.25·Pi·d[hole]2; Iyy[hole] :=
 $\frac{1}{64}$ ·Pi·d[hole]4;

 $d_{hole} := 0.16$ 
 $R_{hole} := 0.080000000000$ 
 $A_{holes} := 0.1005309649$ 
 $Iyy_{hole} := 0.00003216990878$  (1)

> b[i] := 1.2; h[i] := 0.24; A[c] := b[i]·h[i] - A[holes]; Iyy :=  $\frac{1}{12}$ ·b[i]·h[i]3 - n[holes]
·  $\frac{1}{64}$ ·Pi·d[hole]4; z :=  $\frac{1}{2}$ ·h[i]; W :=  $\frac{\left(\frac{1}{12} \cdot b[i] \cdot h[i]^3 - n[holes] \cdot \frac{1}{64} \cdot \text{Pi} \cdot d[hole]^4\right)}{z}$ ;
w[i] := b[i]; l[i] := 7.8; e[p, kern] :=  $\frac{W}{A[c]}$ ; e[p] := 0.05; f[ck] := 45·103; f[cd] :=
 $\frac{f[ck]}{\text{gamma}_c}$ ; f[cm] :=  $\left(\frac{f[ck]}{10^3} + 8\right) \cdot 10^3$ ; f[ctm] := evalf $\left(0.30 \cdot \left(\frac{f[ck]}{1000}\right)^{\frac{2}{3}}\right)$ ; Iyy1 :=
 $\frac{1}{12}$ ·b[i]·h[i]3;

 $b_i := 1.2$ 
 $h_i := 0.24$ 
 $A_c := 0.1874690351$ 
 $Iyy := 0.001221550456$ 
 $W := 0.01017958713$ 
 $l_i := 7.8$ 
 $e_{p, kern} := 0.05430009881$ 
 $e_p := 0.05$ 
 $f_{ctm} := 3.795446994$ 
 $Iyy1 := 0.001382400000$  (2)

```

$$\begin{aligned}
> E[cm] &:= 36000 \cdot 10^3 : E[p, strand] := 195 \cdot 10^6 : E[c, eff] := \frac{E[cm]}{1 + \varphi_{t, t0}}; EI := E[cm] \\
&\cdot I_{yy}; EI[long] := E[c, eff] \cdot I_{yy}; \\
&E_{c, eff} := \frac{36000000}{1 + \varphi_{t, t0}} \\
&EI := 43975.81642 \\
&EI_{long} := \frac{43975.81642}{1 + \varphi_{t, t0}} \tag{3}
\end{aligned}$$

$$\begin{aligned}
> \psi_{i0} &:= 0.4 : \psi_{i1} := 0.5 : \psi_{i2} := 0.3 : g[sw, c] := 25.0 : \gamma_s := 1.1 : \gamma_c := \\
&1.5 :
\end{aligned}$$

$$> f[ctk, 0.05] := 0.7 \cdot f[ctm]; f[ctd] := \frac{f[ctk, 0.05]}{\gamma_c};$$

General factors inserted here [-]:

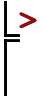
$$\begin{aligned}
&f_{ctk, 0.05} := 2.656812896 \\
&f_{ctd} := 1.771208597 \tag{4}
\end{aligned}$$

General (imposed) loads inserted here [kN/m2]:

$$\begin{aligned}
> q[k, cat A] &:= 1.75; q[k, walls] := 0.8; q[k] := q[k, cat A] + q[k, walls]; \\
&q_{k, cat A} := 1.75 \\
&q_{k, walls} := 0.8 \\
&q_k := 2.55 \tag{5}
\end{aligned}$$

$$> g[k, sw] := \frac{A[c]}{b[i]} \cdot g[sw, c]; g[k, services] := 0.25; g[k, raised floor] := 0.30; g[k] := g[k,
sw] + g[k, services] + g[k, raised floor];$$

$$\begin{aligned}
&g_{k, sw} := 3.905604898 \\
&g_{k, services} := 0.25 \\
&g_{k, raised floor} := 0.30 \\
&g_k := 4.455604898 \tag{6}
\end{aligned}$$



Characteristic load equations per unit width: $w[i]=b[i] \rightarrow$
 [kN/m1]:

```
> eq[6.10 a] := 1.35·g[k] + 1.50·psi0·q[k] :
> eq[6.10 b] := 1.20·g[k] + 1.50·q[k] :
> eq[6.10 c] := 0.9·g[k] :
> q[ed, sls] := (1.0·g[k] + 1.0·q[k])·w[i];
      qed, sls := 8.406725878 (7)
```

```
> q[ed, uls] := max(eq[6.10 a], eq[6.10 b], eq[6.10 c])·w[i];
      qed, uls := 11.00607105 (8)
```

```
> M[q, sls] := 1/8 · (q[k]·w[i])·l[i]2; M[g, sls] := 1/8 · (g[k]·w[i])·l[i]2; M[q + g, sls] := 1/8
      · q[ed, sls]·l[i]2; M[q + g, uls] := 1/8 · q[ed, uls]·l[i]2; M[p, 0] := P[m, 0]·e[p];
      Mq, sls := 23.27130000
      Mg, sls := 40.66185030
      Mq + g, sls := 63.93315030
      Mq + g, uls := 83.70117034
      Mp, 0 := 0.05 Pm, 0 (9)
```

```
> sigma[c, top, midspan] := -0.6·f[ck]; sigma[c, bottom, midspan] := 0·103;
      σc, top, midspan := -27000.0
      σc, bottom, midspan := 0 (10)
```

```
> eq1 := sigma[c, top, midspan] ≤ -0.85·P[m, 0]/A[c] + 0.85·P[m, 0]·e[p]/W - M[q + g, sls]/W :
```

```
> eq2 := sigma[c, bottom, midspan] = -0.85·P[m, 0]/A[c] - 0.85·P[m, 0]·e[p]/W
      + M[q + g, sls]/W;
      eq2 := 0 = -8.709104098 Pm, 0 + 6280.524886 (11)
```

```
> sol0 := solve({eq2}, {P[m, 0]}) : assign(sol0) : P[m, 0];
      721.1447716 (12)
```

```
> evalb(eq1);
      true (13)
```



Required amount of strands:

$$\begin{aligned}
 &> \text{phi}[\text{strand}] := 15.7; \text{phi}[\text{duct}] := 21; A[p, 1 \text{ strand}] := 150 : f[pk, \text{strand}] := 1860 : f[p, \\
 &01 k, \text{strand}] := 1640; \text{sigma}[p, m, 0, \text{strand}] := \min(0.75 \cdot f[pk, \text{strand}], 0.85 \cdot f[p, 01 k, \\
 &\text{strand}]); \\
 &\quad \phi_{\text{strand}} := 15.7 \\
 &\quad \phi_{\text{duct}} := 21 \\
 &\quad f_{p, k, \text{strand}} := 1640 \\
 &\quad \sigma_{p, m, 0, \text{strand}} := 1394.00 \tag{14}
 \end{aligned}$$

$$\begin{aligned}
 &> A[p, \text{req}, \text{strand}] := \frac{P[m, 0] \cdot 10^3}{\text{sigma}[p, m, 0, \text{strand}]}; n[\text{strands}] := \frac{A[p, \text{req}, \text{strand}]}{A[p, 1 \text{ strand}]}, \\
 &N[\text{strands}] := \text{ceil}(n[\text{strands}]); \\
 &\quad A_{p, \text{req}, \text{strand}} := 517.3204961 \\
 &\quad n_{\text{strands}} := 3.448803307 \\
 &\quad N_{\text{strands}} := 4 \tag{15}
 \end{aligned}$$

$$\begin{aligned}
 &> \text{if } N[\text{raveel}] = 1.0 \text{ then } N[\text{strands}] := \text{ceil}(n[\text{strands}]) + 1; \text{else } N[\text{strands}] := \\
 &\text{ceil}(n[\text{strands}]); \text{end if}; \\
 &\quad N_{\text{strands}} := 4 \tag{16}
 \end{aligned}$$

$$\begin{aligned}
 &> A[p, \text{total}, \text{strand}] := N[\text{strands}] \cdot A[p, 1 \text{ strand}]; P[m, 0, \text{total}, \text{strand}] := \\
 &\frac{A[p, \text{total}, \text{strand}] \cdot \text{sigma}[p, m, 0, \text{strand}]}{10^3}; M[p, 0, \text{total}, \text{strand}] := P[m, 0, \text{total}, \text{strand}] \\
 &\cdot e[p]; \\
 &\quad A_{p, \text{total}, \text{strand}} := 600 \\
 &\quad P_{m, 0, \text{total}, \text{strand}} := 836.4000000 \\
 &\quad M_{p, 0, \text{total}, \text{strand}} := 41.82000000 \tag{17}
 \end{aligned}$$

First cross-sectional checks at t=0 before all losses

At section A-A (x = L/2) in [MPa]:

$$\begin{aligned}
 > \text{eq3} := \frac{\left(\frac{-P[m, 0, total, strand]}{A[c]} + \frac{M[p, 0, total, strand]}{W} - 1.00 \cdot \frac{M[q + g, sls]}{W} \right)}{1000} : \\
 \text{sigma}[top[AA], before all losses] &:= \text{eq3}; \\
 \sigma_{top_{AA}, before all losses} &:= -6.633840065 \quad (18)
 \end{aligned}$$

$$\begin{aligned}
 > \text{eq4} := \frac{\left(\frac{-P[m, 0, total, strand]}{A[c]} - \frac{M[p, 0, total, strand]}{W} + 1.00 \cdot \frac{M[q + g, sls]}{W} \right)}{1000} : \\
 \text{sigma}[bottom[AA], before all losses] &:= \text{eq4}; \\
 \sigma_{bottom_{AA}, before all losses} &:= -2.289233547 \quad (19)
 \end{aligned}$$

At section B-B (x = 0) in [MPa]:

$$\begin{aligned}
 > \text{eq5} := \frac{\left(\frac{-P[m, 0, total, strand]}{A[c]} + \frac{M[p, 0, total, strand]}{W} - 0 \cdot \frac{M[q + g, sls]}{W} \right)}{1000} : \\
 \text{sigma}[top[BB], before all losses] &:= \text{eq5}; \\
 \sigma_{top_{BB}, before all losses} &:= -0.353315179 \quad (20)
 \end{aligned}$$

$$\begin{aligned}
 > \text{eq6} := \frac{\left(\frac{-P[m, 0, total, strand]}{A[c]} - \frac{M[p, 0, total, strand]}{W} + \frac{0 \cdot M[q + g, sls]}{W} \right)}{1000} : \\
 \text{sigma}[bottom[BB], before all losses] &:= \text{eq6}; \\
 \sigma_{bottom_{BB}, before all losses} &:= -8.569758433 \quad (21)
 \end{aligned}$$

Direct losses

Friction

$$\begin{aligned} > x := l[i] : \mu[\text{strand}] := 0.06 : k[\text{strand}] := 0.9 \cdot 10^{-2} : \text{angle} := 0 : \alpha[\text{friction}] := \\ & \frac{\text{angle}}{180} \cdot \text{Pi}; \\ & \alpha_{\text{friction}} := 0 \end{aligned} \quad (22)$$

$$\begin{aligned} > \text{delP}[\mu] := P[m, 0, \text{total}, \text{strand}] \cdot (1 - \exp(-\mu[\text{strand}] \cdot (\alpha[\text{friction}] + k[\text{strand}] \\ \cdot x))); \\ & \text{delP}_{\mu} := 3.515507969 \end{aligned} \quad (23)$$

Wedge set

$$\begin{aligned} > \text{slip} := 5 \cdot 10^{-3} : \text{delp}[\text{ws}] := \frac{\text{slip}}{l[i]} \cdot E[p, \text{strand}]; \\ & \text{delp}_{\text{ws}} := 125000.0000 \end{aligned} \quad (24)$$

$$\begin{aligned} > \text{delP}[\text{ws}] := A[p, \text{total}, \text{strand}] \cdot \text{delp}[\text{ws}] \cdot 10^{-6}; \\ & \text{delP}_{\text{ws}} := 75.00000000 \end{aligned} \quad (25)$$

Elastic deformation concrete

$$\begin{aligned} > \text{if } N[\text{strands}] = 1 \text{ then } \text{delP}[\text{el}, \text{check}, 1] := \frac{1}{2} \cdot \frac{E[p, \text{strand}] \cdot A[p, 1 \text{ strand}] \cdot 10^{-6}}{E[\text{cm}] \cdot A[\text{c}]} \cdot P[m, 0, \\ \text{total}, \text{strand}]; \text{ else } \text{delP}[\text{el}, \text{check}, 1] := \frac{N[\text{strands}] - 1}{2} \\ \cdot \frac{E[p, \text{strand}] \cdot A[p, 1 \text{ strand}] \cdot 10^{-6}}{E[\text{cm}] \cdot A[\text{c}]} \cdot P[m, 0, \text{total}, \text{strand}]; \text{ end if}; \\ & \text{delP}_{\text{el}, \text{check}, 1} := 5.437497980 \end{aligned} \quad (26)$$

$$\begin{aligned} > P[m, 0, \text{per strand}] := \frac{P[m, 0, \text{total}, \text{strand}]}{N[\text{strands}]} ; \\ > \text{for } v \text{ to } N[\text{strands}] \text{ do } N[v] := v : \text{delP}[v] := (N[v] - 1) \cdot P[m, 0, \text{per strand}] \\ \cdot \frac{(E[p, \text{strand}] \cdot A[p, 1 \text{ strand}])}{E[\text{cm}] \cdot A[\text{c}]} : \text{delP}[\text{el}, \text{check}, 2] := 10^{-6} \cdot \text{add}(\text{delP}[v], v = 1 \end{aligned}$$


```

..N[strands] :od:
>
> if  $\frac{delP[el, check, 1]}{delP[el, check, 2]} = 1.0$  then  $delP[el] := delP[el, check, 1]$  else  $delP[el] := delP[el, check,$ 
1] end if;

```

$$delP_{el} := 5.437497980 \quad (27)$$

```

>
>
>

```

Total direct losses

```

>  $delP[direct losses] := delP[mu] + delP[ws] + delP[el]$ ;  $Delta[direct losses] :=$ 
 $\frac{delP[direct losses]}{P[m, 0, total, strand]} \cdot 100$ ;

```

$$delP_{direct losses} := 83.95300595$$

$$\Delta_{direct losses} := 10.03742300 \quad (28)$$

```

>
>

```

Time dependent losses

Relaxation

$$\begin{aligned} > \text{sigma}[p, i] := \frac{(P[m, 0, \text{total}, \text{strand}]) \cdot 10^3}{A[p, \text{total}, \text{strand}]}; \text{mu}[r] := \frac{\text{sigma}[p, i]}{f[pk, \text{strand}]}; RHO := 2.5 : \\ & T[\text{time}] := 500000 : \end{aligned}$$

$$\sigma_{p, i} := 1394.000000$$

$$\mu_r := 0.7494623656 \quad (29)$$

$$\begin{aligned} > \text{delsigma}[pr] := \text{sigma}[p, i] \cdot 0.66 \cdot RHO \cdot \exp(9.1 \cdot \text{mu}[r]) \cdot \left(\frac{T[\text{time}]}{1000} \right)^{0.75 \cdot (1 - \text{mu}[r])} \cdot 10^{-5}; \\ & \text{delsigma}_{pr} := 67.73715518 \end{aligned} \quad (30)$$

Creep

$$\begin{aligned} > h[0] := \frac{2 \cdot A[c]}{2 \cdot (b[i] + h[i])} \cdot 10^3; RHI := 50 : \end{aligned}$$

$$h_0 := 130.1868299 \quad (31)$$

$$\begin{aligned} > \text{alpha}[1] := \left(\frac{35}{\frac{f[cm]}{1000}} \right)^{0.7}; \text{alpha}[2] := \left(\frac{35}{\frac{f[cm]}{1000}} \right)^{0.2}; \text{alpha}[3] := \left(\frac{35}{\frac{f[cm]}{1000}} \right)^{0.5}; \end{aligned}$$

$$\alpha_1 := 0.7479189246$$

$$\alpha_2 := 0.9203614824$$

$$\alpha_3 := 0.8126360554 \quad (32)$$

$$\begin{aligned} > \text{beta}[h] := 1.5 \cdot (1 + (0.012 \cdot RHI)^{18}) \cdot h[0] + 250 \cdot \text{alpha}[3] : \end{aligned}$$

$$\begin{aligned} > \text{if } \text{beta}[h] \leq 1500 \cdot \text{alpha}[3] \text{ then } \text{beta}[h] := \text{beta}[h] \\ & \text{else } b[h] := 1500 \cdot \text{alpha}[3] \\ & \text{end if} \end{aligned}$$

$$\beta_h := 398.4590914 \quad (33)$$

$$\begin{aligned} > T0 := 28 : \text{beta}[c] := \left(\frac{\left(\frac{T[\text{time}]}{24} - T0 \right)}{\text{beta}[h] + \left(\frac{T[\text{time}]}{24} - T0 \right)} \right)^{0.3} : \end{aligned}$$

$$\begin{aligned} & \text{if } \text{beta}[c] \leq (1 - 0.02) \text{ then } \text{beta}[c] := \text{beta}[c] \\ & \text{else } \text{beta}[c] := 1.0 \\ & \text{end if} \end{aligned}$$

$$\beta_c := 1.0 \quad (34)$$

$$\begin{aligned}
> \text{beta}[t0] &:= \frac{1}{(0.1 + T0^{0.20})}; \text{beta}[fcm] := \text{evalf}\left(\frac{16.8}{\text{sqrt}\left(\left(\frac{f[cm]}{1000}\right)\right)}\right); \\
&\beta_{t0} := 0.4884495454 \\
&\beta_{fcm} := 2.307657474
\end{aligned} \tag{35}$$

$$\begin{aligned}
> \text{varphi}[RH] &:= \left(1 + \frac{\left(1 - \frac{RHI}{100}\right)}{0.1 \cdot \text{root}(h[0], 3)} \cdot \text{alpha}[1]\right) \cdot \text{alpha}[2]; \\
&\varphi_{RH} := 1.599451392
\end{aligned} \tag{36}$$

$$\begin{aligned}
> \text{varphi}[0] &:= \text{varphi}[RH] \cdot \text{beta}[fcm] \cdot \text{beta}[t0]; \\
&\varphi_0 := 1.802860414
\end{aligned} \tag{37}$$

$$\begin{aligned}
> \text{varphi}[t, t0] &:= \text{varphi}[0] \cdot \text{beta}[c]; \\
&\varphi_{t, t0} := 1.802860414
\end{aligned} \tag{38}$$

$$\begin{aligned}
> \text{sigma}[creep] &:= \min(\text{eq3}, \text{eq4}, \text{eq5}, \text{eq6}); k[\text{sigma}] := \frac{\text{sigma}[creep]}{\frac{f[cm]}{10^3}}; \\
&\sigma_{creep} := -8.569758433 \\
&k_{\sigma} := 0.1616935553
\end{aligned} \tag{39}$$

$$\begin{aligned}
> \text{if } \text{sigma}[creep] < -\frac{0.45 \cdot f[ck]}{10^3} \\
\text{then } \text{varphi}[t, t0] &:= \text{varphi}[t, t0] \cdot \exp(1.5 \cdot (k[\text{sigma}] - 0.45)); \\
\text{else } \text{varphi}[t, t0] &:= \text{varphi}[t, t0] \\
\text{end if;} \\
&\varphi_{t, t0} := 1.802860414
\end{aligned} \tag{40}$$

Shrinkage

$$\begin{aligned}
> \text{varepsilon}[cs] &:= \text{varepsilon}[cd] + 0 \cdot \text{varepsilon}[ca]; \text{varepsilon}[cd] := \text{beta}[ds] \cdot k[h] \\
&\cdot \text{varepsilon}[cd, 0]; \text{varepsilon}[ca] := \text{beta}[as] \cdot \text{varepsilon}[ca, \text{infinity}]; \\
&\varepsilon_{cs} := \varepsilon_{cd} \\
&\varepsilon_{cd} := \beta_{ds} k_h \varepsilon_{cd, 0} \\
&\varepsilon_{ca} := \beta_{as} \varepsilon_{ca, \infty}
\end{aligned} \tag{41}$$

$$\begin{aligned}
> \text{beta}[ds] &:= 1.0 : \text{beta}[as] := 1.0 : RHO := 100 : \text{alpha}[ds1] := 4 : \text{alpha}[ds2] := 0.12 : \\
&f[cm0] := 10 \cdot 10^3 : f[cm] :
\end{aligned}$$

$$\begin{aligned}
> x[1] &:= 100 : x[2] := 200 : x[3] := 300 : x[4] := 500 : y[1] := 1.0 : y[2] := 0.85 : y[3] := \\
&0.75 : y[4] := 0.70 :
\end{aligned}$$

$$\begin{aligned}
&> \text{if } x[1] < h[0] \leq x[2] \text{ then } k[h] := y[1] + \frac{(y[2] - y[1])}{(x[2] - x[1])} \cdot (h[0] - x[1]) \\
&\quad \text{elif } x[2] < h[0] \leq x[3] \text{ then } k[h] := y[2] + \frac{(y[3] - y[2])}{(x[3] - x[2])} \cdot (h[0] - x[2]) \\
&\quad \text{elif } x[3] < h[0] \leq x[4] \text{ then } k[h] := y[3] + \frac{(y[4] - y[3])}{(x[4] - x[3])} \cdot (h[0] - x[3]) \\
&\quad \text{elif } h[0] > x[4] \text{ then } k[h] := y[4] \\
&\quad \text{end if} \\
&\qquad\qquad\qquad k_h := 0.9547197552 \tag{42}
\end{aligned}$$

$$\begin{aligned}
&> \text{beta}[RH] := 1.55 \cdot \left(1 - \left(\frac{RHI}{RHO} \right)^3 \right); \\
&\qquad\qquad\qquad \beta_{RH} := 1.356250000 \tag{43}
\end{aligned}$$

$$\begin{aligned}
&> \text{varepsilon}[cd, 0] := 0.85 \cdot \left((220 + 110 \cdot \text{alpha}[ds1]) \cdot \exp\left(-\frac{\text{alpha}[ds2] \cdot f[cm]}{f[cm0]} \right) \right) \cdot 10^{-6} \\
&\quad \cdot \text{beta}[RH]; \\
&\qquad\qquad\qquad \varepsilon_{cd, 0} := 0.0004028017252 \tag{44}
\end{aligned}$$

$$\begin{aligned}
&> \text{varepsilon}[ca, \text{infinity}] := 2.5 \cdot \left(\frac{f[ck]}{1000} - 10 \right) \cdot 10^{-6}; \\
&\qquad\qquad\qquad \varepsilon_{ca, \infty} := 0.00008750000000 \tag{45}
\end{aligned}$$

> Total losses due to creep, shrinkage and relaxation (EN-1992-1-1 clause 5.10.6)

$$\begin{aligned}
&> q[\text{quasi} - \text{permanent}] := (g[k] + \text{psi2} \cdot q[k]) \cdot w[i]; M[\text{ed}, \text{quasi} - \text{permanent}] := \frac{1}{8} \\
&\quad \cdot q[\text{quasi} - \text{permanent}] \cdot l[i]^2 : \sigma[c, QP] := \left(-\frac{P[m, 0]}{A[c]} - \frac{P[m, 0] \cdot e[p]}{W} \right. \\
&\quad \left. + \frac{M[\text{ed}, \text{quasi} - \text{permanent}]}{W} \right) \cdot 1e-3; \text{varepsilon}[cs]; \\
&\qquad\qquad\qquad q_{\text{quasi} - \text{permanent}} := 6.264725878 \\
&\qquad\qquad\qquad \sigma_{c, QP} := -2.708580445 \\
&\qquad\qquad\qquad 0.0003845627645 \tag{46}
\end{aligned}$$

$$\begin{aligned}
&> \text{delsigma}[csr] := \left(\text{abs}(\text{varepsilon}[cs]) \cdot E[p, \text{strand}] + 0.8 \cdot \text{abs}(\text{delsigma}[pr]) \right. \\
&\quad \left. + \frac{E[p, \text{strand}]}{E[cm]} \cdot \text{varphi}[t, t0] \cdot \text{abs}(\sigma[c, QP]) \right) / \left(1 + \frac{E[p, \text{strand}]}{E[cm]} \right) \\
&\quad \cdot \frac{A[p, \text{total}, \text{strand}]}{A[c] \cdot 1e6} \cdot \left(1 + \frac{A[c]}{I_{yy}} \cdot e[p]^2 \right) \cdot (1 + 0.8 \cdot \text{varphi}[t, t0]) \cdot 1e-3; \\
&\qquad\qquad\qquad \text{delsigma}_{csr} := 70.91580635 \tag{47}
\end{aligned}$$



$$\begin{aligned}
 &> \text{delP}[time\ dependent\ losses] := \frac{\text{delsigma}[csr] \cdot A[p, total, strand]}{1000}; \\
 &\Delta[time\ dependent\ losses] := \frac{\text{delP}[time\ dependent\ losses]}{P[m, 0, total, strand]} \cdot 100; \\
 &\text{delP}_{time\ dependent\ losses} := 42.54948381 \\
 &\Delta_{time\ dependent\ losses} := 5.087217098 \qquad \qquad \qquad \mathbf{(48)}
 \end{aligned}$$

Total losses

$$\begin{aligned} & \text{delP}[total] := \text{delP}[direct losses] + \text{delP}[time dependent losses]; \text{Delta}[total] := \\ & \text{Delta}[direct losses] + \text{Delta}[time dependent losses]; \text{Delta}[t = \text{infinity}] := \frac{\text{Delta}[total]}{100}; \\ & \text{delP}_{total} := 126.5024898 \\ & \Delta_{total} := 15.12464010 \\ & \Delta_{t = \infty} := 0.1512464010 \end{aligned} \tag{49}$$

Cross sectional checks SLS

$$\begin{aligned}
 > P[m, 0, sls] := P[m, 0, total, strand] - delP[direct losses]; M[p, 0, sls] := P[m, 0, sls] \cdot e[p]; \\
 & \quad P_{m, 0, sls} := 752.4469940 \\
 & \quad M_{p, 0, sls} := 37.62234970 \tag{50}
 \end{aligned}$$

$$\begin{aligned}
 > P[m, infinity, sls] := P[m, 0, total, strand] - delP[total]; M[p, infinity, sls] := P[m, infinity, \\
 & \quad sls] \cdot e[p]; \\
 & \quad P_{m, \infty, sls} := 709.8975102 \\
 & \quad M_{p, \infty, sls} := 35.49487551 \tag{51}
 \end{aligned}$$

$$\begin{aligned}
 > \text{if } N[raveel] = 1.0 \text{ then } FI[sls] := N[plates] \cdot \frac{q[ed, sls] \cdot (l[i] - a[raveel])}{4}; FI[uls] := \\
 & \quad N[plates] \cdot \frac{q[ed, uls] \cdot (l[i] - a[raveel])}{4} \text{ else } FI[sls] := 0; FI[uls] := 0 \text{ end if;} \\
 & \quad FI_{sls} := 0 \\
 & \quad FI_{uls} := 0 \tag{52}
 \end{aligned}$$

$$\begin{aligned}
 > q[quasi - permanent, W3] := (1 - psi2) \cdot q[k] \cdot w[i]; \text{if } N[raveel] = 1.0 \text{ then } FI[quasi \\
 & \quad - permanent] := N[plates] \cdot \frac{q[quasi - permanent] \cdot (l[i] - a[raveel])}{4}; FI[quasi \\
 & \quad - permanent, W3] := N[plates] \cdot \frac{q[quasi - permanent, W3] \cdot (l[i] - a[raveel])}{4} \\
 & \text{else } FI[quasi - permanent] := 0; FI[quasi - permanent, W3] := 0; \text{end if} \\
 & \quad q_{quasi - permanent, W3} := 2.1420 \\
 & \quad FI_{quasi - permanent} := 0 \\
 & \quad FI_{quasi - permanent, W3} := 0 \tag{53}
 \end{aligned}$$

$$\begin{aligned}
 > \text{sigma}[bottom, t = infinity] := \text{proc}(x) \text{ if } x < a[raveel] \text{ then } \frac{-P[m, infinity, sls]}{A[c]} \\
 & \quad + \frac{\frac{FI[sls] \cdot (l[i] - a[raveel]) \cdot x}{l[i]} + \frac{1}{2} \cdot q[ed, sls] \cdot x \cdot (l[i] - x) - M[p, infinity, sls]}{W} \\
 & \text{else } \frac{-P[m, infinity, sls]}{A[c]} \\
 & \quad + \left(\frac{FI[sls] \cdot a[raveel] \cdot (l[i] - x)}{l[i]} + \frac{1}{2} \cdot q[ed, sls] \cdot x \cdot (l[i] - x) - M[p, infinity, sls] \right) \text{ end} \\
 & \text{if end proc:}
 \end{aligned}$$

> $\text{sigma}[top, t = \text{infinity}] := \text{proc}(x) \text{ if } x < a[\text{raveel}] \text{ then } \frac{-P[m, \text{infinity}, sls]}{A[c]}$
 $\frac{FI[sls] \cdot (l[i] - a[\text{raveel}]) \cdot x}{l[i]} + \frac{1}{2} \cdot q[\text{ed}, sls] \cdot x \cdot (l[i] - x) - M[p, \text{infinity}, sls]}$
 $\frac{\quad}{W}$
else $\frac{-P[m, \text{infinity}, sls]}{A[c]}$
 $\left(\frac{FI[sls] \cdot a[\text{raveel}] \cdot (l[i] - x)}{l[i]} + \frac{1}{2} \cdot q[\text{ed}, sls] \cdot x \cdot (l[i] - x) - M[p, \text{infinity}, sls] \right)$
 $\frac{\quad}{W}$ **end**

if end proc:

> $\text{sigma}[bottom, t = 0] := \text{proc}(x) \text{ if } x < a[\text{raveel}] \text{ then } \frac{-P[m, 0, sls]}{A[c]}$
 $\frac{FI[sls] \cdot (l[i] - a[\text{raveel}]) \cdot x}{l[i]} + \frac{1}{2} \cdot q[\text{ed}, sls] \cdot x \cdot (l[i] - x) - M[p, 0, sls]$
 $+$ $\frac{\quad}{W}$
else $\frac{-P[m, 0, sls]}{A[c]}$
 $\left(\frac{FI[sls] \cdot a[\text{raveel}] \cdot (l[i] - x)}{l[i]} + \frac{1}{2} \cdot q[\text{ed}, sls] \cdot x \cdot (l[i] - x) - M[p, 0, sls] \right)$
 $+$ $\frac{\quad}{W}$ **end if**

end proc:

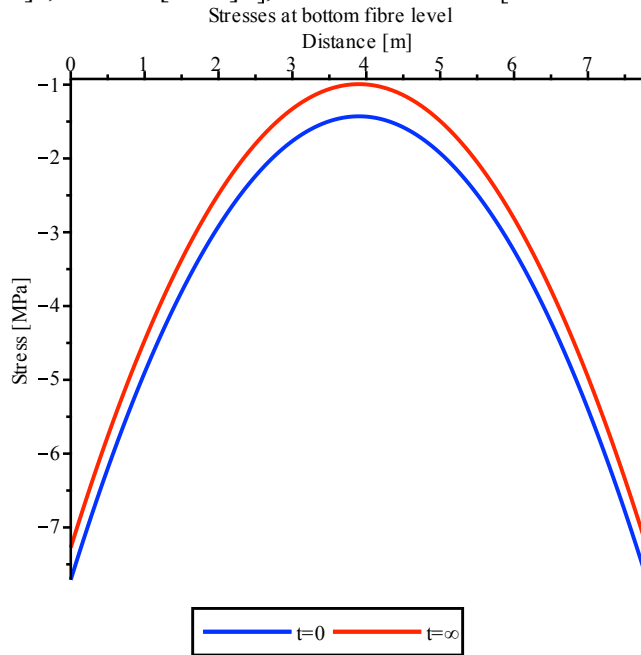
> $\text{sigma}[top, t = 0] := \text{proc}(x) \text{ if } x < a[\text{raveel}] \text{ then } \frac{-P[m, 0, sls]}{A[c]}$
 $\frac{FI[sls] \cdot (l[i] - a[\text{raveel}]) \cdot x}{l[i]} + \frac{1}{2} \cdot q[\text{ed}, sls] \cdot x \cdot (l[i] - x) - M[p, 0, sls]$
 $\frac{\quad}{W}$
else $\frac{-P[m, 0, sls]}{A[c]}$
 $\left(\frac{FI[sls] \cdot a[\text{raveel}] \cdot (l[i] - x)}{l[i]} + \frac{1}{2} \cdot q[\text{ed}, sls] \cdot x \cdot (l[i] - x) - M[p, 0, sls] \right)$
 $\frac{\quad}{W}$ **end if end**

proc:

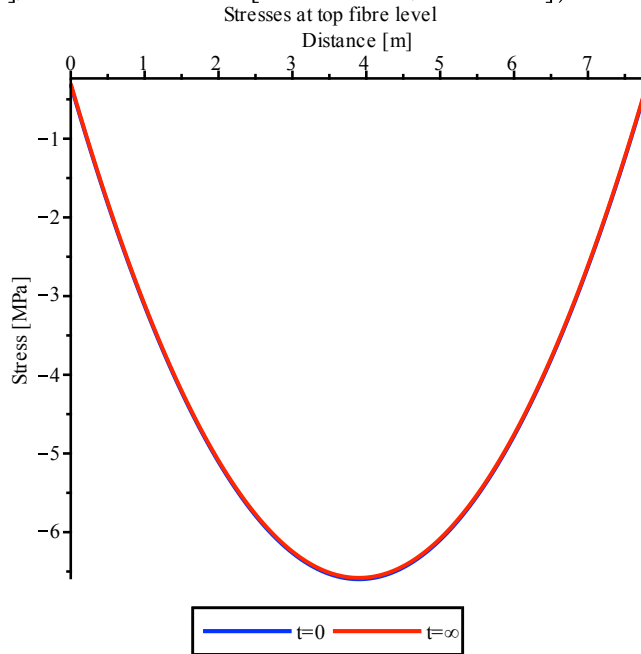
> $\text{Sig1}[0] := \text{plot}\left(\frac{\text{sigma}[bottom, t = 0]}{1e3}, 0..l[i], \text{legend} = ["t=0"], \text{color} = \text{blue}\right) : \text{Sig2}[0] :=$
 $\text{plot}\left(\frac{\text{sigma}[top, t = 0]}{1e3}, 0..l[i], \text{legend} = ["t=0"], \text{color} = \text{blue}\right) :$

> $\text{Sig1}[\text{infinity}] := \text{plot}\left(\frac{\text{sigma}[bottom, t = \text{infinity}]}{1e3}, 0..l[i], \text{legend} = ["t=\infty"], \text{color} = \text{red}\right) :$
 $\text{Sig2}[\text{infinity}] := \text{plot}\left(\frac{\text{sigma}[top, t = \text{infinity}]}{1e3}, 0..l[i], \text{legend} = ["t=\infty"], \text{color} = \text{red}\right) :$

```
> display( {Sig1[0], Sig1[infinity]}, title = ["Stresses at bottom fibre level"], labels
= ["Distance [m]", "Stress [MPa]"], labeldirections = ["horizontal", "vertical"]);
```



```
> display( {Sig2[0], Sig2[infinity]}, title = ["Stresses at top fibre level"], labels = ["Distance [m]",
"Stress [MPa]"], labeldirections = ["horizontal", "vertical"]);
```



```
> M[ed, 0, sls] := proc(x) if x < a[raveel] then  $\frac{Fl[sls] \cdot (l[i] - a[raveel]) \cdot x}{l[i]} + \frac{1}{2} \cdot q[ed, sls]$ 
\cdot (l[i]-x) - M[p, 0, sls] else  $\frac{Fl[sls] \cdot a[raveel] \cdot (l[i]-x)}{l[i]} + \frac{1}{2} \cdot q[ed, sls] \cdot x \cdot (l[i]-x)$ 
- M[p, 0, sls] end if end proc;
```

[>

[>

Bending moment resistance (ULS)

$$\begin{aligned}
 > d[p] := \frac{h[i]}{2} + e[p]; \text{ delta} := 1.0 : b[w] := b[i] - n[\text{holes}] \cdot d[\text{hole}]; \text{ alpha}[M] := 0.80; \\
 & \quad d_p := 0.1700000000 \\
 & \quad b_w := 0.40 \\
 & \quad \alpha_M := 0.80 \tag{54}
 \end{aligned}$$

$$\begin{aligned}
 > M[ed, uls] := \text{proc}(x) \text{ if } x < a[\text{raveel}] \text{ then } \frac{FI[uls] \cdot (l[i] - a[\text{raveel}]) \cdot x}{l[i]} + \frac{1}{2} \cdot q[ed, uls] \cdot x \\
 & \quad \cdot (l[i] - x) - M[p, \text{infinity}, sls] \text{ else } \frac{FI[uls] \cdot a[\text{raveel}] \cdot (l[i] - x)}{l[i]} + \frac{1}{2} \cdot q[ed, uls] \cdot x \cdot (l[i] \\
 & \quad - x) - M[p, \text{infinity}, sls] \text{ end if end proc:}
 \end{aligned}$$

$$> M[\text{Max}] := 0.0 : \text{NrPoints} := 1000 :$$

$$\begin{aligned}
 > \text{for } r \text{ from } 0 \text{ by } 1 \text{ to } \text{NrPoints} \text{ do } x := r \cdot \frac{l[i]}{\text{NrPoints}}; MI := M[ed, uls](x); M[\text{Max}] := \text{if}(MI \\
 & \quad > M[\text{Max}], MI, M[\text{Max}]) \text{ end do:}
 \end{aligned}$$

$$> M[\text{max}, uls] := M[\text{Max}];$$

$$M_{\text{max}, uls} := 48.20629484 \tag{55}$$

$$\begin{aligned}
 > M[ed, uls](0); M[ed, uls](a[\text{raveel}]); M[ed, uls]\left(\frac{l[i]}{2}\right); M[ed, uls](l[i]); \\
 & \quad -35.49487551 \\
 & \quad 8.08916585 \\
 & \quad 48.20629484 \\
 & \quad -35.49487551 \tag{56}
 \end{aligned}$$

$$> \text{MMMM} := M[\text{max}, uls] + M[p, \text{infinity}, sls];$$

$$\text{MMMM} := 83.70117035 \tag{57}$$

$$> \text{sigma}[pm, \text{infinity}] := \frac{(P[m, \text{infinity}, sls]) \cdot 1000}{A[p, \text{total}, \text{strand}]};$$

$$\sigma_{pm, \infty} := 1183.162517 \tag{58}$$

$$\begin{aligned}
 > \text{delsigma}[p, uls, \text{lowerbound}] := 50; \text{delP}[uls, \text{lowerbound}] := \\
 & \quad \text{evalf}\left(\frac{\text{delsigma}[p, uls, \text{lowerbound}] \cdot A[p, \text{total}, \text{strand}]}{1000}\right);
 \end{aligned}$$

$$\text{delsigma}_{p, uls, \text{lowerbound}} := 50$$

$$\text{delP}_{uls, \text{lowerbound}} := 30. \tag{59}$$

$$> N[cu, \text{lowerbound}] := \text{alpha}[M] \cdot 2 \cdot \text{eta}[\text{lowerbound}] \cdot h[i] \cdot b[i] \cdot f[cd] :$$

$$\begin{aligned}
& \text{eq100} := N[cu, lowerbound] = (P[m, infinity, sls]) + delP[uls, lowerbound] : \\
& \text{eta}[lowerbound] := solve(\text{eq100}, \text{eta}[lowerbound]); x[u, lowerbound] := \text{eta}[lowerbound] \\
& \quad \cdot h[i] \cdot 1e3; N[cu, lowerbound]; \\
& \quad \eta_{lowerbound} := 0.05352267869 \\
& \quad x_{u, lowerbound} := 12.84544289 \\
& \quad \quad \quad 739.8975102 \tag{60}
\end{aligned}$$

$$\begin{aligned}
& M[uls, failure, EC2] := (P[m, infinity, sls] + delP[uls, lowerbound]) \cdot \left(\frac{h[i]}{2} + e[p] - x[u, \right. \\
& \quad \left. lowerbound] \cdot 1e-3 \right); \\
& \quad M_{uls, failure, EC2} := 116.2782655 \tag{61}
\end{aligned}$$

$$\begin{aligned}
& UC[moment, EC2] := \frac{M[\max, uls] + M[p, infinity, sls]}{M[uls, failure, EC2]}; \\
& \quad UC_{moment, EC2} := 0.7198350439 \tag{62}
\end{aligned}$$

$$\begin{aligned}
& \#q[uls, failure, lowerbound] := \\
& \quad \frac{1}{l[i]^2} \left(8 \cdot (P[m, infinity, sls] + delP[uls, lowerbound]) \cdot \left(\frac{h[i]}{2} + e[p] \right. \right. \\
& \quad \left. \left. - \text{eta}[lowerbound] \cdot h[i] \right) \right); M[uls, failure, lowerbound] := \frac{1}{8} \cdot q[uls, failure, lowerbound] \\
& \quad \cdot l[i]^2;
\end{aligned}$$

$$\#UC[moment, lowerbound] := \frac{M[\max, uls] + M[p, infinity, sls]}{M[uls, failure, lowerbound]};$$

$$\begin{aligned}
& \text{varepsilon}[cu] := 0.0030; \Omega[u] := 0.09 \cdot \frac{d[p] - \frac{h[i]}{2}}{0.25 \cdot d[p]} \cdot \left(1.41 + \frac{18}{\frac{l[i]}{d[p]}} \right); \\
& \quad \varepsilon_{cu} := 0.0030 \\
& \quad \Omega_u := 0.1908325792 \tag{63}
\end{aligned}$$

$$\begin{aligned}
& \text{delf}[ps] := \Omega[u] \cdot \left(\frac{E[p, strand]}{1e3} \right) \cdot \text{varepsilon}[cu] \cdot \left(\frac{d[p]}{x[u, Alqam]} - 1 \right); \\
& \quad \text{delf}_{ps} := \frac{18.97830000}{x_{u, Alqam}} - 111.6370588 \tag{64}
\end{aligned}$$

$$\text{eq200} := 0.86 \cdot f[pk, strand] = \text{sigma}[pm, infinity] + \text{delf}[ps]; x[u, Alqam] := solve(\text{eq200},$$

$$\begin{aligned}
x[u, Alqam]; delf[ps]; delP[uls, Alqam] &:= \frac{delf[ps] \cdot A[p, total, strand]}{1e3}, \\
x_{u, Alqam} &:= 0.03593867625 \\
&416.4374832 \\
delP_{uls, Alqam} &:= 249.8624899
\end{aligned} \tag{65}$$

$$\begin{aligned}
> M[uls, failure, Alqam] &:= (P[m, infinity, sls] + delP[uls, Alqam]) \cdot \left(\frac{h[i]}{2} + e[p] \right. \\
&\quad \left. - \frac{x[u, Alqam]}{2} \right); \\
M_{uls, failure, Alqam} &:= 145.9129481
\end{aligned} \tag{66}$$

$$\begin{aligned}
> \#q[uls, failure, upperbound] &:= \\
&\frac{8 \cdot (P[m, infinity, sls] + delP[uls, upperbound]) \cdot \left(\frac{h[i]}{2} + e[p] - \frac{x[u, upperbound]}{2} \right)}{l[i]^2}; \\
M[uls, failure, upperbound] &:= \frac{1}{8} \cdot q[uls, failure, upperbound] \cdot l[i]^2;
\end{aligned}$$

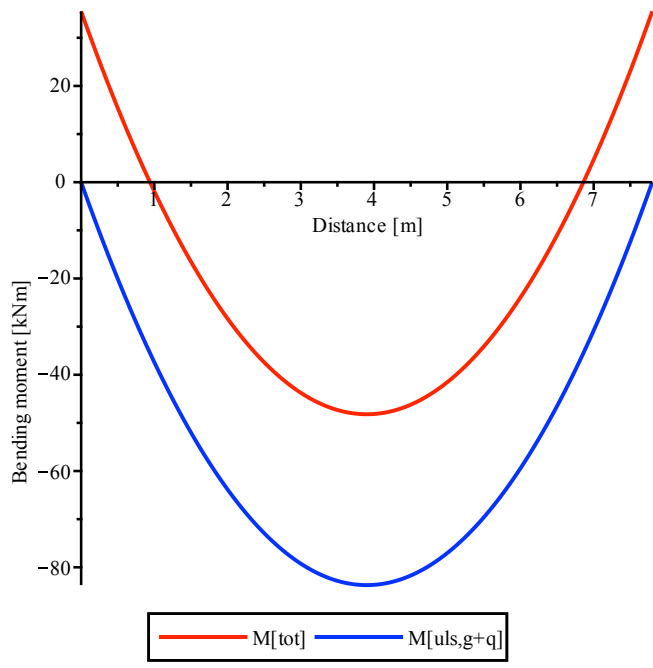
$$\begin{aligned}
> UC[moment, Alqam] &:= \frac{M[\max, uls] + M[p, infinity, sls]}{M[uls, failure, Alqam]}, \\
UC_{moment, Alqam} &:= 0.5736377165
\end{aligned} \tag{67}$$

$$\begin{aligned}
> MMM &:= \text{proc}(x) \text{ if } x < a[raveel] \text{ then } \frac{FI[uls] \cdot (l[i] - a[raveel]) \cdot x}{l[i]} + \frac{1}{2} \cdot q[ed, uls] \cdot x \\
&\quad \cdot (l[i] - x) \text{ else } \frac{FI[uls] \cdot a[raveel] \cdot (l[i] - x)}{l[i]} + \frac{1}{2} \cdot q[ed, uls] \cdot x \cdot (l[i] - x) \text{ end if end proc;}
\end{aligned}$$

> ZZ := plot(-MMM, 0..l[i], labels = ["Distance [m]", "Bending moment [kNm]"],
labeldirections = ["horizontal", "vertical"], color = "Blue", legend = "M[uls,g+q]");

> ZZZ := plot(-M[ed, uls], 0..l[i], labels = ["Distance [m]", "Bending moment [kNm]"],
labeldirections = ["horizontal", "vertical"], color = "Red", legend = "M[tot]");

> display({ZZ, ZZZ});



Shear Resistance (ULS)

Cross-section

```

>
>
> SI := proc(x) if x < a[raveel] then  $\frac{Fl[uls] \cdot (l[i] - a[raveel])}{l[i]} + \frac{1}{2} \cdot q[ed, uls] \cdot (l[i] - 2$ 
    ·x) else  $-\frac{Fl[uls] \cdot a[raveel]}{l[i]} + \frac{1}{2} \cdot q[ed, uls] \cdot (l[i] - 2 \cdot x)$  end if end proc:
>
> Smax := 0.0 : NrPoints := 1000 :
> for r from 0 by 1 to NrPoints do x :=  $r \cdot \frac{l[i]}{NrPoints}$ ; SS := SI(x) : Smax := 'if(SS > Smax,
    SS, Smax) end do:
> V[max] := Smax :
>
> V[ed, uls] := V[max]; S :=  $\frac{1}{8} \cdot b[i] \cdot h[i]^2 - n[holes] \cdot \left( \frac{1}{2} \cdot Pi \cdot R[hole]^2 \cdot \left( \frac{4 \cdot R[hole]}{3 \cdot Pi} \right) \right)$ ;
sigma[cp, lowerbound] :=  $\frac{P[m, infinity, sls] + delP[uls, lowerbound]}{A[c] \cdot 1000}$ ; sigma[cp,
Alqam] :=  $\frac{P[m, infinity, sls] + delP[uls, Alqam]}{A[c] \cdot 1000}$ ; f[ctk, 0.05] :=  $\frac{0.7 \cdot f[ctm]}{1000}$ ; f[ctk,
0.05, d] :=  $\frac{f[ctk, 0.05]}{gamma\_c}$ ; alpha[l] := 1.0;
    Ved, uls := 42.92367710
    S := 0.0069333333334
    σcp, lowerbound := 3.946771849
    σcp, Alqam := 5.119565477
    fctk, 0.05 := 0.002656812896
    fctk, 0.05, d := 0.001771208597
    αl := 1.0

```

(68)

```

>
>
>
> V[rd, c, lowerbound] :=  $\left( \frac{I_{yy} \cdot b[w]}{S} \cdot (f[ctd]^2 + alpha[l] \cdot sigma[cp, lowerbound] \cdot f[ctd])^{0.5} \right)$ 

```


$$\cdot 10^3; V[rd, c, Alqam] := \left(\frac{I_{yy} \cdot b[w]}{S} \cdot (f[ctd]^2 + \alpha[l] \cdot \sigma[cp, Alqam] \cdot f[ctd])^{0.5} \right) \cdot 10^3;$$

$$V_{rd, c, lowerbound} := 224.2773985$$

$$V_{rd, c, Alqam} := 246.2057449 \quad (69)$$

$$> b[w, out] := 68 \cdot 1e-3; T[ed] := \frac{FI[uls] \cdot b[i]}{2};$$

$$b_{w, out} := 0.068$$

$$T_{ed} := 0. \quad (70)$$

$$> \text{if } n[holes] > 0 \text{ then } V[etd] := \frac{T[ed]}{2 \cdot b[w, out]} \cdot \frac{b[w]}{b[i] - b[w, out]}; \text{ else } V[etd] := T[ed]$$

$$\cdot \frac{3 + 1.8 \cdot \left(\frac{b[i]}{h[i]} \right)}{b[i]} \text{ end if;}$$

$$V_{etd} := 0. \quad (71)$$

$$> V[rd, n, lowerbound] := V[rd, c, lowerbound] - V[etd];$$

$$V_{rd, n, lowerbound} := 224.2773985 \quad (72)$$

$$> V[rd, n, Alqam] := V[rd, c, Alqam] - V[etd];$$

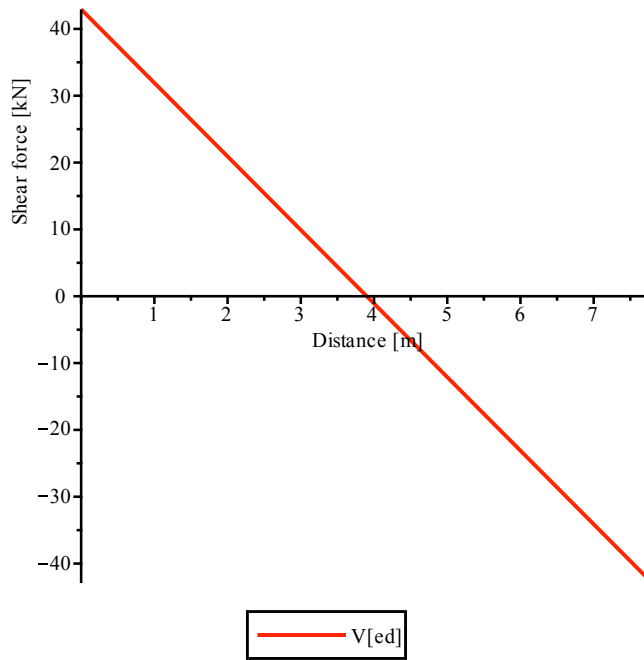
$$V_{rd, n, Alqam} := 246.2057449 \quad (73)$$

$$> UC[shear, EC2] := \frac{V[ed, uls]}{V[rd, n, lowerbound]}; UC[shear, alqam] := \frac{V[ed, uls]}{V[rd, n, Alqam]};$$

$$UC_{shear, EC2} := 0.1913865480$$

$$UC_{shear, alqam} := 0.1743406805 \quad (74)$$

> SSI := plot(SI, 0 .. l[i], labels = ["Distance [m]", "Shear force [kN]"], labeldirections = ["horizontal", "vertical"], color = "Red", legend = "V[ed]");



> $V[\max]$;

42.92367710

(75)

Interface

> $\beta[\textit{shear}] := 1.0$; $\mu[\textit{shear}] := 0.5$; $\sigma[n, \textit{lowerbound}] := \frac{P[m, \textit{infinity}, \textit{sls}] + \textit{del}P[\textit{uls}, \textit{lowerbound}]}{A[c]}$; $\sigma[n, \textit{Alqam}] := \frac{P[m, \textit{infinity}, \textit{sls}] + \textit{del}P[\textit{uls}, \textit{Alqam}]}{A[c]}$;

$\beta_{\textit{shear}} := 1.0$

$\mu_{\textit{shear}} := 0.5$

$\sigma_{n, \textit{lowerbound}} := 3946.771849$

(76)

> $v[\textit{ed}, i] := \frac{\beta[\textit{shear}] \cdot V[\textit{ed}, \textit{uls}]}{d[p] \cdot b[w]} \cdot 1e-3$;

$v_{\textit{ed}, i} := 0.6312305455$

(77)

> $v[\textit{rd}, i, \textit{lowerbound}] := \mu[\textit{shear}] \cdot \sigma[n, \textit{lowerbound}] \cdot 1e-3$; $v[\textit{rd}, i, \textit{Alqam}] := \mu[\textit{shear}] \cdot \sigma[n, \textit{Alqam}] \cdot 1e-3$;

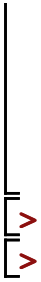
$v_{\textit{rd}, i, \textit{lowerbound}} := 1.973385924$

$v_{\textit{rd}, i, \textit{Alqam}} := 2.559782738$

(78)

> $UC[\textit{shear}, \textit{interface}, \textit{lowerbound}] := \frac{v[\textit{ed}, i]}{v[\textit{rd}, i, \textit{lowerbound}]}$; $UC[\textit{shear}, \textit{interface},$

$$\begin{aligned}
 \text{upperbound}] &:= \frac{v[ed, i]}{v[rd, i, Alqam]}; \\
 UC_{\text{shear, interface, lowerbound}} &:= 0.3198718192 \\
 UC_{\text{shear, interface, upperbound}} &:= 0.2465953599
 \end{aligned}
 \tag{79}$$



Deflections quasi-permanent combination (SLS)

```

> q[quasi - permanent]; q[quasi - permanent, W3]; FI[quasi - permanent]; FI[quasi
  - permanent, W3]; EI[short] := E[cm]·Iyy; EI[long] := E[c, eff]·Iyy; a[raveel];
  6.264725878
  2.1420
  0
  0
  EI_short := 43975.81642
  EI_long := 15689.62058
  1.2

```

(80)

```

> def1 := proc(x) if x < a[raveel] then 1/6
  . FI[quasi - permanent]·(a[raveel] - l[i])·x·(x2 + a[raveel]2 - 2·a[raveel]·l[i])
  . EI[short]·l[i]
  + 1/24 · q[quasi - permanent]·x · (l[i]3 - 2·l[i]·x2 + x3) +
  - M[p, infinity, sls]·x·(-x + l[i])
  . 2·EI[short] else 1/6 · 1/EI[short]·l[i] ((x3 - 3·x2·l[i] + x
  ·a[raveel]2 + 2·x·l[i]2 - l[i]·a[raveel]2)·FI[quasi - permanent]·a[raveel]) + 1/24
  . q[quasi - permanent]·x · (l[i]3 - 2·l[i]·x2 + x3) +
  - M[p, infinity, sls]·x·(-x + l[i])
  . 2·EI[short] end if end proc:

```

```

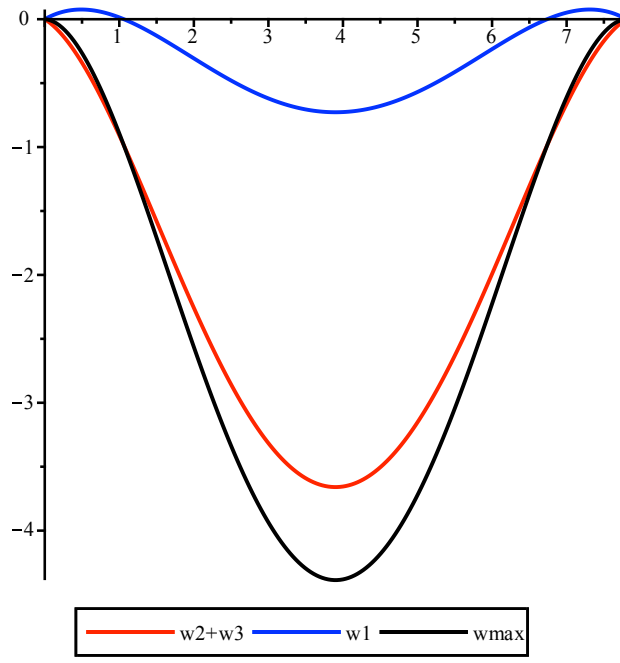
> def2 := proc(x) if x < a[raveel] then 1/6
  . FI[quasi - permanent]·(a[raveel] - l[i])·x·(x2 + a[raveel]2 - 2·a[raveel]·l[i])
  . EI[long]·l[i]
  + 1/24 · q[quasi - permanent]·x · (l[i]3 - 2·l[i]·x2 + x3) +
  - M[p, infinity, sls]·x·(-x + l[i])
  . 2·EI[long] else 1/6 · 1/EI[long]·l[i] ((x3 - 3·x2·l[i] + x
  ·a[raveel]2 + 2·x·l[i]2 - l[i]·a[raveel]2)·FI[quasi - permanent]·a[raveel]) + 1/24
  . q[quasi - permanent]·x · (l[i]3 - 2·l[i]·x2 + x3) +
  - M[p, infinity, sls]·x·(-x + l[i])
  . 2·EI[long]

```

```

-  $\frac{M[p, \text{infinity}, \text{sls}] \cdot x \cdot (-x + l[i])}{2 \cdot EI[\text{long}]}$  end if end proc:
>
>
> def3 := proc(x) if x < a[raveel] then  $\frac{1}{6}$ 
.  $\frac{FI[\text{quasi} - \text{permanent}, W3] \cdot (a[\text{raveel}] - l[i]) \cdot x \cdot (x^2 + a[\text{raveel}]^2 - 2 \cdot a[\text{raveel}] \cdot l[i])}{EI[\text{short}] \cdot l[i]}$ 
+  $\frac{1}{24} \cdot \frac{q[\text{quasi} - \text{permanent}, W3] \cdot x}{EI[\text{short}]} \cdot (l[i]^3 - 2 \cdot l[i] \cdot x^2 + x^3)$  else  $\frac{1}{6}$ 
.  $\frac{1}{EI[\text{short}] \cdot l[i]} ((x^3 - 3 \cdot x^2 \cdot l[i] + x \cdot a[\text{raveel}]^2 + 2 \cdot x \cdot l[i]^2 - l[i] \cdot a[\text{raveel}]^2) \cdot FI[\text{quasi}$ 
-  $\text{permanent}, W3] \cdot a[\text{raveel}])$  +  $\frac{1}{24} \cdot \frac{q[\text{quasi} - \text{permanent}, W3] \cdot x}{EI[\text{short}]} \cdot (l[i]^3 - 2 \cdot l[i] \cdot x^2$ 
+  $x^3)$  end if end proc:
>
>
> DEF1 := def1 · 1e3 : DEF2 := (def2 - def1) · 1e3 : DEF3 := def3 · 1e3 :
> DEF23 := DEF2 + DEF3 :
> DEFMAX := DEF1 + DEF2 + DEF3 :
>
>
> defmax := 0.0 : NrPoints := 1000 :
> for r from 0 by 1 to NrPoints do x :=  $r \cdot \frac{l[i]}{\text{NrPoints}}$ ; deldel := def1(x) + (def2(x) - def1(x))
+ def3(x); defmax := `if` (deldel > defmax, deldel, defmax) end do:
> def[max, sls] := defmax · 1e3 :
>
>
> defmax23 := 0.0 : NrPoints := 1000 :
> for r from 0 by 1 to NrPoints do x :=  $r \cdot \frac{l[i]}{\text{NrPoints}}$ ; deldel23 := (def2(x) - def1(x))
+ def3(x); defmax23 := `if` (deldel23 > defmax23, deldel23, defmax23) end do:
> def[w2 + w3] := defmax23 · 1e3 :
>
>
>
> PP1 := plot(-DEF1, 0 ..l[i], legend = ["w1"], color = "Blue", labels = ["Distance [m]",
"Deflection [mm]"], labeldirections = ["horizontal", "vertical"]) : PP2 := plot(-DEF2, 0
..l[i], legend = ["w2"], color = "Green") : PP3 := plot(-DEF3, 0 ..l[i], legend = ["w3"],
color = "Red") : PP23 := plot(-DEF23, 0 ..l[i], legend = "w2 + w3", color = "Red") :
PPMAX := plot(-DEFMAX, 0 ..l[i], legend = ["wmax"], color = "black") :
>
> display({PP1, PP23, PPMAX});

```



```
> def[w2 + w3]; def[max, sls];
```

3.659505733
4.387189937

(81)

Deflections frequent combination (SLS)

$$\begin{aligned} > q[\text{freq}] := (g[k] + \text{psil} \cdot q[k]) \cdot w[i]; \\ & \qquad \qquad \qquad q_{\text{freq}} := 6.876725878 \end{aligned} \quad (82)$$

$$\begin{aligned} > q[\text{freq}, W3] := (1 - \text{psil}) \cdot q[k] \cdot w[i]; \\ & \qquad \qquad \qquad q_{\text{freq}, W3} := 1.5300 \end{aligned} \quad (83)$$

$$\begin{aligned} > \text{if } N[\text{raveel}] = 1.0 \text{ then } FI[\text{freq}] := N[\text{plates}] \cdot \frac{q[\text{freq}] \cdot (l[i] - a[\text{raveel}])}{4}; FI[\text{freq}, W3] := \\ & \quad N[\text{plates}] \cdot \frac{q[\text{freq}, W3] \cdot (l[i] - a[\text{raveel}])}{4} \text{ else } FI[\text{freq}] := 0; FI[\text{freq}, W3] := 0; \text{end} \\ \text{if} \\ & \qquad \qquad \qquad FI_{\text{freq}} := 0 \\ & \qquad \qquad \qquad FI_{\text{freq}, W3} := 0 \end{aligned} \quad (84)$$

$$\begin{aligned} > M[\text{ed}, \text{freq}] := \frac{1}{8} \cdot q[\text{freq}] \cdot l[i]^2; \\ & \qquad \qquad \qquad M_{\text{ed}, \text{freq}} := 52.29750030 \end{aligned} \quad (85)$$

$$\begin{aligned} > q[\text{freq}]; q[\text{freq}, W3]; FI[\text{freq}]; FI[\text{freq}, W3]; EI[\text{short}]; EI[\text{long}]; \\ & \qquad \qquad \qquad 6.876725878 \\ & \qquad \qquad \qquad 1.5300 \\ & \qquad \qquad \qquad 0 \\ & \qquad \qquad \qquad 0 \\ & \qquad \qquad \qquad 43975.81642 \\ & \qquad \qquad \qquad 15689.62058 \end{aligned} \quad (86)$$

$$\begin{aligned} > \text{def100} := \text{proc}(x) \text{ if } x < a[\text{raveel}] \text{ then } \frac{1}{6} \\ & \quad \cdot \frac{FI[\text{freq}] \cdot (a[\text{raveel}] - l[i]) \cdot x \cdot (x^2 + a[\text{raveel}]^2 - 2 \cdot a[\text{raveel}] \cdot l[i])}{EI[\text{short}] \cdot l[i]} + \frac{1}{24} \\ & \quad \cdot \frac{q[\text{freq}] \cdot x}{EI[\text{short}]} \cdot (l[i]^3 - 2 \cdot l[i] \cdot x^2 + x^3) + - \frac{M[p, \text{infinity}, \text{sls}] \cdot x \cdot (-x + l[i])}{2 \cdot EI[\text{short}]} \text{ else } \frac{1}{6} \\ & \quad \cdot \frac{(x^3 - 3 \cdot x^2 \cdot l[i] + x \cdot a[\text{raveel}]^2 + 2 \cdot x \cdot l[i]^2 - l[i] \cdot a[\text{raveel}]^2) \cdot FI[\text{freq}] \cdot a[\text{raveel}]}{EI[\text{short}] \cdot l[i]} \\ & \quad + \frac{1}{24} \cdot \frac{q[\text{freq}] \cdot x}{EI[\text{short}]} \cdot (l[i]^3 - 2 \cdot l[i] \cdot x^2 + x^3) + - \frac{M[p, \text{infinity}, \text{sls}] \cdot x \cdot (-x + l[i])}{2 \cdot EI[\text{short}]} \text{ end if} \\ \text{end proc;} \end{aligned}$$

```

> def200 := proc(x) if x < a[raveel] then  $\frac{1}{6}$ 
  .  $\frac{FI[freq] \cdot (a[raveel] - l[i]) \cdot x \cdot (x^2 + a[raveel]^2 - 2 \cdot a[raveel] \cdot l[i])}{EI[long] \cdot l[i]} + \frac{1}{24}$ 
  .  $\frac{q[freq] \cdot x}{EI[long]} \cdot (l[i]^3 - 2 \cdot l[i] \cdot x^2 + x^3) + - \frac{M[p, infinity, sls] \cdot x \cdot (-x + l[i])}{2 \cdot EI[long]}$  else  $\frac{1}{6}$ 
  .  $\frac{(x^3 - 3 \cdot x^2 \cdot l[i] + x \cdot a[raveel]^2 + 2 \cdot x \cdot l[i]^2 - l[i] \cdot a[raveel]^2) \cdot FI[freq] \cdot a[raveel]}{EI[long] \cdot l[i]}$ 
+  $\frac{1}{24} \cdot \frac{q[freq] \cdot x}{EI[long]} \cdot (l[i]^3 - 2 \cdot l[i] \cdot x^2 + x^3) + - \frac{M[p, infinity, sls] \cdot x \cdot (-x + l[i])}{2 \cdot EI[long]}$  end if
end proc:

```

```

> def300 := proc(x) if x < a[raveel] then  $\frac{1}{6}$ 
  .  $\frac{FI[freq, W3] \cdot (a[raveel] - l[i]) \cdot x \cdot (x^2 + a[raveel]^2 - 2 \cdot a[raveel] \cdot l[i])}{EI[short] \cdot l[i]} + \frac{1}{24}$ 
  .  $\frac{q[freq, W3] \cdot x}{EI[short]} \cdot (l[i]^3 - 2 \cdot l[i] \cdot x^2 + x^3)$  else  $\frac{1}{6}$ 
  .  $\frac{(x^3 - 3 \cdot x^2 \cdot l[i] + x \cdot a[raveel]^2 + 2 \cdot x \cdot l[i]^2 - l[i] \cdot a[raveel]^2) \cdot FI[freq, W3] \cdot a[raveel]}{EI[short] \cdot l[i]}$ 
+  $\frac{1}{24} \cdot \frac{q[freq, W3] \cdot x}{EI[short]} \cdot (l[i]^3 - 2 \cdot l[i] \cdot x^2 + x^3)$  end if end proc:

```

```

> DEF100 := def100 · 1e3 : DEF200 := (def200 - def100) · 1e3 : DEF300 := def300 · 1e3 :

```

```

> DEF230 := DEF200 + DEF300 :

```

```

> DEFMAX00 := DEF100 + DEF200 + DEF300 :

```

```

> defmax := 0.0 : NrPoints := 1000 :

```

```

> for r from 0 by 1 to NrPoints do x :=  $r \cdot \frac{l[i]}{NrPoints}$ ; deldel100 := def100(x) + (def200(x)
  - def100(x)) + def300(x); defmax := `if` (deldel100 > defmax, deldel100, defmax) end
do:

```

```

> def[max, freq] := defmax · 1e3;

```

$def_{max, freq} := 5.596441912$ (87)

```

> defmax230 := 0.0 : NrPoints := 1000 :

```

```

> for r from 0 by 1 to NrPoints do x :=  $r \cdot \frac{l[i]}{NrPoints}$ ; deldel230 := (def200(x) - def100(x))
  + def300(x); defmax230 := `if` (deldel230 > defmax230, deldel230, defmax230) end do:

```

```

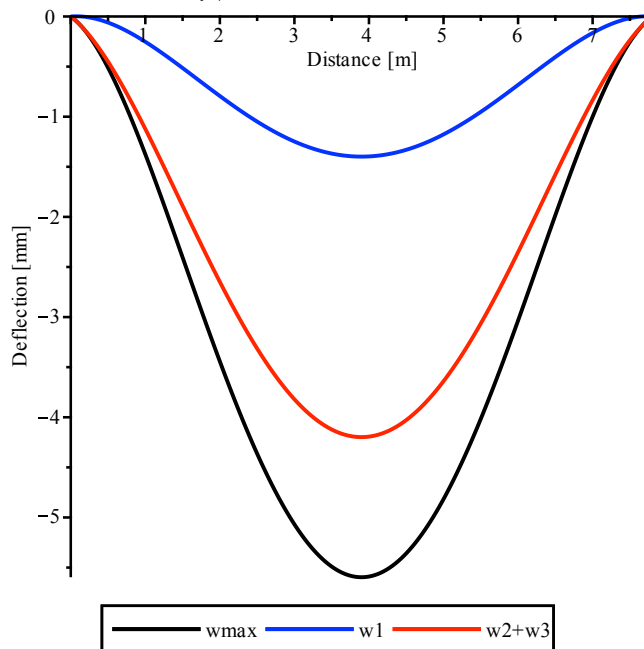
> def[w2 + w3, freq] := defmax230 · 1e3;

```


$$def_{w2 + w3, freq} := 4.198016941$$

(88)

```
> PPP1 := plot(-DEF100, 0 ..l[i], legend = ["w1"], color = "Blue", labels = ["Distance [m]",  
"Deflection [mm]"], labeldirections = ["horizontal", "vertical"]) : PPP2 := plot(-DEF200, 0  
..l[i], legend = ["w2"], color = "Green", labels = ["Distance [m]", "Deflection [mm]"],  
labeldirections = ["horizontal", "vertical"]) : PPP3 := plot(-DEF300, 0 ..l[i], legend  
= ["w3"], color = "Red", labels = ["Distance [m]", "Deflection [mm]"], labeldirections  
= ["horizontal", "vertical"]) : PPP23 := plot(-DEF230, 0 ..l[i], legend = "w2 + w3", color  
= "Red", labels = ["Distance [m]", "Deflection [mm]"], labeldirections = ["horizontal",  
"vertical"]) : PPPMAX := plot(-DEFMAX00, 0 ..l[i], legend = ["wmax"], color = "black",  
labels = ["Distance [m]", "Deflection [mm]"], labeldirections = ["horizontal", "vertical"]) :  
>  
> display({PPP1, PPP23, PPPMAX});
```

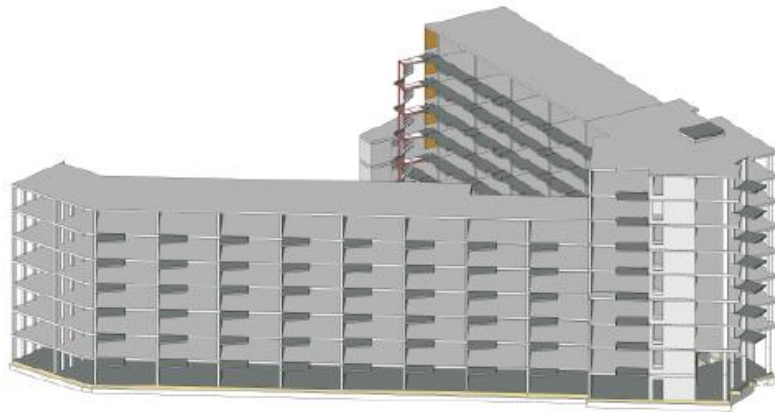


Case study Project

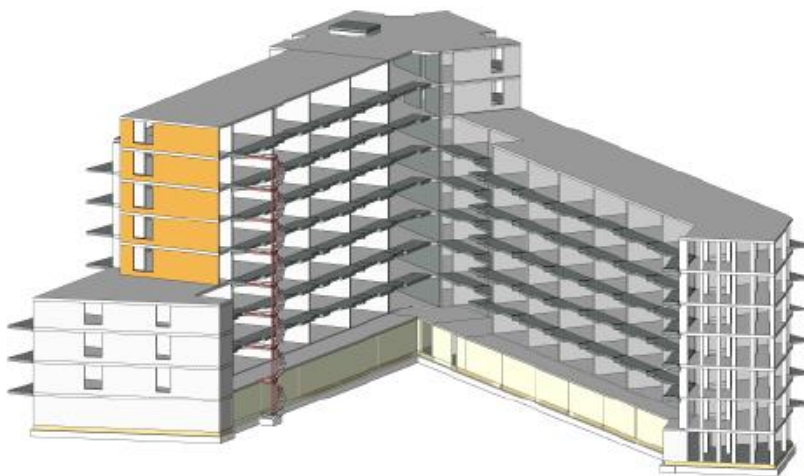
This sections consists figures related to the case study project. The case study adopted in this thesis report is a recent project of C.A.E. B.V. The project is divided in two parts: (i) a medium to high-rise apartment building and 16 blocks of ground based housing units. The proposed floor system is designed according to the span lengths adopted for all buildings considered in this project. The span lengths vary from 5.4 meters to 6.6 meters for the ground-based housing units. The largest span length for the apartment building is 7.8 meters. Apart from the span lengths, the apartment building is taken as a reference situation to determine impact of the horizontal loads due to wind. The apartment building consists of two sections, one with seven storeys and one with nine storeys. For the horizontal loads, the highest section is taken as the reference case. All storeys have a residential purpose. An overview of the plot is presented in figure F.1. Front and back views of the building are provided in figure F.2.



Figure F.1: Overview of the building plot of the case study



(a) Front view of the case study apartment building



(b) Back view of the case study apartment buildings

Figure F.2: Front and back view of the case study apartment building